Sieves for powders separation

Sieve number and relative spacing

TABLE 20.6 Aperture Size of U.S. Standard Sieves

Sieve number	*Aperture (μm)*	*Sieve number*	*Aperture (μm)*
3.5	5,660	60	250
4	4,760	70	210
5	4,000	80	177
6	3,360	100	149
7	2,830	120	125
8	2,380	140	105
10	2,000	170	88
12	1,680	200	74
14	1,410	230	63
16	1,190	270	53
18	1,000	325	44
20	841	400	37
25	707	600	30
30	595	1,200	15
35	500	1,800	9
40	420	3,000	6
45	354	8,000	3
50	297	14,000	1

Dynamic light scattering

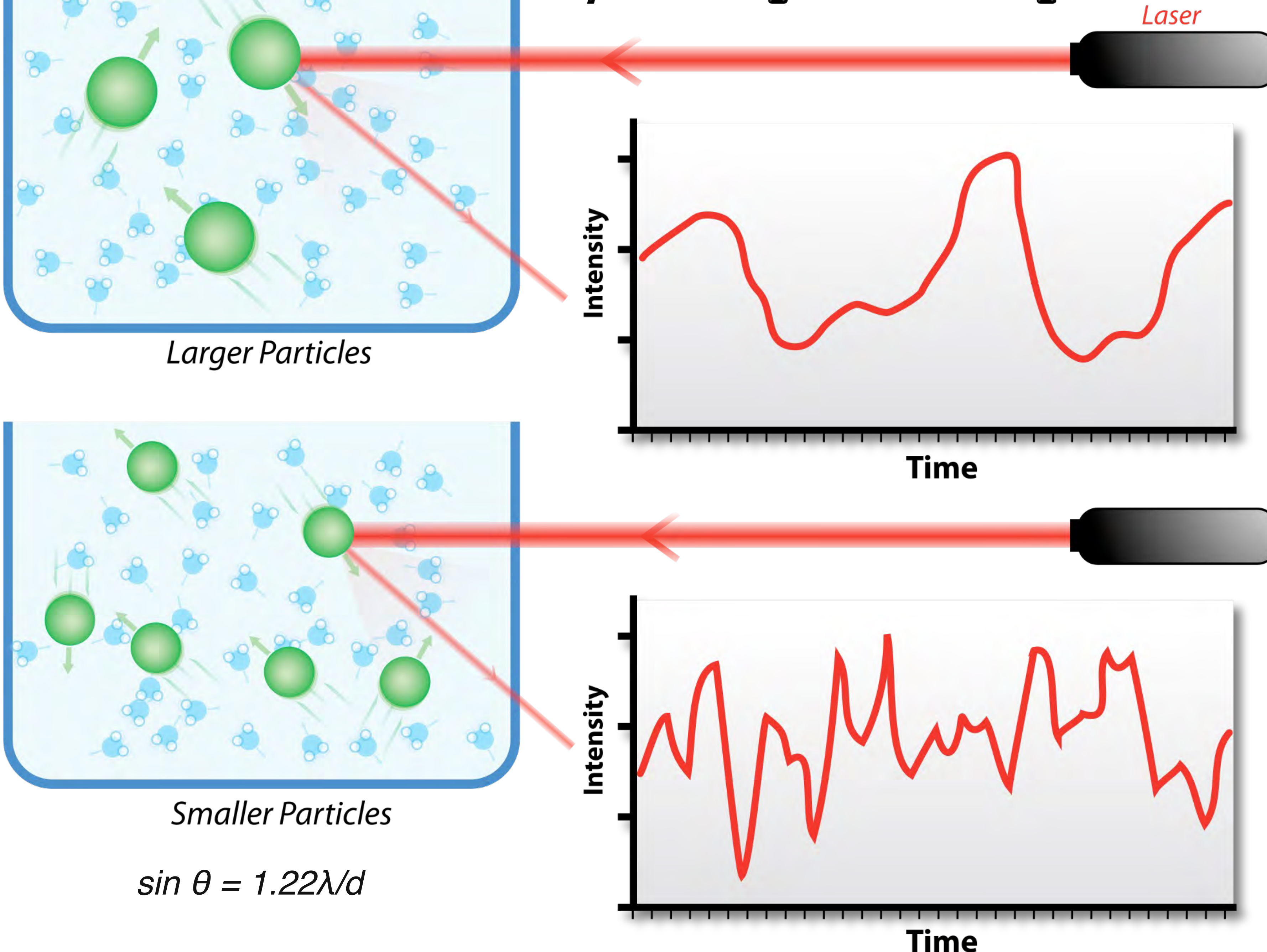

$$\sin \theta = 1.22\lambda/d$$

Dynamic light scattering

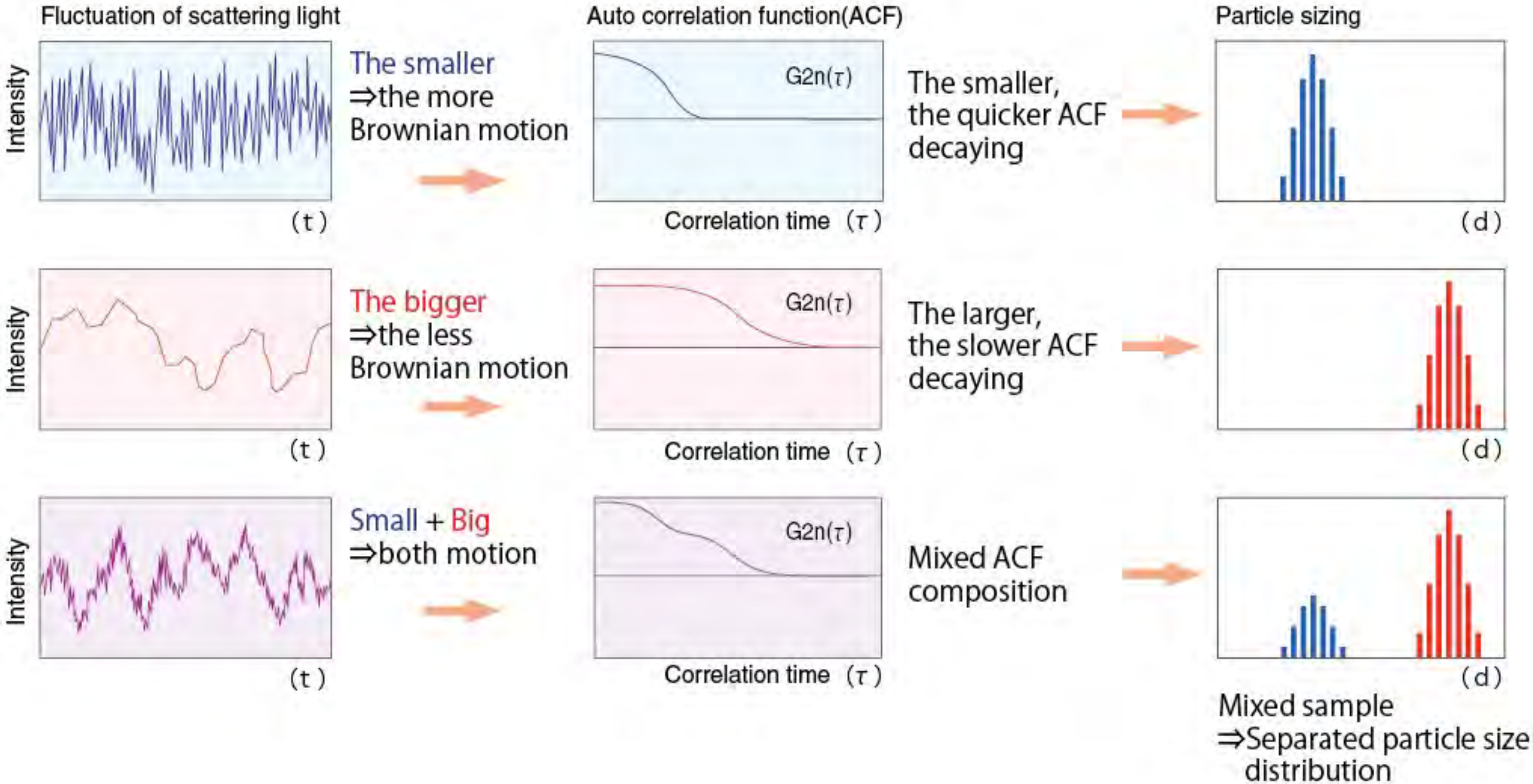

Perfectly spherical ceramic particles

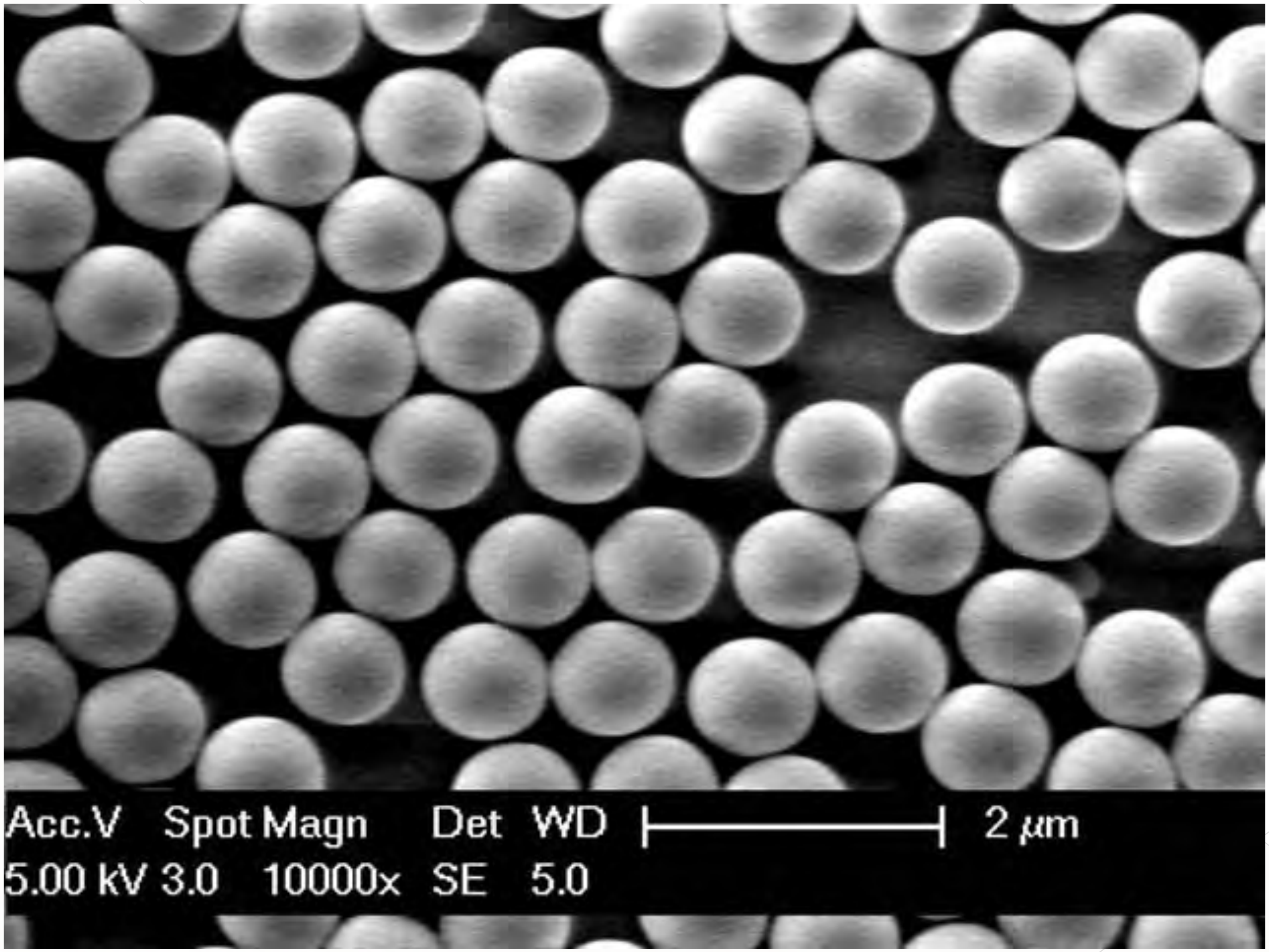

Particle size distribution and % finer plot

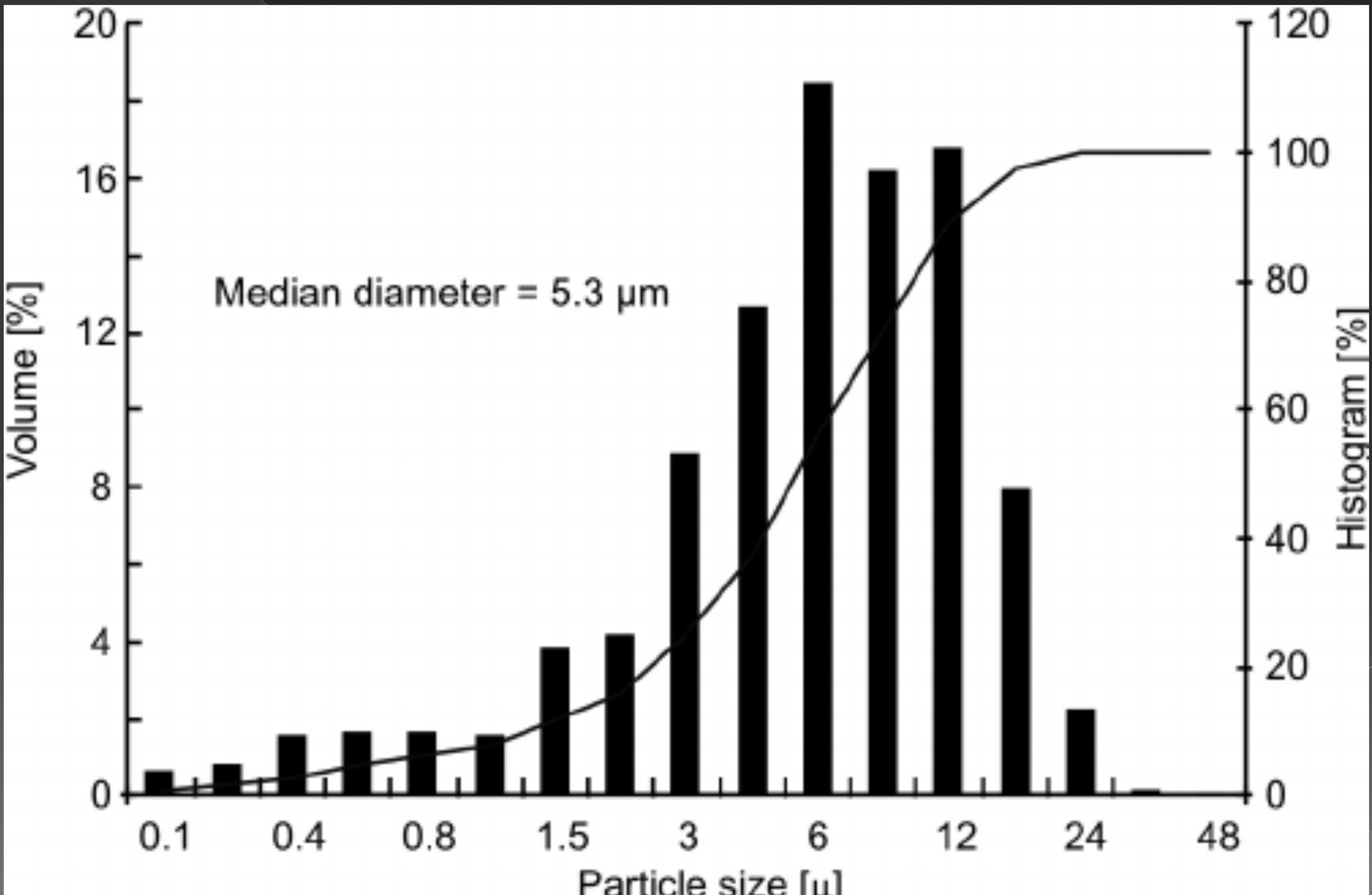

TEM image of Si_3N_4 powder

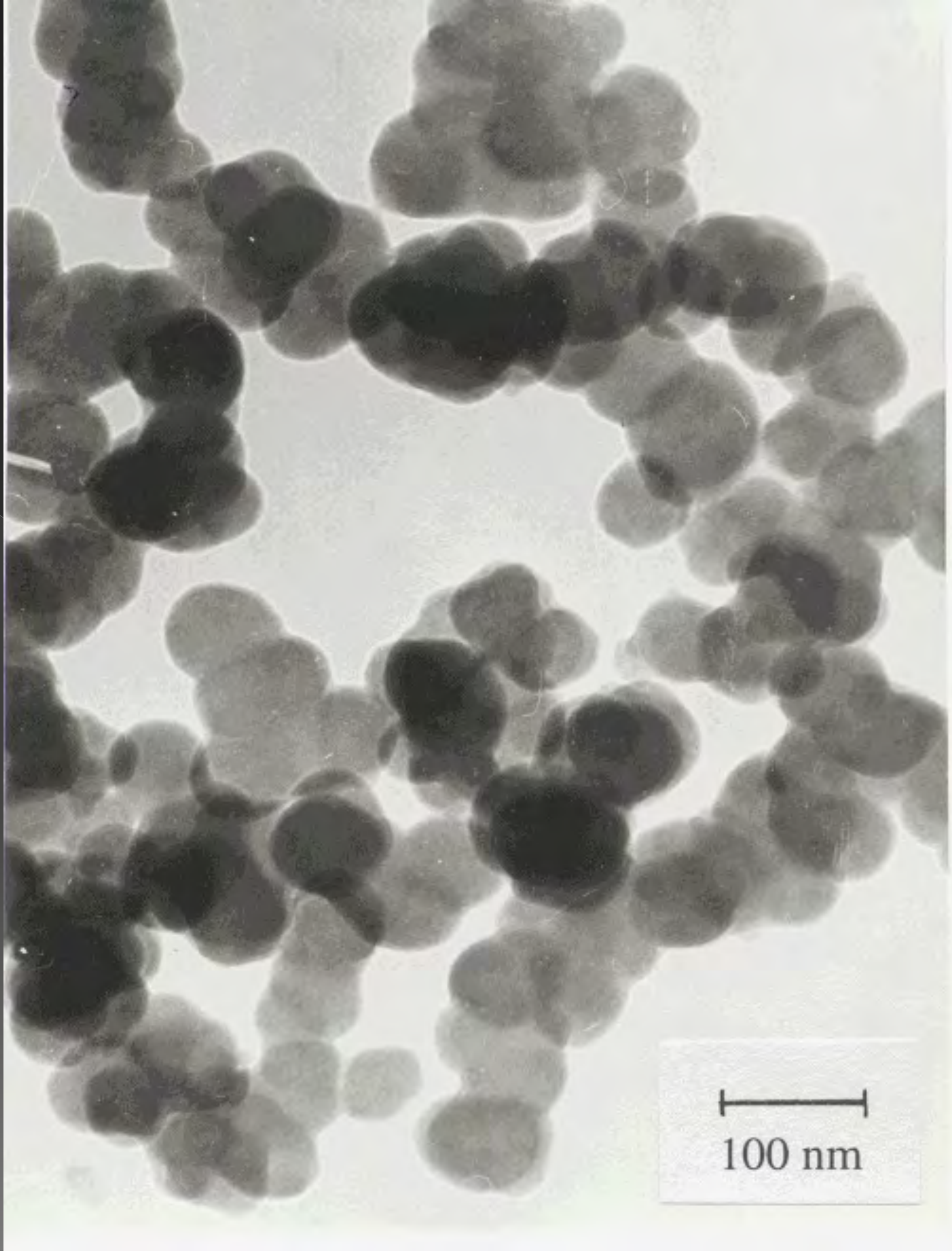

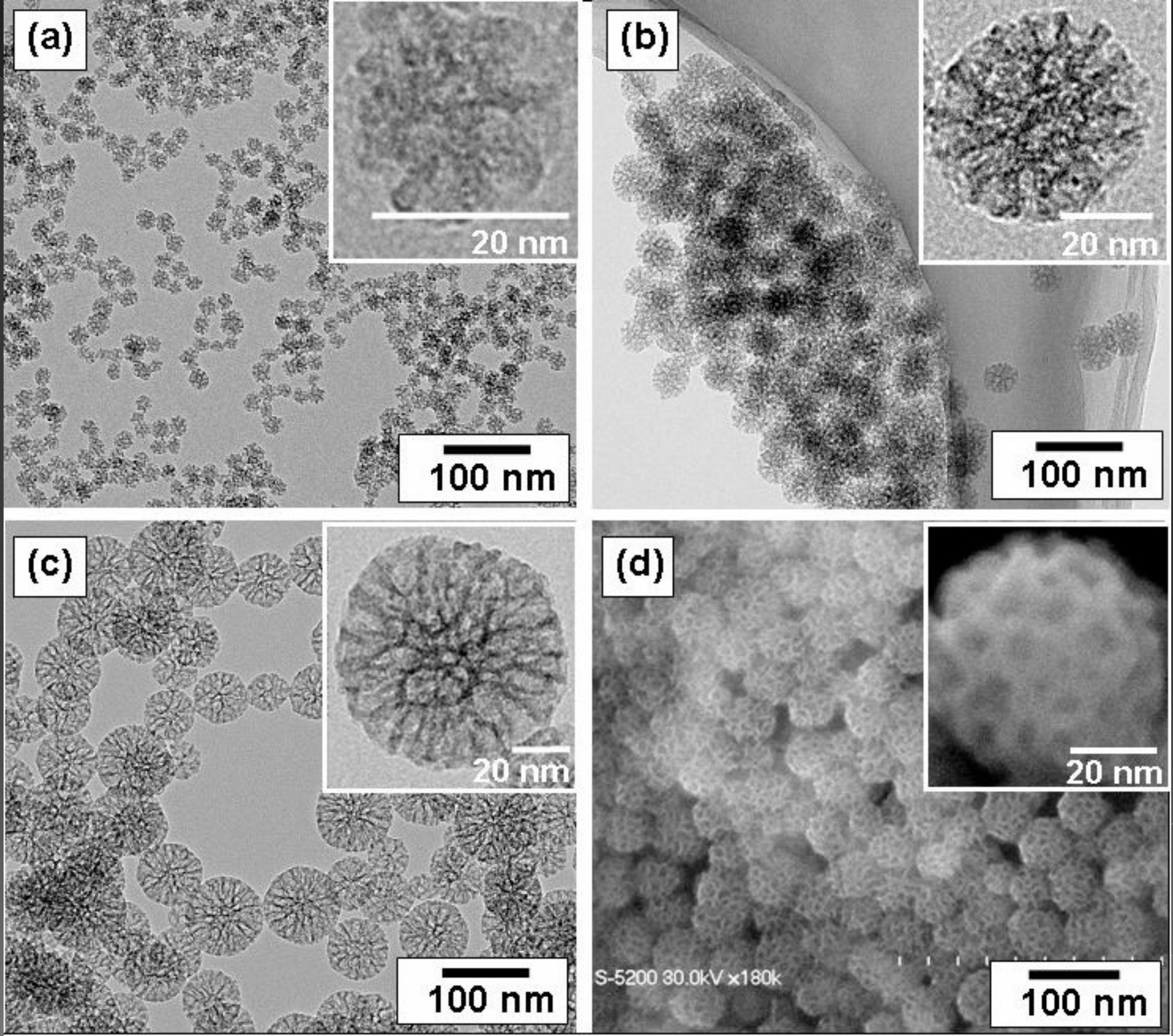

(a)
20 nm
100 nm
(b)
20 nm
100 nm
(c)
20 nm
100 nm
(d)
20 nm
S-5200 30.0kV x180k
100 nm

Reducing particle size: Ball milling

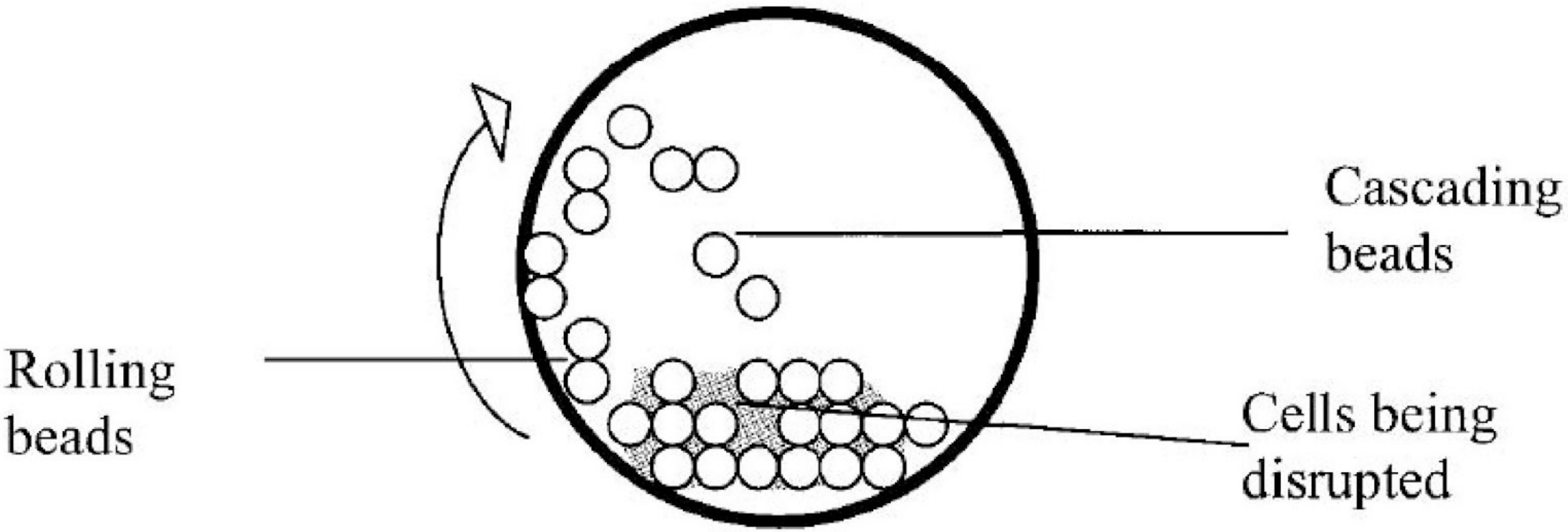

Industrial ball mills

Attrition milling

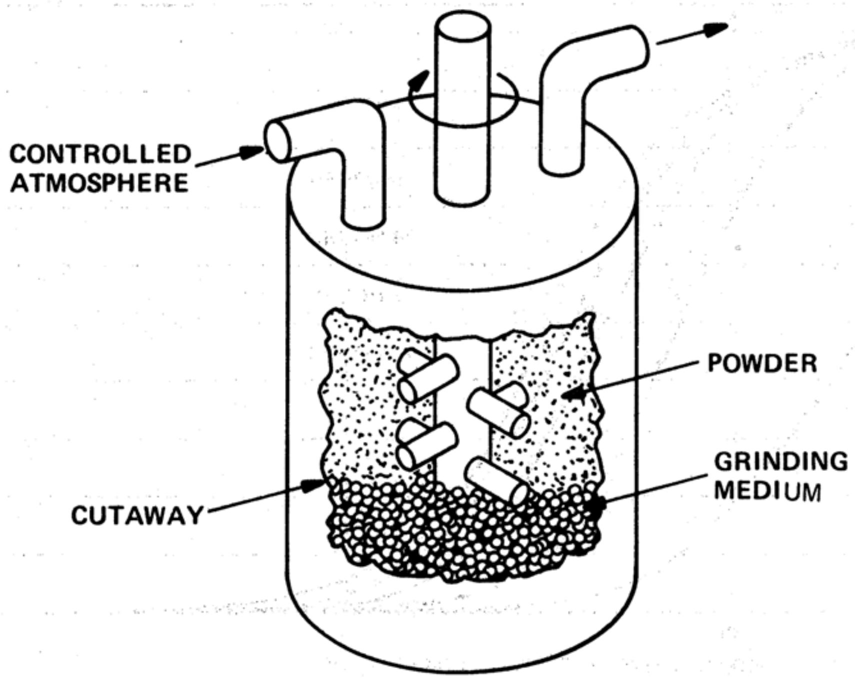

Figure 9.7 Schematic of an attrition mill. (Adapted from T. P. Herbell and T. K. Glasgow, NASA, paper presented at the DOE Highway Vehicle Systems Contractors Coordination Meeting, Dearborn, Mich., Oct. 17–20, 1978.)

Industrial attrition mills

CENTRIFUGAL IMPACT MILLS

Effect of milling time on particle size reduction

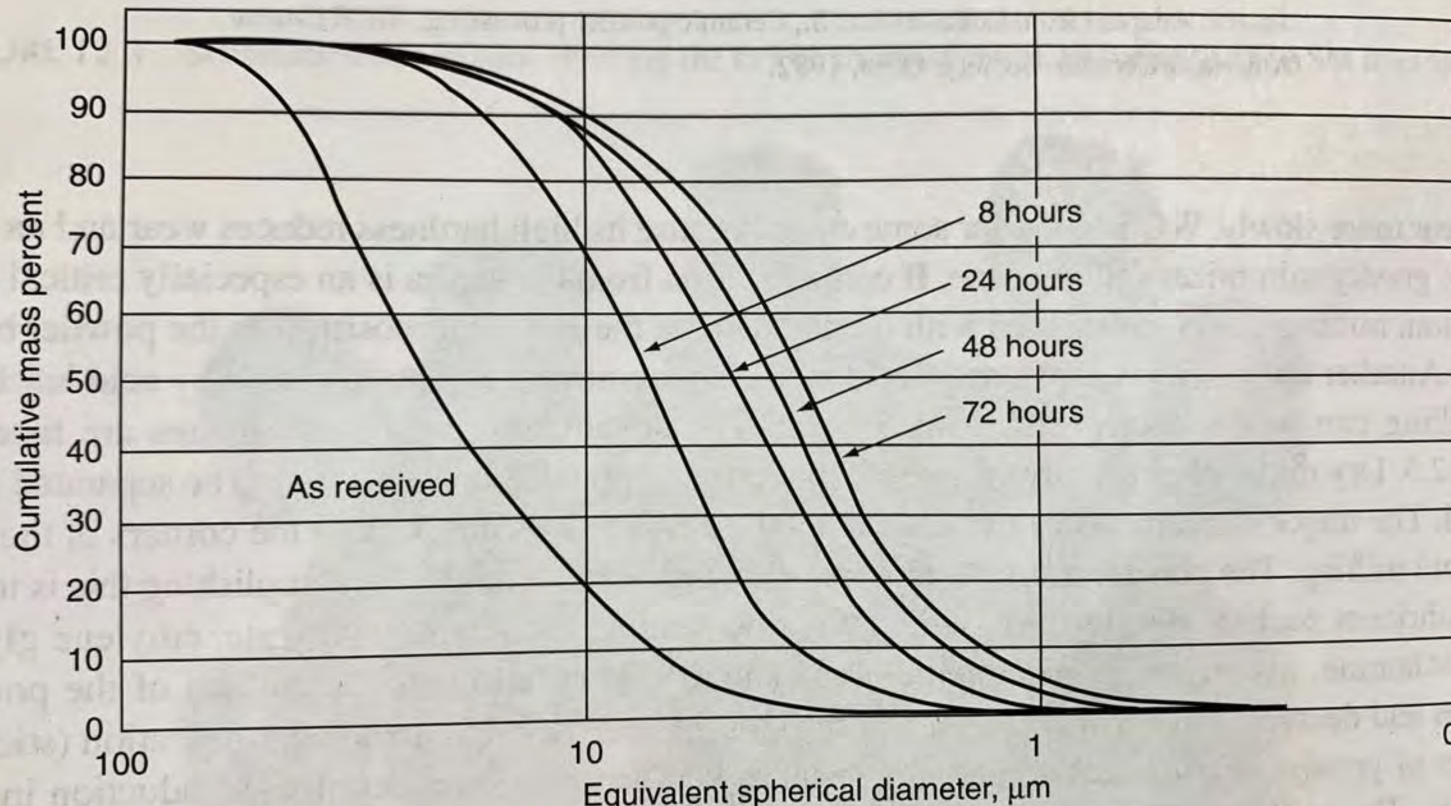

FIGURE 12.6 Particle size distribution of silicon powder as a function of milling time.

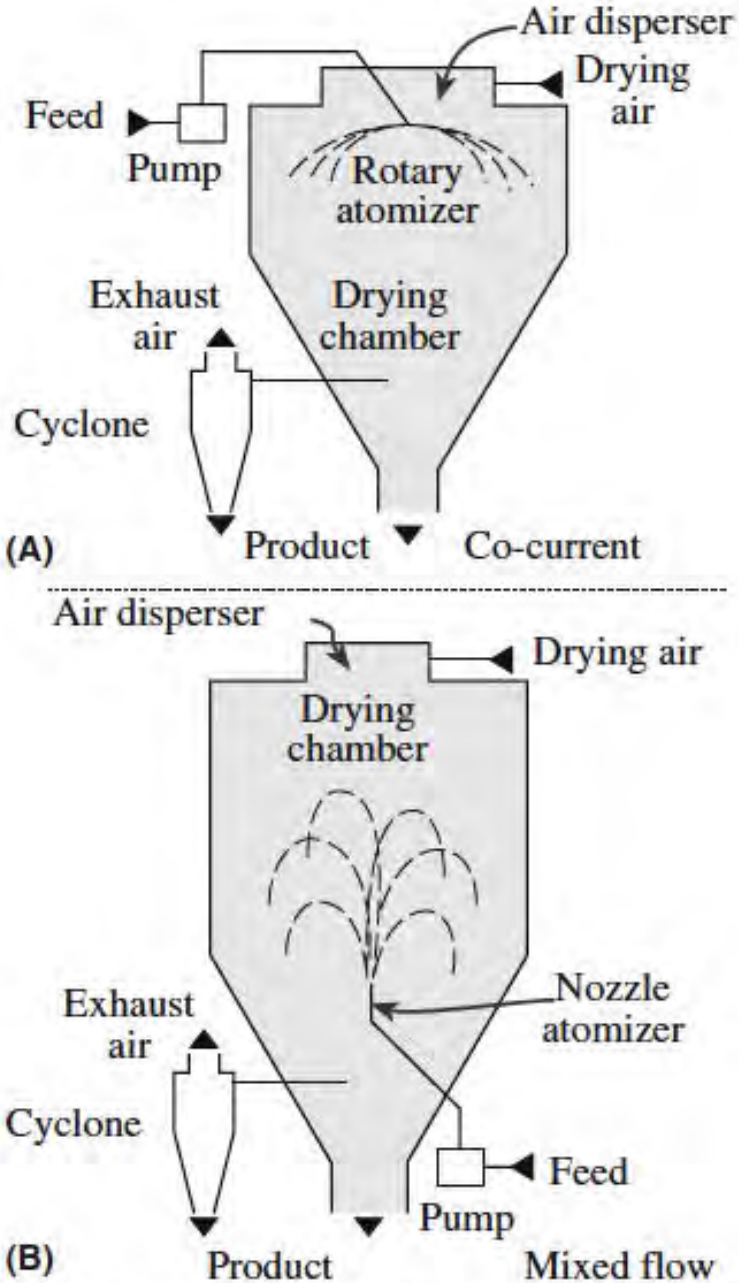

FIGURE 20.3 Spray dryers: (a) Centrifugal atomizer with cocurrent air flow. (b) Nozzle atomizer using mixed-flow conditions.

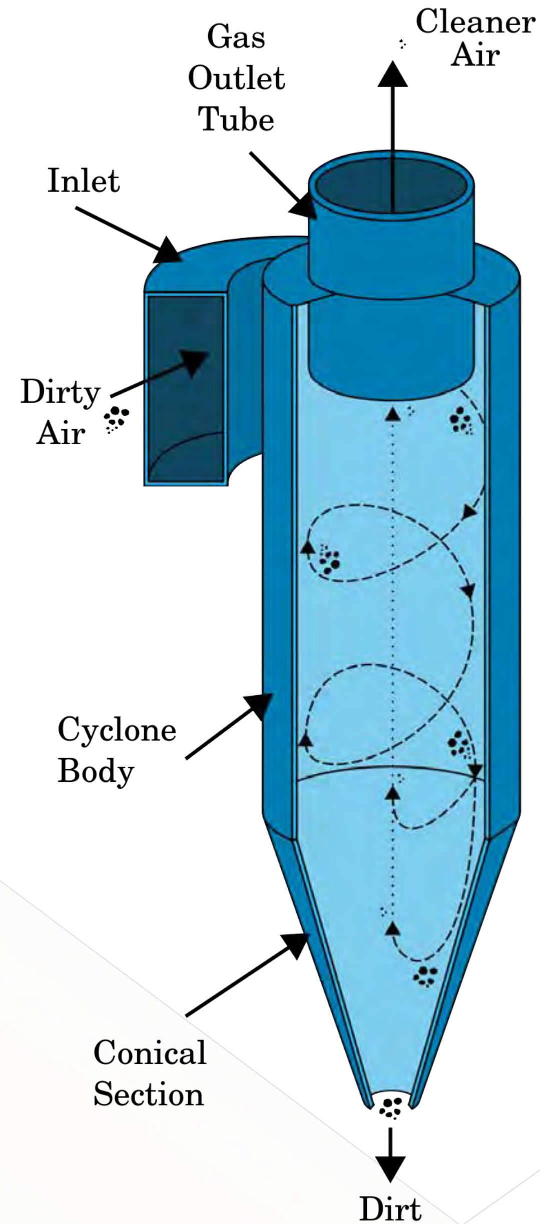

Cyclone

Spray drier

Shaping

- Pressing
  - Uniaxial
    - Cold
    - Hot
  - isostatic
    - Cold
    - Hot
- Casting
  - -Drain
  - -Squeeze
  - -Centrifugal
  - TAPE casting
- Extrusion
- Injection Moulding (very rare)

Overall process from starting powder to slurry:
https://www.youtube.com/watch?v=UHD1SzAJjU8

Slurry preparation (impasto/barbottina)

- Ceramic powder 50%
- Water (or other suspension media) 40%
- Binder (legante) 5%
  - Organic: PVA, PEG, Cellulose, starch
  - Inorganic: Clay, colloidal silica, aluminates
- Plasticizer (plasticizzante) 2-3%
- Lubricant (lubrificante) 1-2%
  - Stearic acid or stearato
  - Graphite, BN, steatite

Typical composition of slurry

Components	Amounts (%)
PZT powder	65–70
Dispersant	1.25
Solvent	25
Plasticizer	1.75
Binder	2

TABLE 23.3 Examples of Compositions of Extruded Bodies (Composition in vol%)

Refractory alumina		*High alumina*		*Electrical porcelain*	
Alumina (<20 µm)	50	Alumina (<20 µm)	46	Quartz (<44 µm)	16
Hydroxyethyl cellulose	6	Ball clay	4	Feldspar (<44 µm)	16
Water	44	Methylcellulose	2	Kaolin	16
$AlCl_3$ (pH > 8.5)	<1	Water	48	Ball clay	16
		$MgCl_2$	<1	Water	36
				$CaCl_2$	<1

TABLE 23.4 Additives for Injection Molding of SiC

Function	*Example*	*Quantity (wt%)*	*Volatilization temperature*
Thermoplastic resin	Ethyl cellulose Polyethylene Polyethylene glycol	9–17	200–400°C
Wax or high-temperature volatilizing oil	Paraffin Mineral oils Vegetable oils	2–3.5	150–190°C
Low-temperature volatilizing hydrocarbon or oil	Animal oils Vegetable oils Mineral oils	4.5–8.5	50–150°C
Lubricant or mold release	Fatty acids Fatty alcohols Fatty esters	1–3	
Thermosetting resin	Epoxy Polyphenylene Phenol formaldehyde		Gives carbon 450–1000°C

Uuniaxial pressing

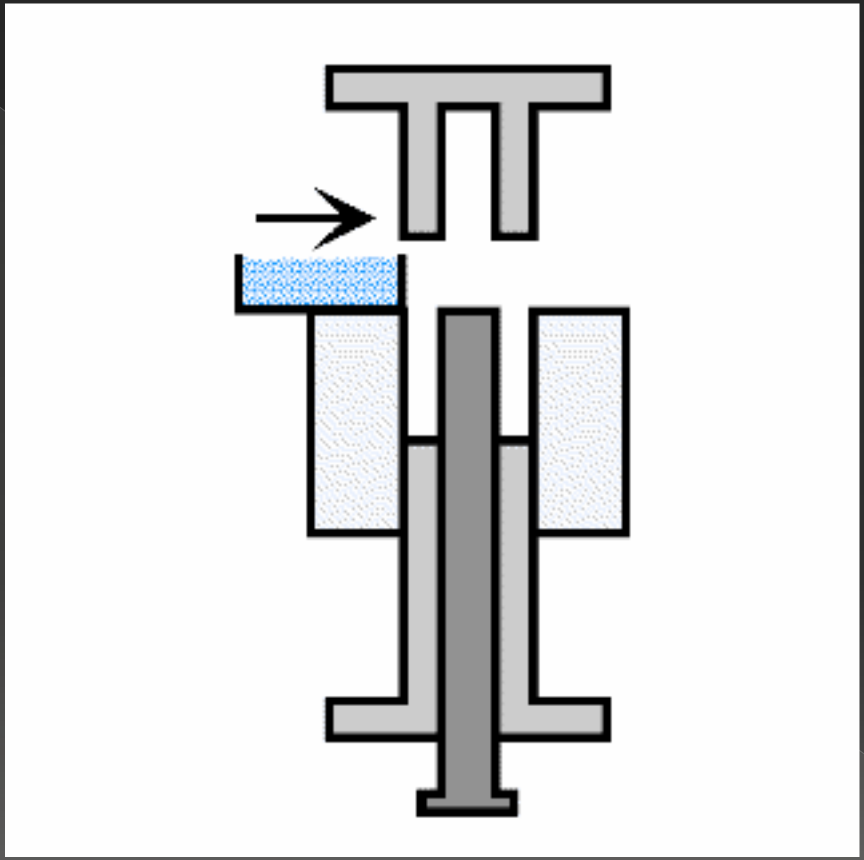

https://www.youtube.com/watch?v=WuxRkt_icso

Cold Isostatic Pressing

Animation

Animation 2

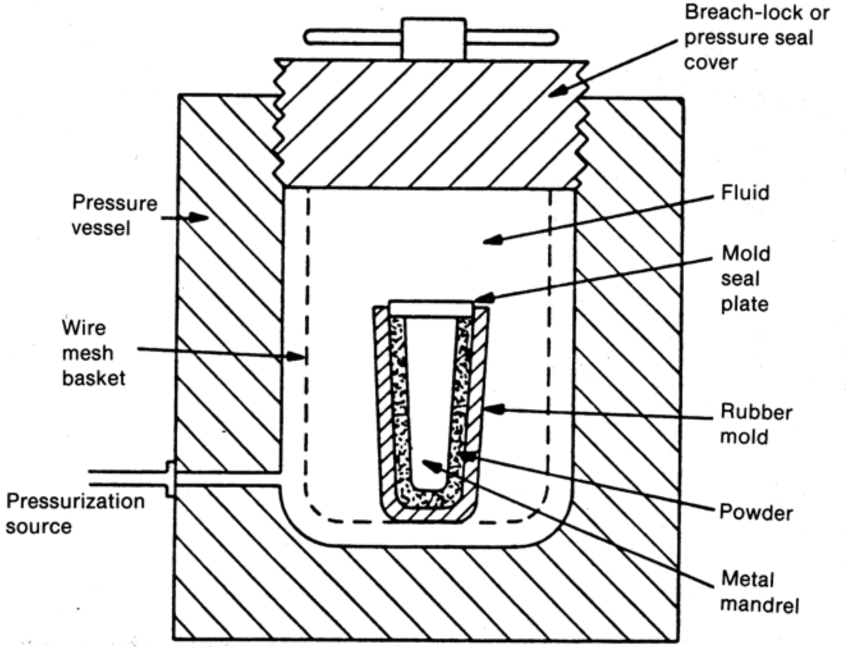

Figure 10.18 Schematic of a wet-bag isostatic pressing system. (© ASM International.)

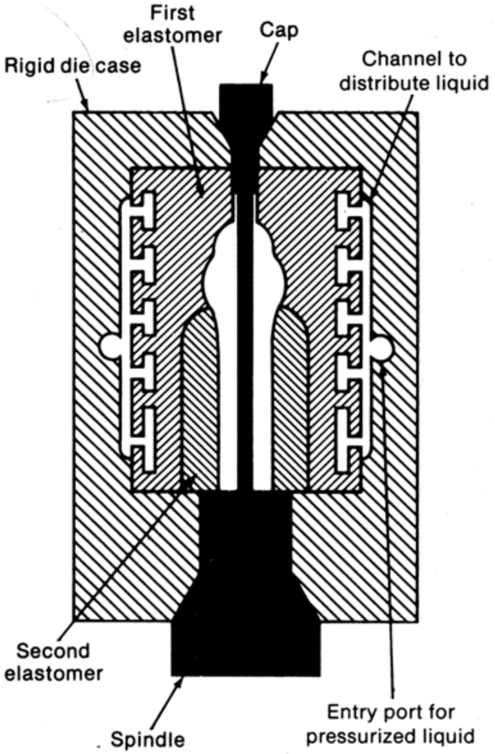

Figure 10.19 Schematic of a die for dry-bag isostatic pressing of a spark plug insulator. (© ASM International.)

Uniaxial hot press

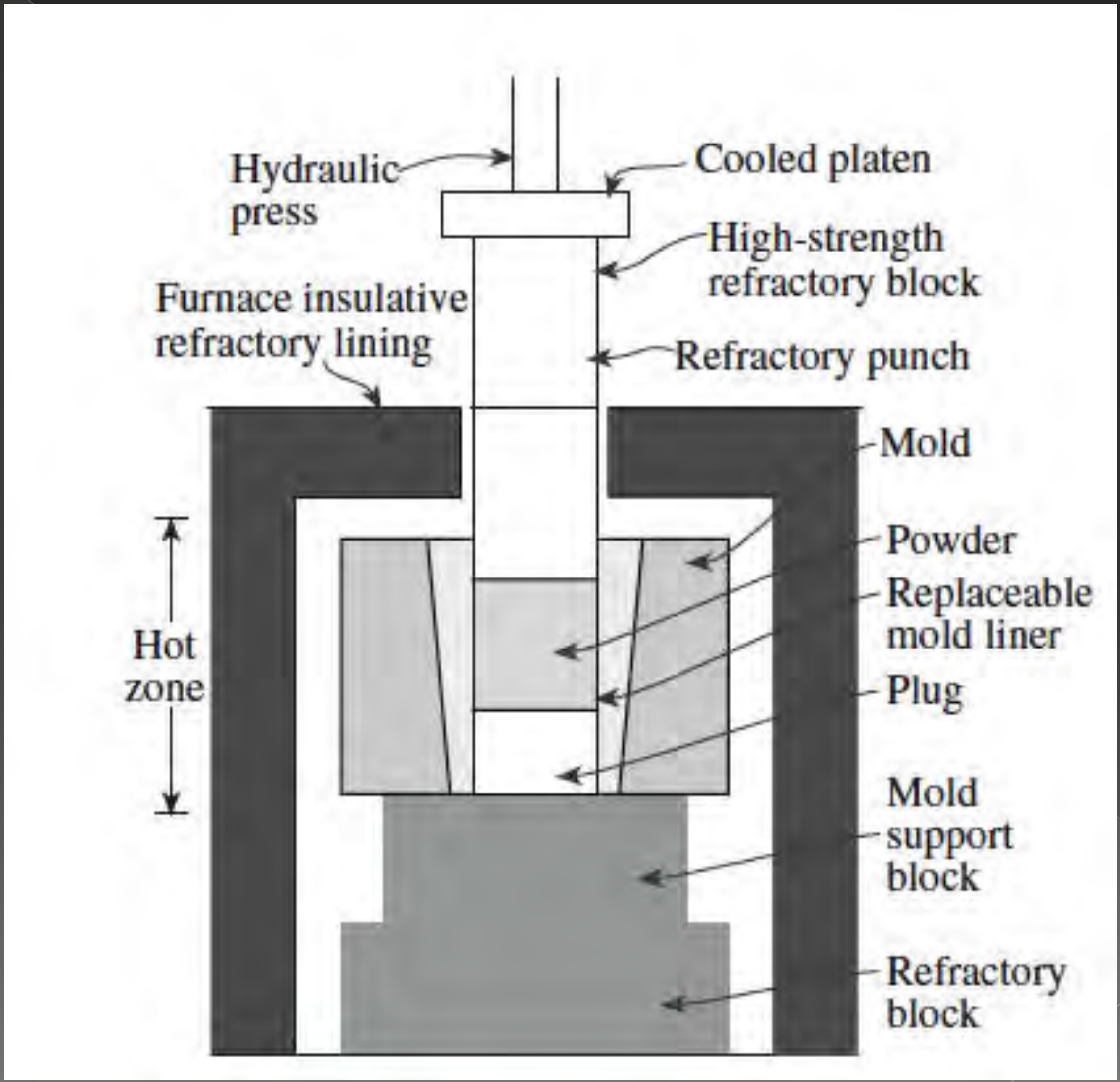

Isostatic Hot press

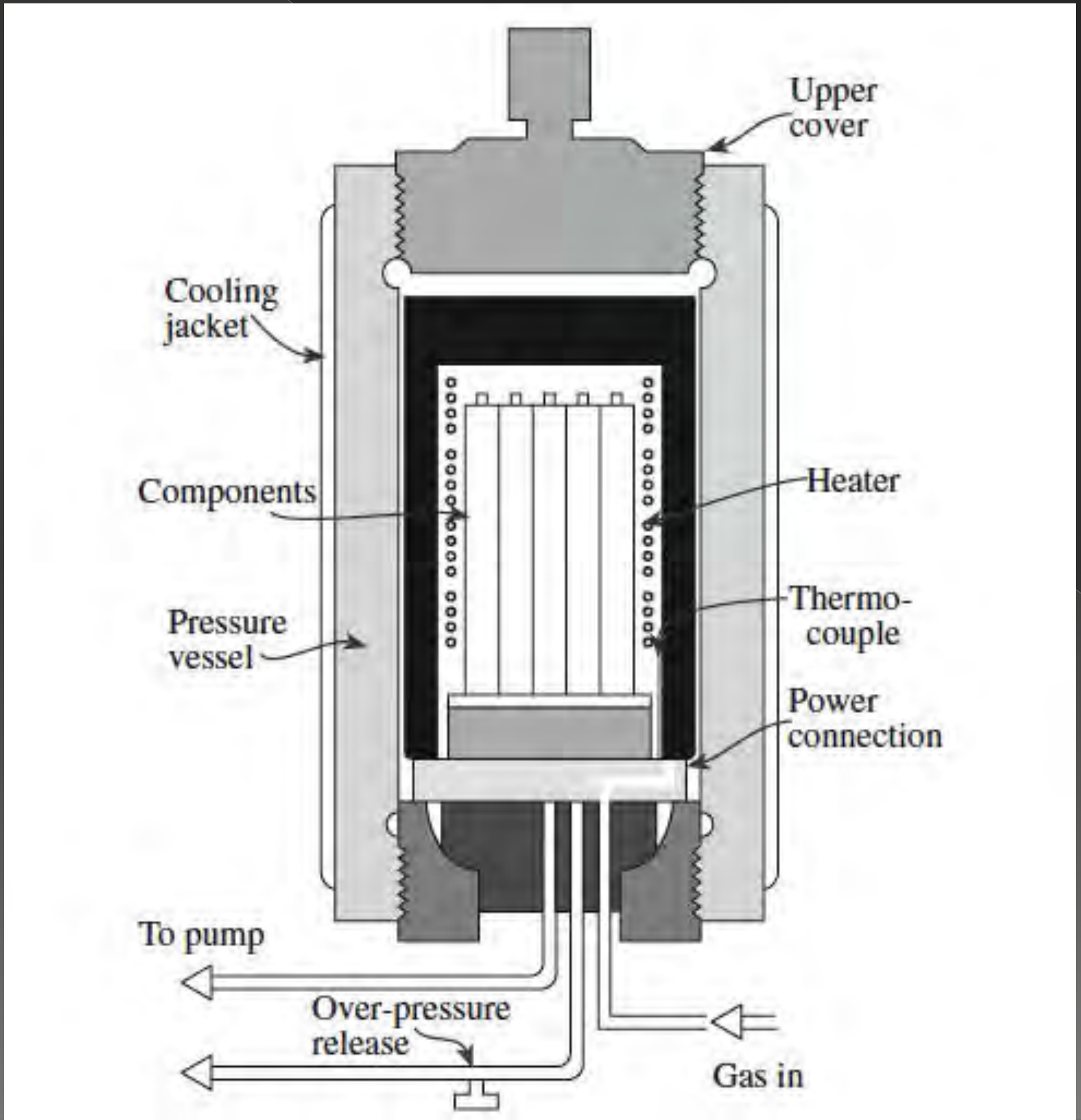

video

Drain Casting

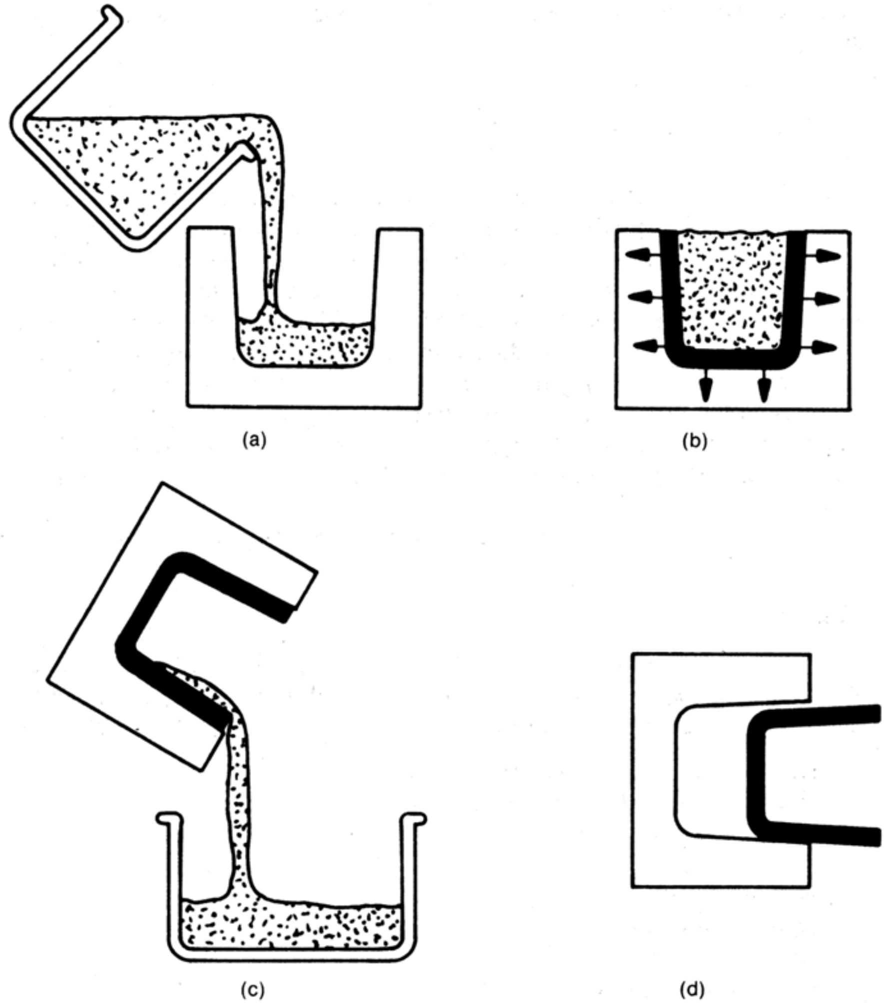

Figure 10.34 Schematic illustrating the drain-casting process. (a) Fill mold with slip, (b) mold extracts liquid, forms compact along mold walls, (c) excess slip drained, and (d) casting removed after partial drying.

Casting

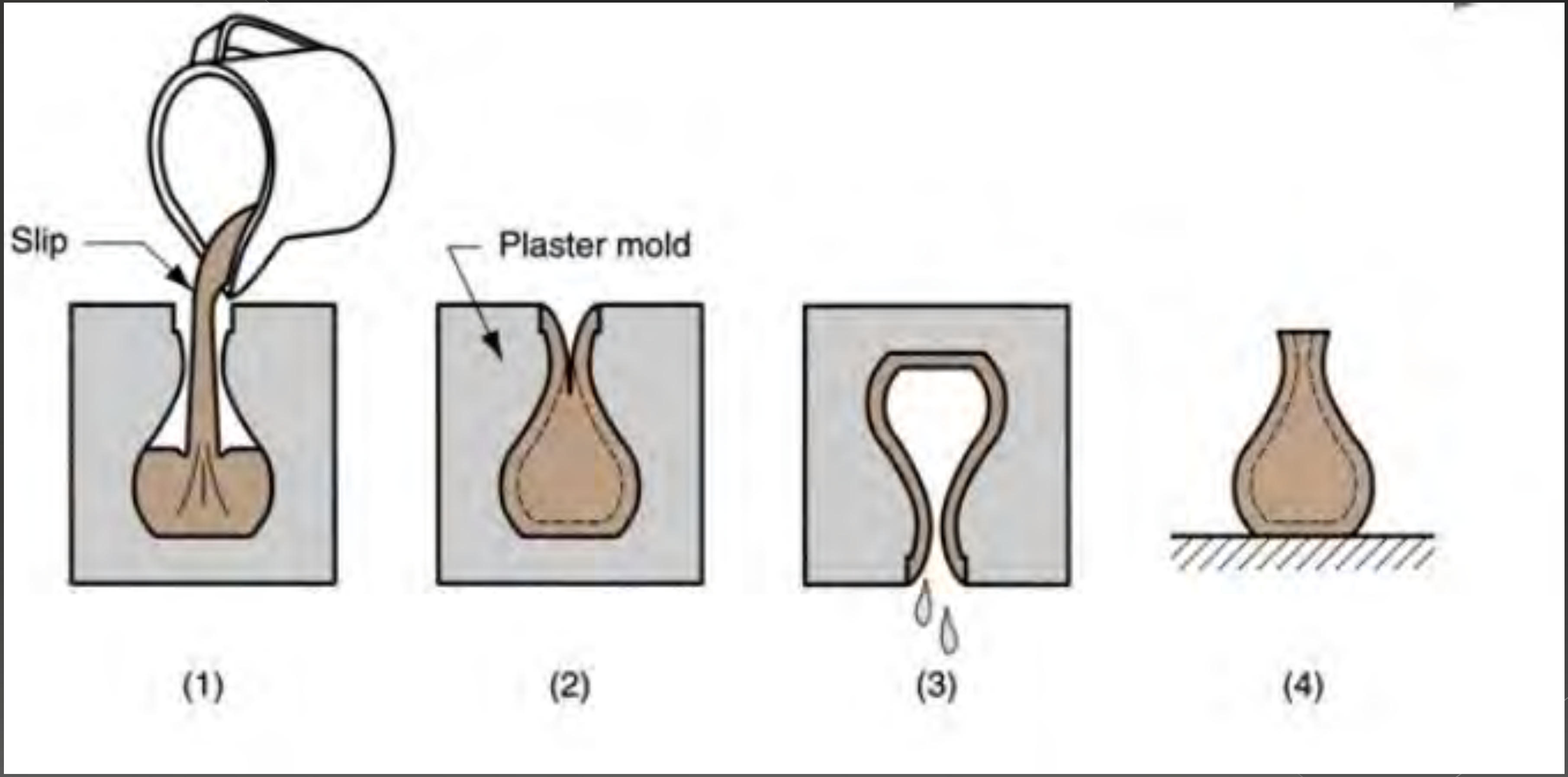

https://www.youtube.com/watch?v=FZzOTX9Ihqs

SLIP CASTING

Tape Casting

Fabrication process for thin ceramic sheets

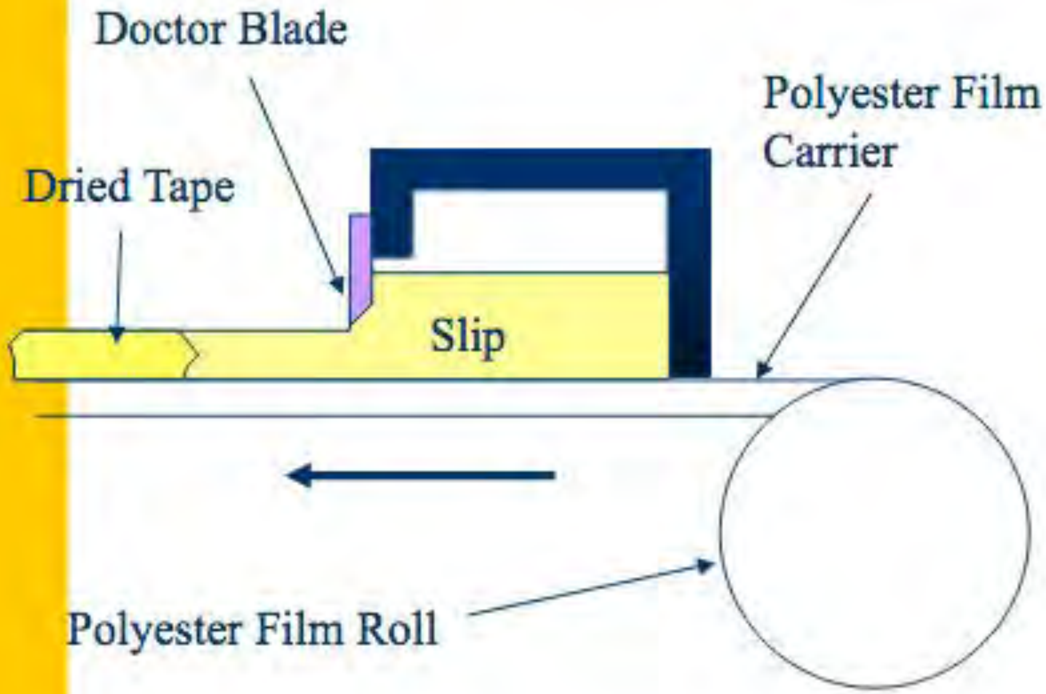

Presentazione Della Mea su Tape casting video

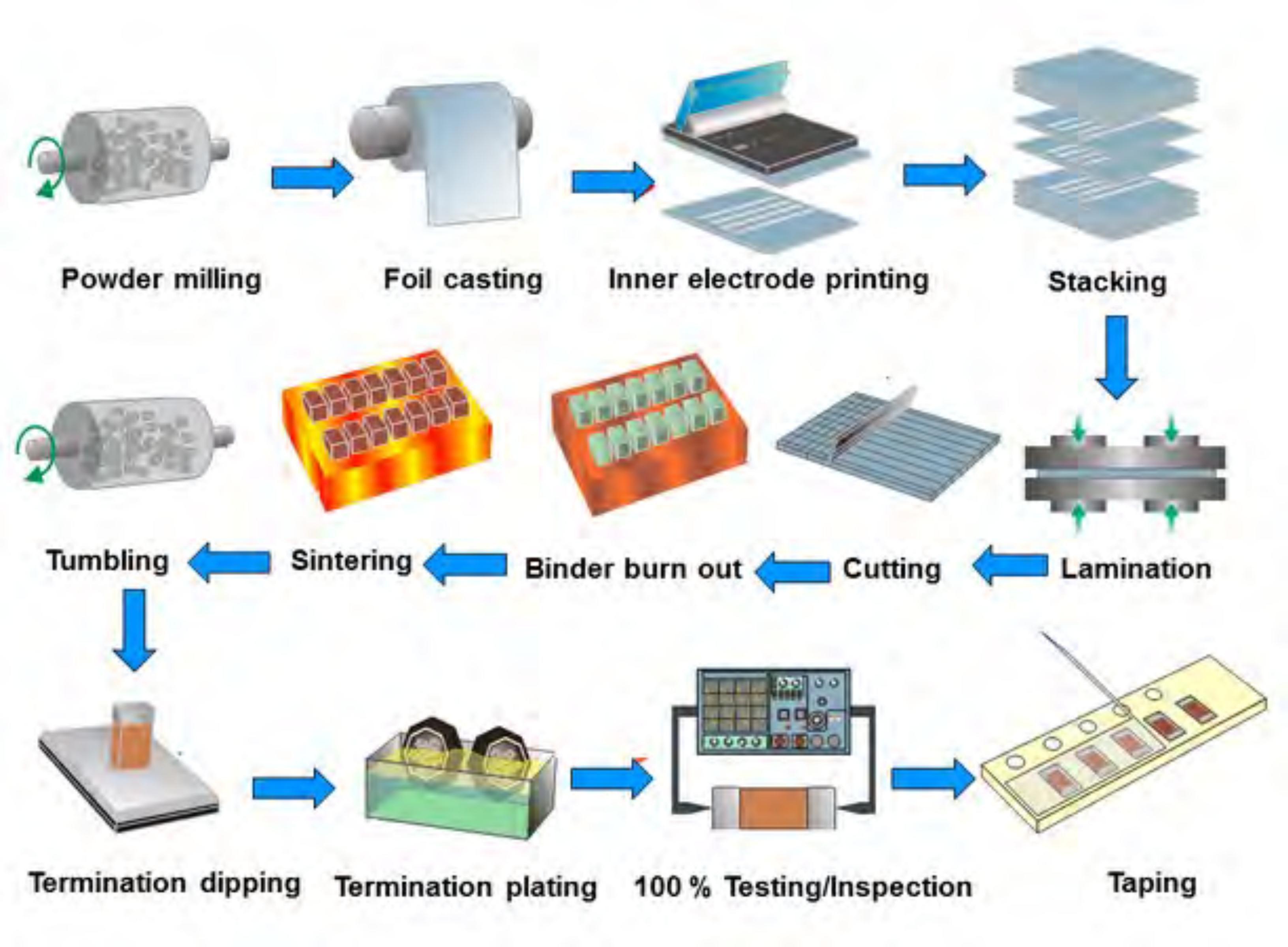

Powder milling
Foil casting
Inner electrode printing
Stacking
Lamination
Cutting
Binder burn out
Sintering
Tumbling
Termination dipping
Termination plating
100 % Testing/Inspection
Taping

Multilayer capacitors

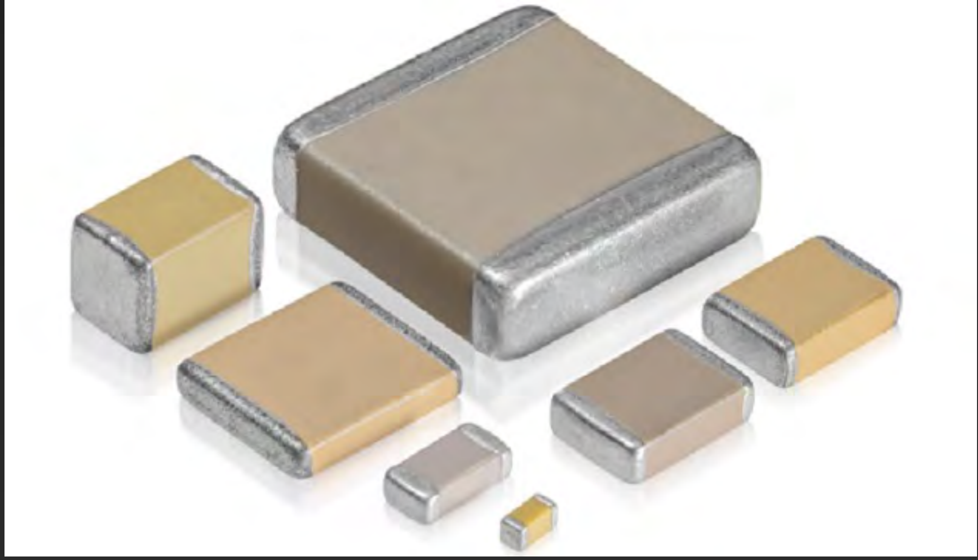

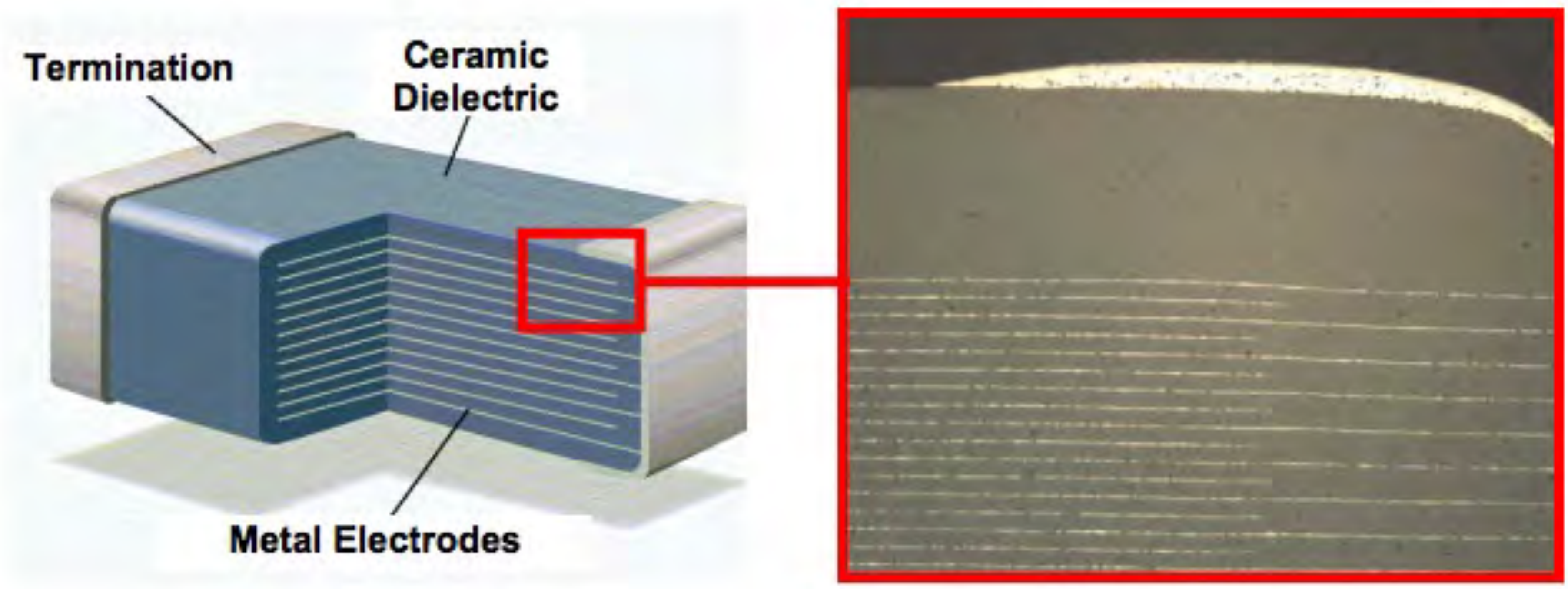

Figure 1: Cross-section of a multilayer ceramic chip capacitor (MLCC)

Extruder Sectional View

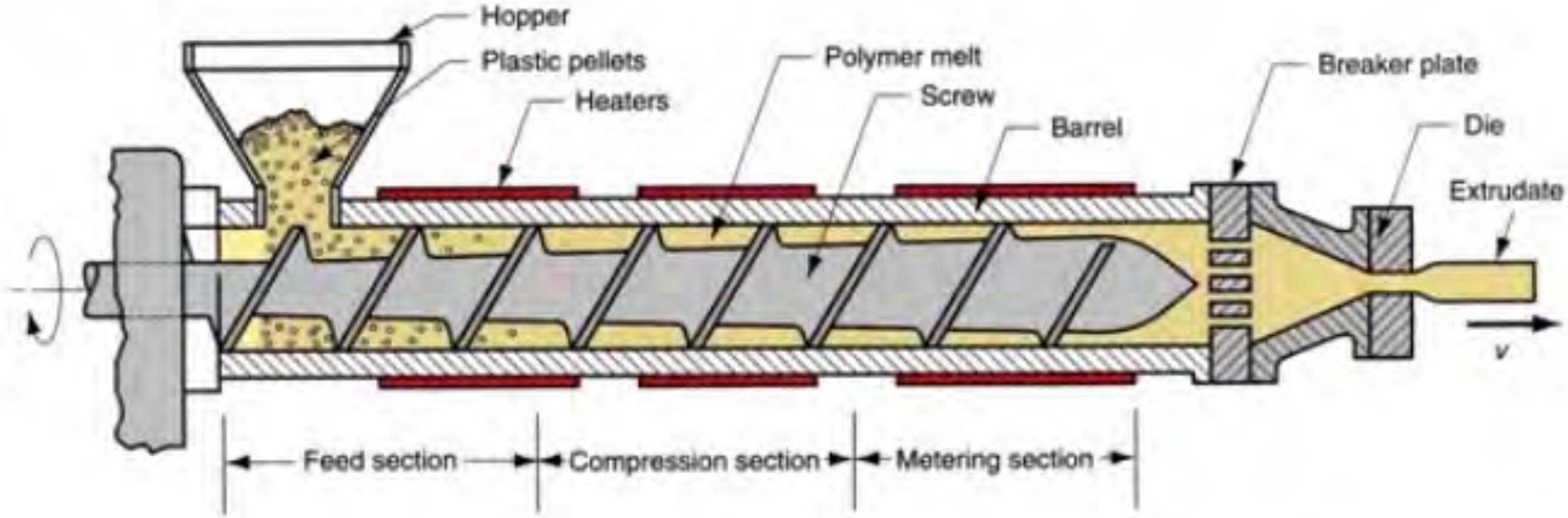

Components and features of a (single-screw) extruder for plastics and elastomers

https://www.youtube.com/watch?v=OqloeOubnmY

TABLE 23.3 Examples of Compositions of Extruded Bodies (Composition in vol%)

Refractory alumina		*High alumina*		*Electrical porcelain*	
Alumina (<20 µm)	50	Alumina (<20 µm)	46	Quartz (<44 µm)	16
Hydroxyethyl cellulose	6	Ball clay	4	Feldspar (<44 µm)	16
Water	44	Methylcellulose	2	Kaolin	16
$AlCl_3$ (pH > 8.5)	<1	Water	48	Ball clay	16
		$MgCl_2$	<1	Water	36
				$CaCl_2$	<1

Injection moulding

- https://www.youtube.com/watch?v=ohI7wVDa9Ww

Complexity vs productivity

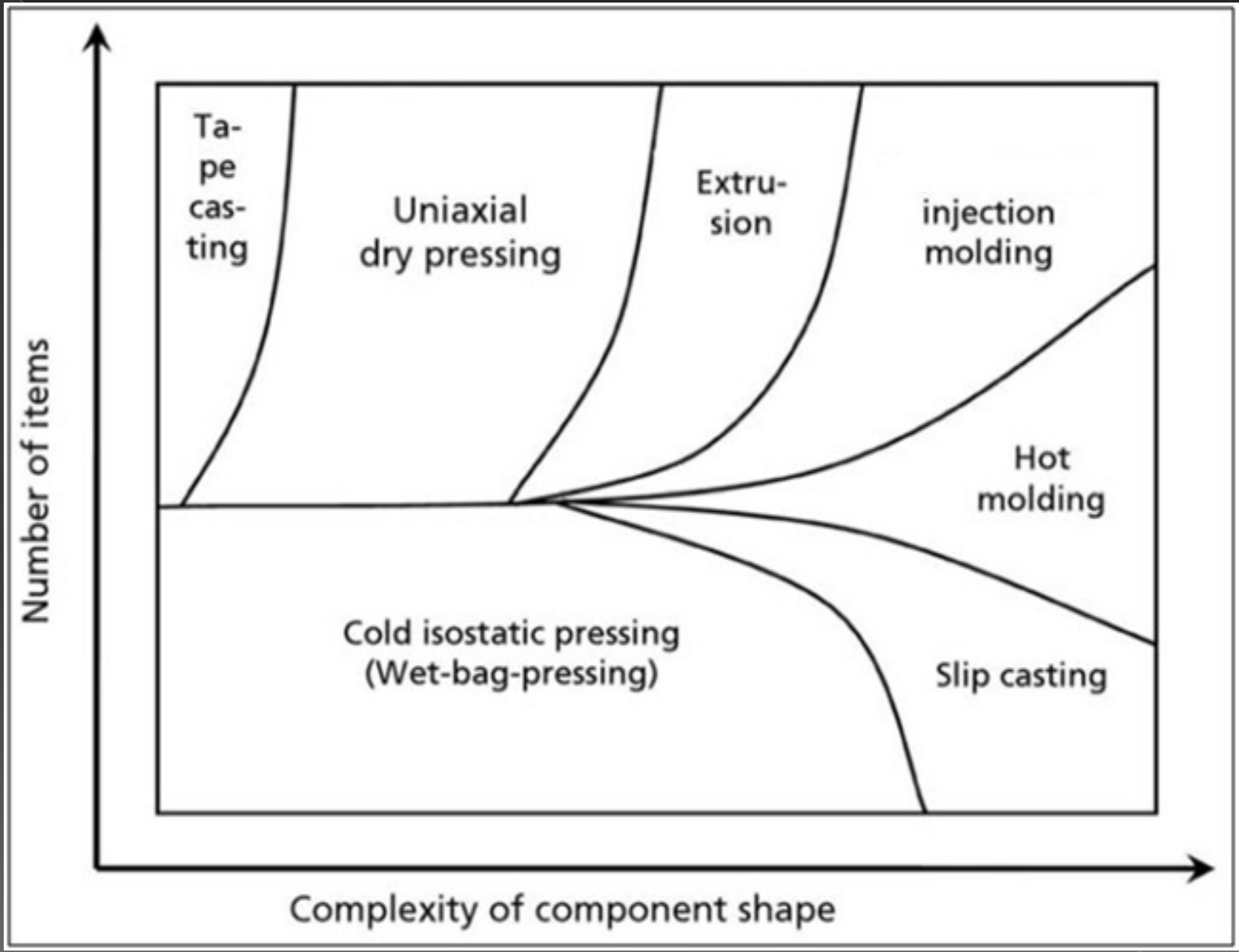

Additive Manufactoring

https://www.youtube.com/watch?v=yiUUZxp7b

Ceramic 3D printing

Ceramics 3D printing

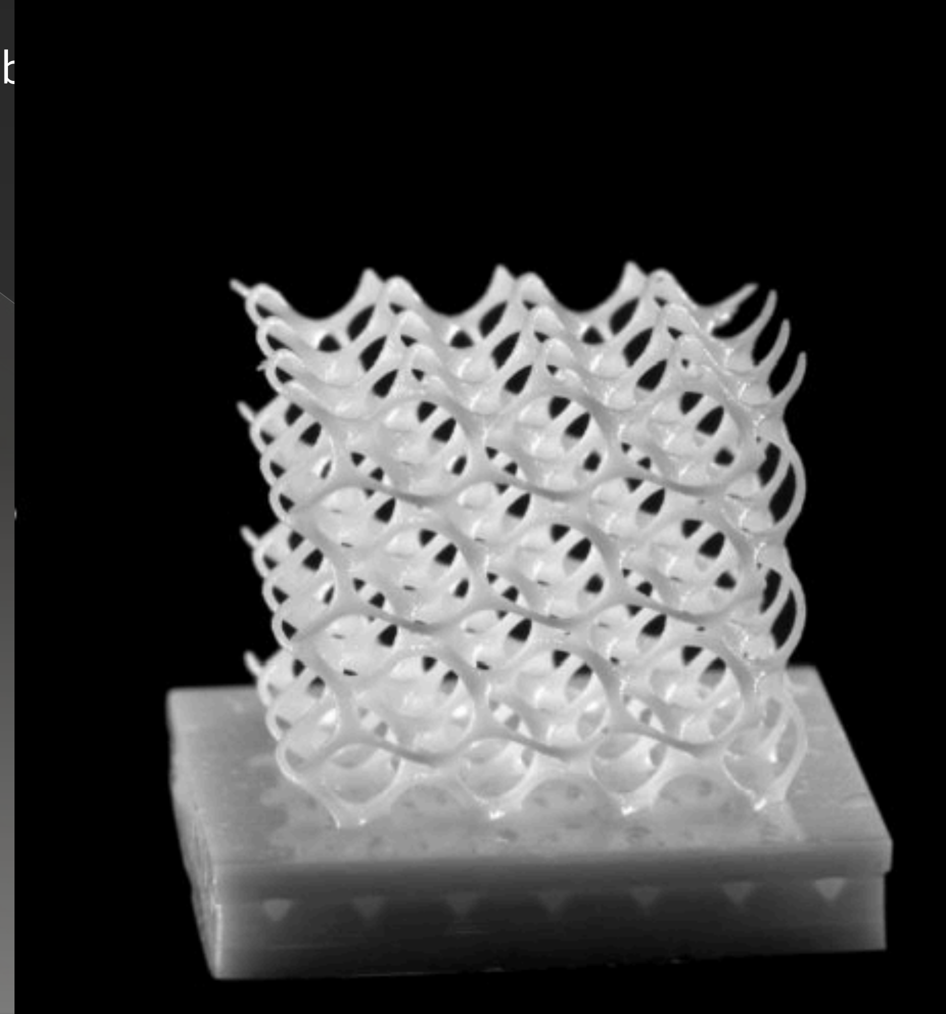

SINTERING PROCESS

Silvia Dalla Marta
(dal corso di Scienza e tecnologia dei materiali ceramici prof. V. Sergo)

It is a thermal process of microstructural rearrangement in which the particles of powder are compacted and the porosity decreases to form a dense piece of ceramic.

monodisperse powder fcc or hcp: PF=74.5%

ceramic matherial with porosity:
before sintering

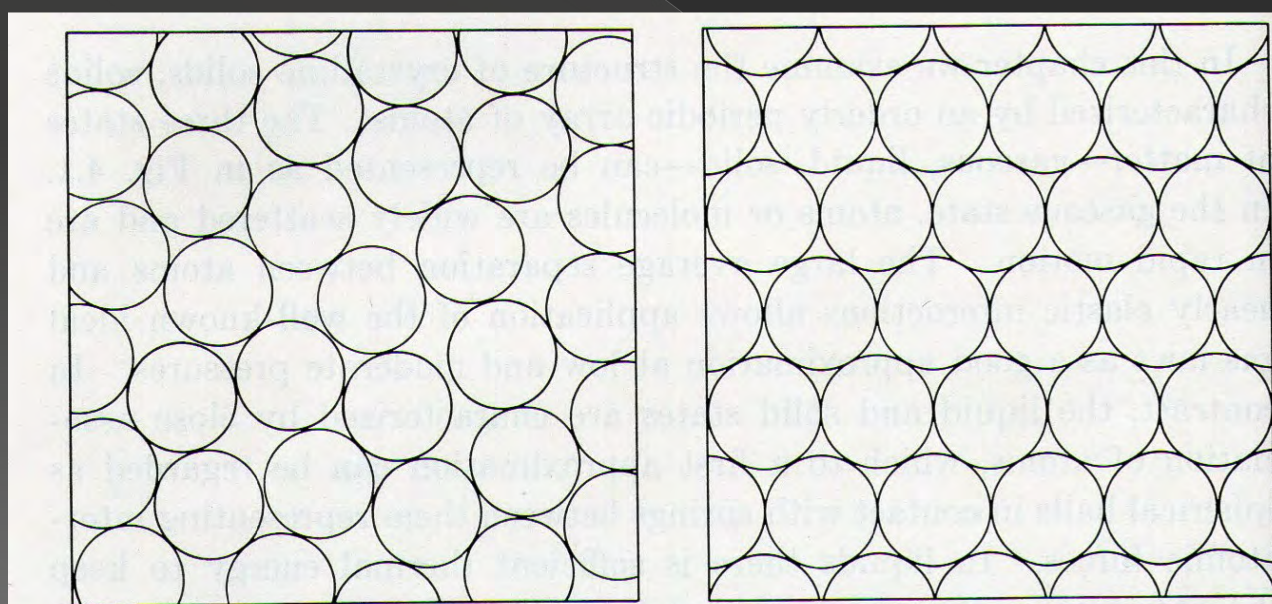

FORMATURE?

The absence of defects and porosity is very important for the *mechanical properties*:

$$K_{IC} = y\sigma\sqrt{c}$$

K: the parameter for the determination of the stress at the tip of the crack.
y: dimensionless constant that depends on defect's geometry and load
c: length of defect (m)

For the polycrystalline alumina: $K_{IC} = 3MPa\sqrt{m}$

In ceramics materials these values are very low compared to metals.
A very small defect or porosity lead to failure during an application of stress.

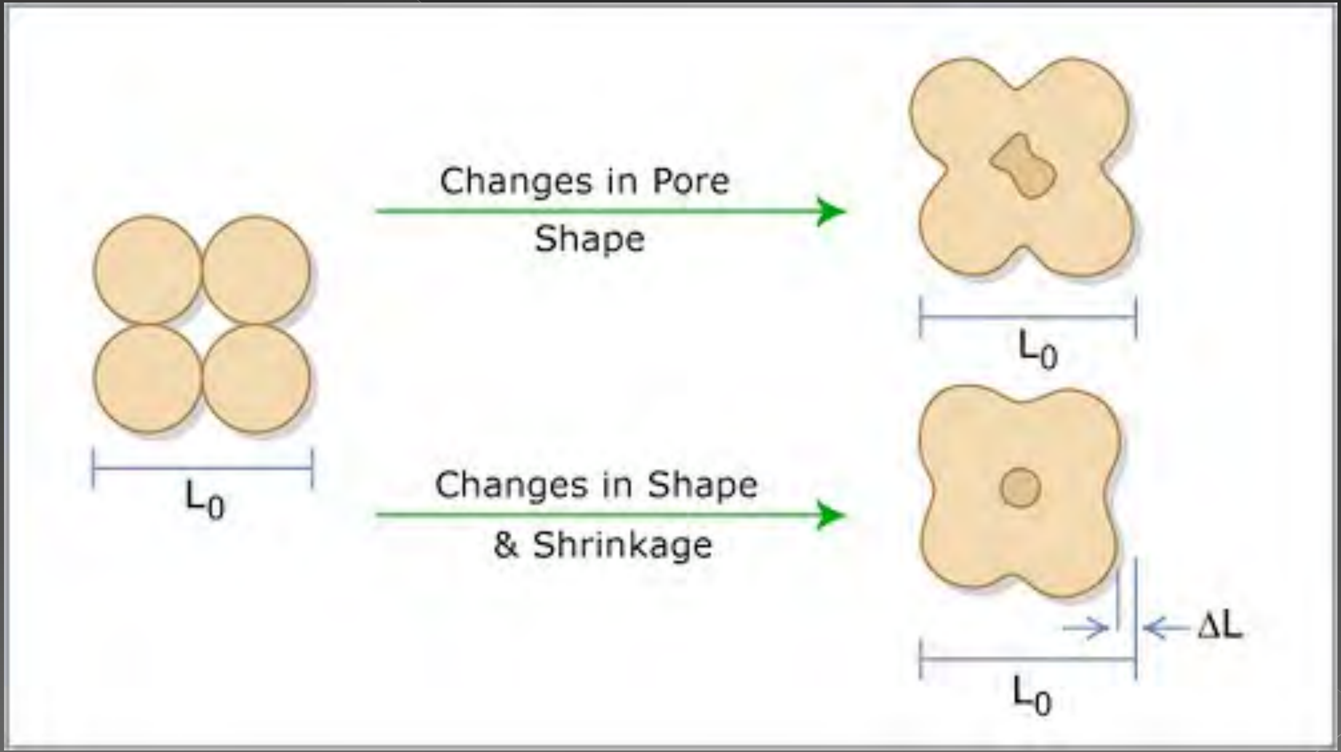

Changes in Pore
Shape
Changes in Shape
& Shrinkage
L_0
L_0
ΔL
L_0

BEFORE SINTERING:

- powder compact united by weaks Van der Waals forces
- individual grains separated by 25-60% of volume porosity

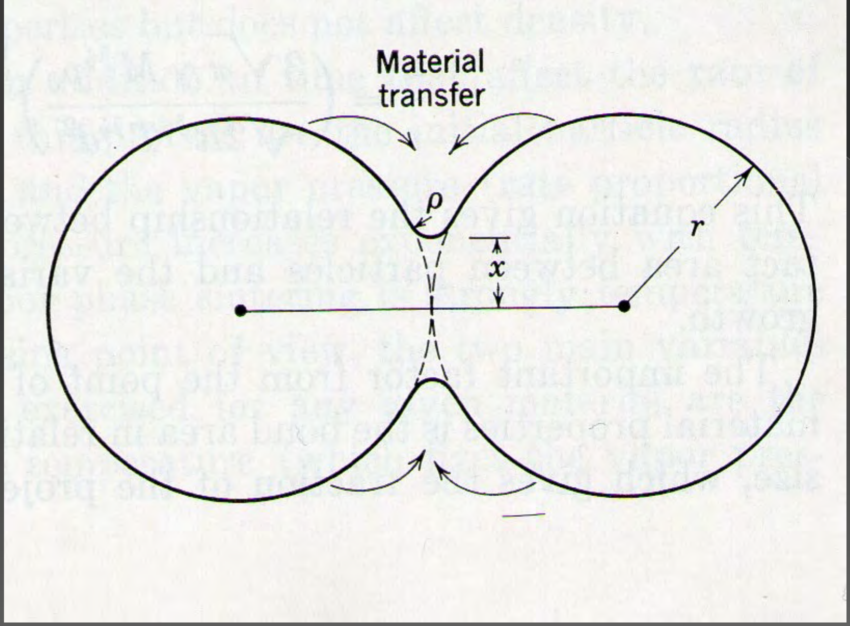

Considering two particles of ceramic material in contact with each other:

- concave zone
- convex zone

The atoms in a convex zone tend to *migrate* in a concave zone in according to a diffusion process actived by temperature.

DIFFUSION PROCESS

- Thermodinamically favored
- kinetically slow

FICK'S LAW (1D):

$$\frac{dC}{dt} = D\frac{d^2C}{dx^2}$$

Diffusion coefficient:

$$D = D_0 e^{-\frac{Ea}{RT}}$$

In order of kinetics to be fast enough for microstructural rearrangment to occur in *short time*, the sintering temperature must be:

$$T = \frac{2}{3}T_m$$

SINTERING MECHANISMS

- *SURFACE DIFFUSION*
- *VAPOR TRANSPORT*

↓

NO ***densification***

thinning of the particles

- *BULK DIFFUSION*
- *GRAIN BOUNDARY DIFFUSION*

↓

densification

decrease of the distance between particle centres

Thinning due to vapor phase matherial transfer:

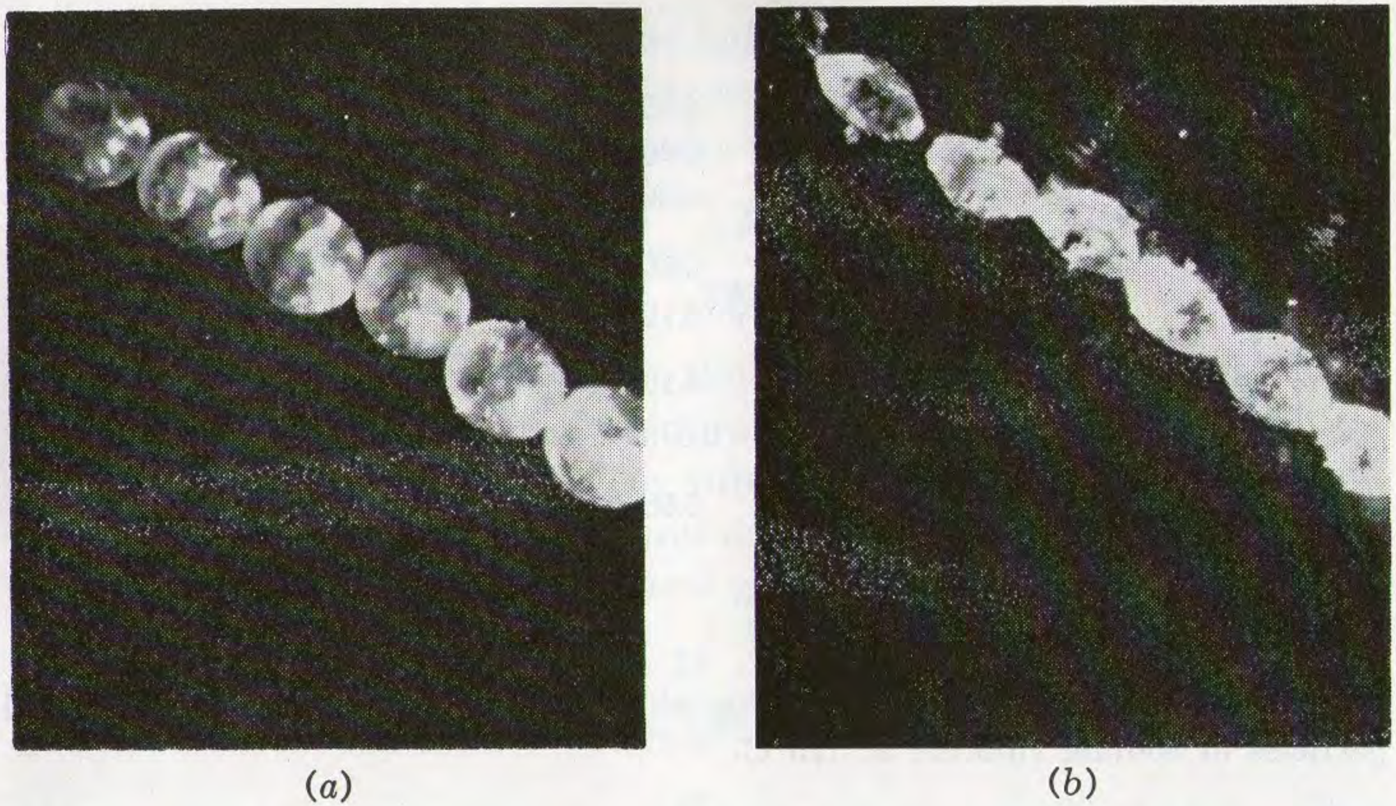

Fig. 12.17. Photomicrographs of sintering sodium chloride at 750°C: (*a*) 1 min, (*b*) 90 min.

DENSIFICATION:

- atoms migration in the neck zone
- pores disappearence
- obtaining straight grain boundaries
- same chemical potential
- thermodynamically stable

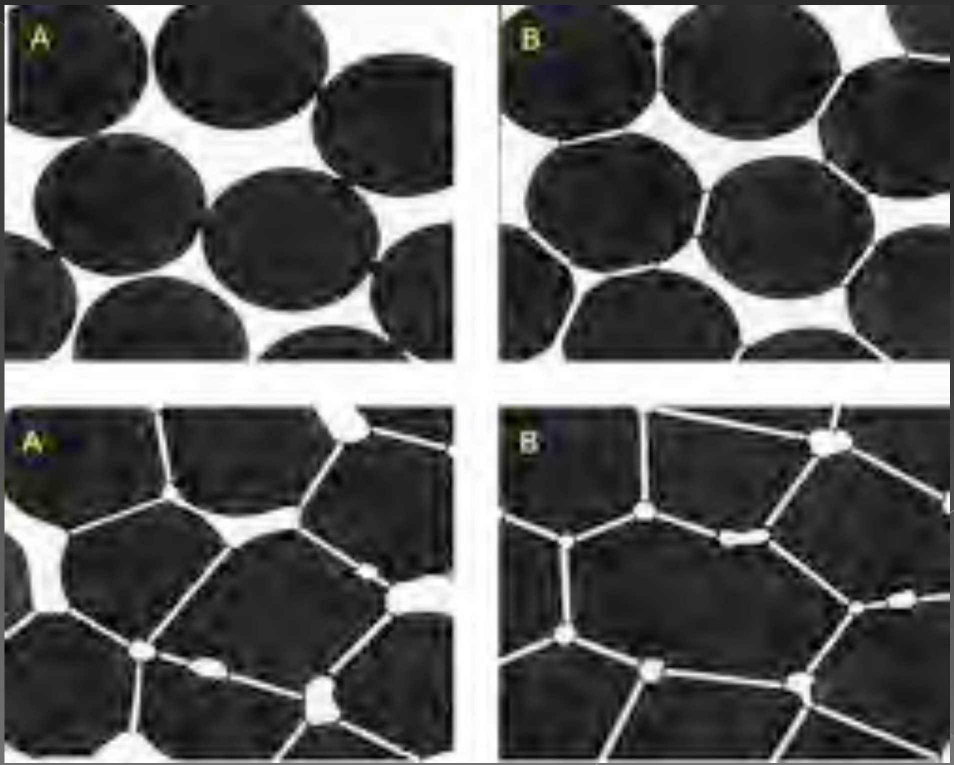

Monodispersed powder:
rare and expensive!

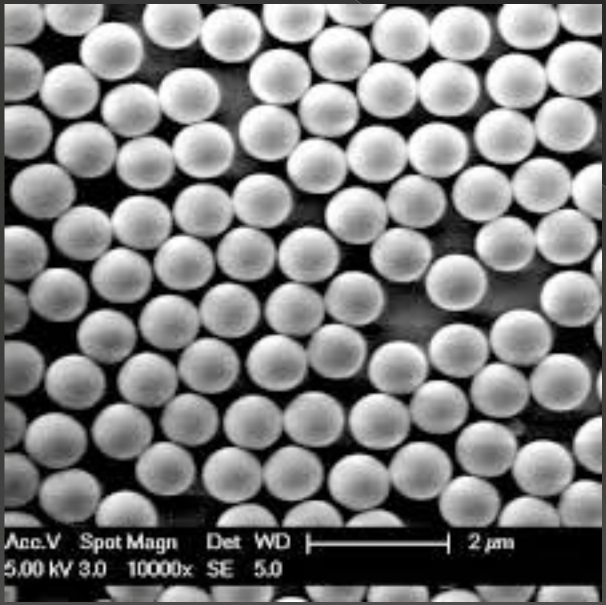

More frequent:
Grain size distribution!

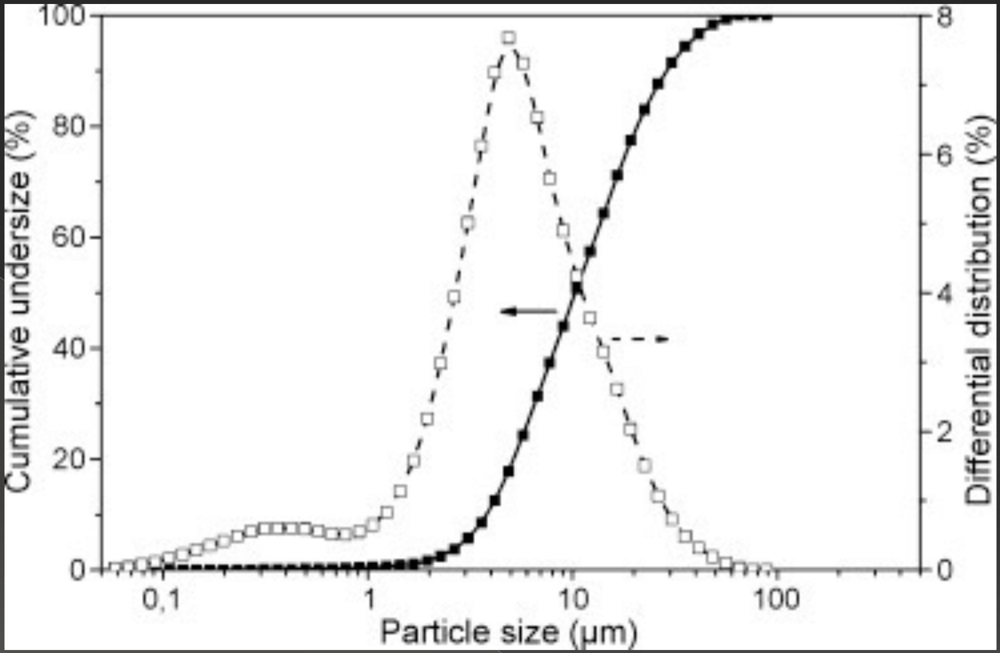

SECONDARY, ABNORMAL GRAIN GROWTH

Since grain boundaries migrate toward their centre of curvature,

grains with more than 6 sides tend to incorporate grains with less than 6 sides.

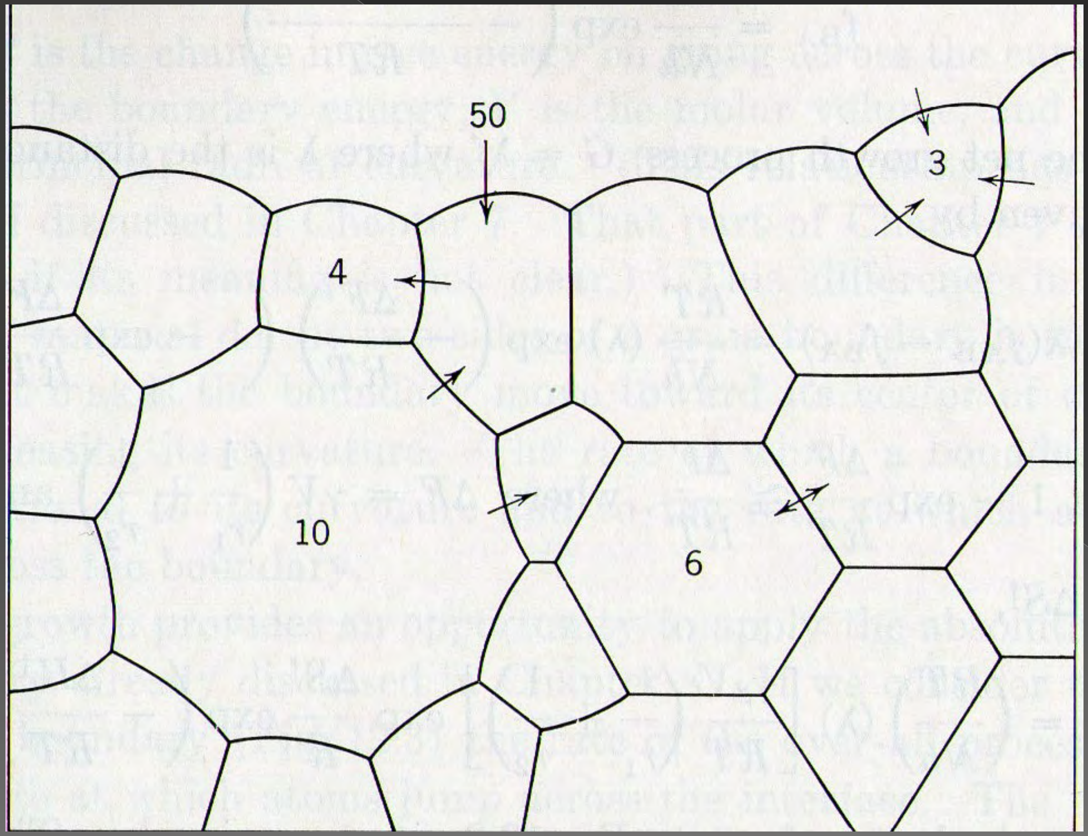

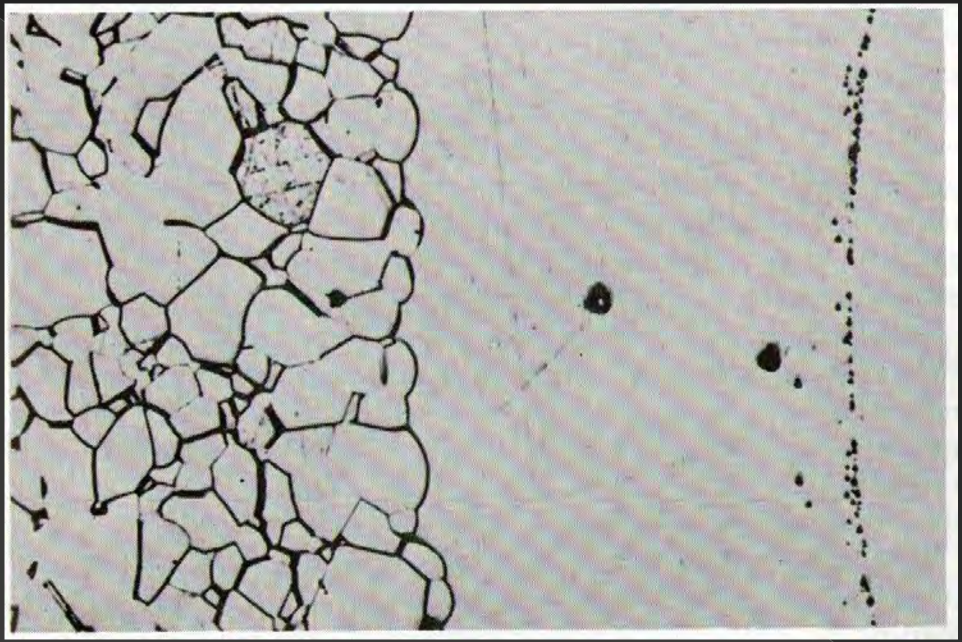

Growth of a large Al_2O_3 crystal into a matrix of uniformly sized grain.

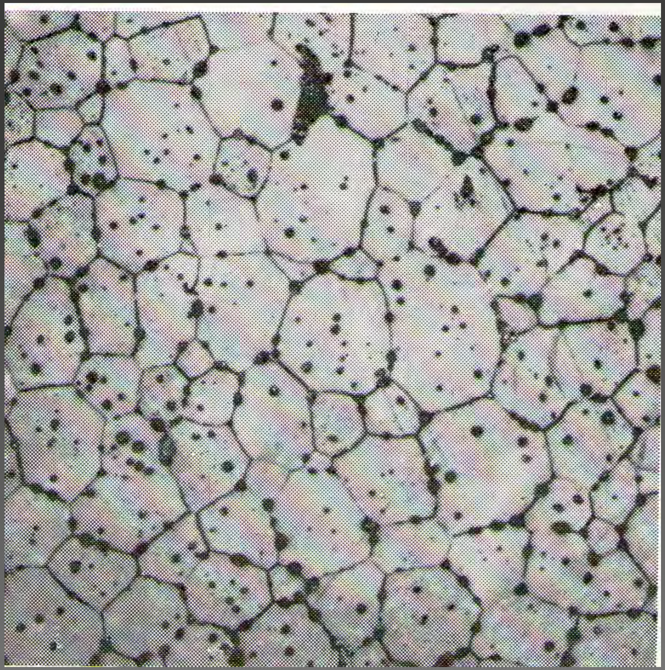

Polycrystalline flurite CaF_2 illustrating normal grain growth

PROGRESSIVE DEVELOPMENT OF MICROSTRUCTURE IN *LUCALOX ALUMINA*

a) SEM of initial particles befor sintering (5000x)

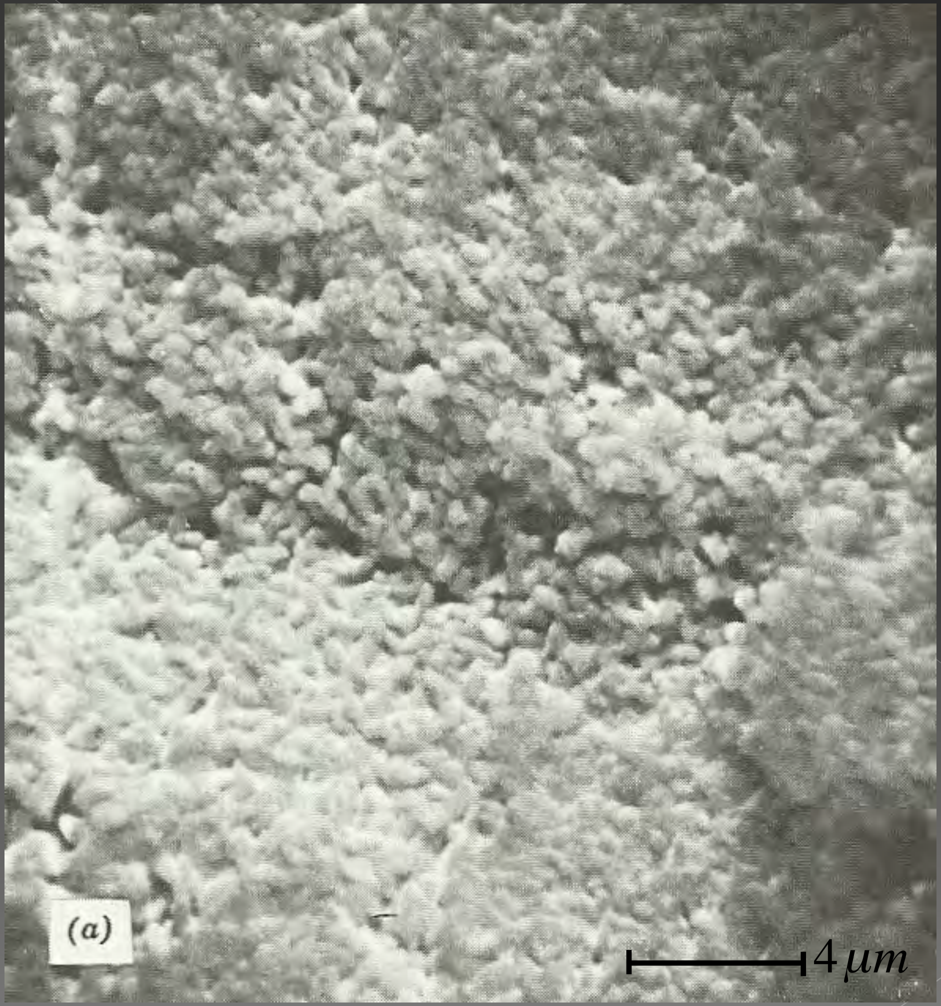

b) SEM of particles after 1 minute at 1700°C (5000x)

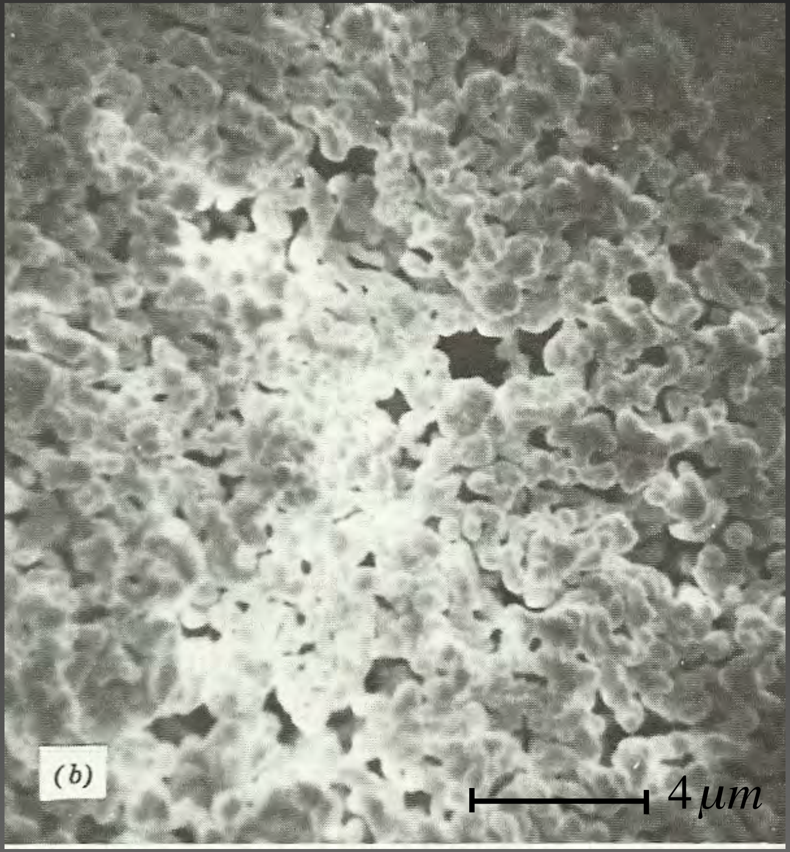

c) SEM of particles after 2 minutes at 1700°C (5000x)

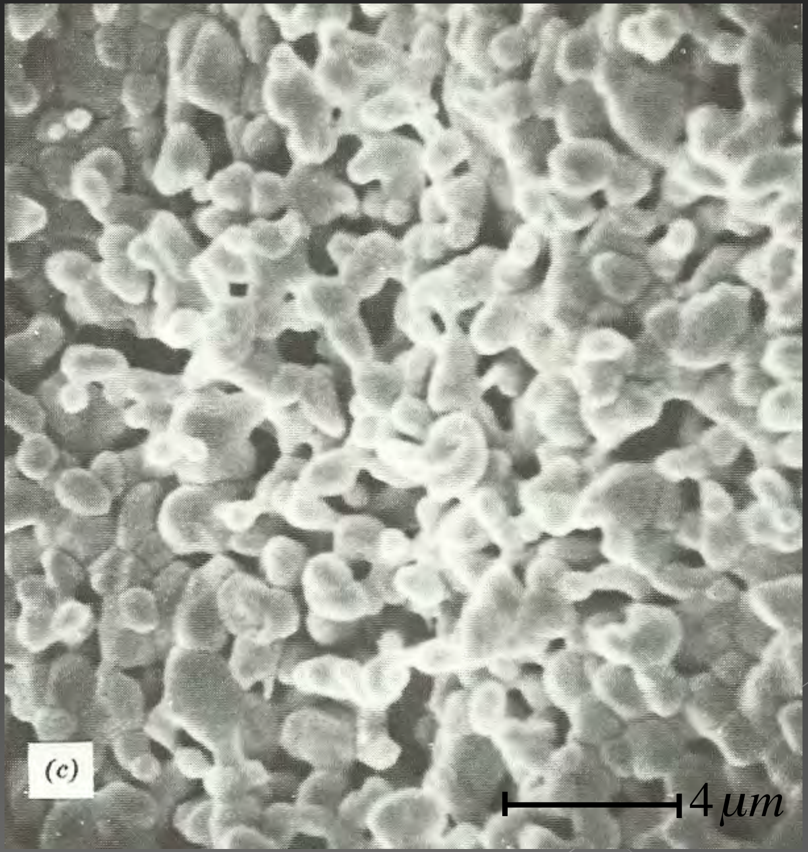

d) SEM of particles after 6 minutes at 1700°C (5000x)

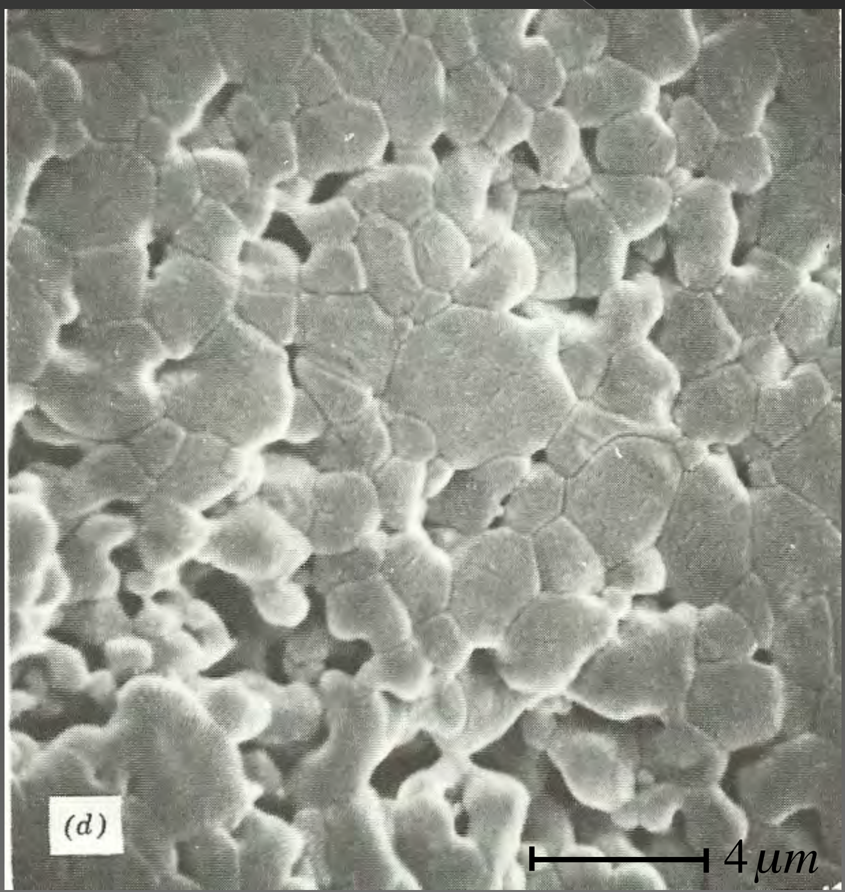

e) SEM of the final microstructure that is nearly porefree, with only a few pores located within grains (500x)

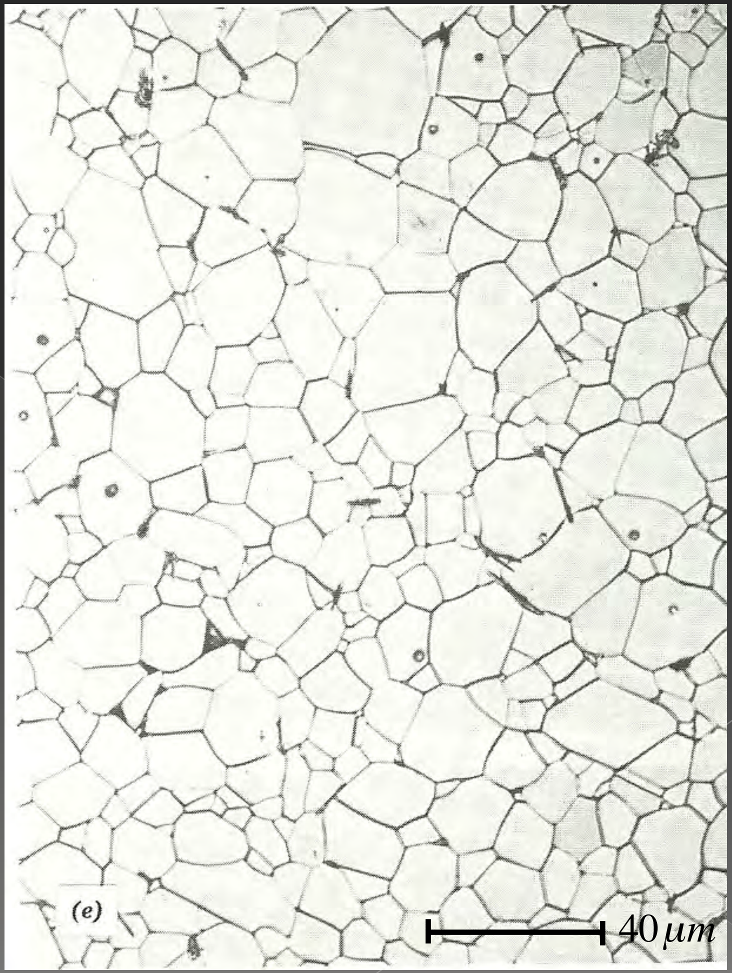

PRESSURE DIFFERENCE ACROSS A CURVED SURFACE

- The differences in the curvature of surface, causes a *pressure difference* in the various part of system, that leads to atoms transport.
- At the surface of the particle there is a positive radius of curvature, so that the vapour pressure is larger than would be observed in a flat surface.
- At the junction between particles there is a NECK whith a small negative radius of curvatures and a vapour pressure lower than that for the particle itself.

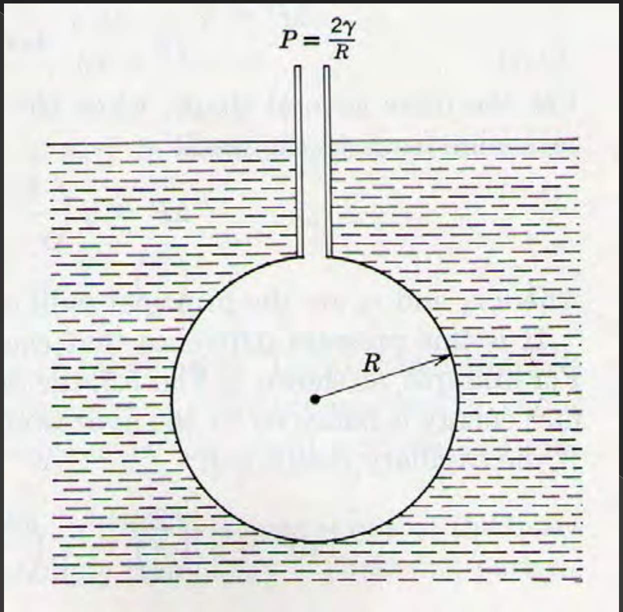

P : Supplementary pressure to create the bubble.

γ: surface tension

SPHERICAL MODEL:

$$A = 4\pi R^2 \qquad V = \frac{4}{3}\pi R^3$$

$$pdV = \gamma_{LV} dA$$

$$\Delta p 4\pi R^2 dR = \gamma_{LV} 8\pi R dR$$

$$\Delta p = \frac{2\gamma_{LV}}{R}$$

GENERICALLY:

$$\Delta p = \gamma_{LV}\left(\frac{1}{R_1} + \frac{1}{R_2}\right)$$

$$H_2O(l) \rightleftharpoons H_2O(g)$$

in equilibrium condition

$$p^\circ = K_e = e^{-\frac{\Delta G^0}{RT}}$$

vapour pressure of water
in a flat liquid-vapour interface

If the liquid-vapour interface is not flat, as in a small drops, the water has a vapour pressure that is larger than that in a flat surface:

$$e^{-\frac{\Delta G}{RT}} = e^{-\frac{\Delta G^0}{RT}} e^{-\frac{\overline{V}\Delta P}{RT}}$$

$$P_{H_2O} = P^0_{H_2O} e^{-\frac{2\gamma \overline{V}}{rRT}}$$

$P^0_{H_2O}$: standard vapour pression

Δp for water drops of different radii at STP

Droplet radius	1 mm	0.1 mm	1 μm	10 nm
Δp (atm)	0.0014	0.0144	1.436	143.6

ENERGY SURFACE

in a densification process in which the only energy is given by radius of curvature:

$$\overline{V} = \frac{MW}{\rho}$$

$$N = \frac{3MW}{4\pi a^3 \rho} = \frac{3\overline{V}}{4\pi a^3}$$

$$S_A = 4\pi a^2 N = \frac{4\pi a^2 3MW}{4\pi a^3 \rho} = 3\frac{\overline{V}}{a}$$

$$E_S = S_A \gamma = \frac{3\overline{V}\gamma}{a}$$

$\overline{V}$	: molecular volume	$\frac{cm^3}{mol}$
ρ	: density	$\frac{g}{cm^3}$
a	: particle radius	$\approx \mu m$
N	: number of particles in a mole of powder	
S_A	: surface area	m^2
E_S	:surface energy	$\frac{J}{mol}$
γ	: surface tension	$\approx 1\frac{J}{m^2}$
MW	: molecular weight	$\frac{g}{mol}$

- Energy available without added pressure in a sintering process of alumina:

$$E_S = \frac{3\bar{V}\gamma}{a} = 75\,\frac{J}{mol}$$

- Energy available with added pressure in the same sintering:

$$w = P_A\bar{V} = 750\,\frac{J}{mol}$$

$$P = 30\,Mpa$$

$$\bar{V}_{Al_2O_3} = 25\cdot 10^{-6}\,\frac{m^3}{mol}$$

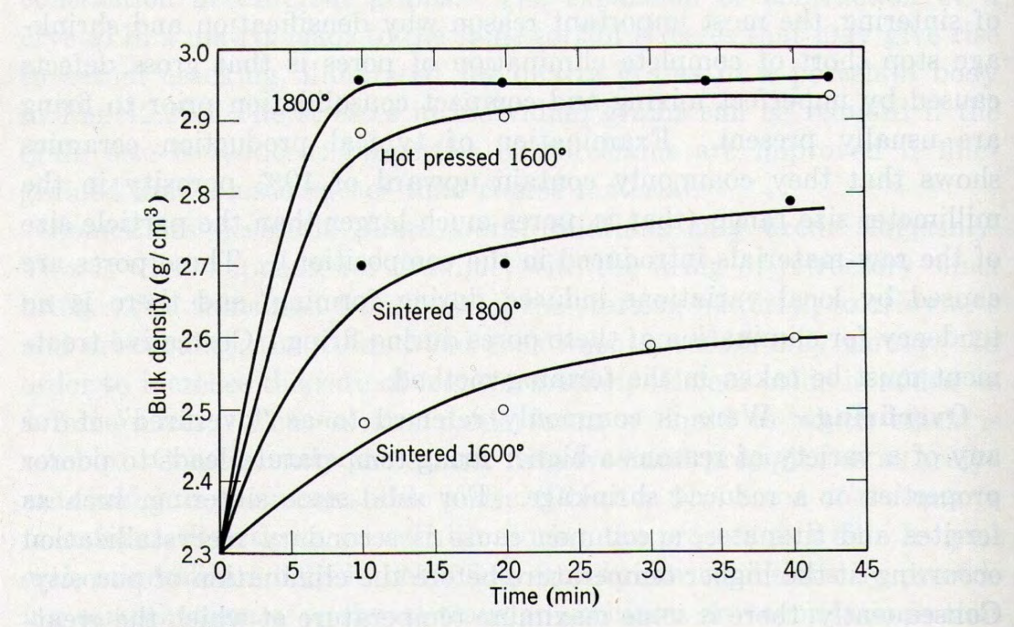

Fig. 12.30. Densification of beryllia by sintering and by hot pressing at 2000 psi.

Image from Kingery

DIFFUSION AND MOBILITY:

true in the absence of friction: $F = ma$

otherwise: $F = m\frac{dv}{dt} + \frac{v}{M}$

Einstein's generalized equation of mobility: $D = MRT$

$\frac{v}{M}$: friction coefficient

M : mobility

D : diffusion coefficient

KINETIC MODELING OF SINTERING PROCESS

PARAMETERS TO DEFINE THE MODEL:

- *define a DRIVING FORCE*
- *define the GEOMETRY*
- *define the MECHANISM OF TRANSPORT*

STAGES OF THE SINTERING:

- *INITIAL STAGE :* from 50-55% to 75% of TD ⟶ *MODELING*
- *INTERMEDIATE STAGE :* from 75% to 92% of TD
- *FINAL STAGE :* from 92% to 100% of TD

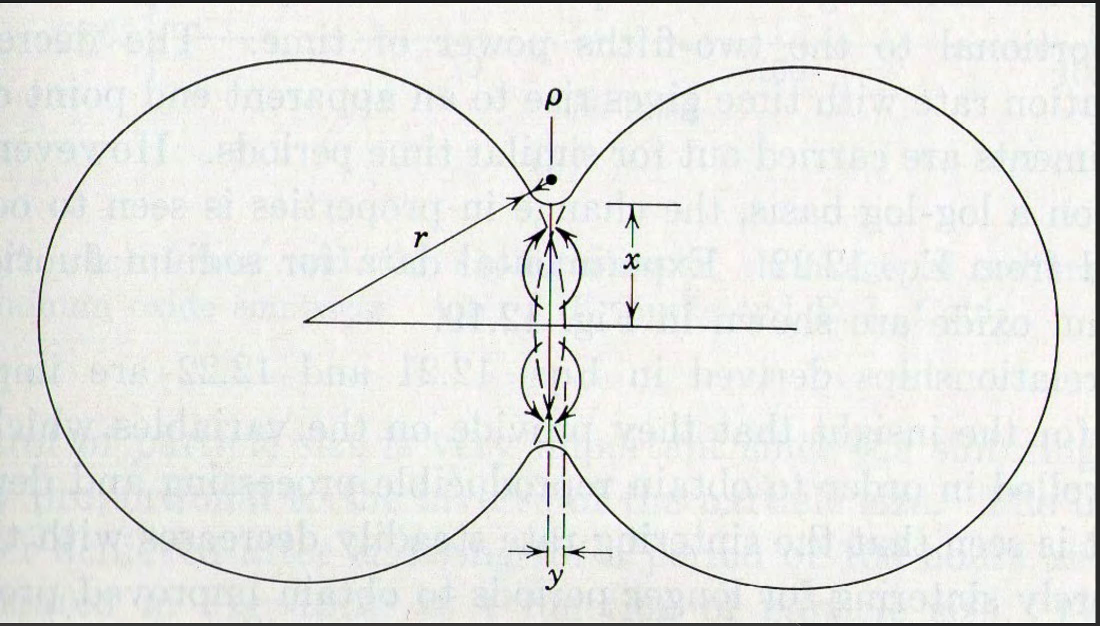

ρ : radius of the neck's curvature

r : radius of particle

x : parameter indicated the progress of the sintering

GEOMETRY

$$(r+\rho)^2 = (r-\rho)^2 + (x+\rho)^2$$

$$\rho = \frac{x^2}{4r}$$

$$A_{Neck} = 2\pi x \cdot \pi\rho = \frac{\pi^2 x^3}{2r}$$

$$V_{Neck} = \frac{\pi x^4}{8r}$$

Approximations :

$$\rho^2 = 0$$

$$x\rho = 0$$

FLUX

The material transfer is linked to the flux.
Considering the area through which the transport takes (the neck area):

$$J = \frac{1}{A_{Neck}} \frac{d}{MW} \frac{dV_{Neck}}{dt}$$

d : density
MW : molecoular weight
J : flux

$$\frac{dV_{Neck}}{dt} = \frac{4\pi x^3}{8r} \frac{dx}{dt} = \frac{\pi x^3}{2r} \frac{dx}{dt}$$

Variation of the neck volume based on the increase of the 'x' parameter:

$$J = \frac{2r}{\pi^2 x^3} \frac{d}{MW} \frac{\pi x^3}{2r} \frac{dx}{dt} = \frac{1}{\pi \bar{V}} \frac{dx}{dt}$$

FLUX expressed as a DRIVING RORCE

$$J = cMF$$

c : concentration

M : mobility of bulk and grain boundary atoms

F : force

$$M = \frac{D}{RT}$$

$J = cMF$

$$F = -\nabla G = -\frac{dG}{dx} \approx \frac{dG}{\rho}$$

Variation of the free energy during the diffusion on the neck area:

$$\Delta G = \Delta p\overline{V} = \overline{V}\gamma\left(\frac{1}{r_1} + \frac{1}{r_2}\right) = \overline{V}\gamma\left(\frac{1}{x} - \frac{1}{\rho}\right) = \frac{\overline{V}\gamma}{\rho}$$

$$F = \frac{\Delta G}{\rho} = \frac{\overline{V}\gamma}{\rho^2}$$

$$J = cMF = c\frac{D}{RT}\frac{\overline{V}\gamma}{\rho^2}$$

$$\frac{1}{\overline{V}\pi}\frac{dx}{dt} = \frac{cD}{RT}\frac{\overline{V}\gamma}{\frac{x^4}{16r^2}}$$

integration between o and x

t=o, x=o

$$\frac{1}{5}x^5 = \frac{5\pi\overline{V}^2 cD\gamma r^2}{RT}t$$

$$x = \left(\frac{5\pi\overline{V}^2 cD\gamma r^2}{RT}\right)^{\frac{1}{5}} t^{\frac{1}{5}}$$

t: sintering time

Variation of the volume of the particles in the sintering process during the time:

Variation of the relative density variatung time and temperature:

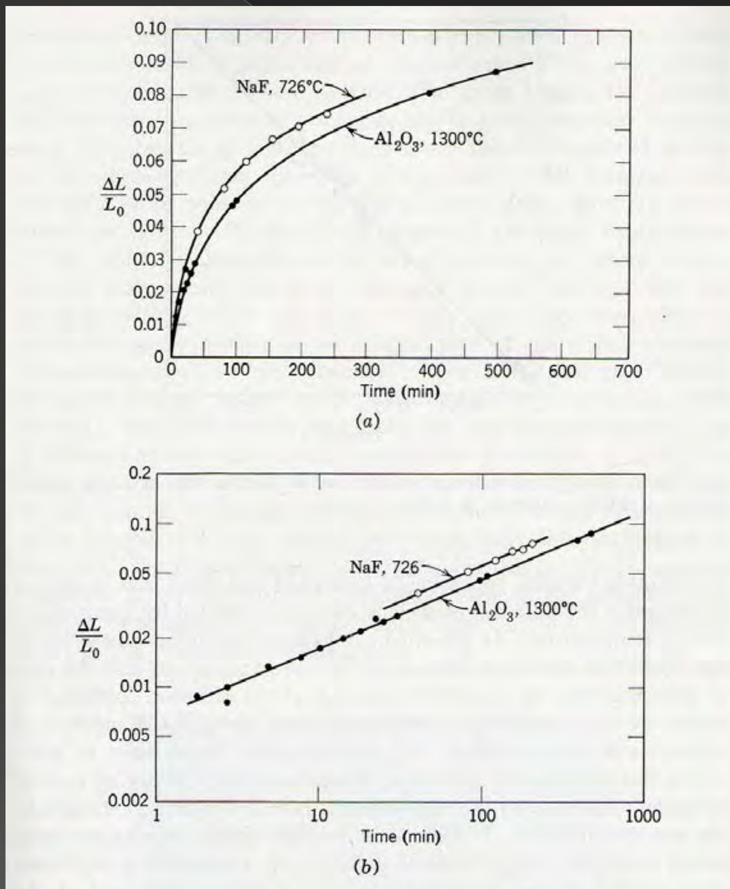

Fig. 12.19. (a) Linear and (b) log-log plots of shrinkage of sodium fluoride and aluminum oxide compacts. After J. E. Burke and R. L. Coble.

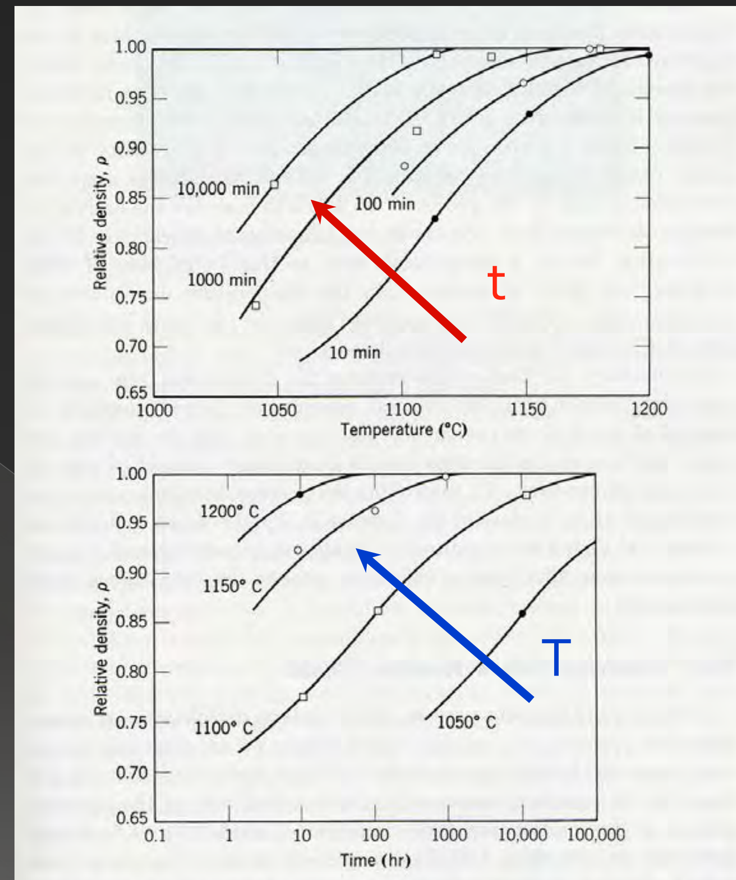

Fig. 12.25. Effect of time and temperature on the vitrification of a porcelain body. Data from F. H. Norton and F. B. Hodgdon, *J. Am. Ceram. Soc.*, **14**, 177 (1931).

The increase of a few degrees in temperature has much more influence on the grain size than the increase of a one order of magnitude of the time

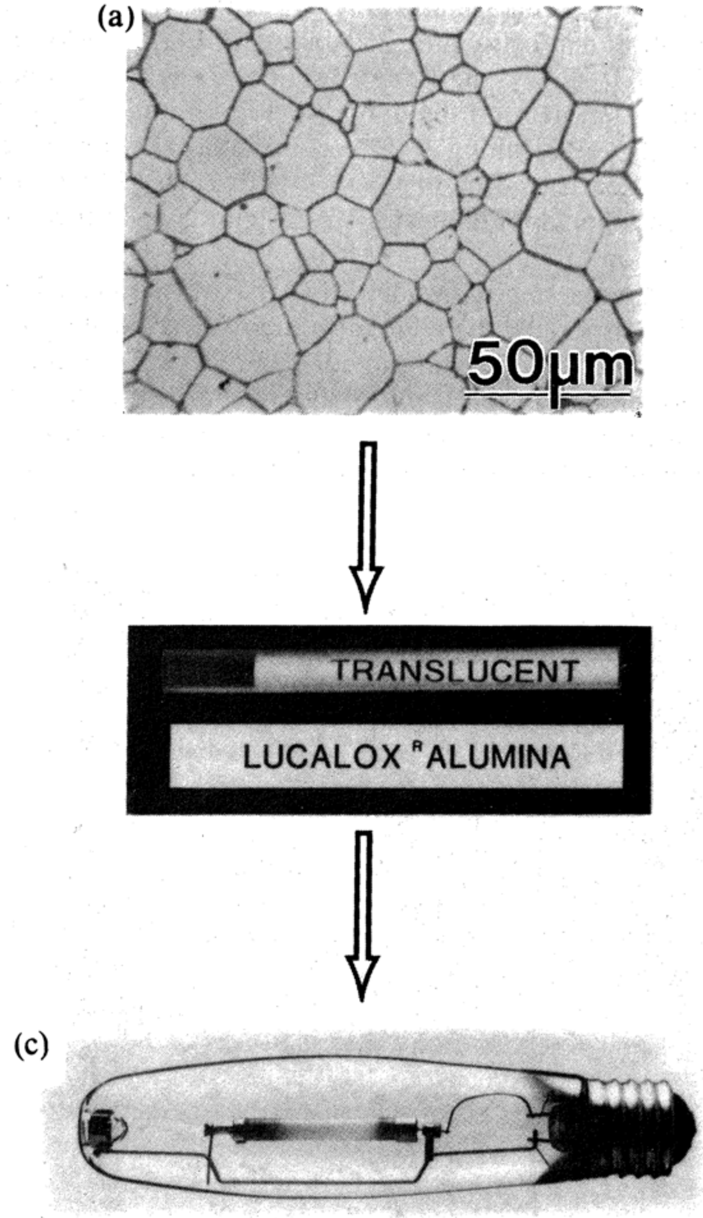

Figure 11.9 Comparison of the microstructure and translucency of relatively pore-free Al_2O_3 (a) with that of opaque Al_2O_3 containing pores trapped in grains (b). Translucent Al_2O_3 tubes are used in sodium vapor lamps that provide energy efficient street lights. (Courtesy of General Electric.)

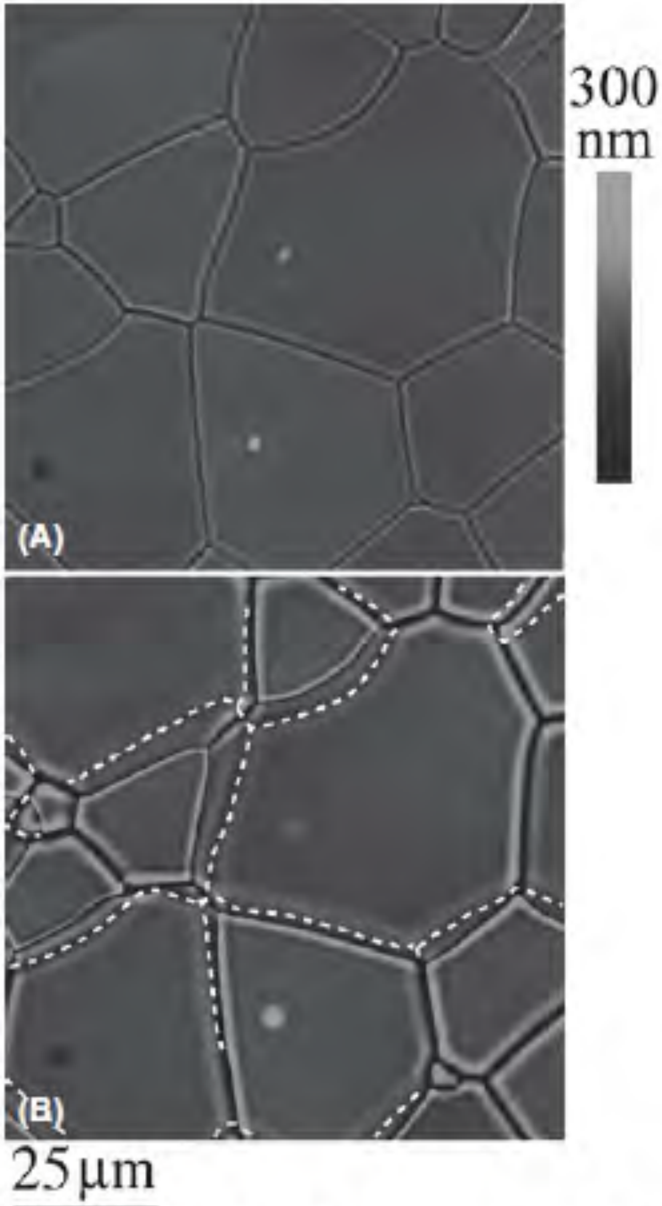

FIGURE 24.17 (a, b) AFM of grooves at migrating GBs

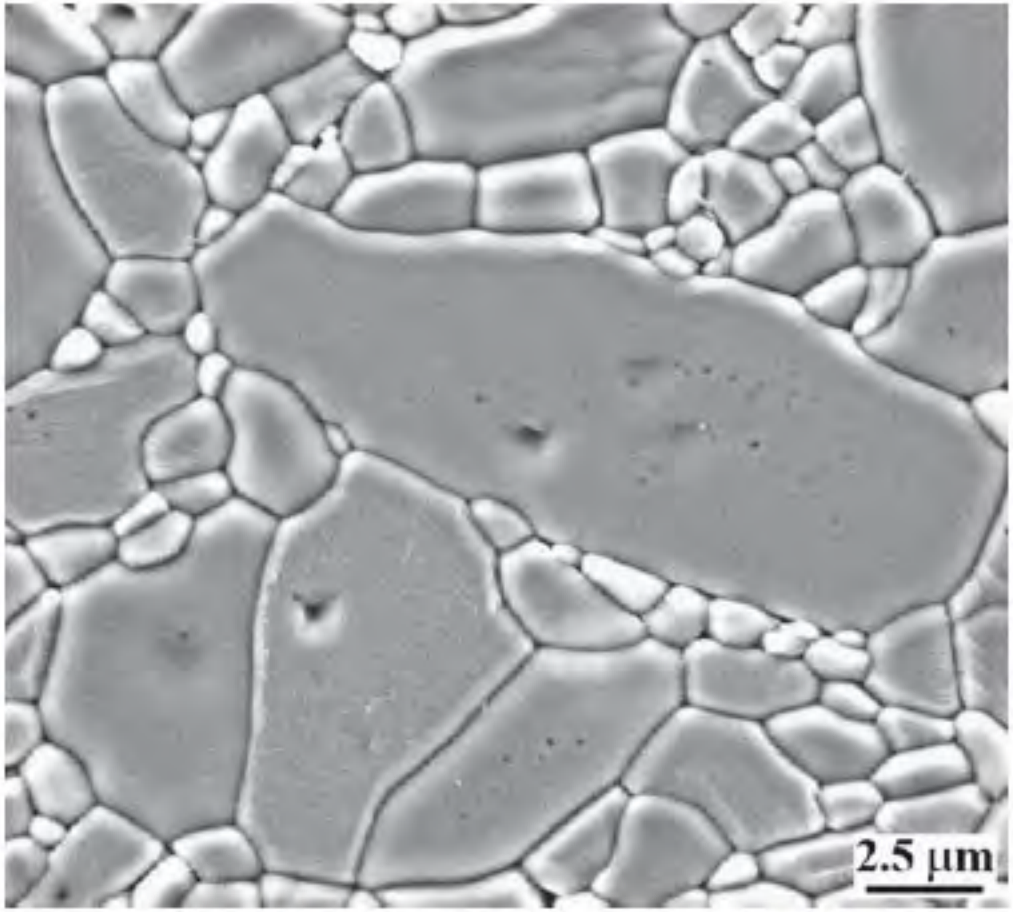

FIGURE 24.21 Elongated exaggerated grain in Al_2O_3.

- During the growth, the larger grain leaves behind a lot of pores and the piece can not achive the 100% of theoretical density (DT).
- To avoid the pore incorporation inside the grain, the speed of grain boudaries must be lower than that of the pores.
- Some impurities can segregate on grain boundary (*GRAIN BOUNDARY PINNING)* slowing the growth and so it’s possible to achive the 100% of DT.

v pore > v grain boundary

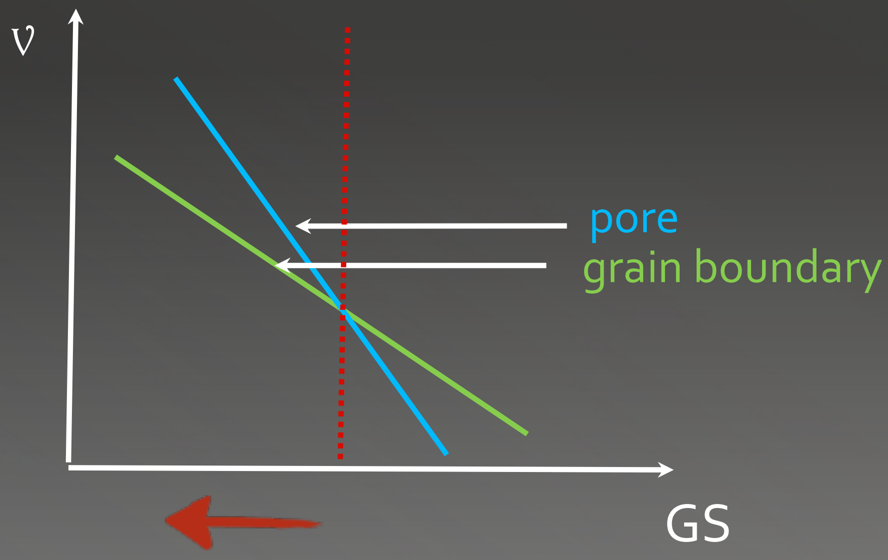

E.G. :

ALUMINA ‘LUCALOX ‘:
polycrystalline Al_2O_3 - 1% MgO

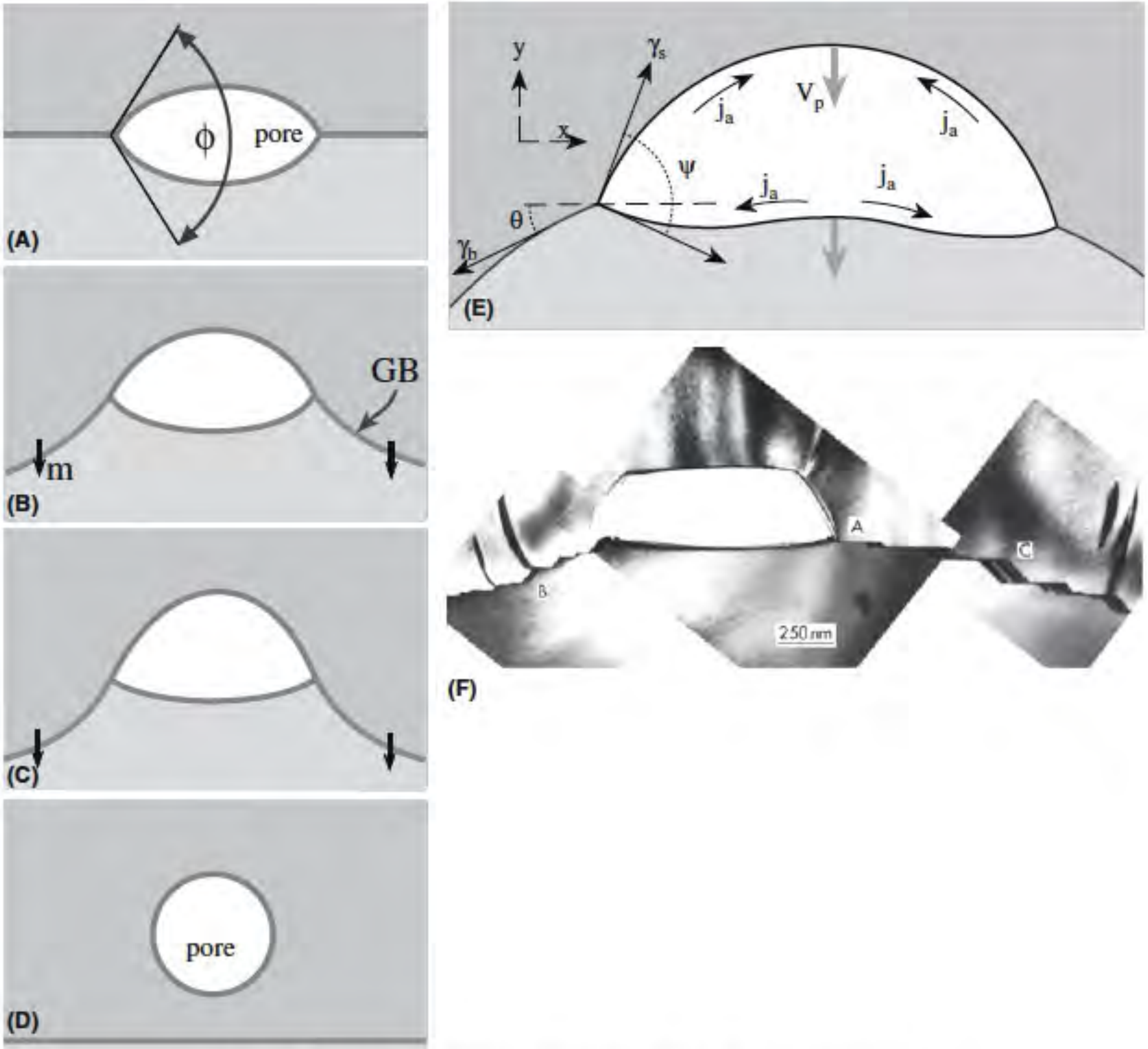

FIGURE 24.14 (a–e) GB/pore interaction: the break-away process.

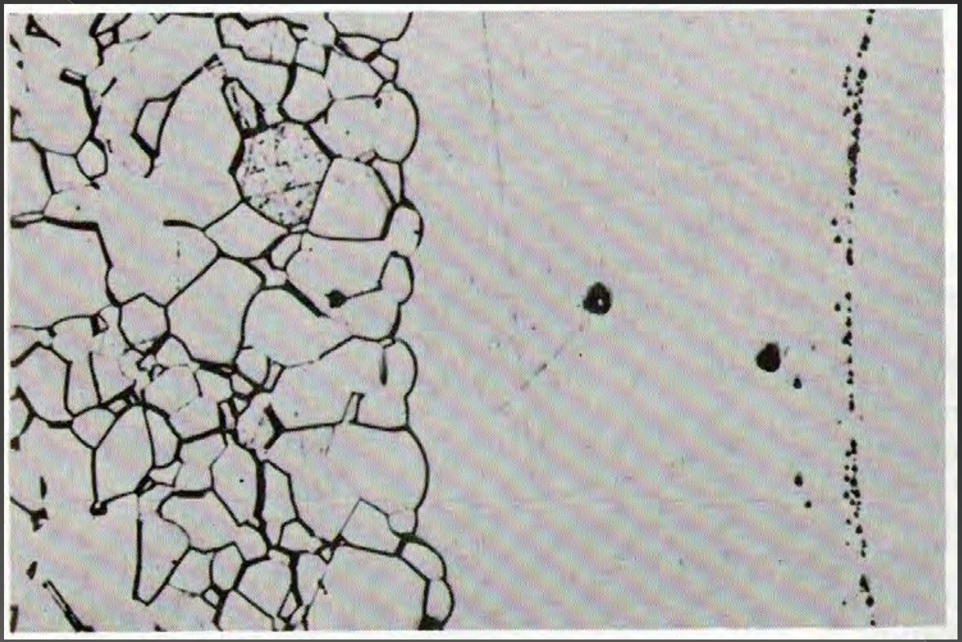

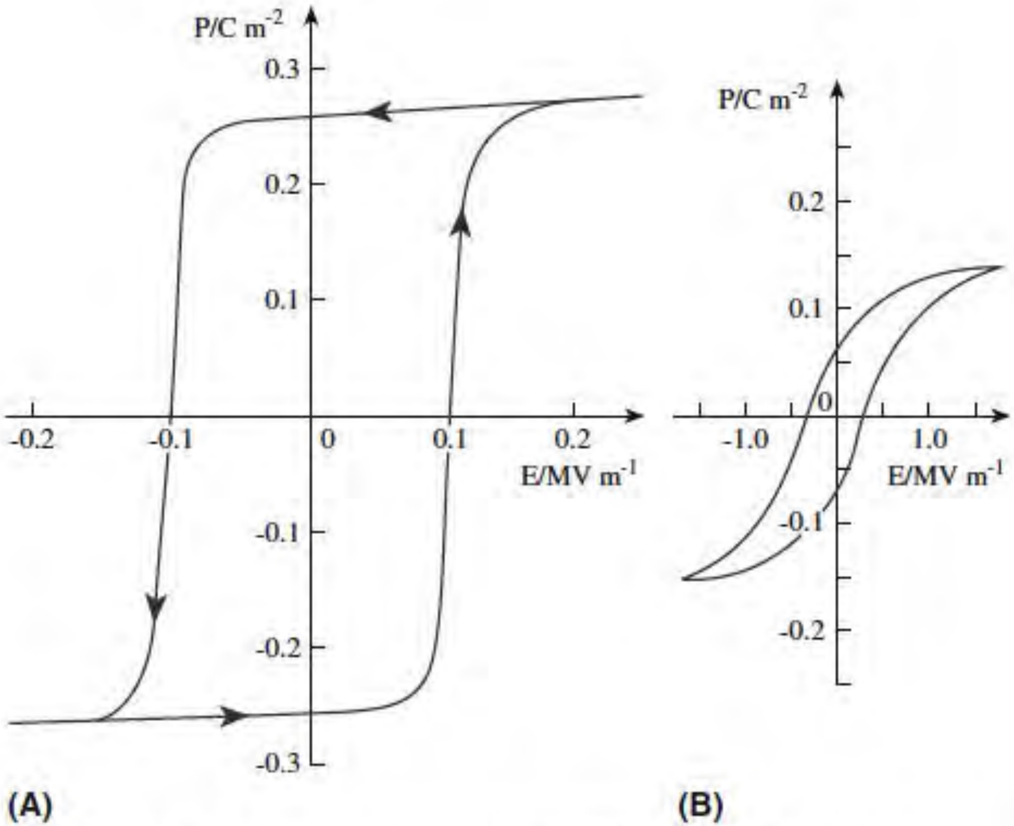

FIGURE 31.10 Hysteresis loops for $BaTiO_3$. (a) Single-domain single crystal. (b) Polycrystalline ceramic.

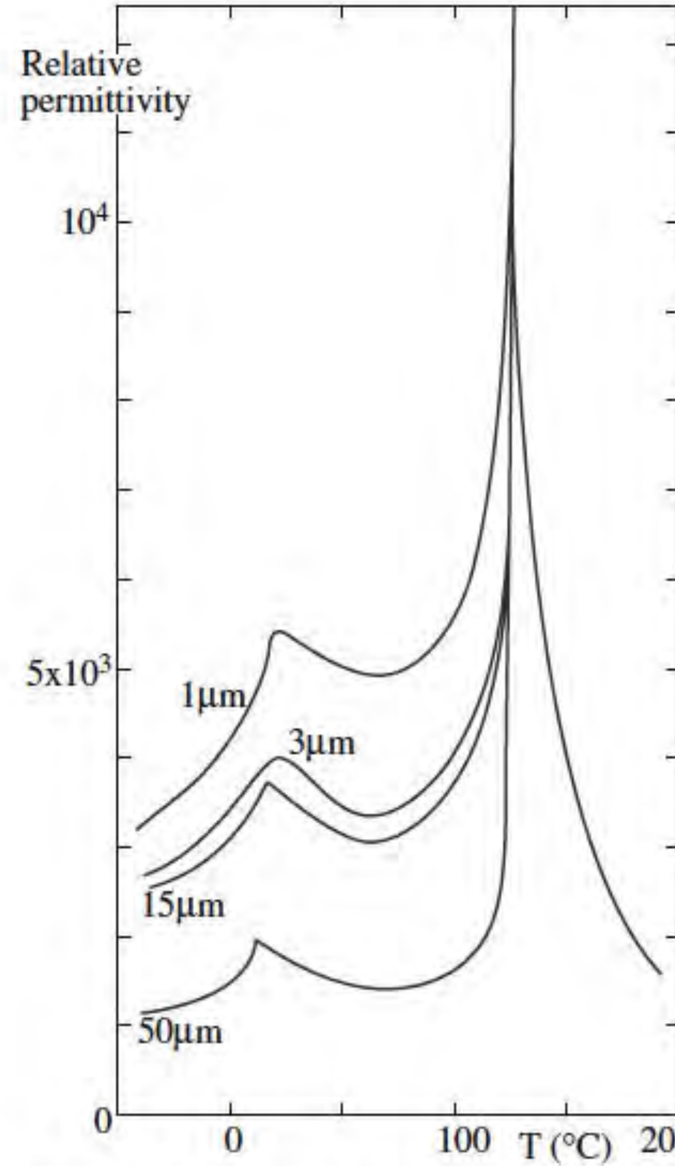

FIGURE 31.15 Effect of grain size on the dielectric con
$BaTiO_3$.

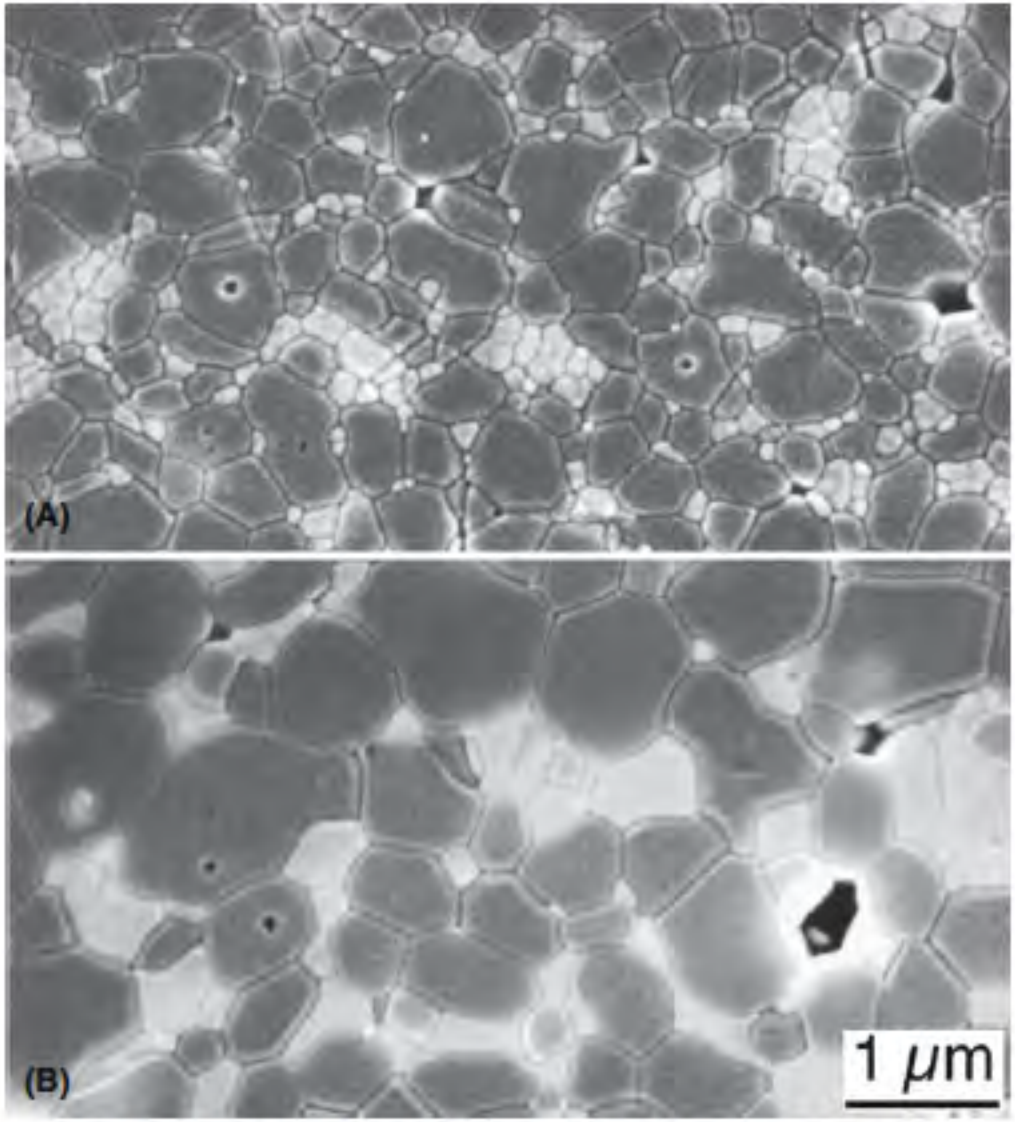

FIGURE 24.27 Two-phase ceramics. (a) As sintered and (b) heat treated at 1600°C for 30 hours. ZTA 30% (zirconia-toughened alumina with 30 vol% YSZ containing 10 molar% yttria).

WETTABILITY

Is the ability of a drop of liquid to recline on a solid surface.

Varying the pressure changes the wettability.

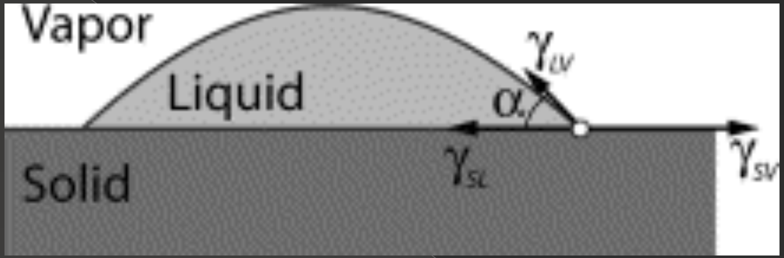

α : contact angle

γ_{LV} : liquid-vapour interfacial energy

γ_{LS} : liquid-solid interfacial energy

γ_{SV} : solid-vapour interfacial energy

The contact angle specifies the condition for minimum energy, according to the relation:

$$\gamma_{SL} + \gamma_{LV} \cos\alpha = \gamma_{SV}$$

$$\cos\alpha = \frac{\gamma_{SV} - \gamma_{SL}}{\gamma_{LV}}$$

possible cases:

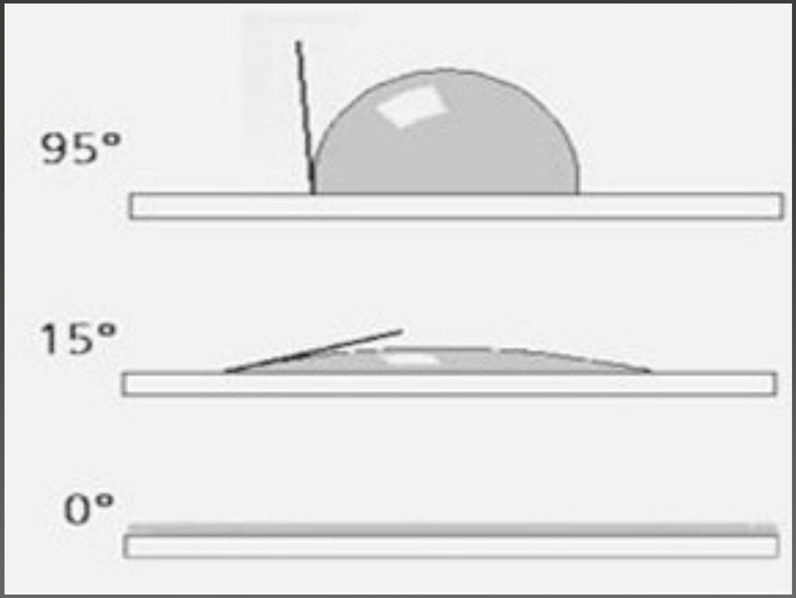

$\alpha > 90°$ ⟶ non-wettability

$\alpha < 90°$ ⟶ wettability

$\alpha = 0$ ⟶ spreading

LIQUID PHASE SINTERING

- It is the process of adding an additive to the powder which will melt before the ceramic grains.
- The metal added, at high temperatures, melt and WET the grains. The intergranulary spaces are such as to have a capillary forces which attract the grain one another.
- (By lowering the temperature, the amorphous phase does not wet the grains anymore and ritires in triple junctions.)
- (This gives good mechanical proprieties.)
- E.G. : WIDIA (93% WC in a Co matrix).

Liquid phase sintered SiC

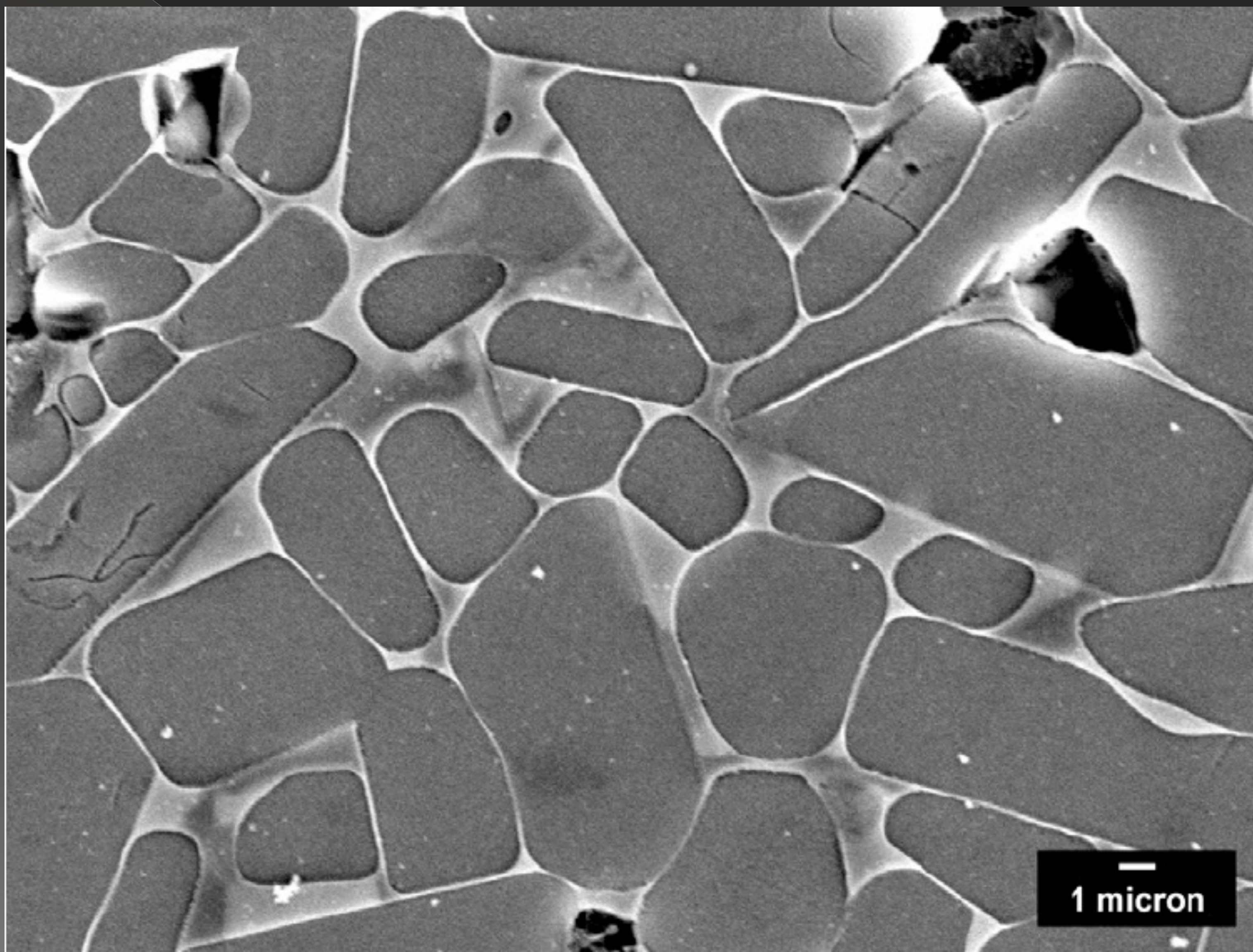

Liquid phase sintered Si_3N_4

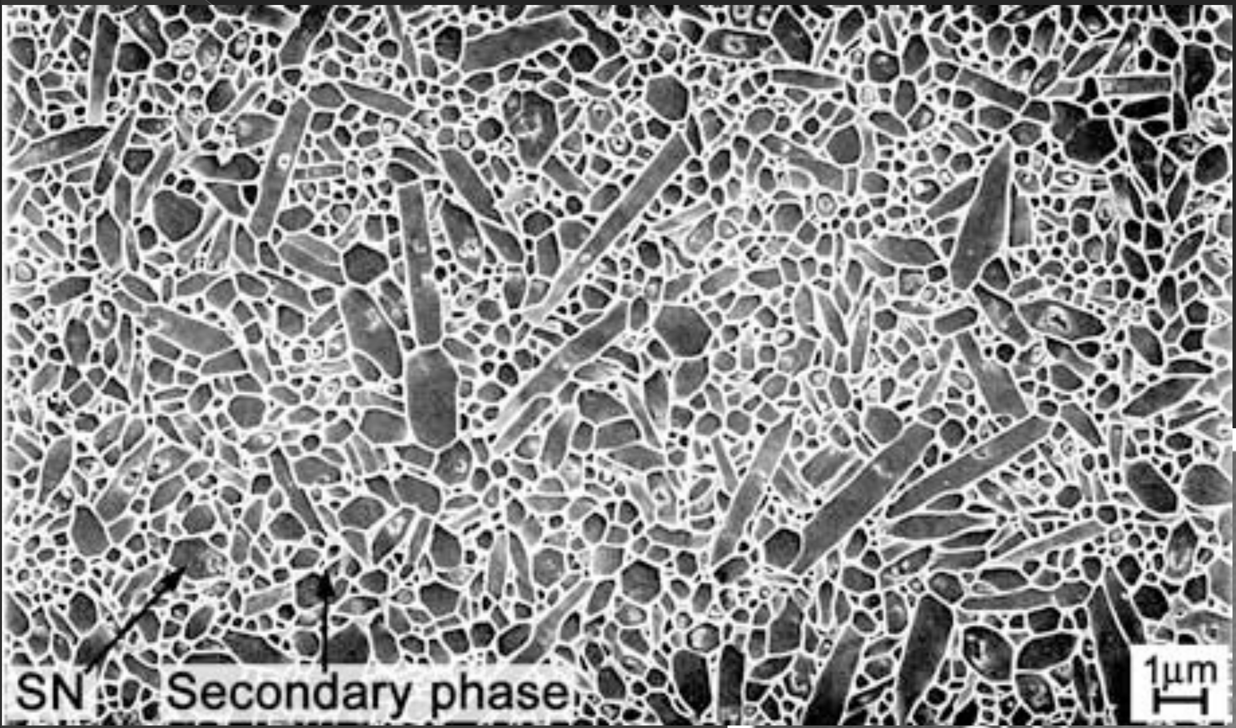

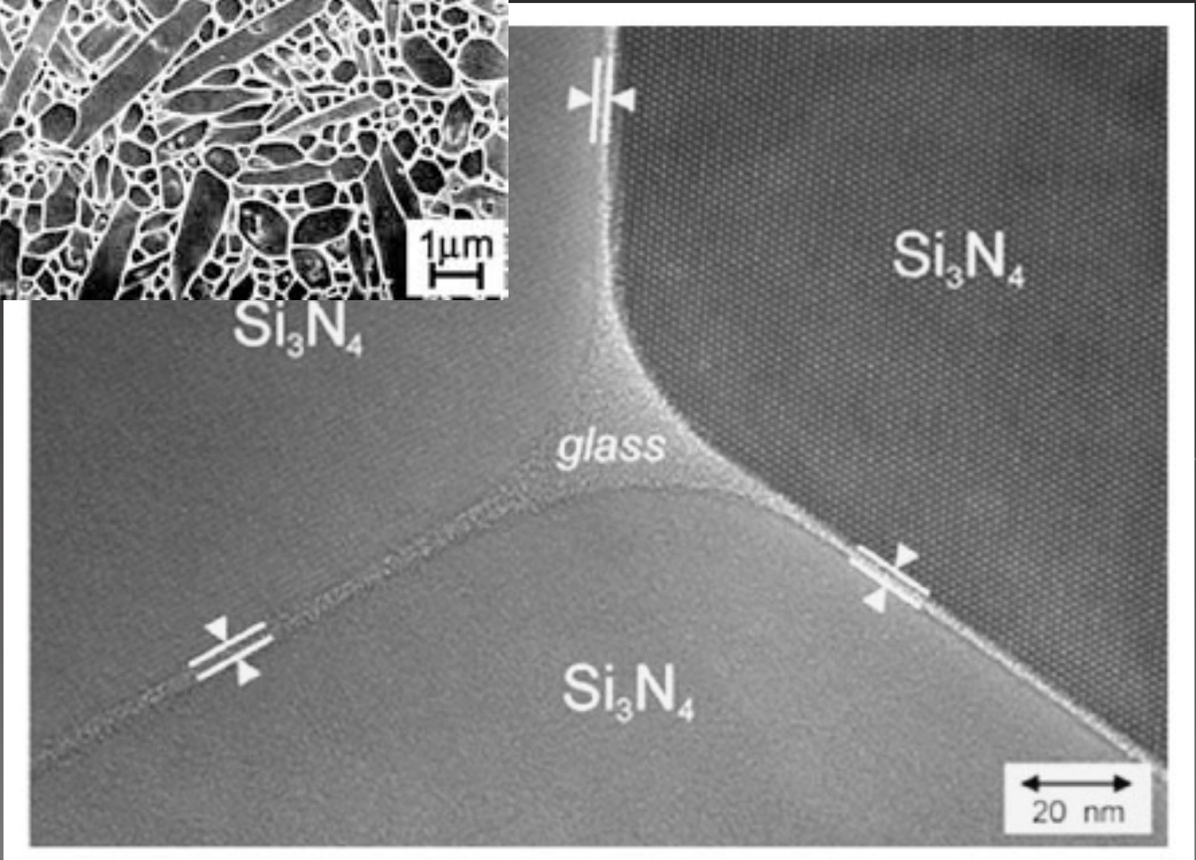

Lquid phase sintered SiAlON

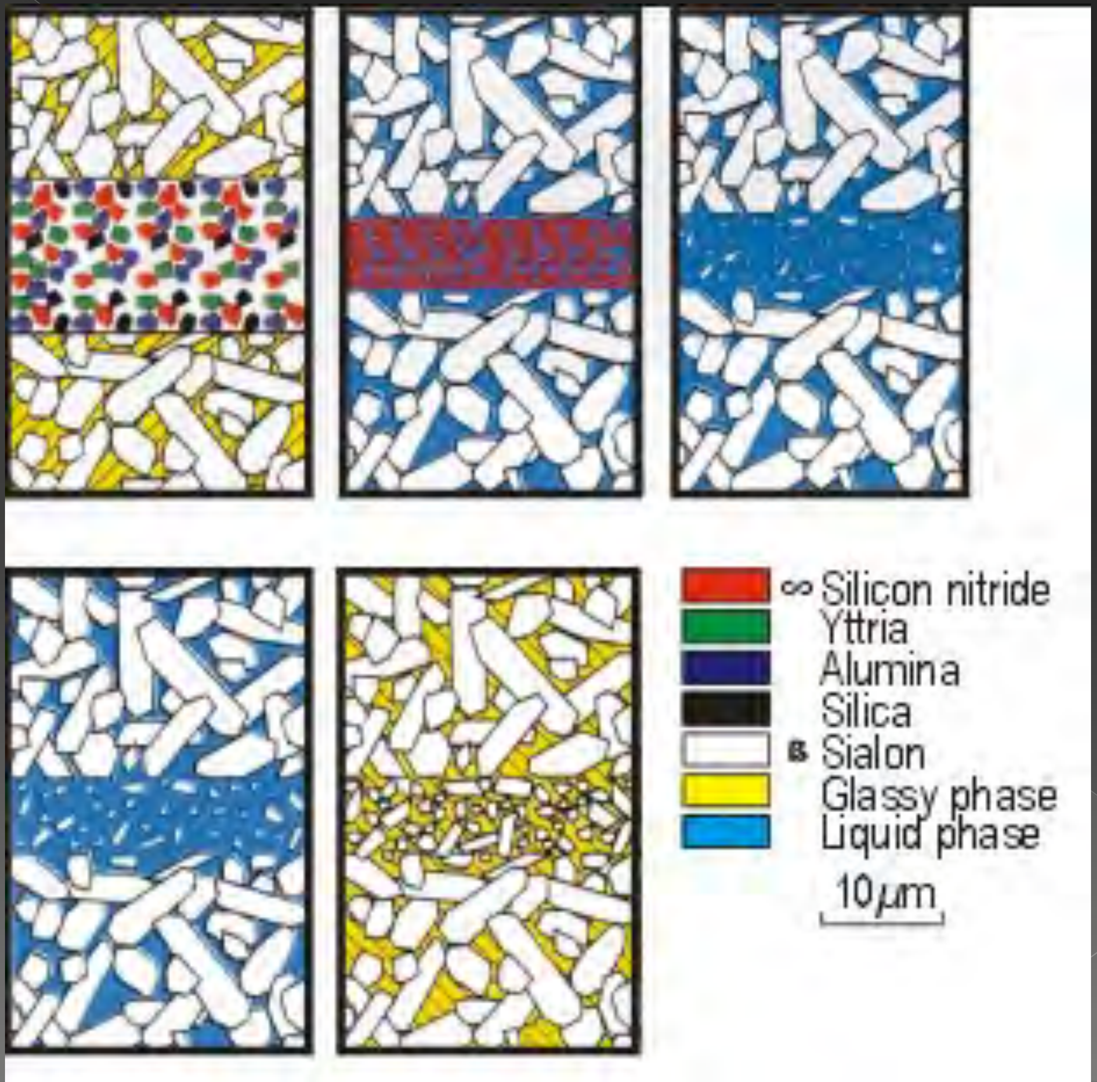

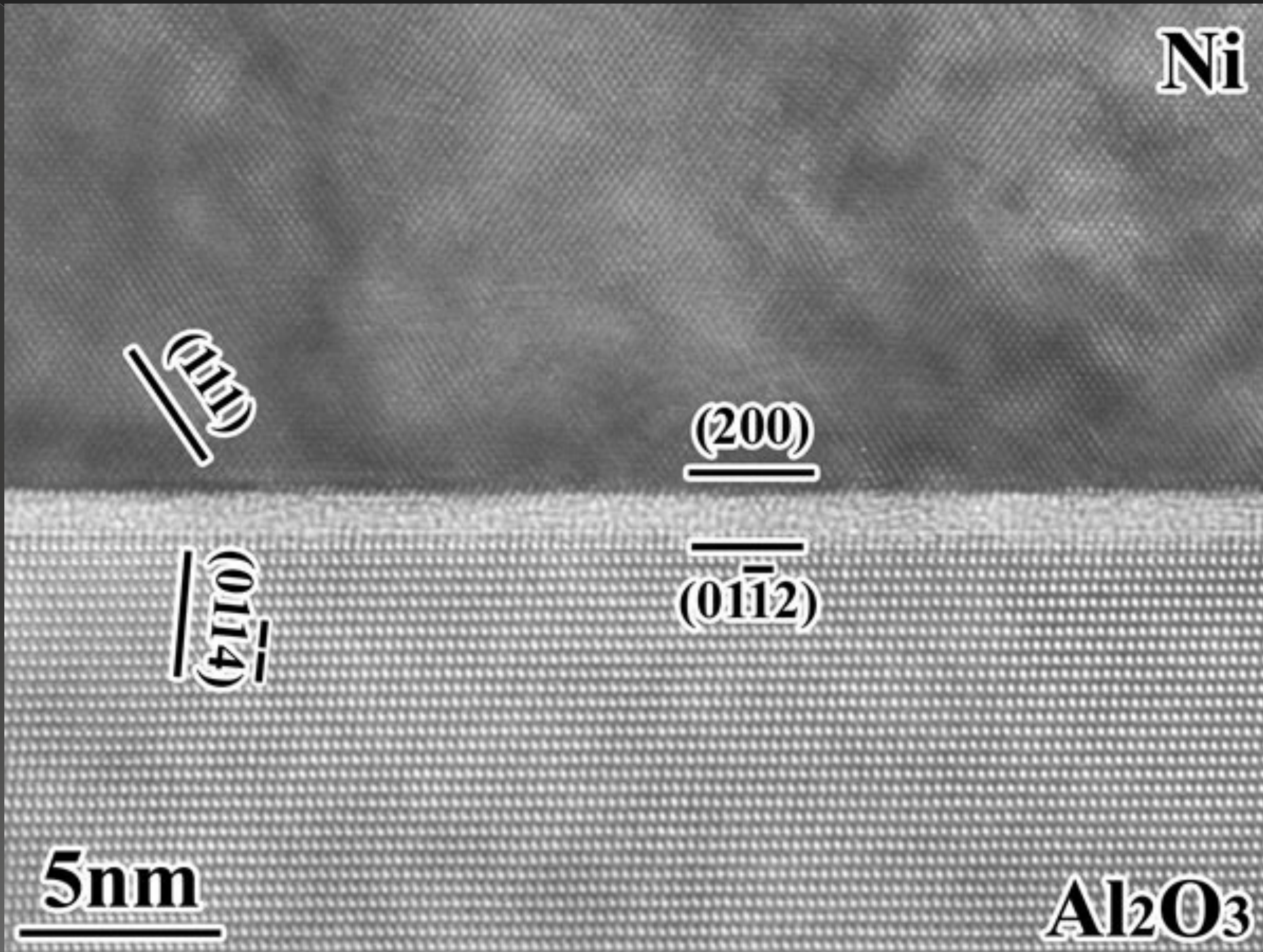
Ni
(111)
(200)
(01$\bar{1}$2)
(01$\bar{1}$4)
5nm
Al_2O_3

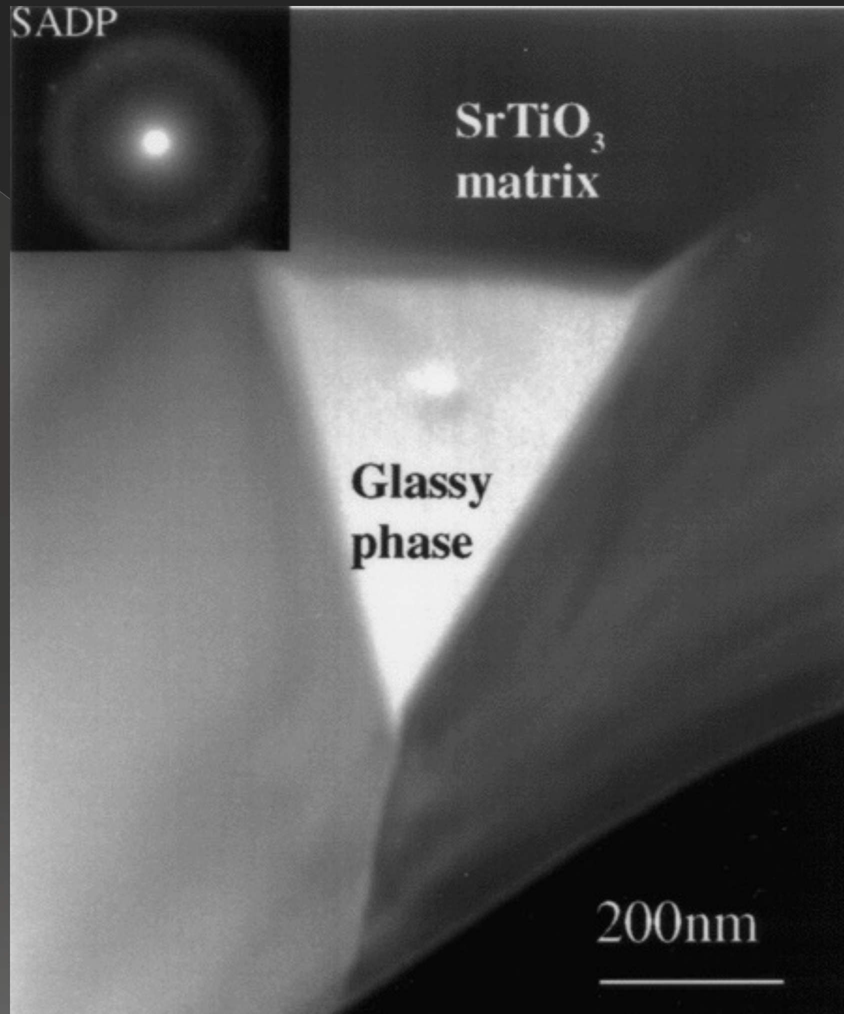
SADP
SrTiO3
matrix
Glassy
phase
200nm

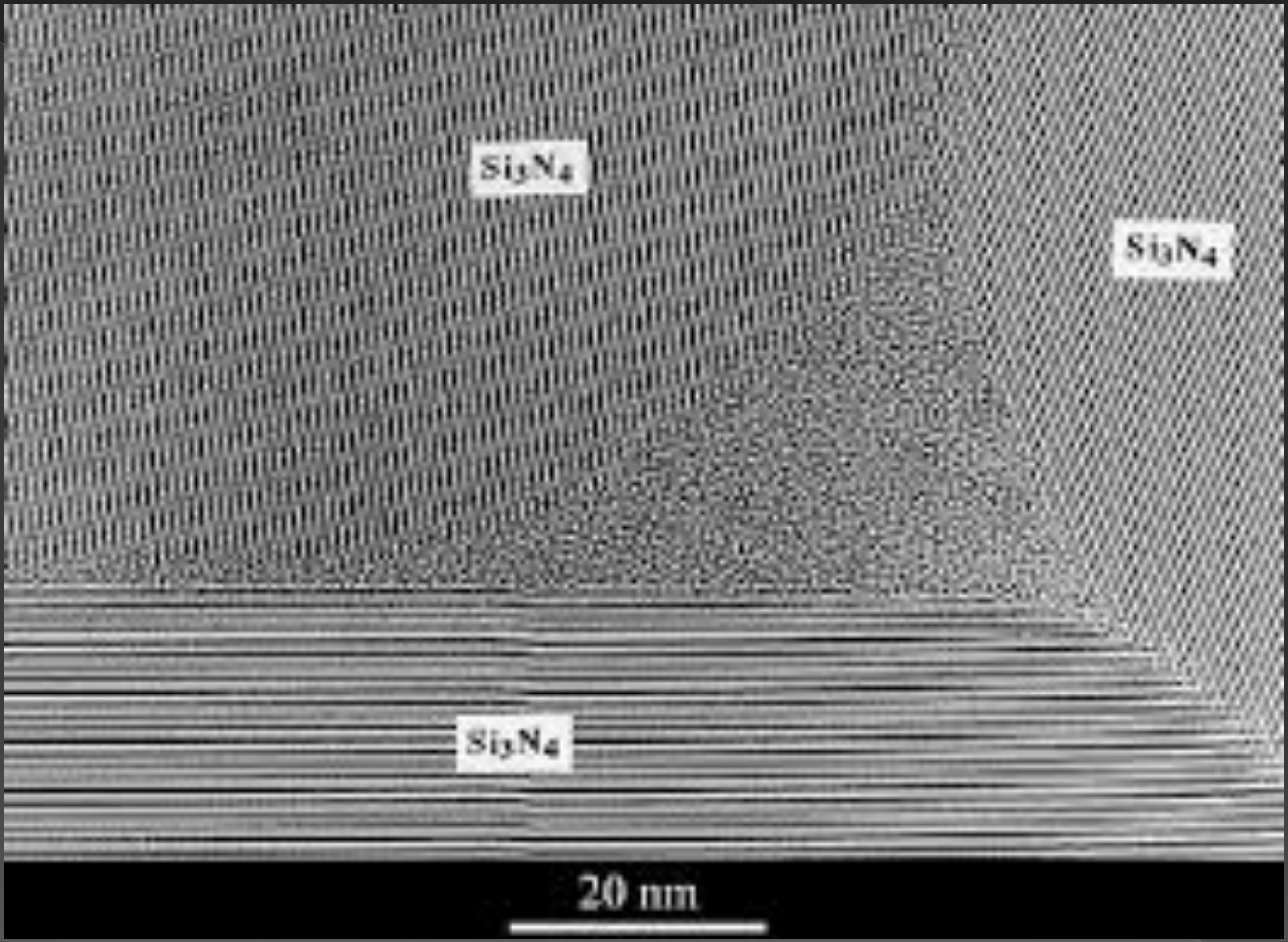

Si_3N_4
Si_3N_4
Si_3N_4
20 nm

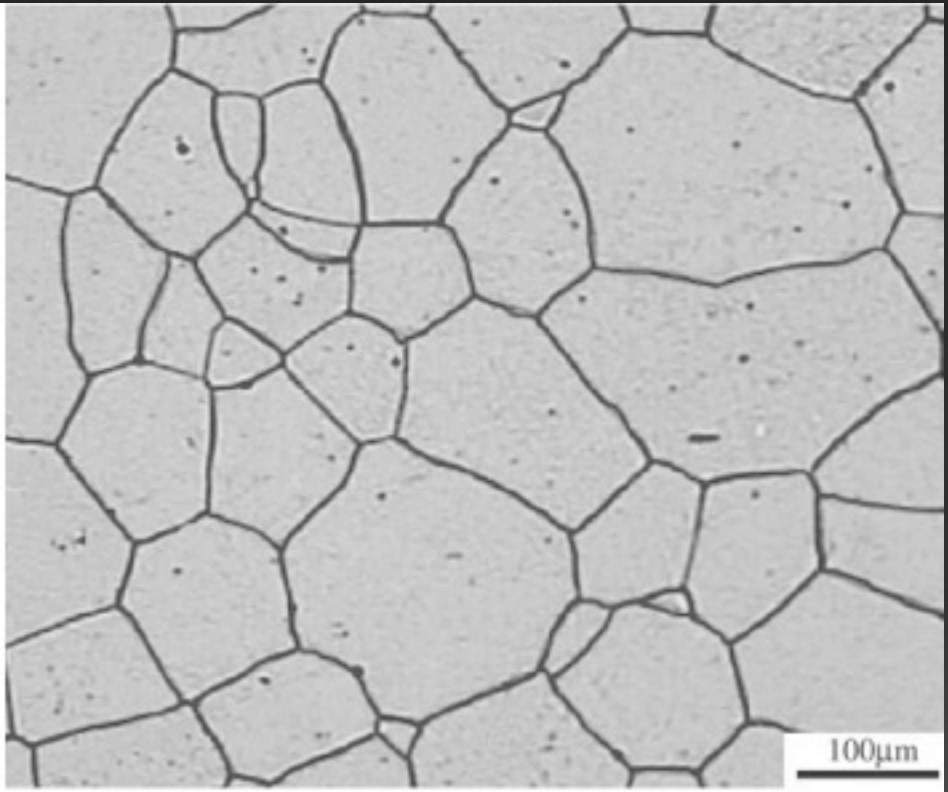

Figure 1. Typical microstructure of polycrystalline ZnO used in this work, after thermal etching at 1150 °C, for 1 h, in air.

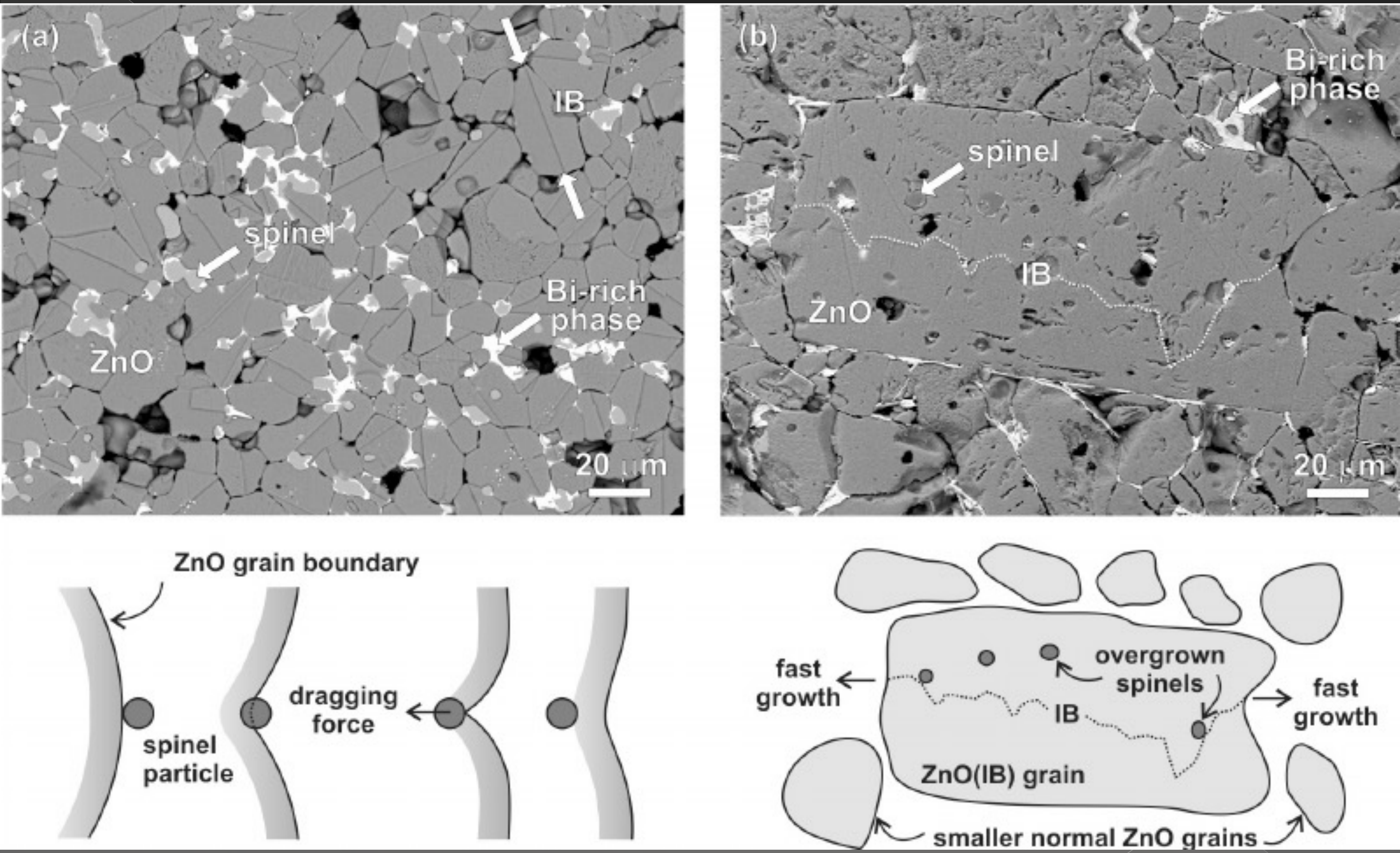
(a)
IB
spinel
Bi-rich phase
ZnO
20 μm
(b)
Bi-rich phase
spinel
IB
ZnO
20 μm
ZnO grain boundary
spinel particle
dragging force
fast growth
overgrown spinels
IB
fast growth
ZnO(IB) grain
smaller normal ZnO grains

PROCEDURE FOR THE SINTERING PROCESS

- Determination of the T_m $T_{sintering} = 2/3\, T_m$ E.G. : Al_2O_3
  $T_m = 2400°C$ $T_{sintering} = 1600°C$
- CALCINATION (200°C-300°C under the sintering temperature)
  E.G. : ZrO_2 stabilized by CaO, Y_2O_3, CeO_2
- FORMING the ceramic parts
- SINTERING

$$\frac{\sqrt{D \cdot t}}{a} \approx 1$$

DENSITY DETERMINATION BY ARCHIMEDE'S PRINCIPLE

- D = dry weight
- boil the piece for 5 hours
- W = wet weight in air
- S = wet weight in water suspended
- V = external volume of the piece: $V = W - S$
- BULK DENSITY $B = D/V$
- P = apparent porosity $P = (W-D)/V$

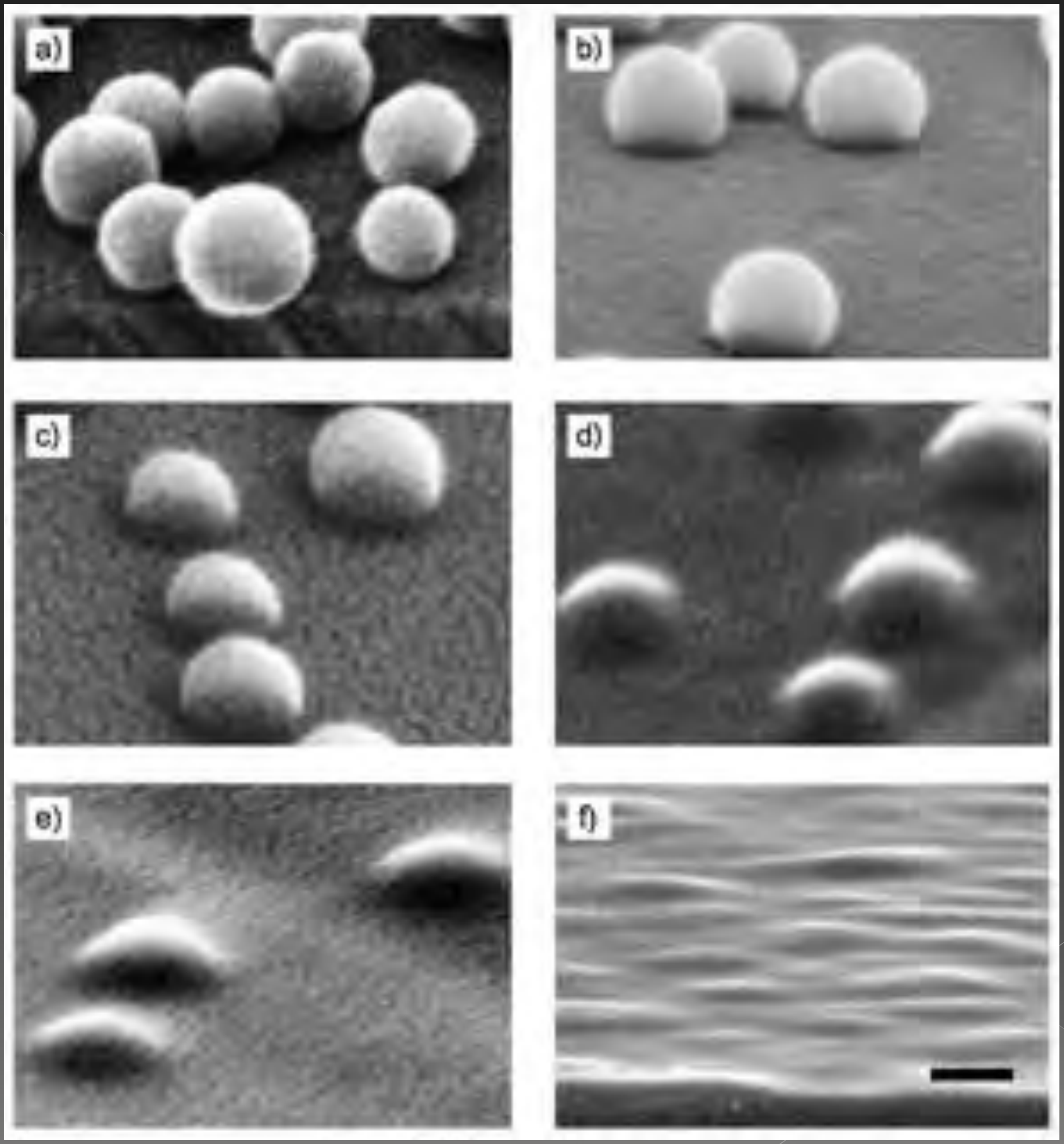
a)
b)
c)
d)
e)
f)

TYPICAL SINTERING TIME-TEMPERATURE PROFILE

Non destructive testing Techniques

- Visual inspection
- Penetrant dyes https://www.youtube.com/watch?v=xEK-c1pkTUI
- Ultrasonic testing https://www.youtube.com/watch?v=UM6XKvXWVFA
- Radiographic testing https://www.youtube.com/watch?v=IcWjZbXiFkM
- Magnetoscopic testing
- Eddy currents

Proof testing:
1) load configuration as similar as possible to service condiction

2) one single test slightly above load/stress values in service

Liquid penetrant dyes

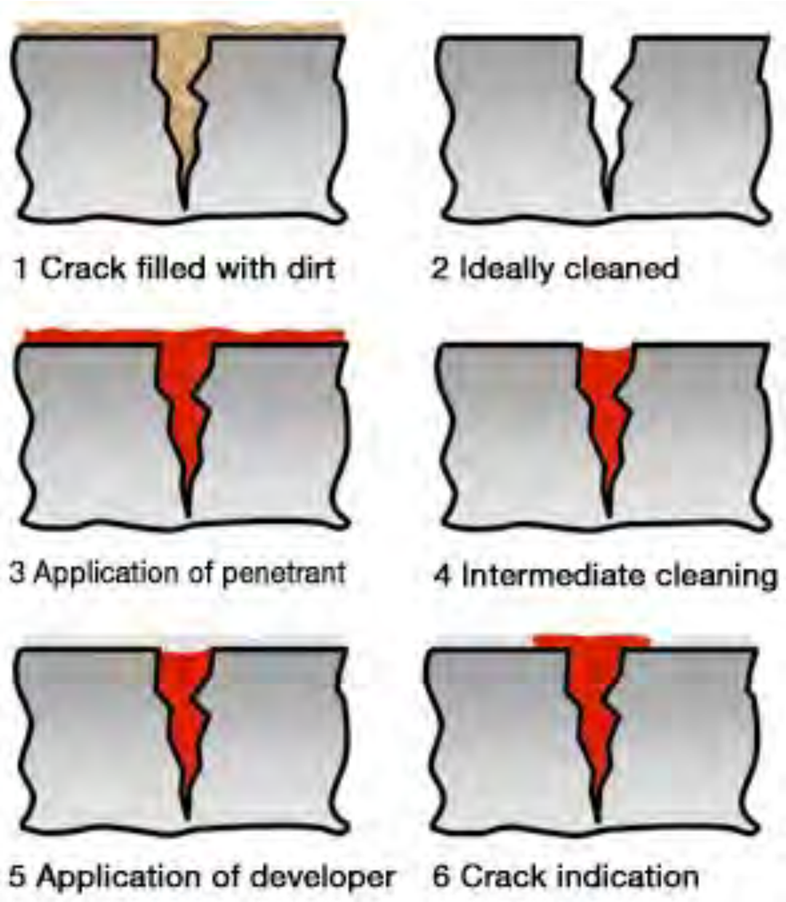

Fluorescent penetrant dye revealed with a Wood lamp

Ultrasonic testing

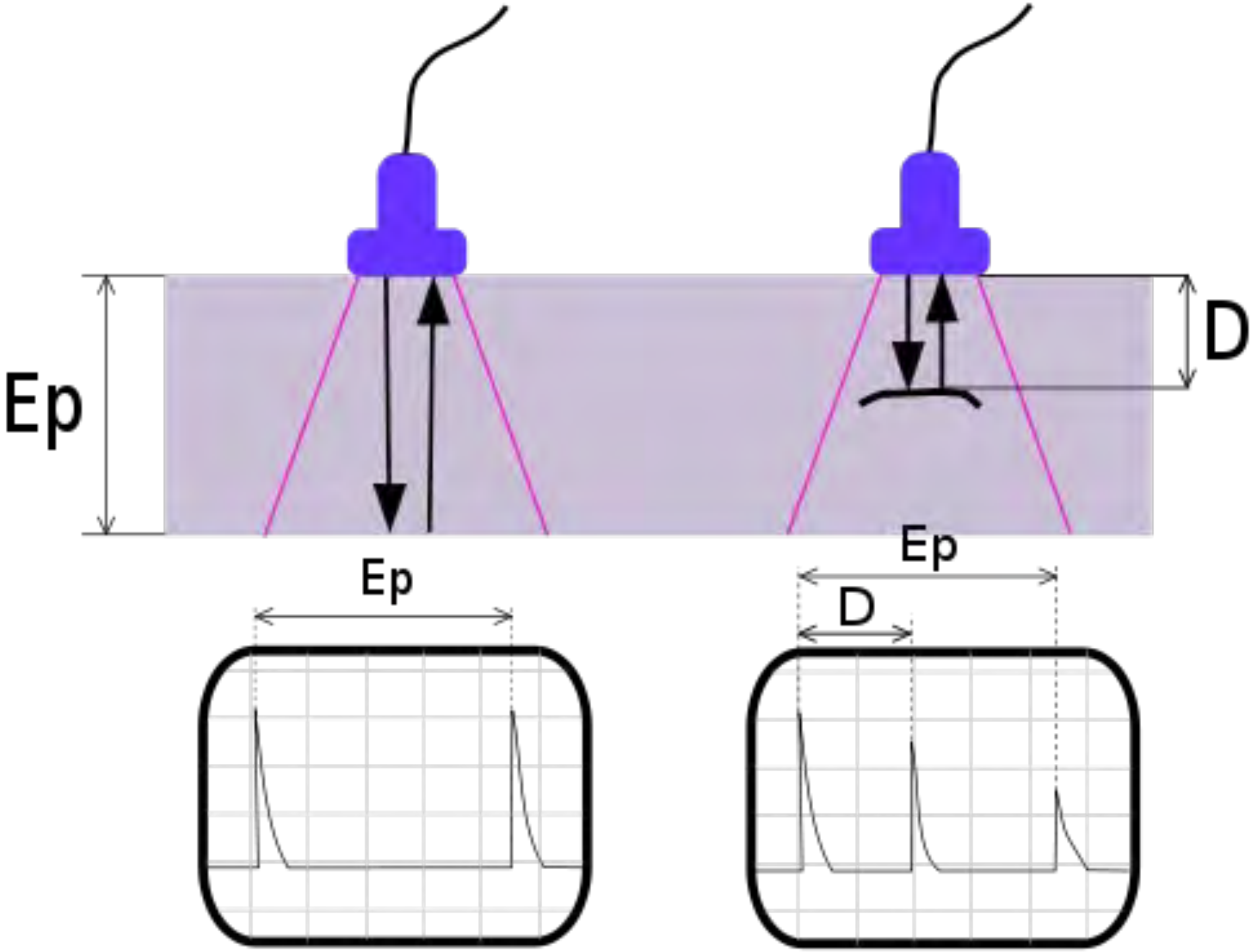

https://www.youtube.com/watch?v=UM6XKvXWVFA

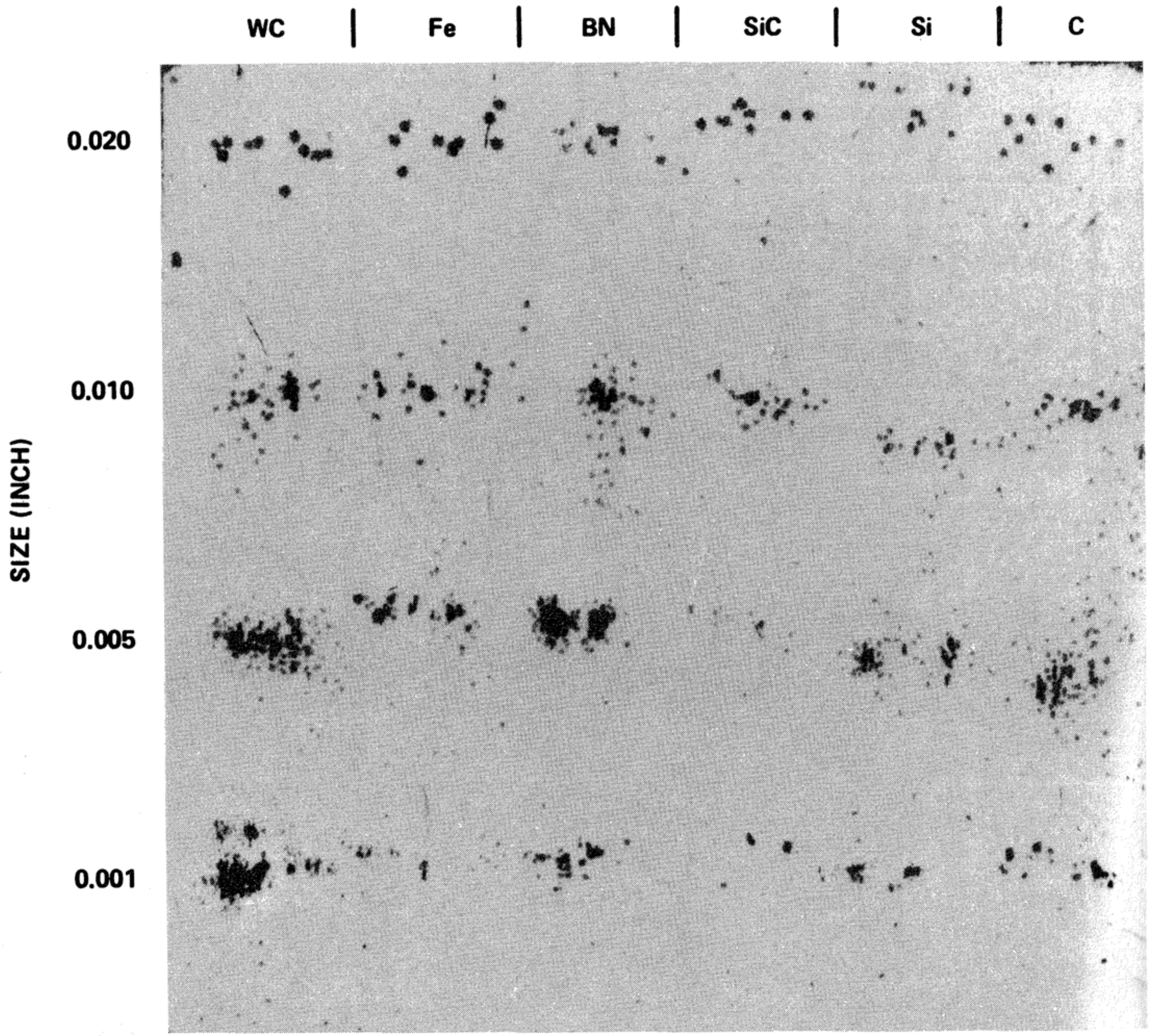

Figure 13.10 Ultrasonic C-scan with a 25-MHz transducer of a 0.64-cm (0.25-in.)-thick hot-pressed Si_3N_4 plate. (Courtesy Garrett Turbine Engine Company, Phoenix, Ariz., Division of Allied-Signal Aerospace.)

Radiographic testing

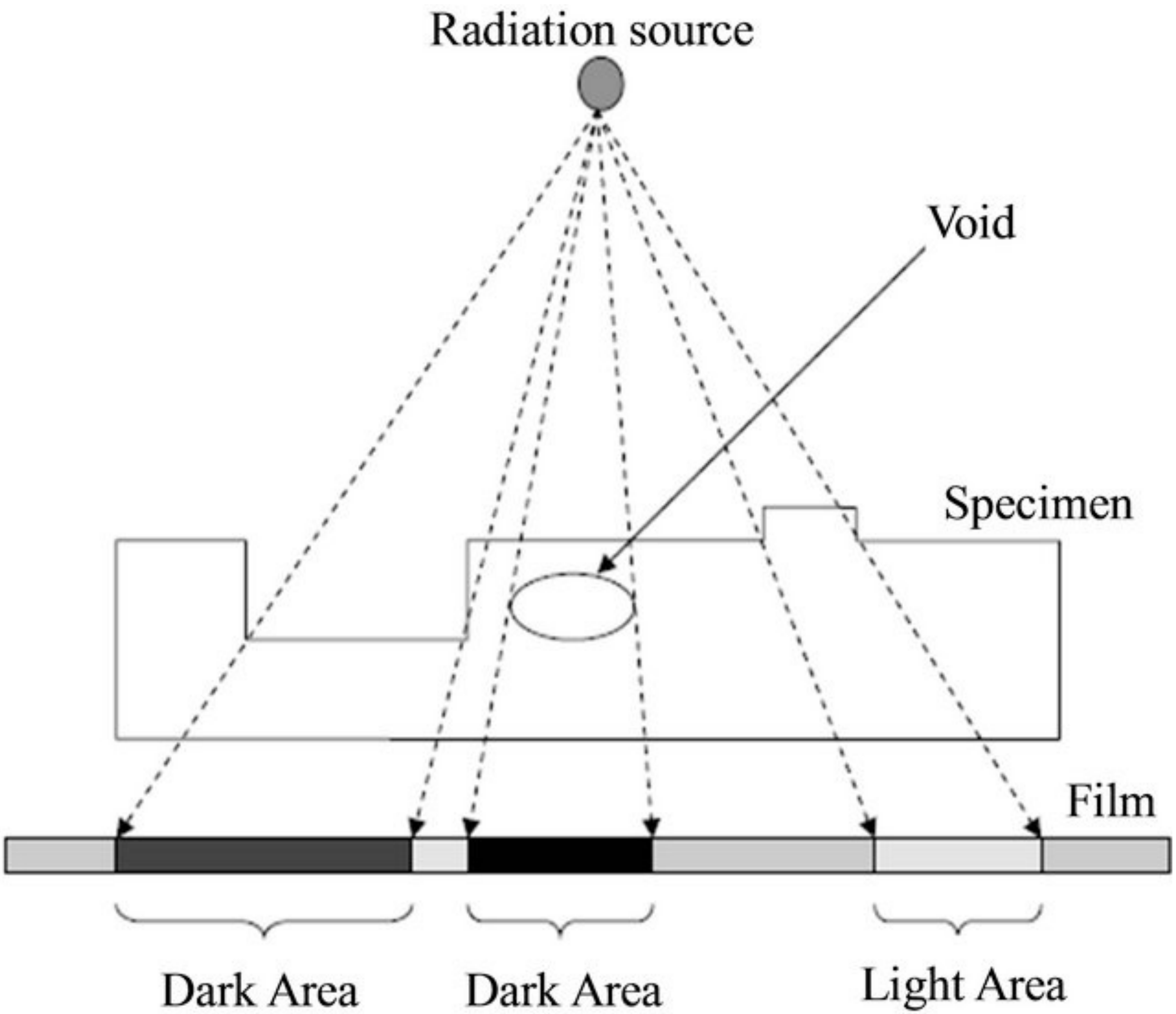

Radiographic testing of two chips

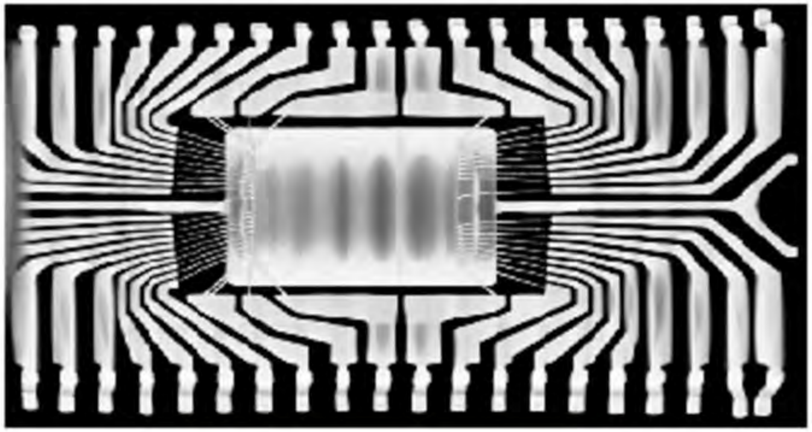

Counterfeit

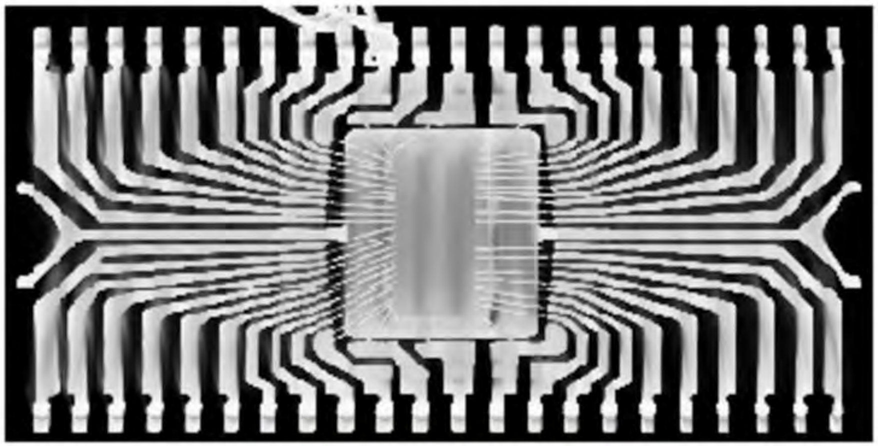

Authentic

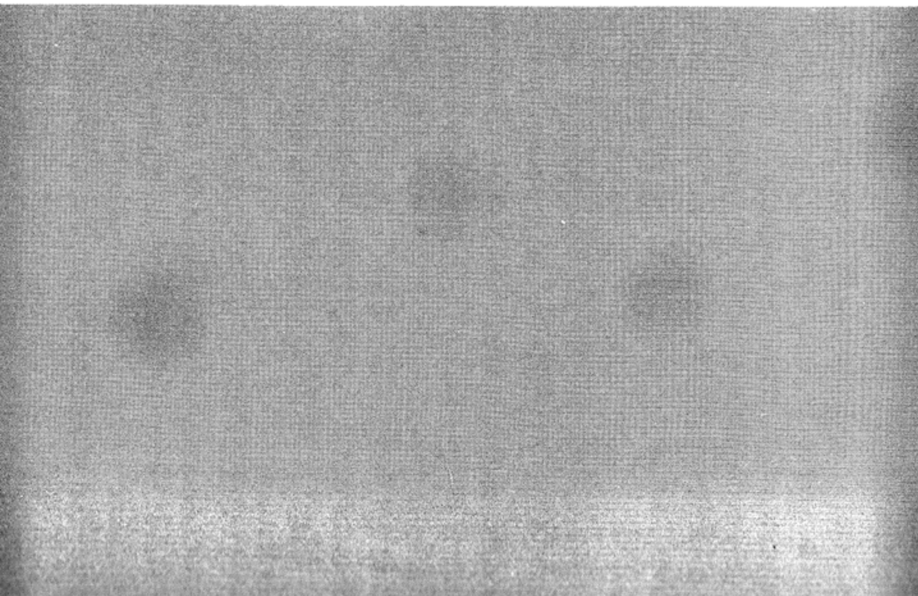

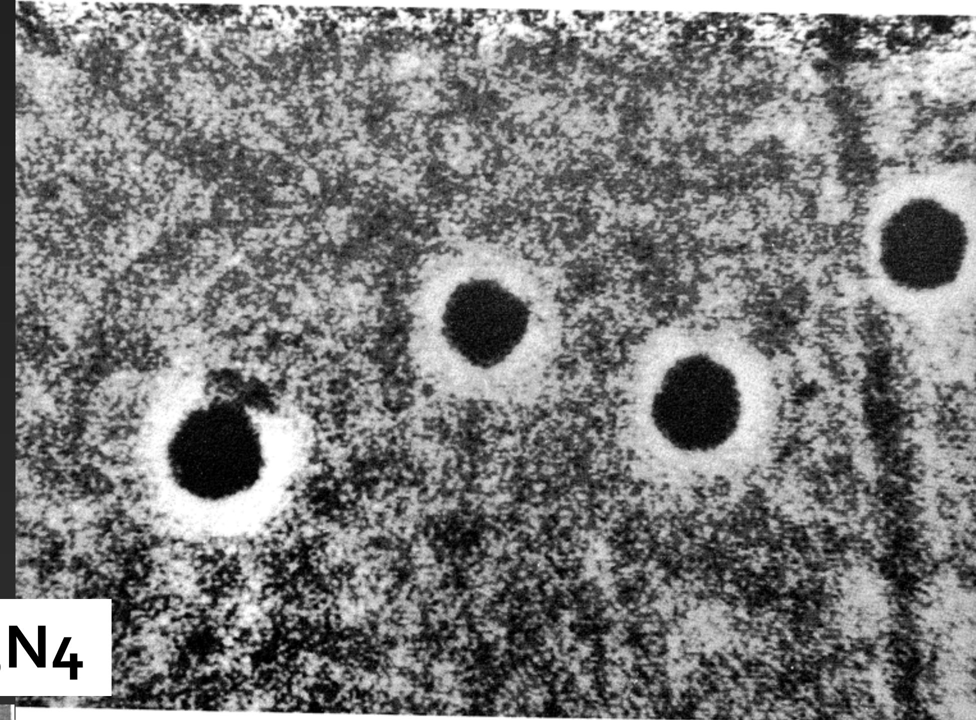

X ray image of C inclusions in Si_3N_4

X ray image of WC inclusions in Si_3N_4

https://www.youtube.com/watch?v=SZgPBbbo-Cw

Magnetoscopic testing

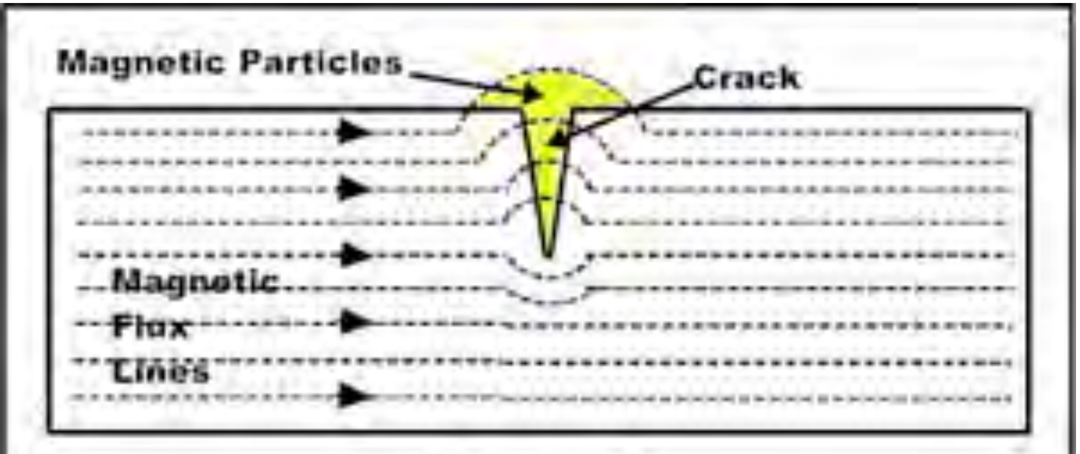

Figure 1

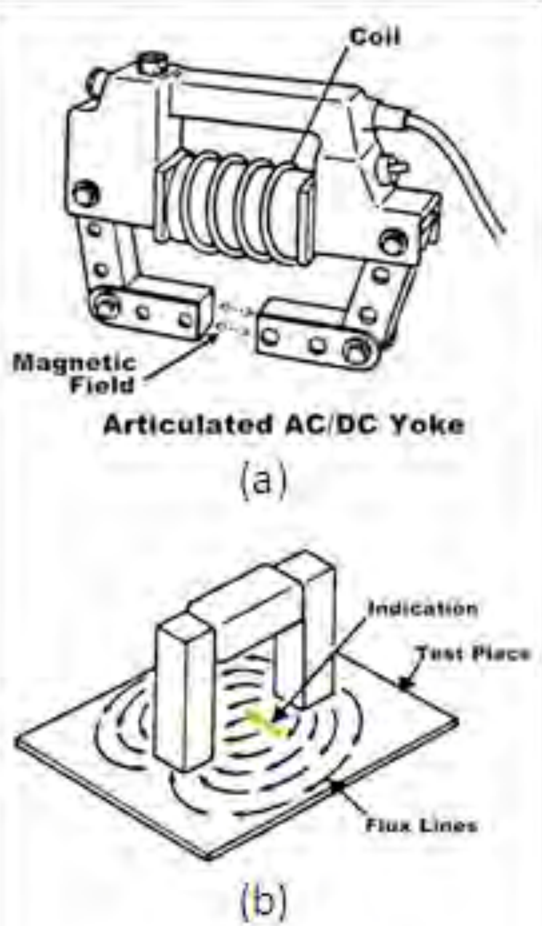

Figure 2

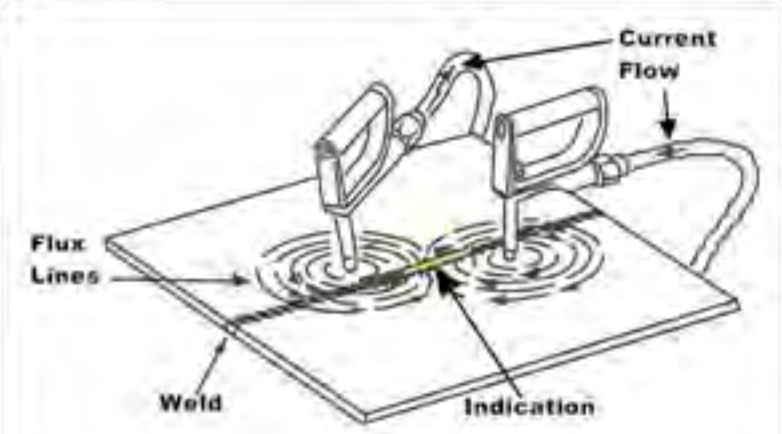

Figure 3

Eddy current testing

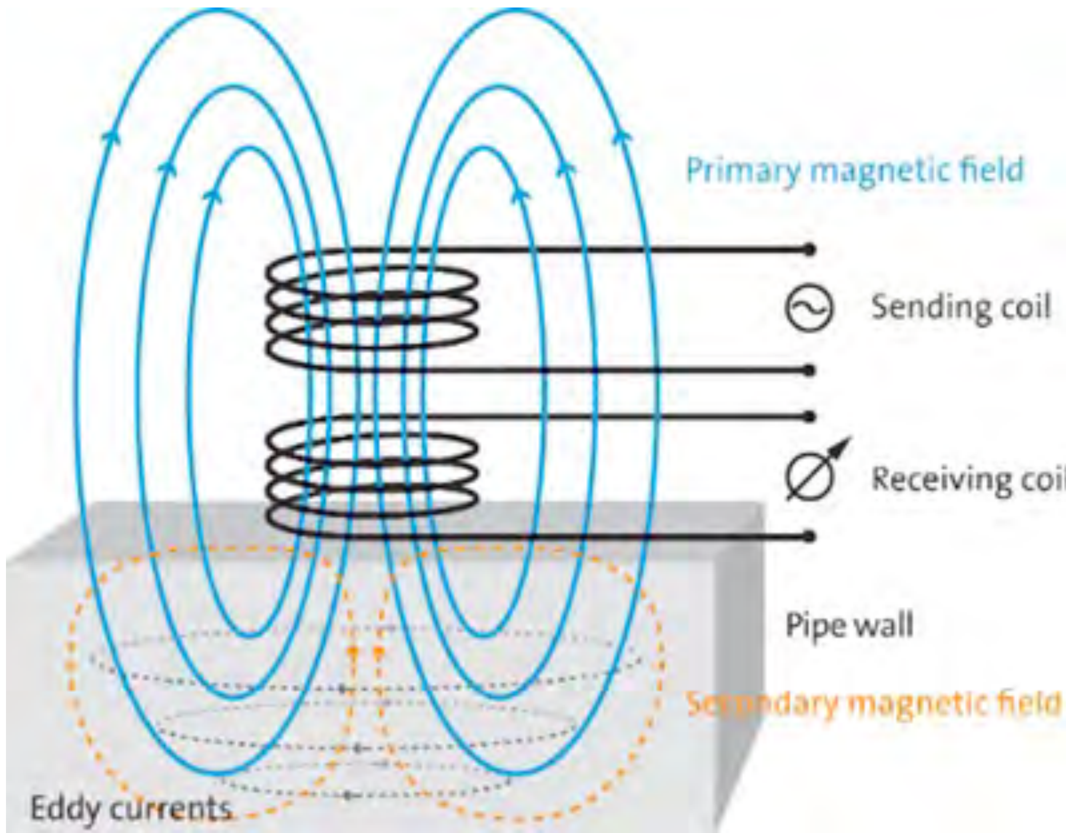

Flaws are Stress Concentrators

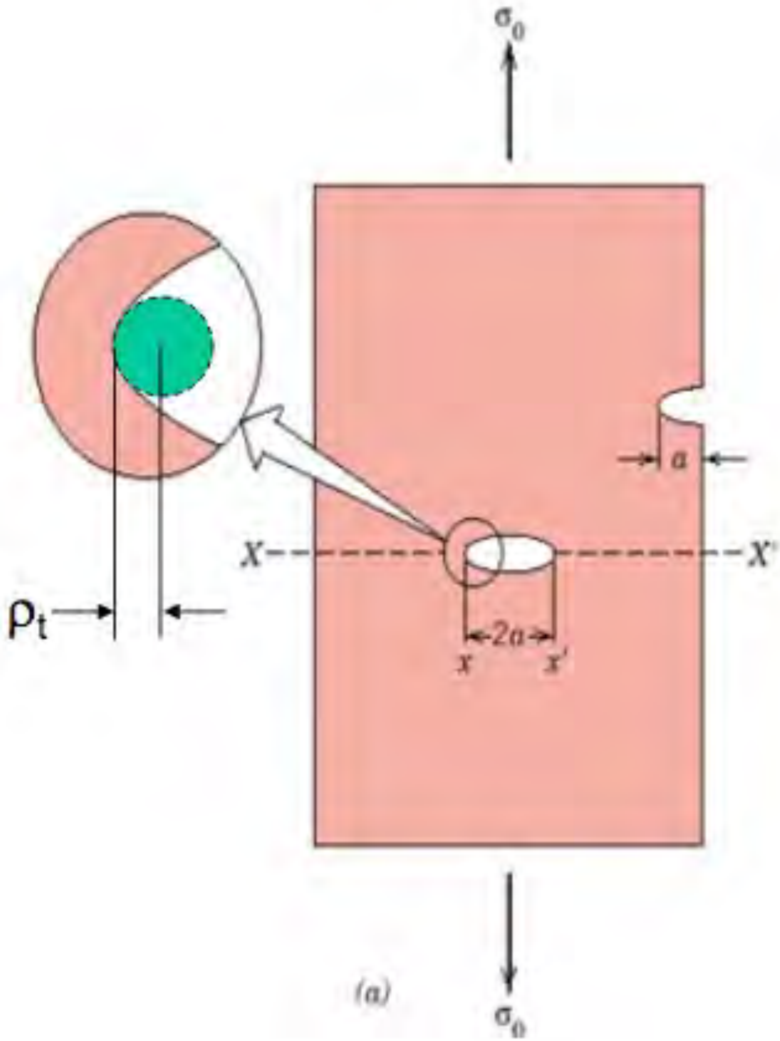

If the crack is similar to an elliptical hole through plate, and is oriented perpendicular to applied stress, the maximum stress σ_m=

$$\sigma_m = 2\sigma_o\left(\frac{a}{\rho_t}\right)^{1/2} = K_t\sigma_o$$

where

ρ_t = radius of curvature

σ_o = applied stress

σ_m = stress at crack tip

a = length of surface crack or ½ length of internal crack

$\sigma_m/\sigma_o = K_t$ the stress concentration factor

Brittle Fracture of Ceramics

- Most ceramics (at room temperature) fracture before any plastic deformation can occur.
- Typical crack configurations for 4 common loading methods.

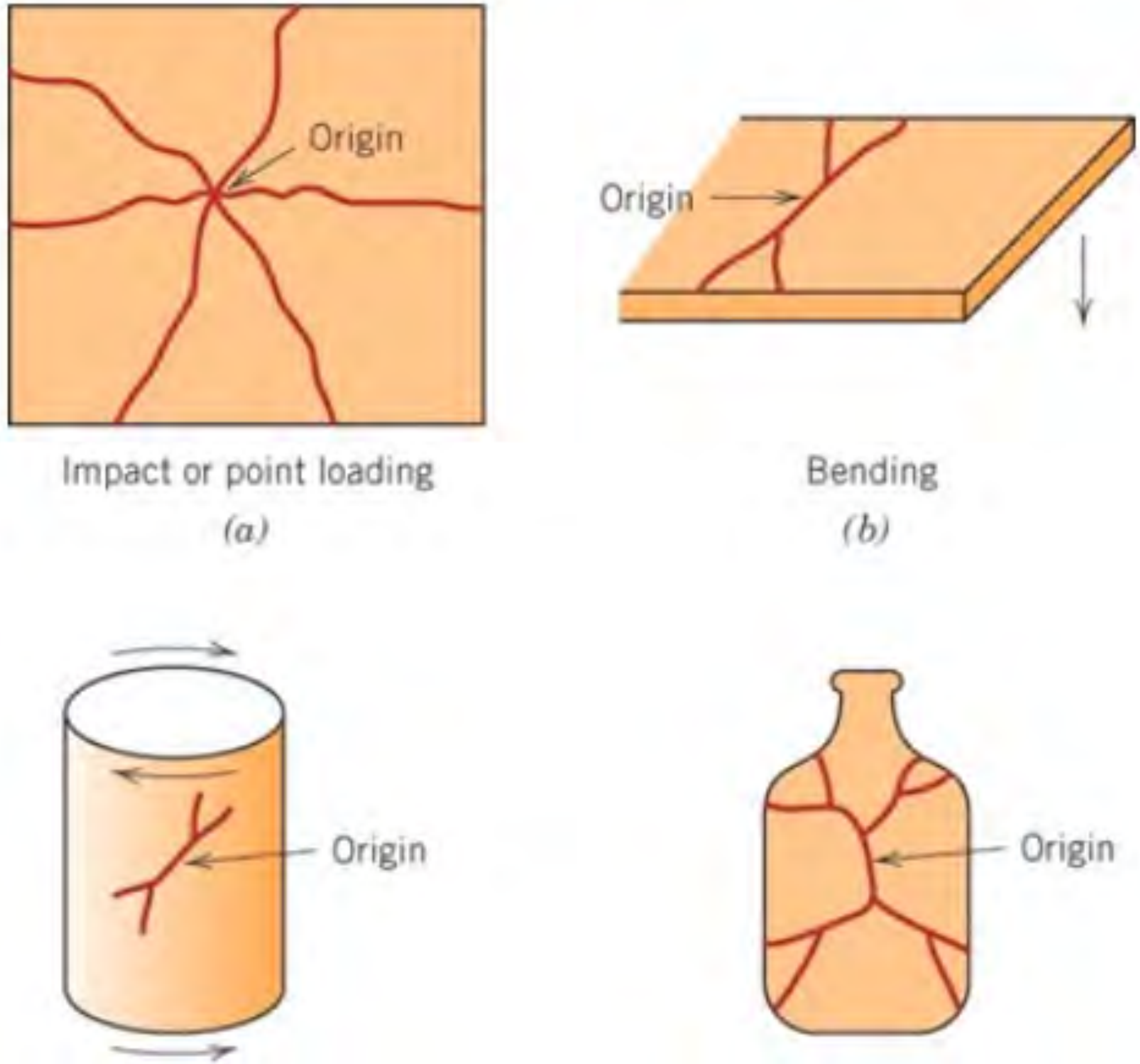

Impact or point loading (a) Bending (b) Torsion (c) Internal pressure (d)

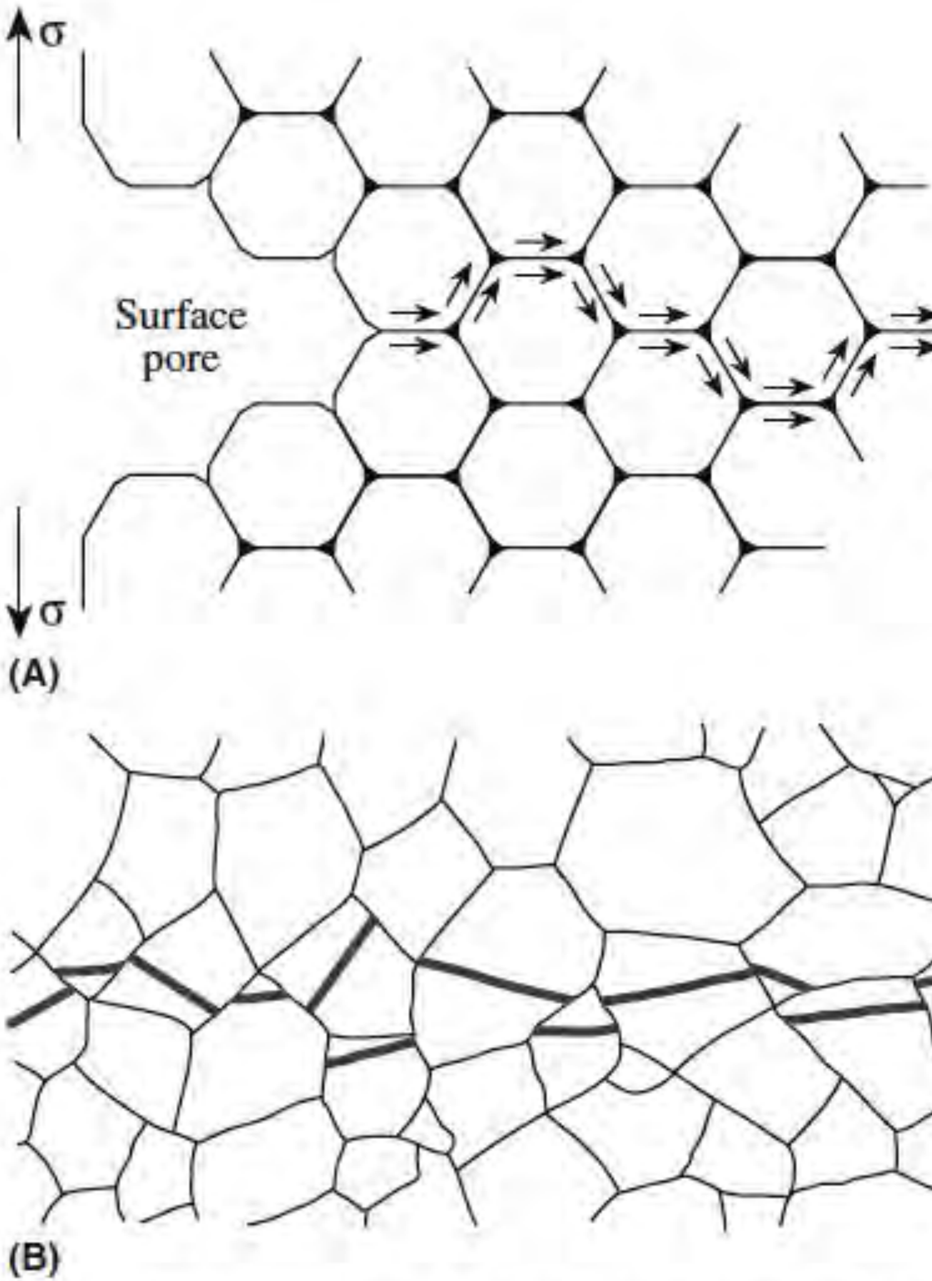

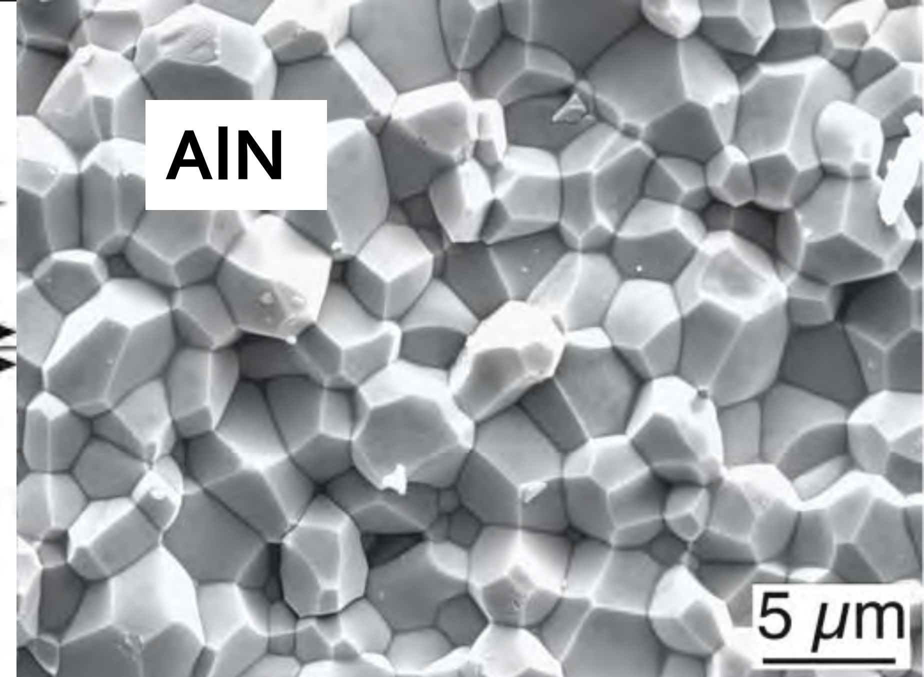

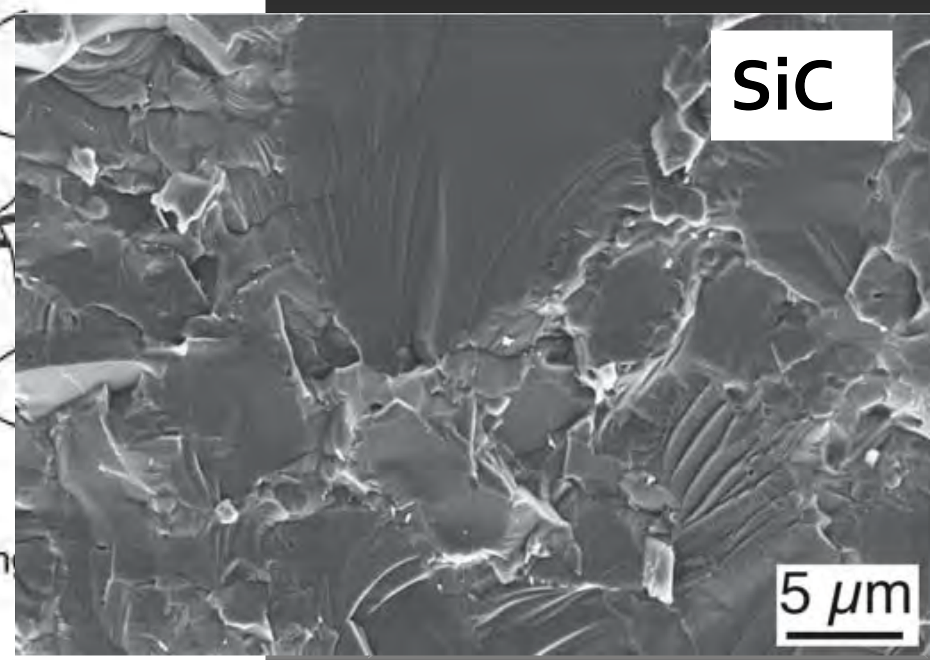

FIGURE 18.12 (a) Illustration of intergranular crackin
Illustration of transgranular cracking.

Undistinct features: brittle fracture (SiC)

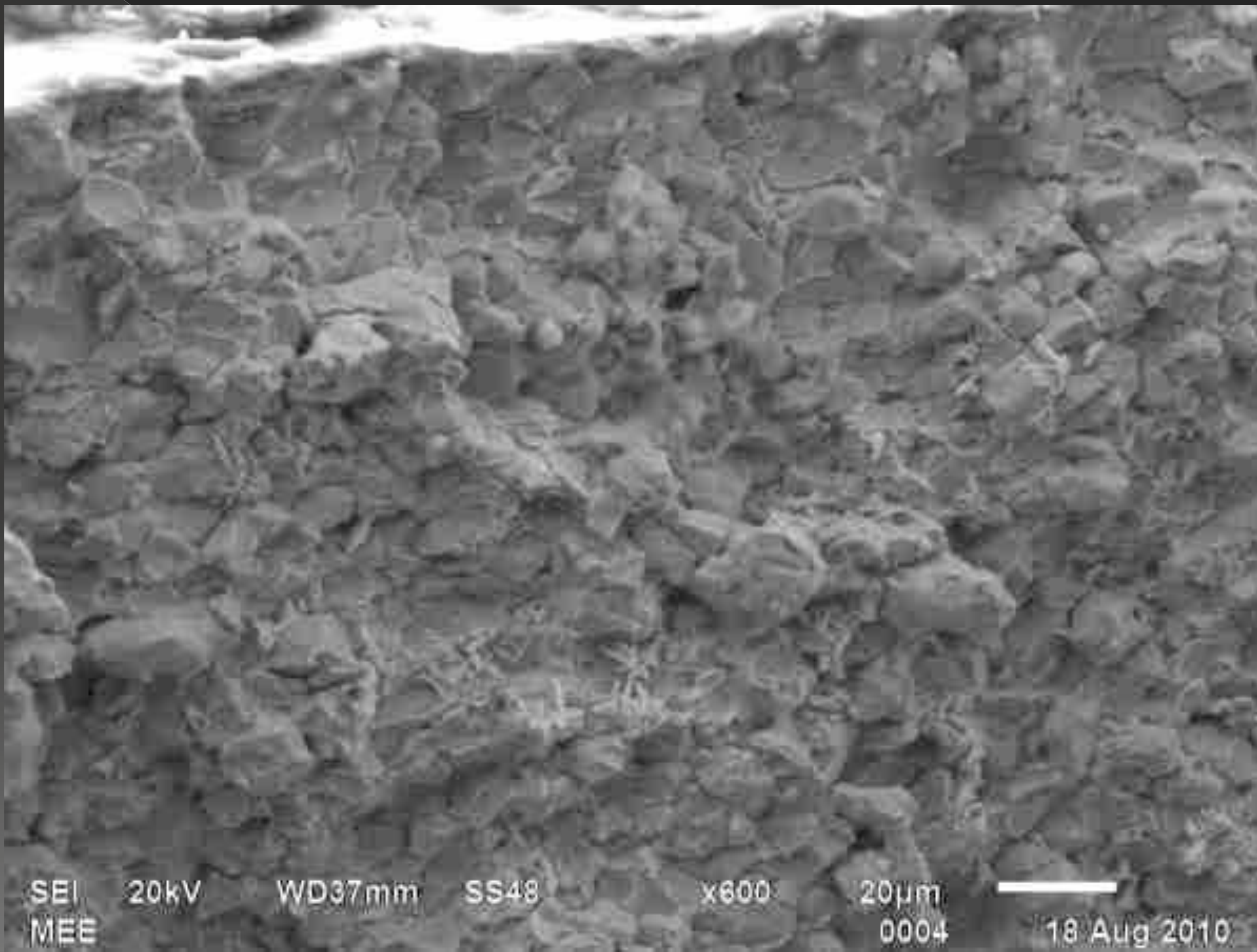

Fatigue

- Fracture surface with crack initiation at top. Surface shows predominantly dull fibrous texture where rapid failure occurred after crack achieved critical size.

- Fatigue failure
  1. Crack initiation
  2. Crack propagation
  3. Final failure

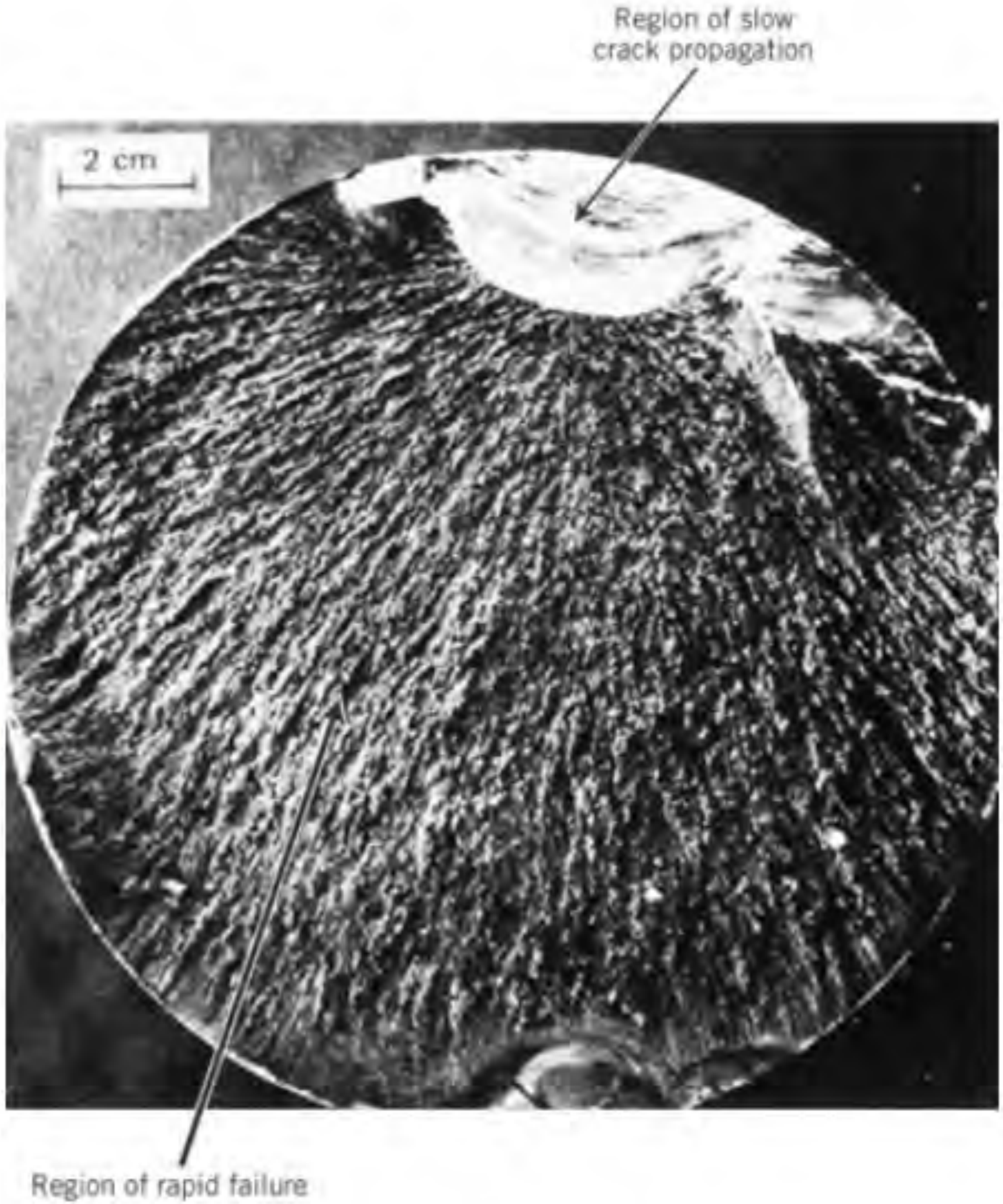

Brittle Fracture of Ceramics

- Surface of a 6-mm diameter fused silica rod.
- Characteristic fracture behavior in ceramics
  - Origin point
  - Initial region (mirror) is flat and smooth
  - After reaches critical velocity crack branches
    - mist
    - hackle

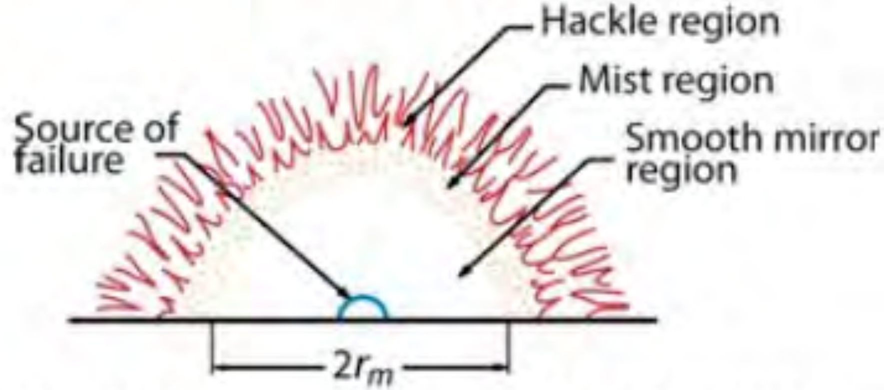

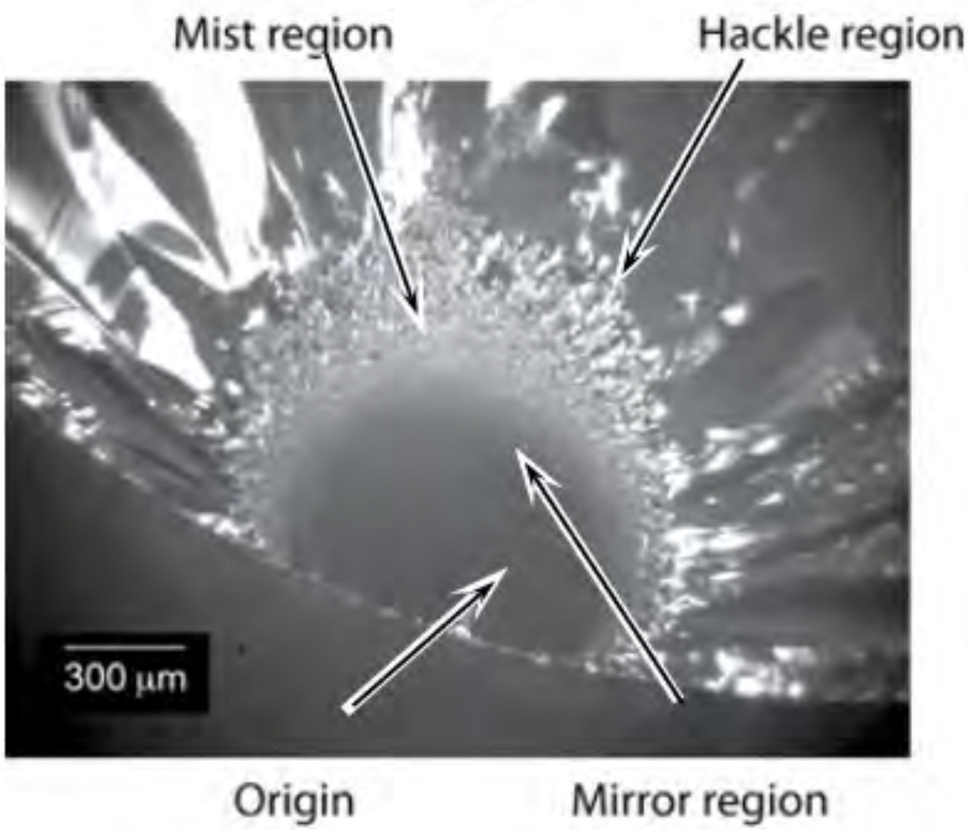

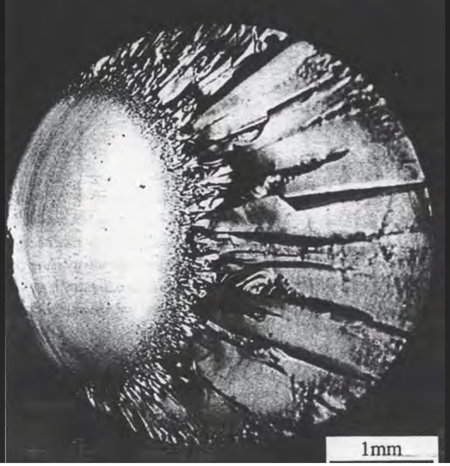
1mm

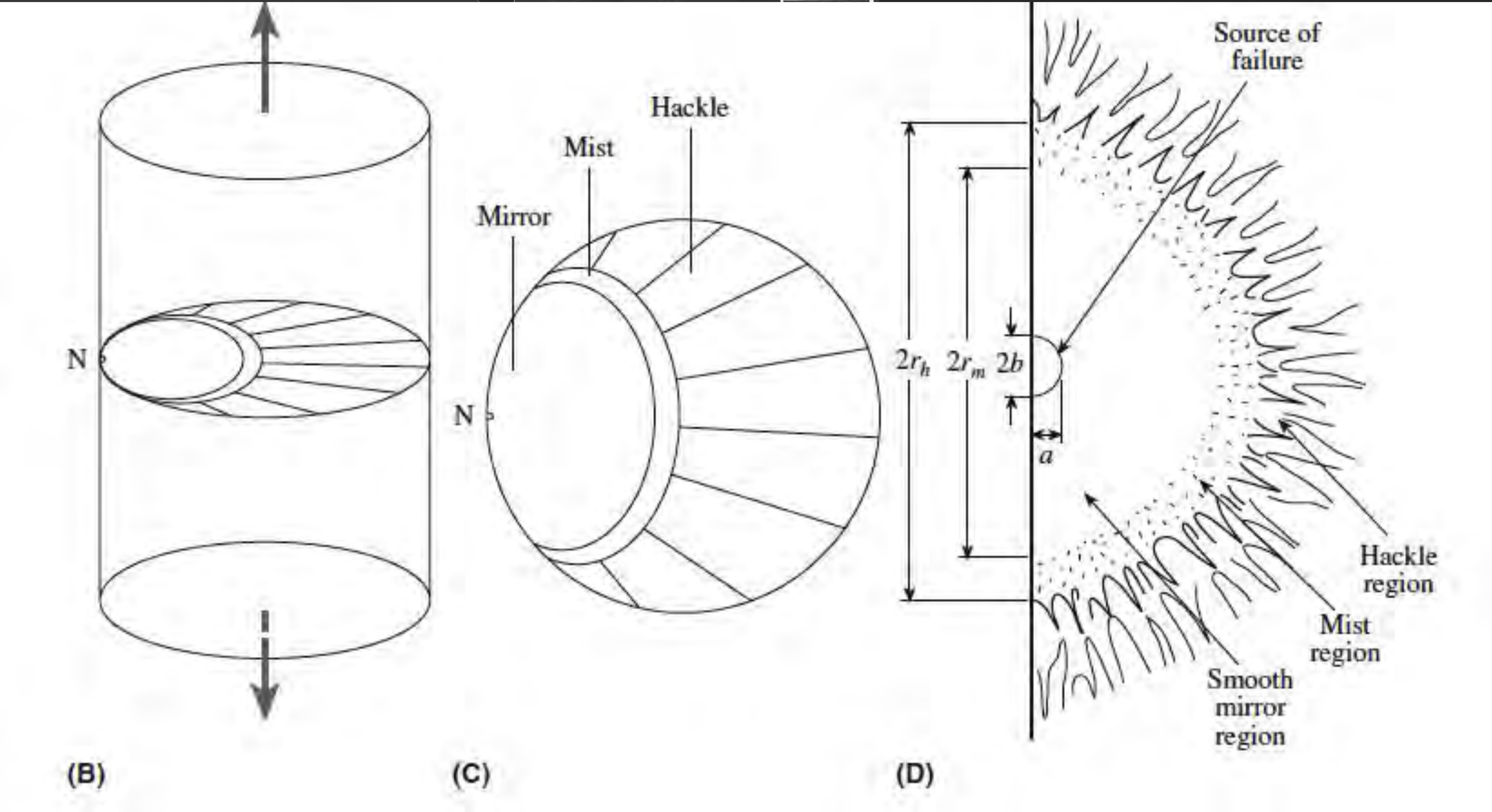
N
Hackle
Mist
Mirror
N
Source of failure
$2r_h$
$2r_m$
$2b$
a
Hackle region
Mist region
Smooth mirror region
(B)
(C)
(D)

Fracture of glass

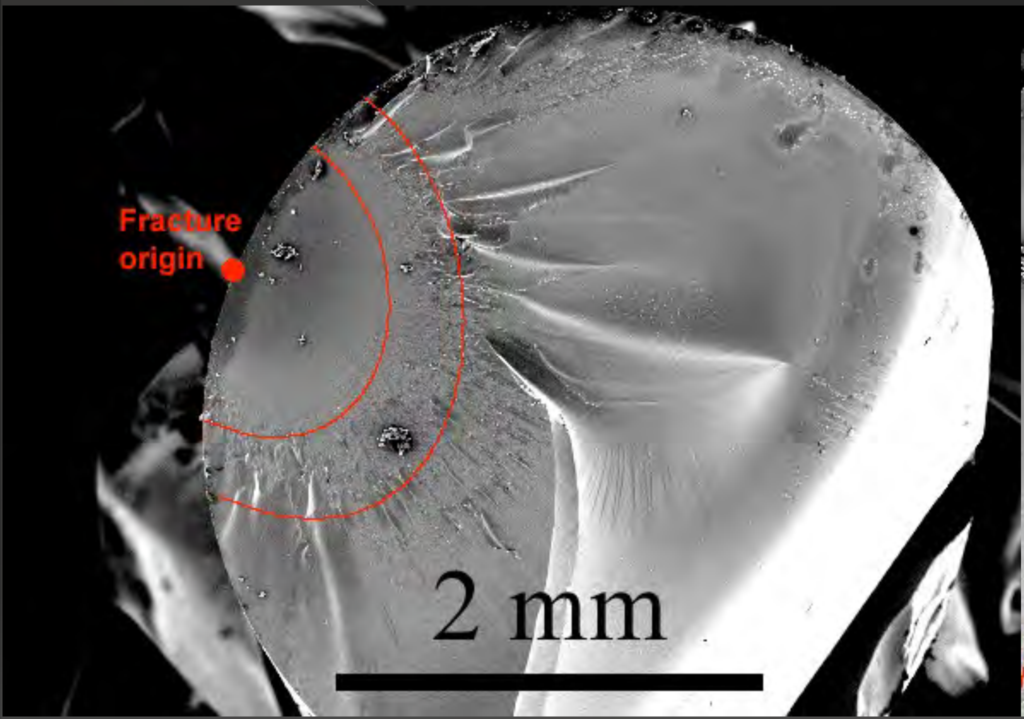

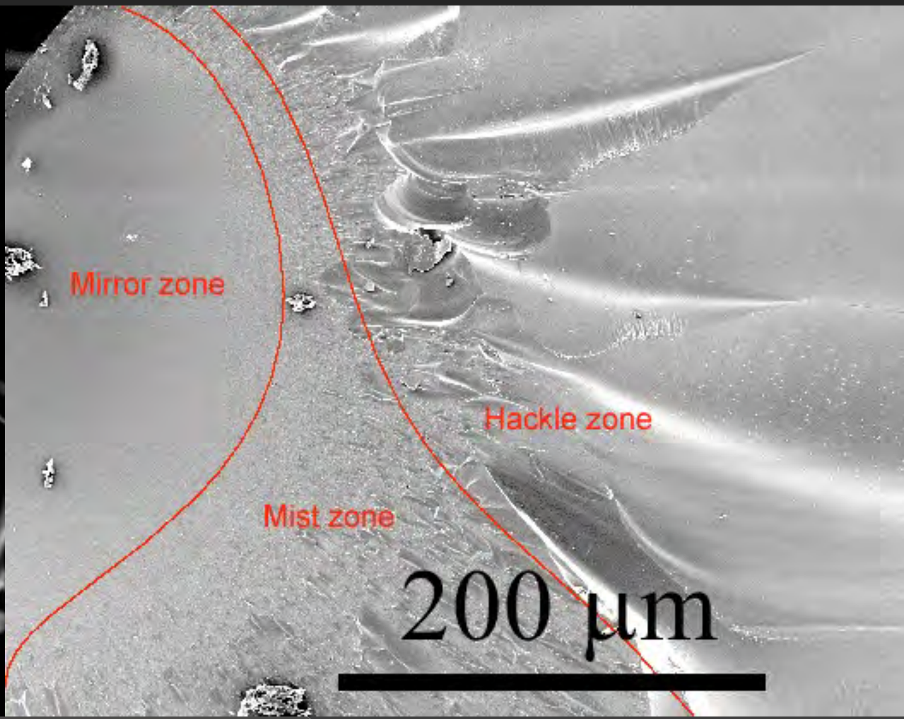

Fracture surface of silicon nitride with steel impurity

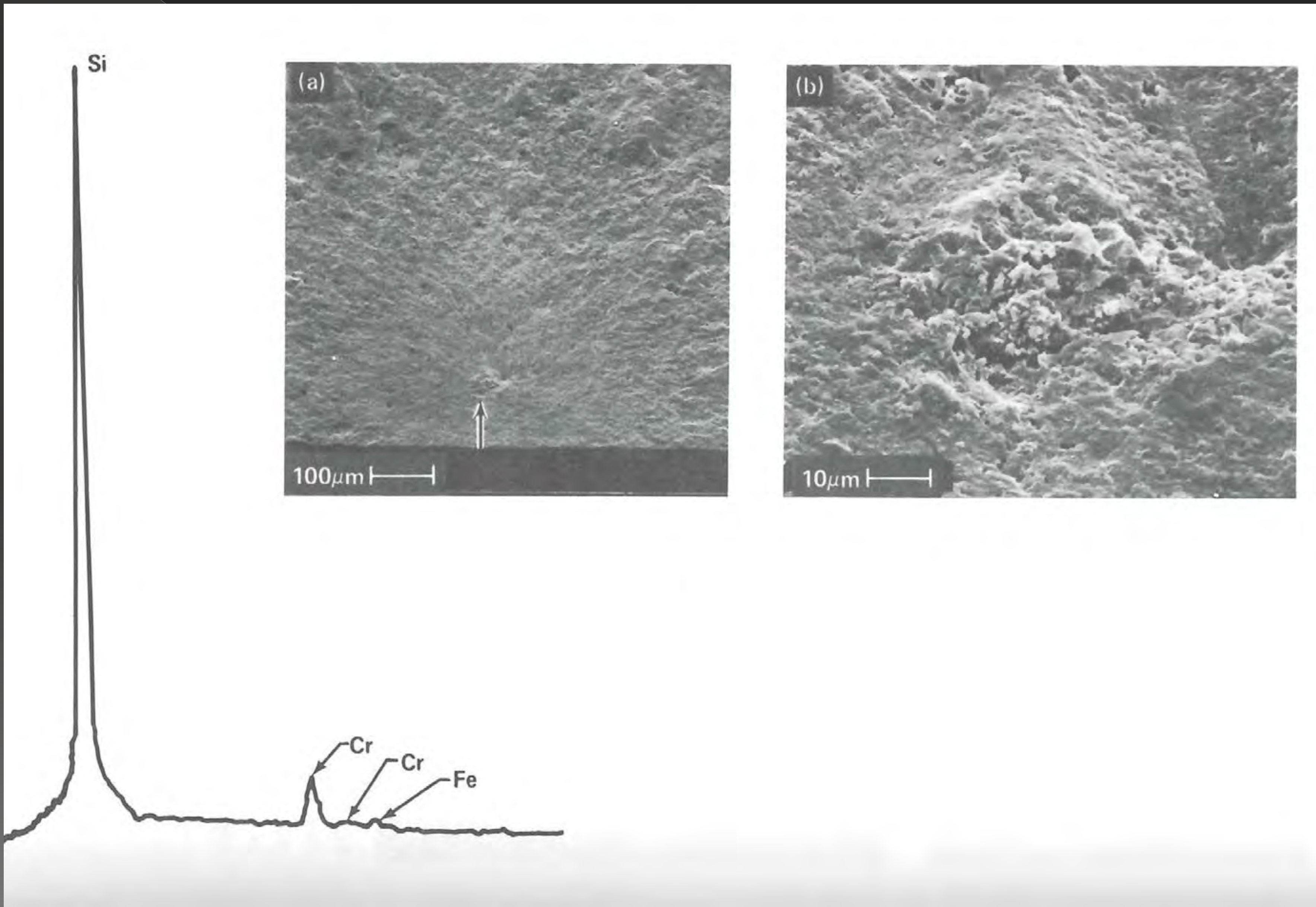

Fracture surface of lathe machined Silicon nitride

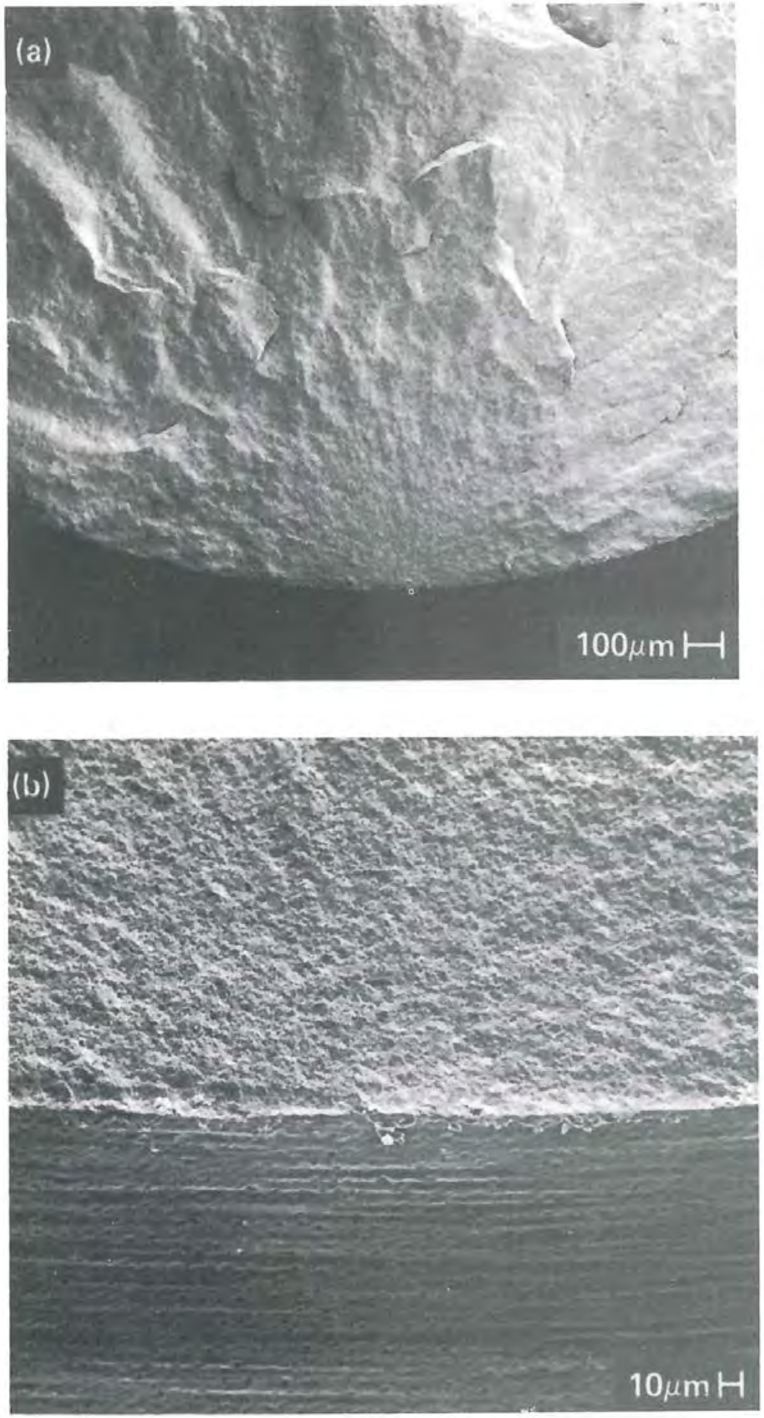

Roadmap for fractography

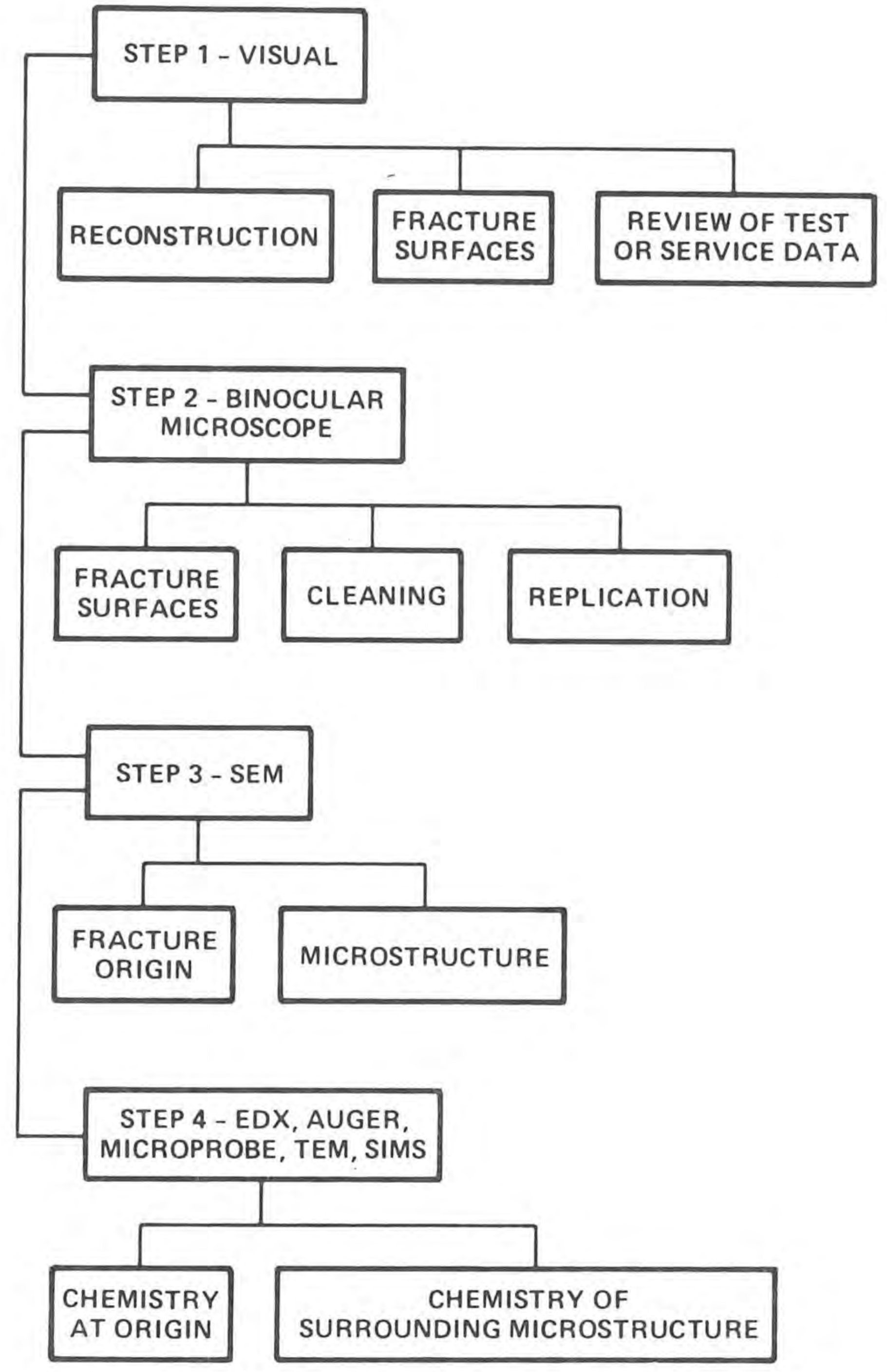

Roadmap for correcting failure

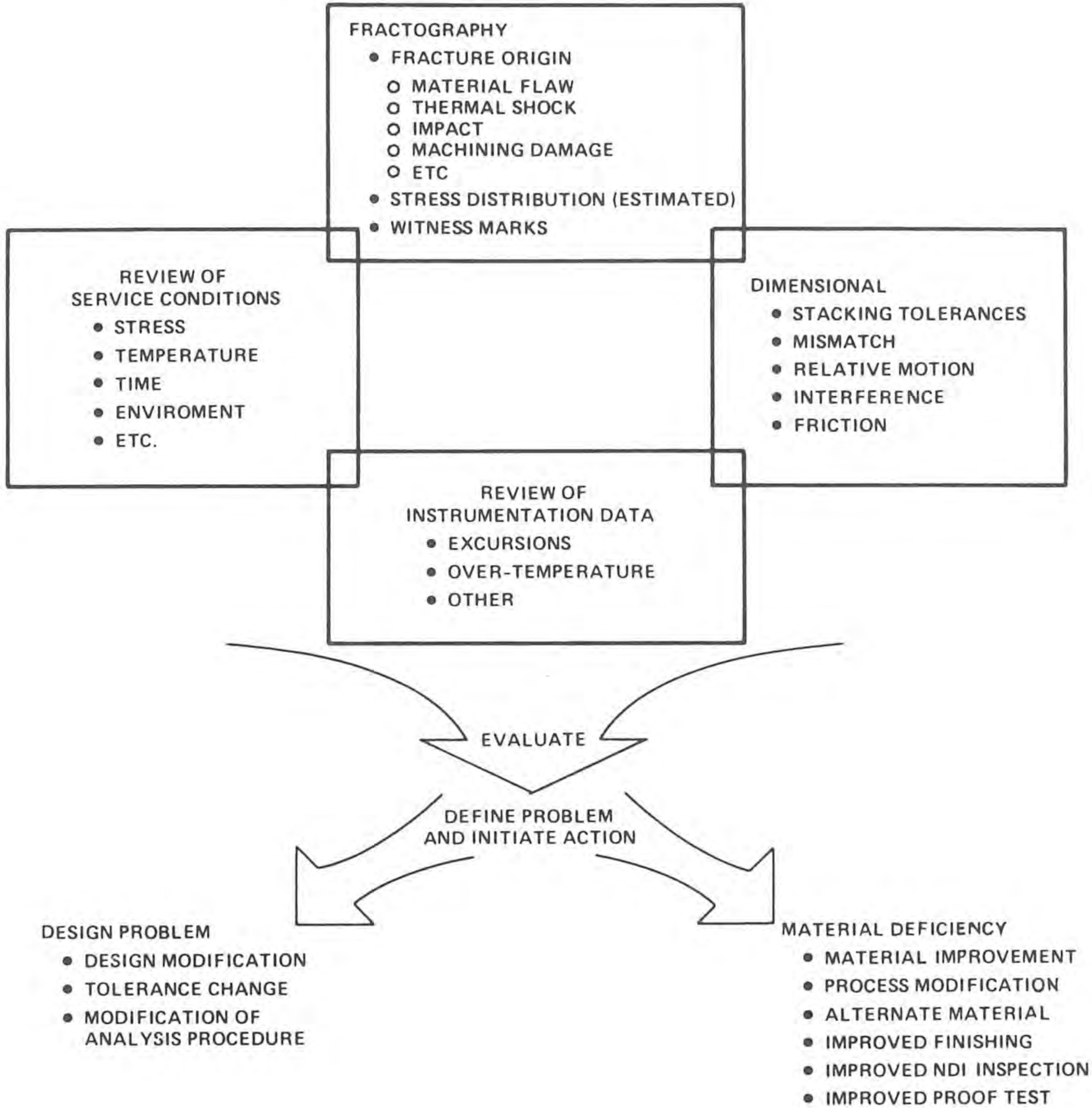

Toughening by whiskers and fibers

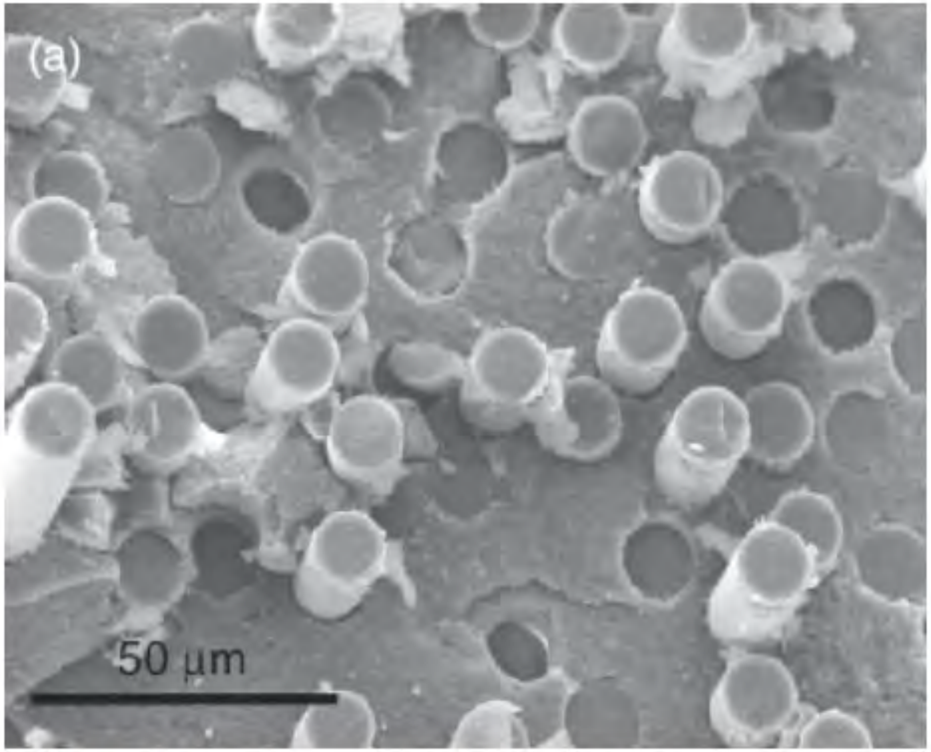

FIGURE 18.18 SEM image showing fiber pullout on the fracture surface of $AlPO_4$-coated alumina/mullite fiber/Al_2O_3 CMC, hot pressed at 1250°C for 1 h.

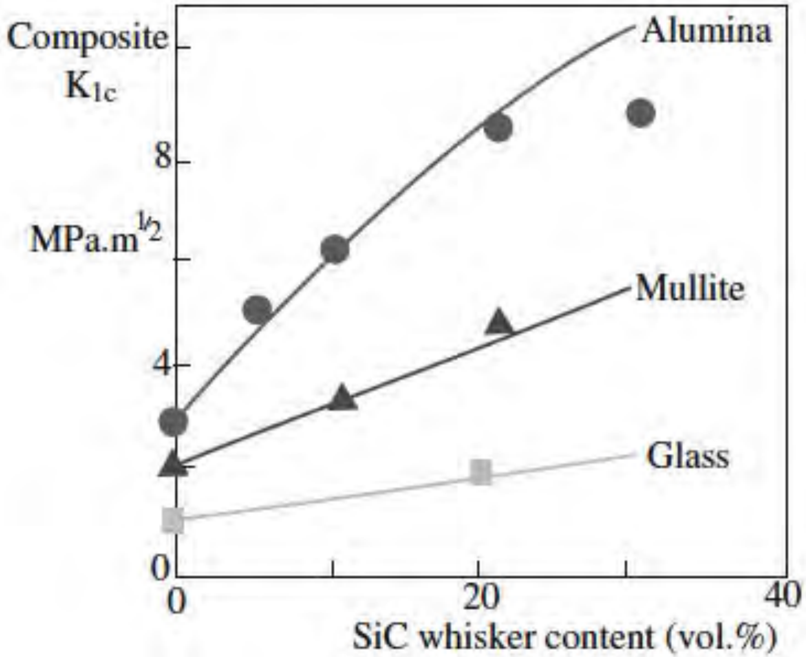

Glass theory

- Glasses lack the periodic (long range) order of a crystal
- •
- Infinite unit cell (no repeating large scale structures)
- •
- 3D network lacking symmetry and periodicity
- •
- ISOTROPIC: same average packing and properties in all directions
- •
- Crystals in different directions(see above):
- •
- different atom packing and so different properties

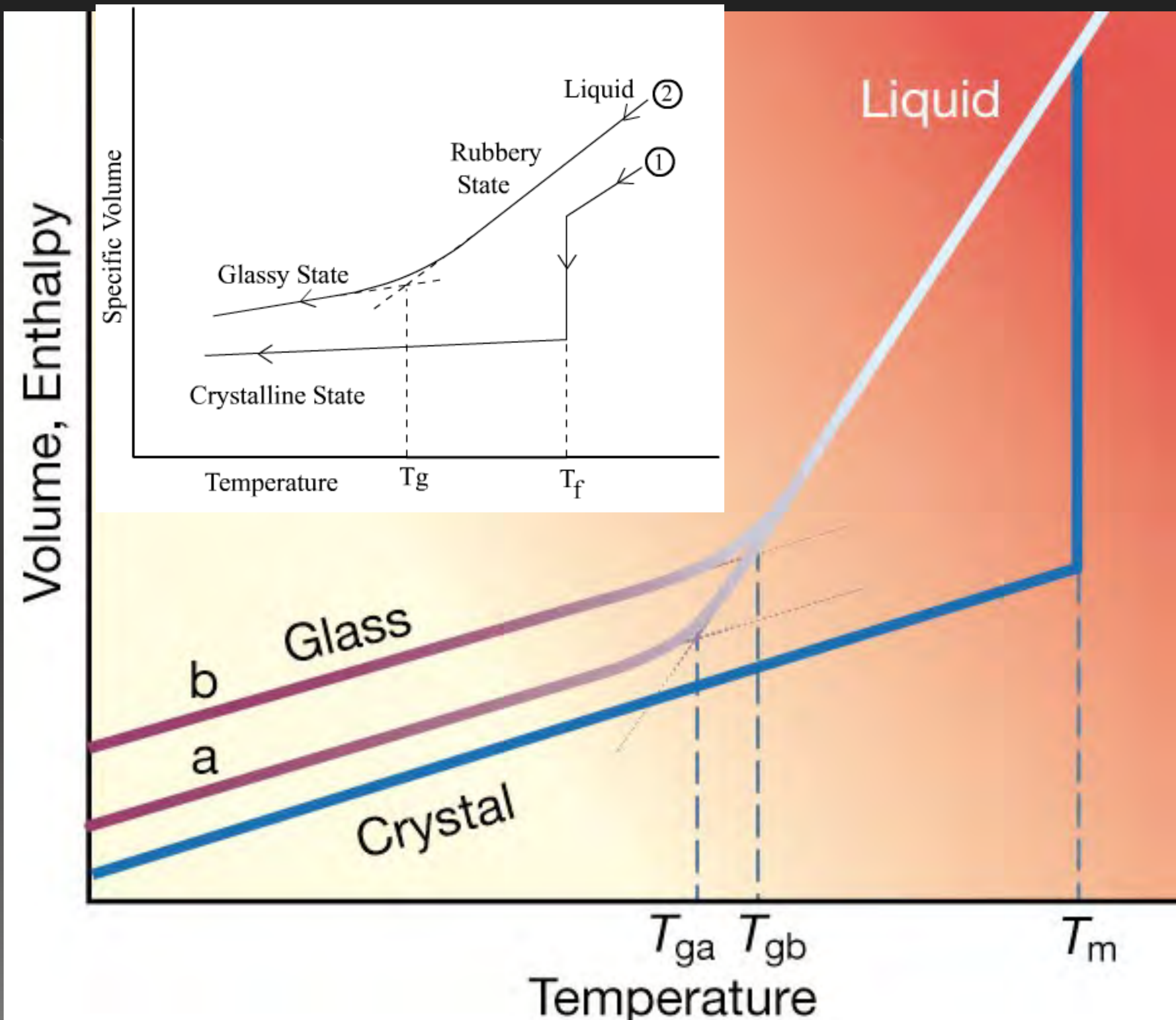
Liquid
Rubbery
State
Glassy State
Crystalline State
Specific Volume
Temperature
Tg
Tf
Liquid
Glass
b
a
Crystal
Volume, Enthalpy
Tga
Tgb
Tm
Temperature

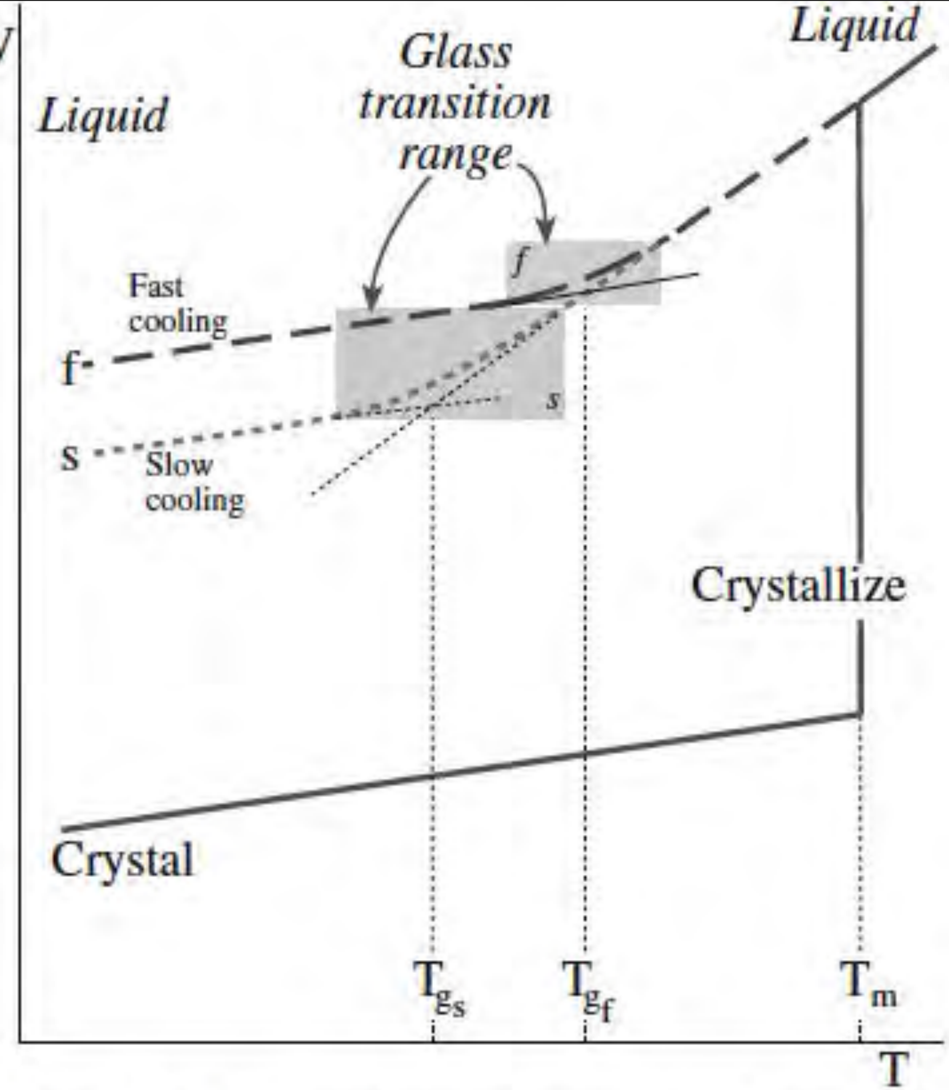

FIGURE 21.1 Plot of volume versus temperature for a liquid that forms a glass on cooling and one that forms a crystalline solid. The glass transition temperature, T_g, depends on the cooling rate and is not fixed like T_m.

Pair distribution function of SiO2 glass

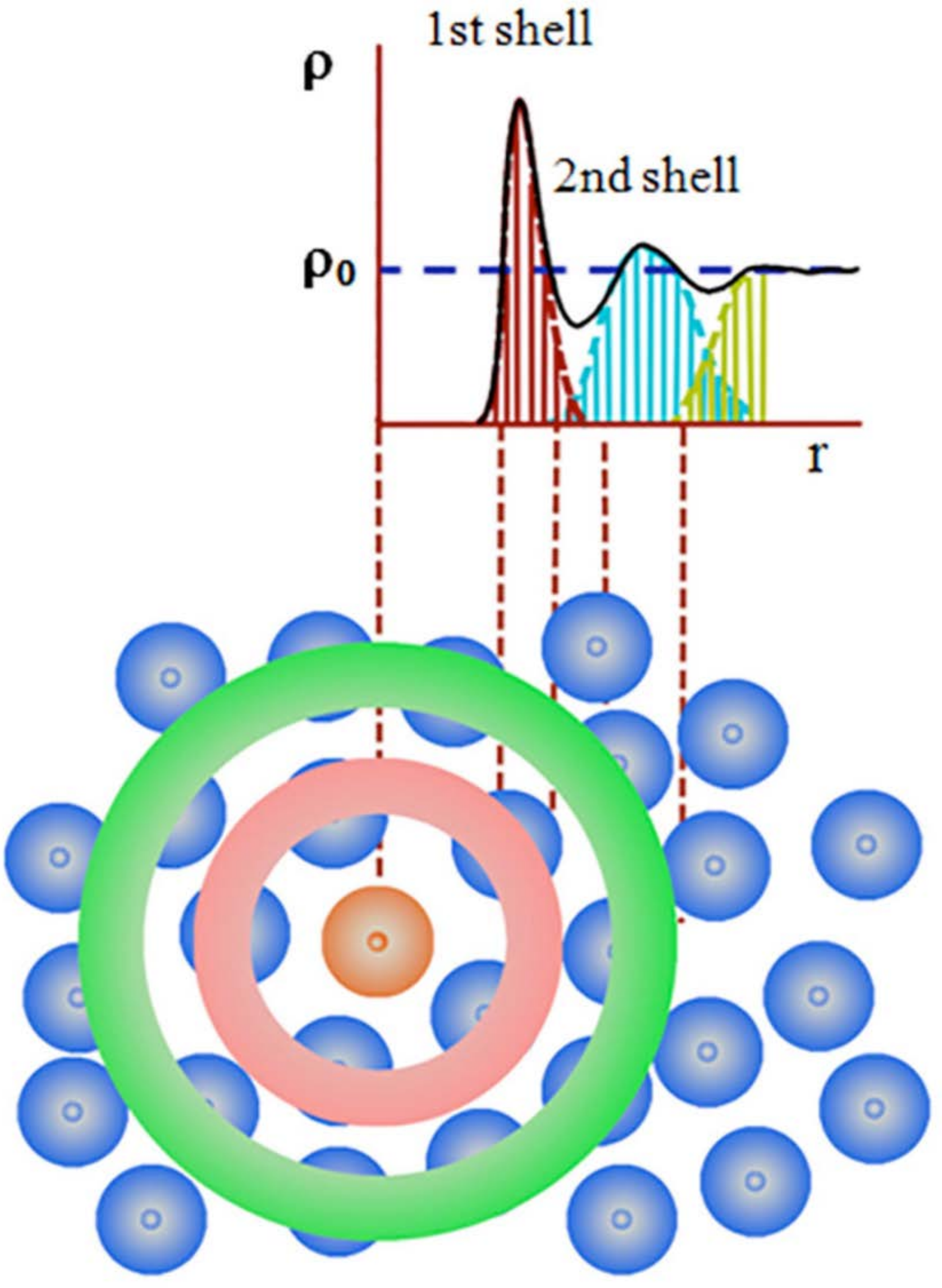

Radial distribution function for SiO_2

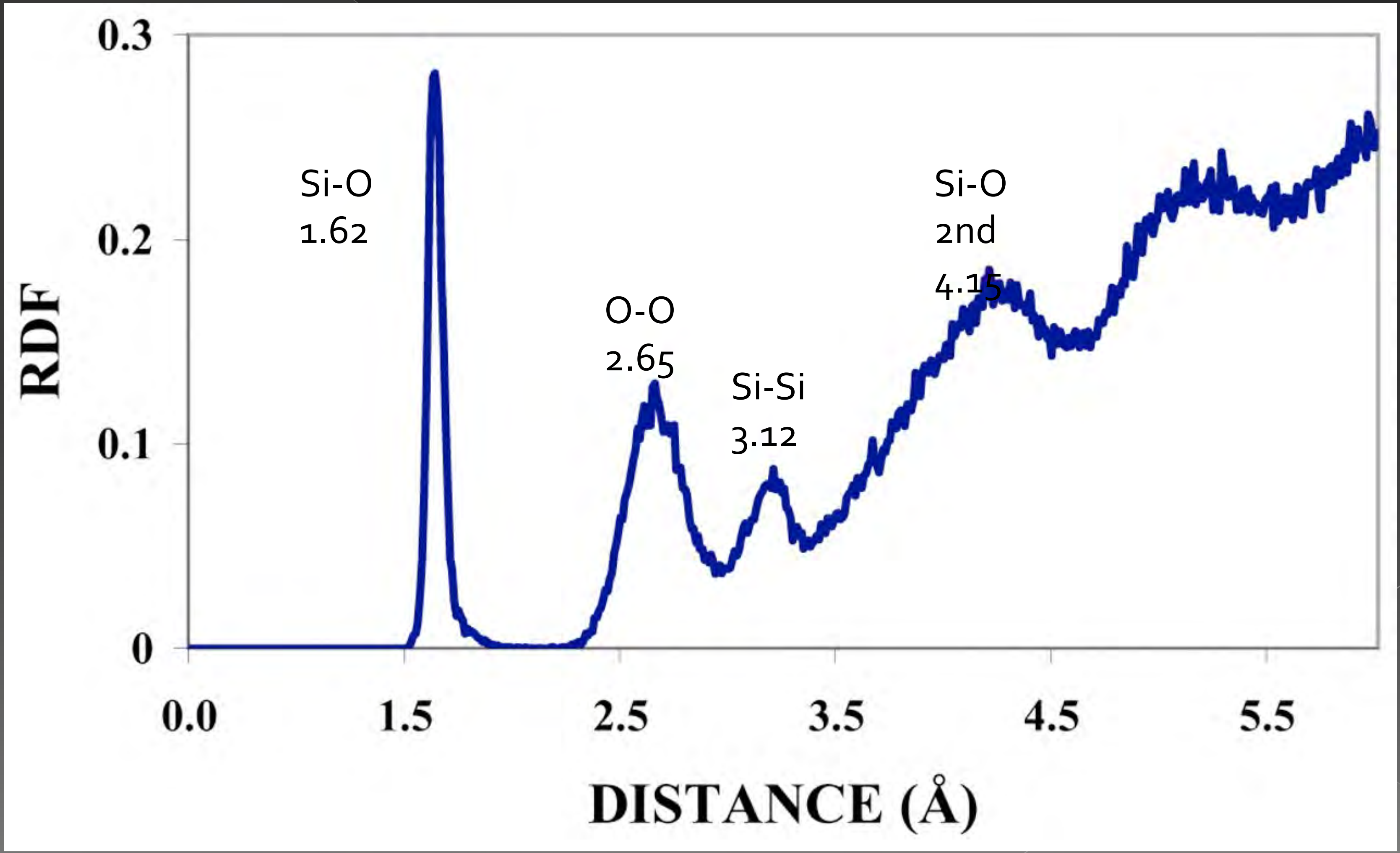

Glass structure:
SiO2 quartz compared to SiO2 glass

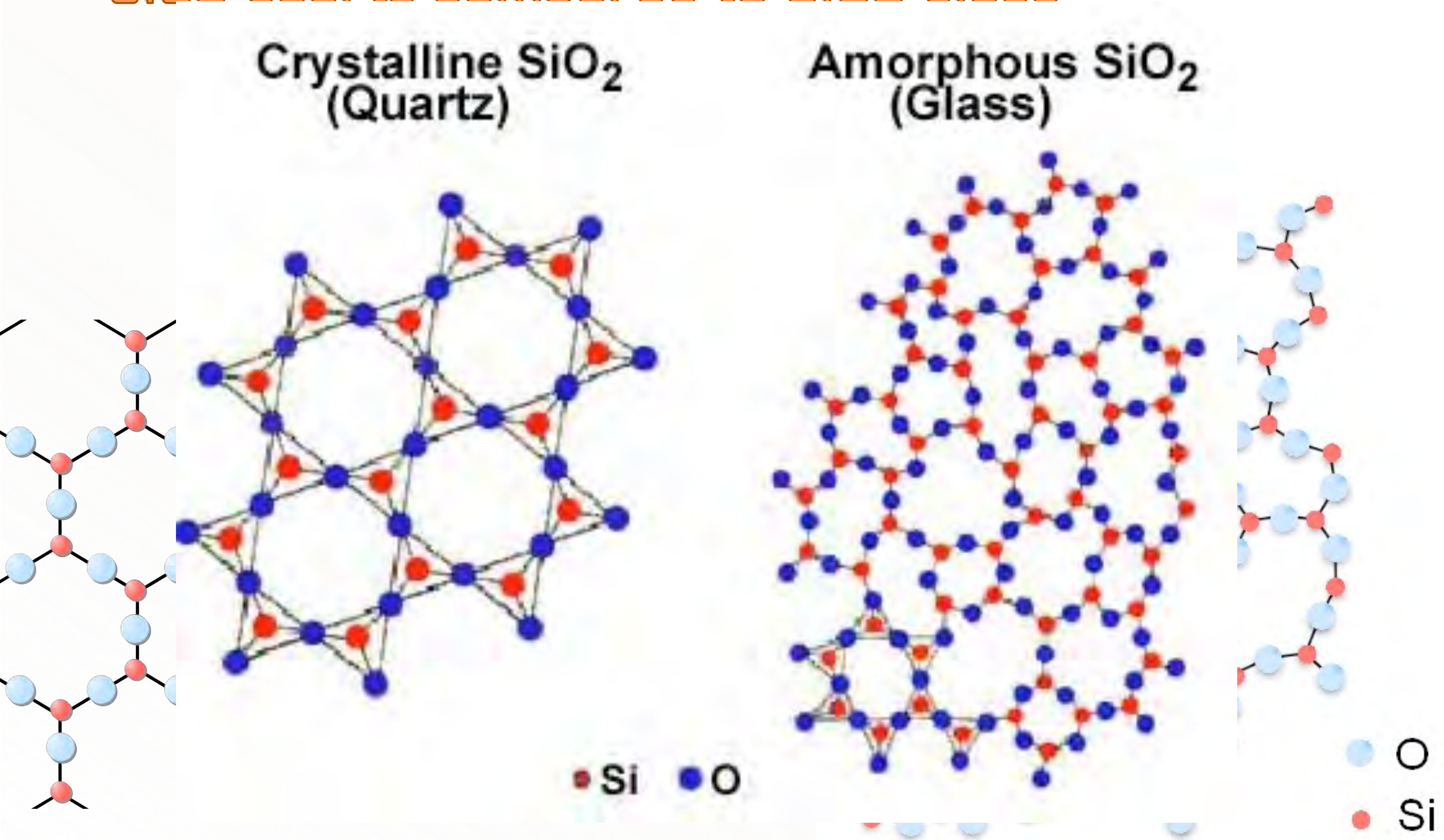

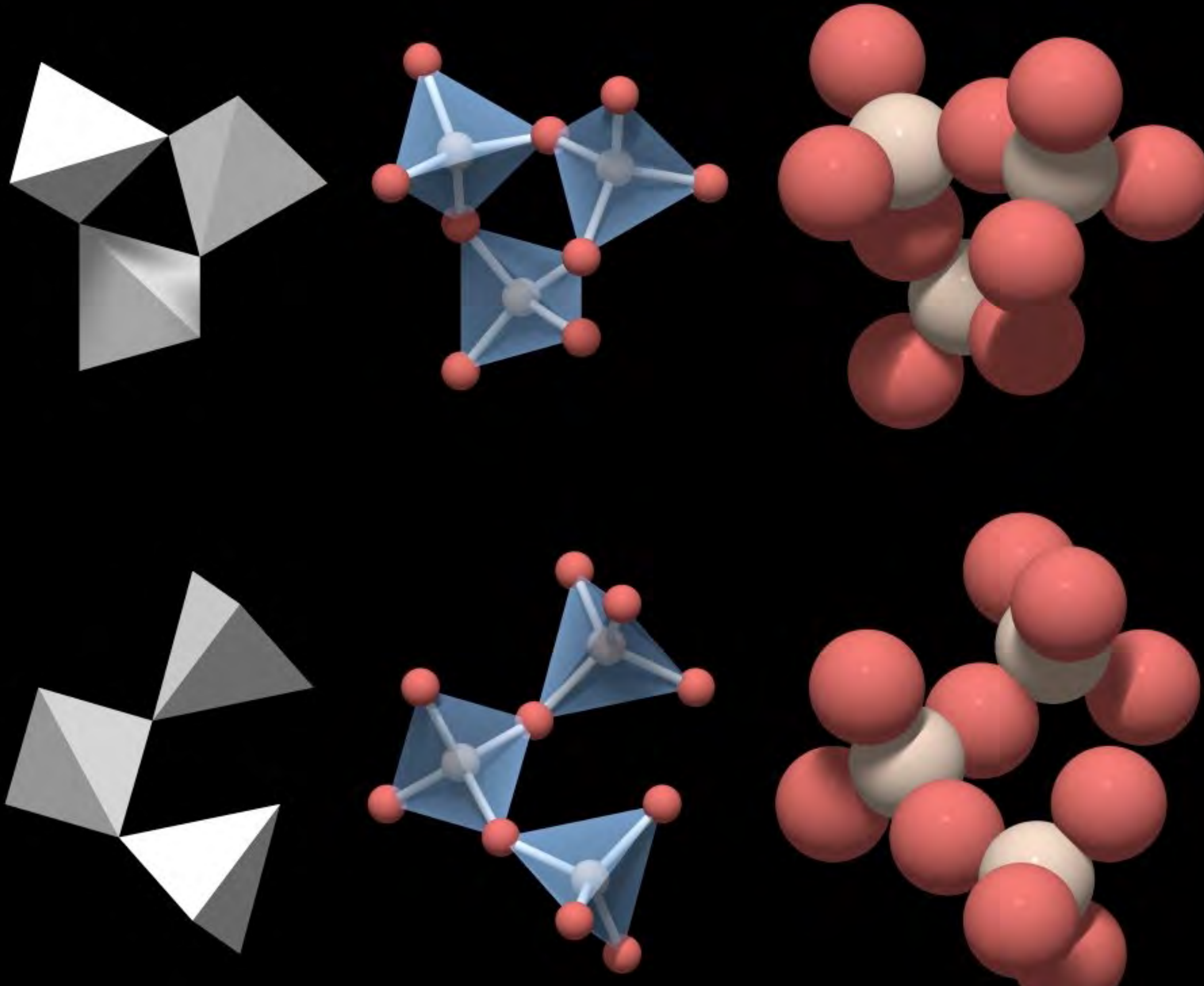

Zachariasen rules for glass A_mO_n

1) An oxygen atom is linked to no more than two glass-forming atoms A.
2) The number of oxygen atoms around each glass-forming atom A is small, perhaps 3 or 4.
3) Among the oxygen-containing polyhedra, a polyhedron cation A shares corners, but no sides or faces.
4) For three-dimensional networks of oxygen-containing polyhedra, at least three corners must be shared.

In general, all four rules should be satisfied for glass formation to occur.

Low coordination numbers, corner-sharing rules imply that glass formation is more likely with open, low density polyhedral structures.

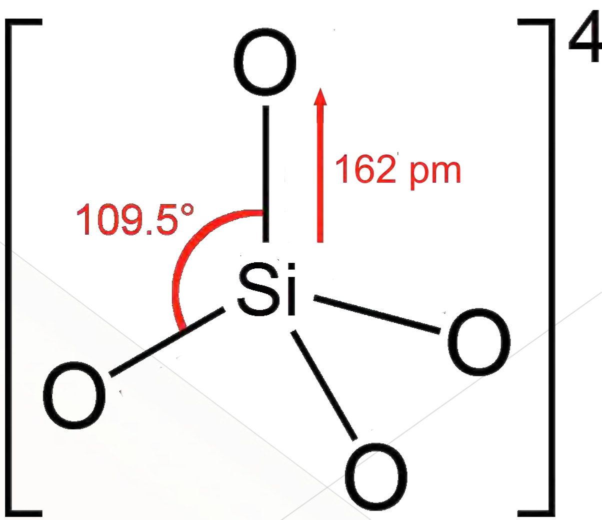

1. Consider Silica:
    - covalent Si-O bond: sp^3 hybrid
        - tetrahedral bonding
- Pauling's packing rule:

$$\frac{r(Si^{4+})}{r(O^{2-})} = \frac{0.40}{1.40} \approx 0.29 \quad \textit{prefers tetrahedral bonding}$$

- satisfies Zachariasen's rule #2.

$$\frac{charge(Si^{4+})}{CN(Si^{4+})} = \frac{4}{4} = \frac{charge(O^{2-})}{CN(O^{2-})} = \frac{2}{2} \quad CN(O^{2-}) \textit{ is } 2.$$

- satisfies Zachariasen's rule #1.

Crystal structure: sharing four corners:

All Rules are Satisfied: SiO_2 forms a glass.

β-cristobalite (SiO_2)

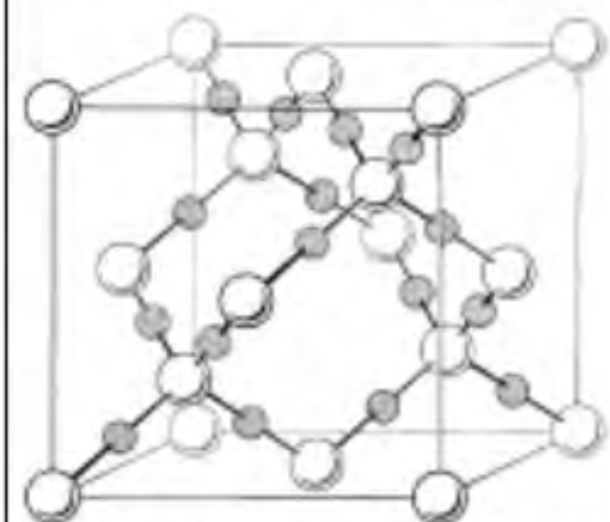

Cation CN:Anion CN = 4:2

2. Consider Magnesia (MgO):

- ionic Mg-O bond
  - Pauling's packing rule:

$$\frac{r(Mg^{2+})}{r(O^{2-})} = \frac{0.72}{1.40} \approx 0.51 \quad \textit{prefers octahedral bonding}$$

  - violates Zachariasen's rule #2.

$$\frac{charge(Mg^{2+})}{CN(Mg^{2+})} = \frac{2}{6} = \frac{charge(O^{2-})}{CN(O^{2-})} = \frac{2}{6} \quad CN(O^{2-}) \textit{ is } 6.$$

  - violates Zachariasen's rule #1.

Crystal structure: edge-sharing polyhedra;
Rules are Not Satisfied: MgO does not form a glass.

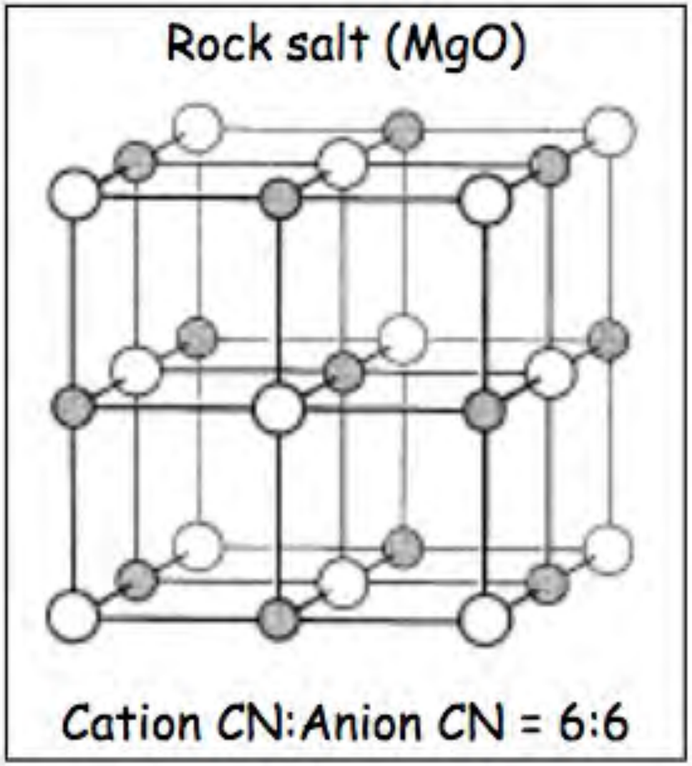

3. Consider Alumina (Al_2O_3):

- Pauling's packing rule:

$$\frac{r(Al^{3+})}{r(O^{2-})} = \frac{0.53}{1.40} \approx 0.38 \qquad \textit{octahedral / tetrahedral boundary}$$

- octahedral CN preferred in Al_2O_3.

$$\frac{charge(Al^{3+})}{CN(Al^{3+})} = \frac{3}{6} = \frac{charge(O^{2-})}{CN(O^{2-})} = \frac{2}{4} \qquad CN(O^{2-}) \text{ is } 4.$$

- violates Zachariasen's rule #1.

Al_2O_3 does not form a glass.

Elements for glass formation

Formers	Modifiers	Intermediate
B	Sc	Ti
Si	La	Zr
Ge	Na	Pb
Al	K	Al
V	Rb	Th
As	Cs	

Log Glass Viscosity vs. Temperature

- Viscosity decreases with *T*

- soda-lime glass: 70% SiO_2 balance Na_2O (soda) & CaO (lime)
- borosilicate (Pyrex): 13% B_2O_3, 3.5% Na_2O, 2.5% Al_2O_3
- Vycor: 96% SiO_2, 4% B_2O_3
- fused silica: > 99.5 wt% SiO_2

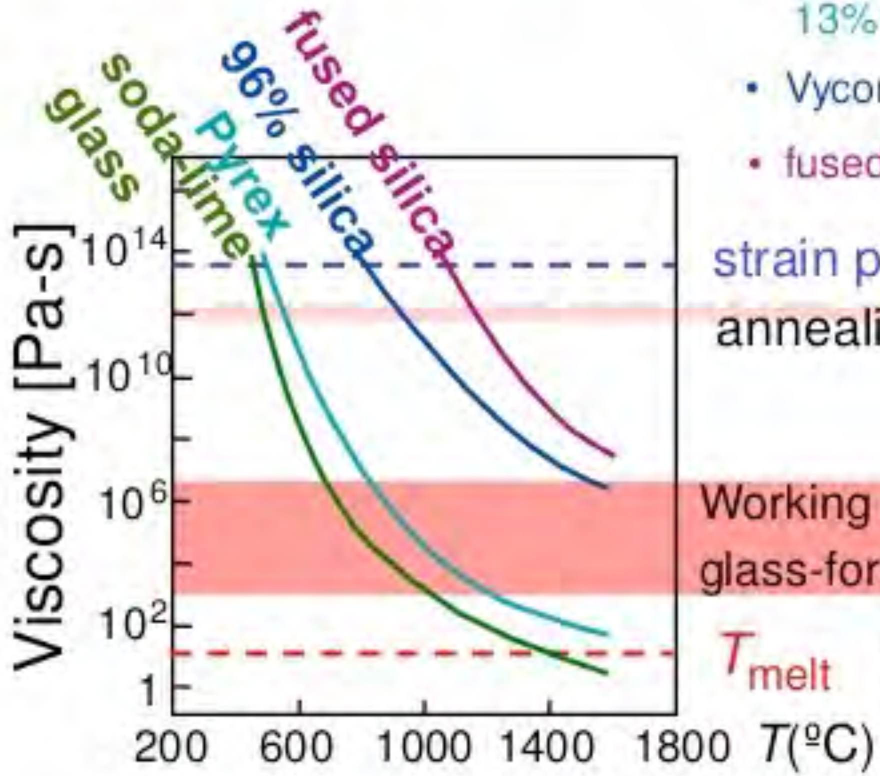

Adapted from Fig. 13.7, *Callister & Rethwisch 8e.* (Fig. 13.7 is from E.B. Shand, *Engineering Glass*, Modern Materials, Vol. 6, Academic Press, New York, 1968, p. 262.)

Glass Viscosity and Workability

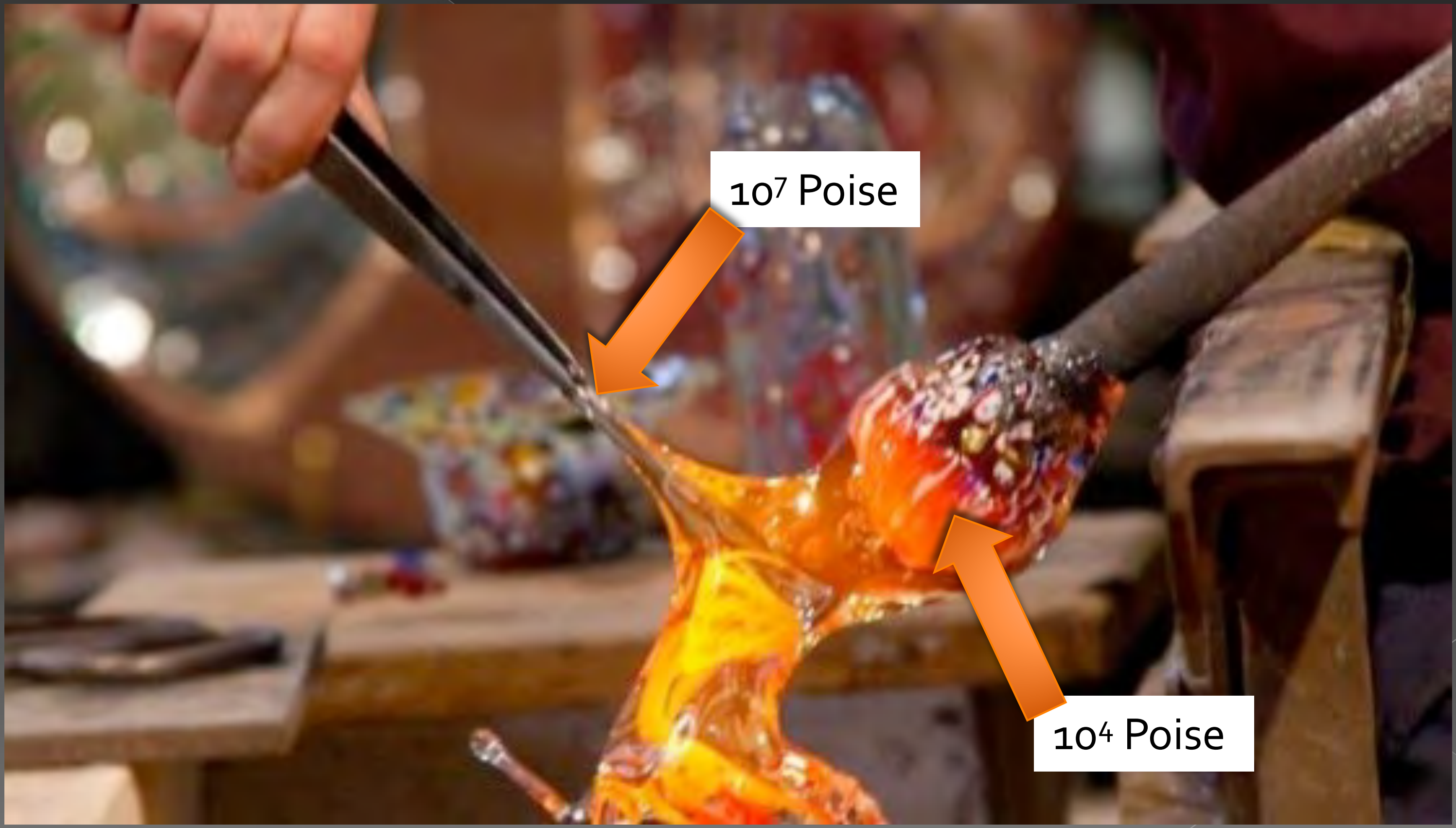

Pilkington process

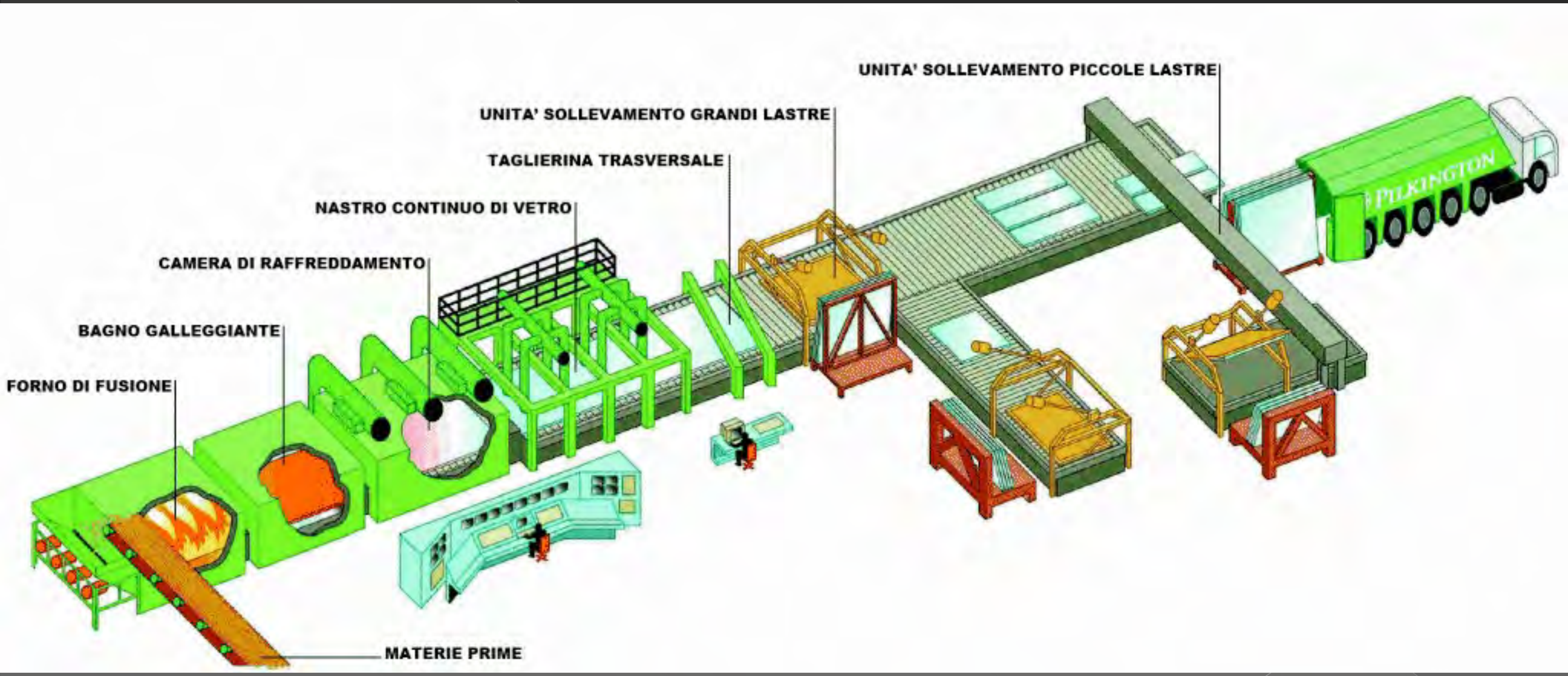

https://www.youtube.com/watch?v=ig4G5WbOMLc

Glass bending

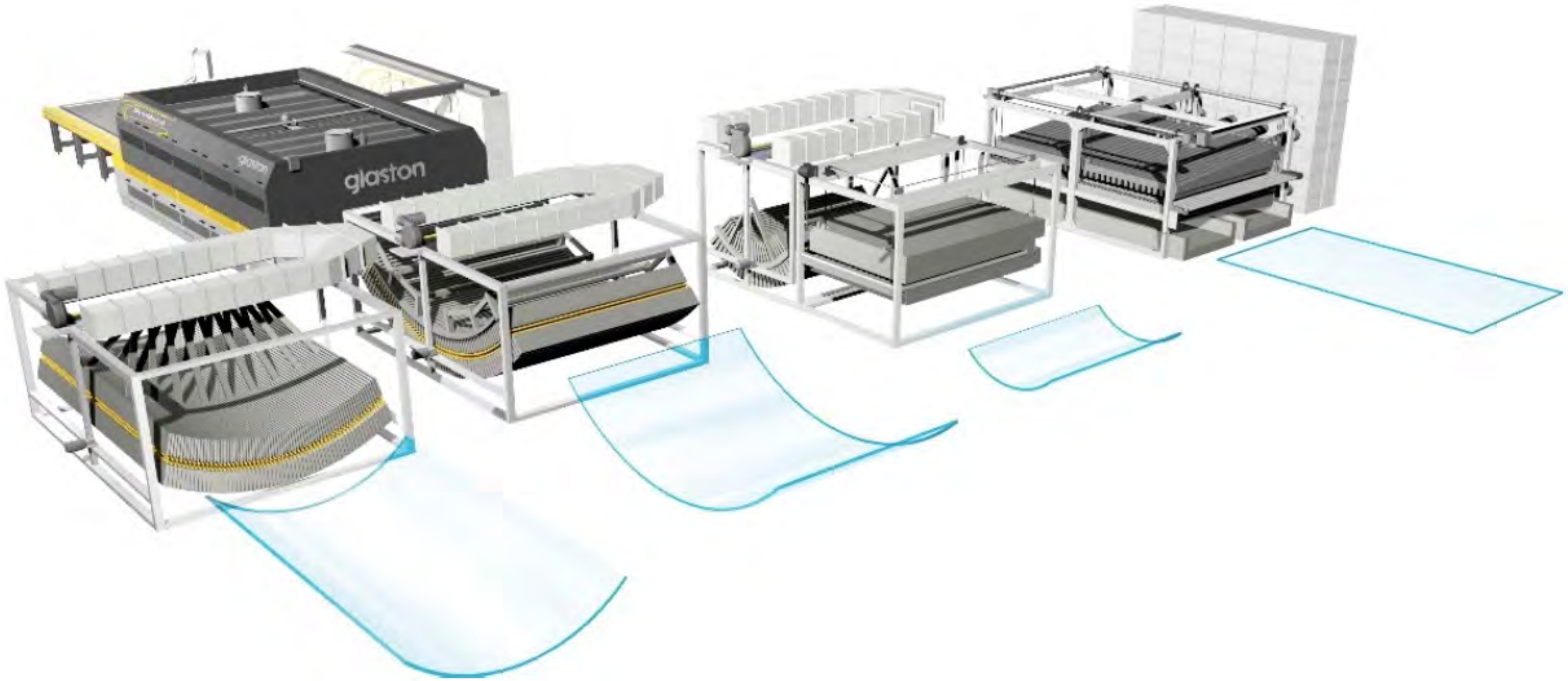

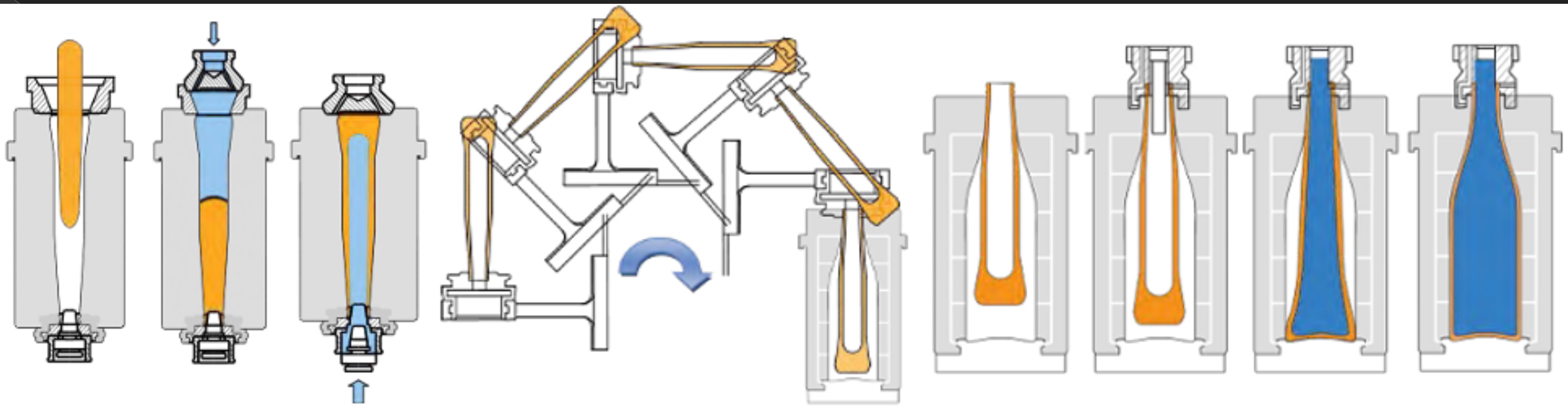

Bottle production line

http://www.youtube.com/watch?v=A_M8WBJMcMo

Functional ceramics

- Insulators: Al_2O_3, BeO, AlN
- Conductors (+ and -): $LaCrO_3$, ZnO, ITO, ZrO_2
- Dielectrics: $BaTiO_3$
- Ferroelectrics: $BaTiO_3$
- Piezoelectrics: PZT
- Pyroelectrics: $LiTaO_3$, PZT
- Magnets
- Optics

Dielectrics

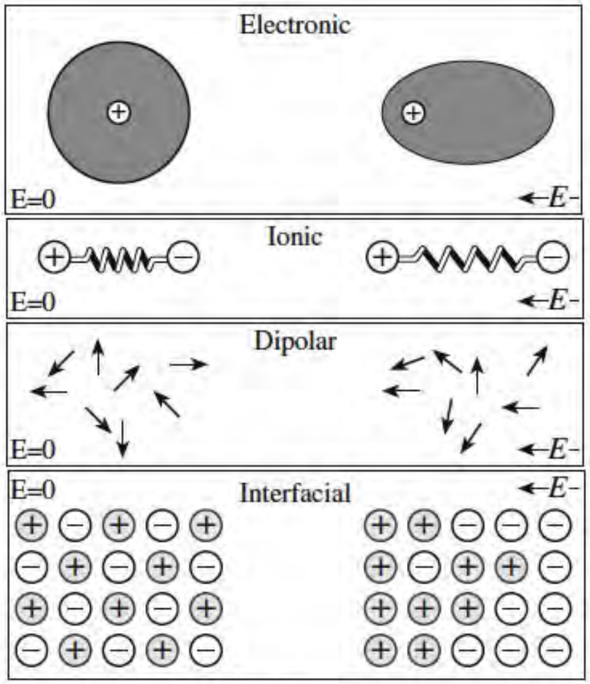

FIGURE 31.1 Illustration of the different polarization mechanisms in a solid.

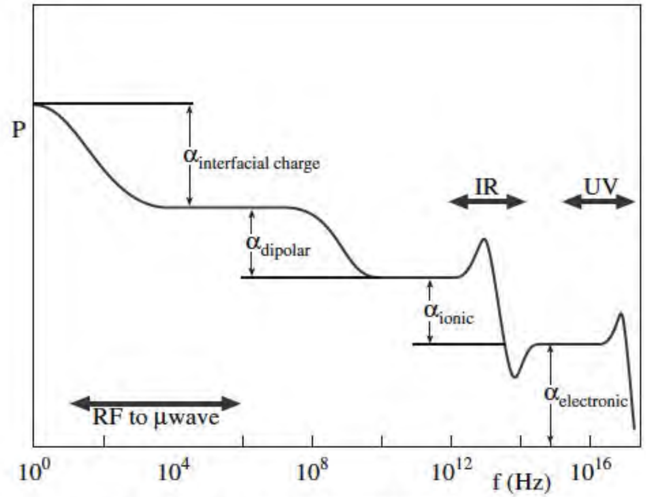

FIGURE 31.2 Frequency dependence of polarization.

TABLE 31.2 Dielectric Constants of Various Ceramics

Material	*κ at 1 MHz*	*Material*	*κ at 1 MHz*
Diamond	5.5–6.6	Al_2O_3	8.8
SiO_2	3.7–3.8	MgO	9.6
NaCl	5.9	$BaTiO_3$	3000
Mica	5.4–8.7	Pyrex glass	4.0–6.0
Soda-lime glass	7.0–7.6	TiO_2	14–110
Steatite (SiO_2 + MgO + Al_2O_3)	5.5–7.5	Forsterite ($2MgO \cdot SiO_2$)	6.2
Cordierite (SiO_2 + MgO + Al_2O_3)	4.5–5.4	Mullite	6.6
High-lead glass	19		

TABLE 31.4 Dielectric Strengths for Various Ceramics

Material	*Dielectric strength (MV/cm at 25°C)*
Al_2O_3 (99.5%)	0.18
Al_2O_3 (94.0%)	0.26
High-voltage porcelain	0.15
Steatite porcelain	0.10
Lead glass	0.25
Lime glass	2.5
Borosilicate glass	5.8
Fused quartz	6.6
Quartz crystal	6.0
NaCl [100], [111], [110]	2.5, 2.2, 2.0
Muscovite mica	10.1

$BaTiO_3$ cristalline structure

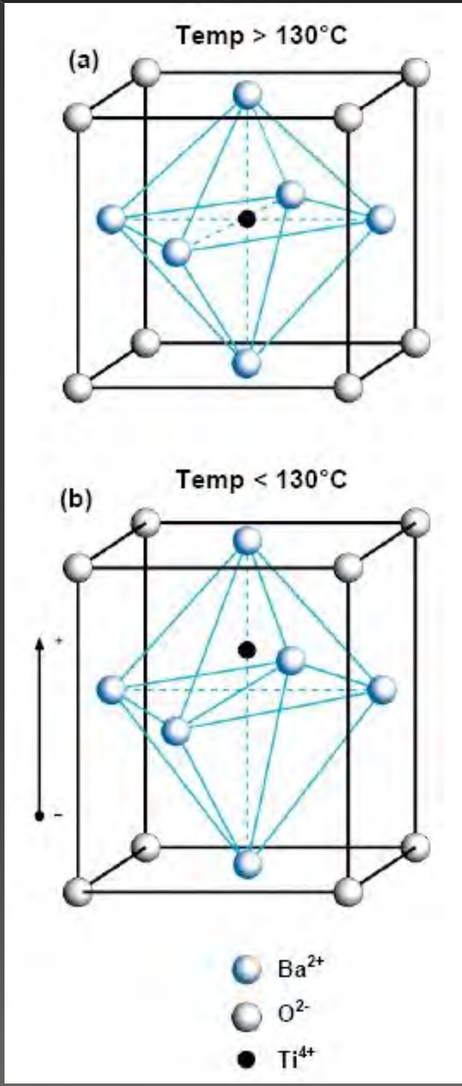

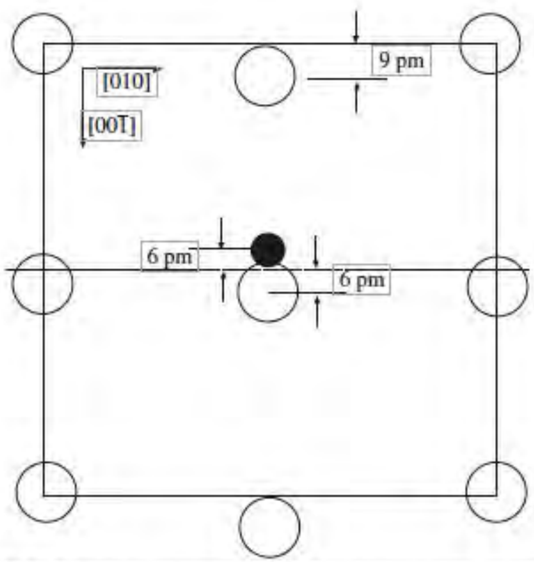

FIGURE 31.7 [100] projection of $BaTiO_3$ showing ion displacements below θ_c (not to scale).

Dielectric constant of $BaTiO_3$

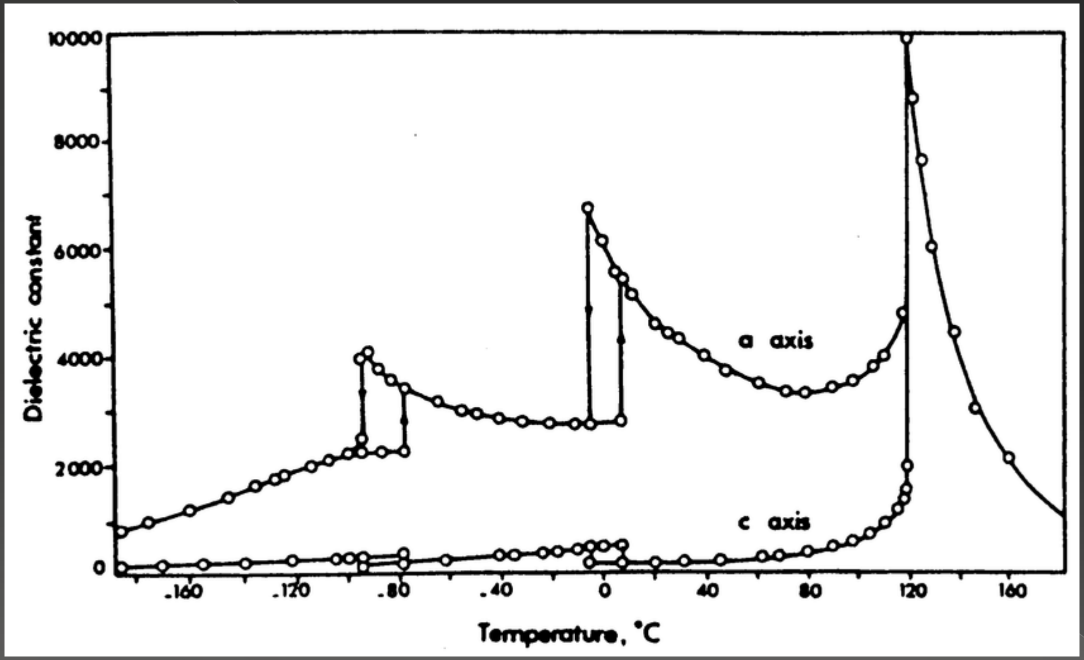

Histeresis loop in $BaTiO_3$

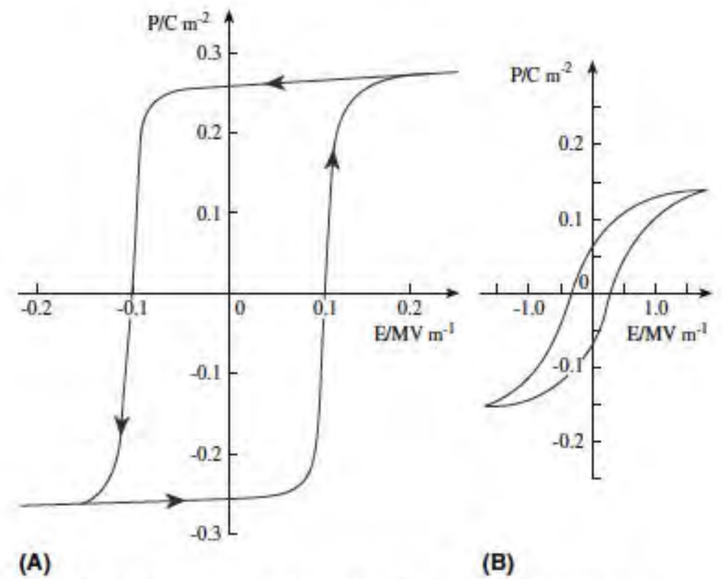

FIGURE 31.10 Hysteresis loops for $BaTiO_3$. (a) Single-domain single crystal. (b) Polycrystalline ceramic.

Grain size influence on dielectric constant in BaTiO3

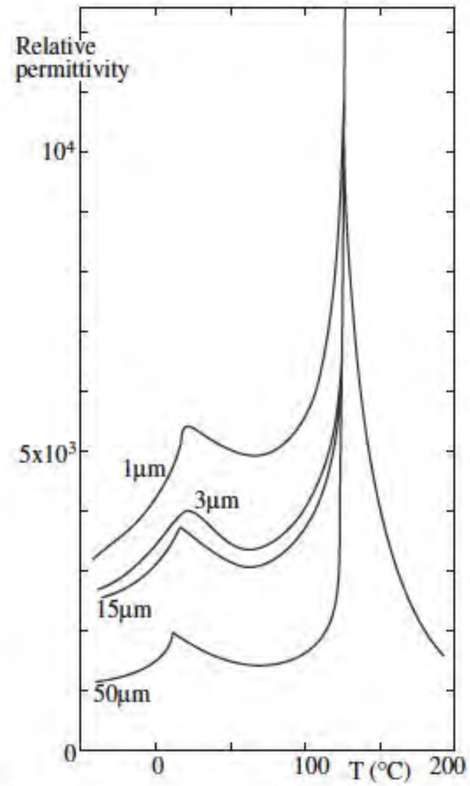

FIGURE 31.15 Effect of grain size on the dielectric constant of $BaTiO_3$.

Engineering the Curie temperature in $BatiO_3$

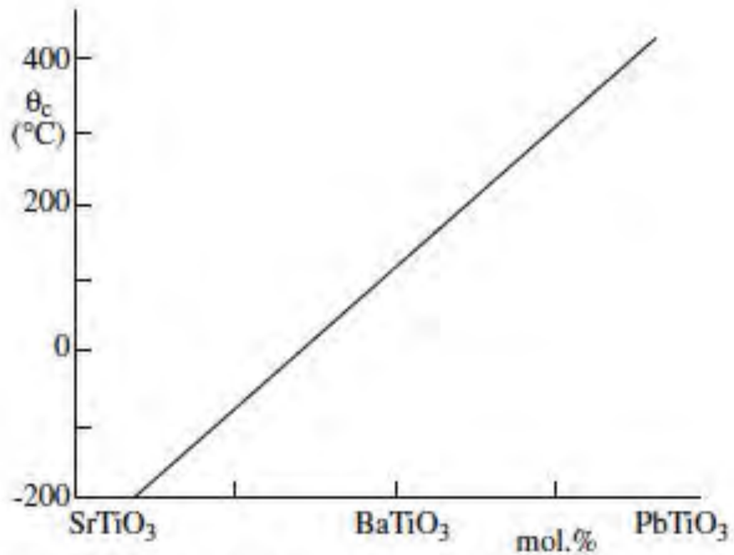

FIGURE 31.16 Effect of substitution on θ_c for $BaTiO_3$ solid solutions with $SrTiO_3$ and $PbTiO_3$.

Domains in ferroelectric depend on the orientation of the polarization

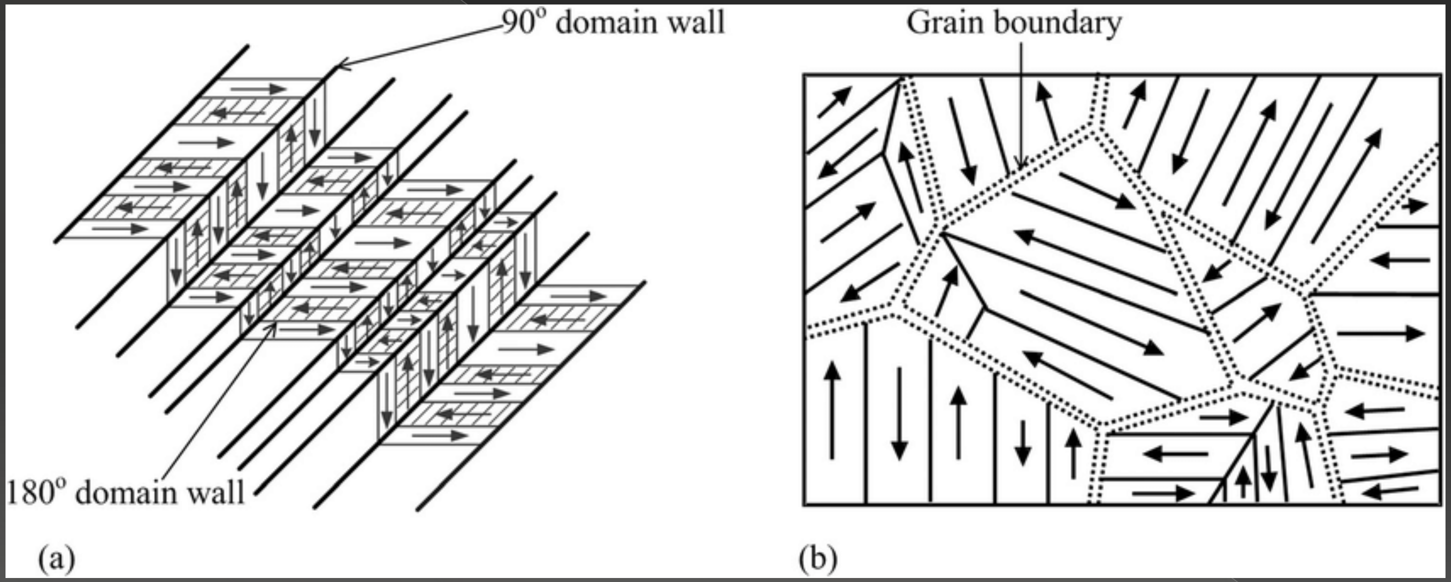

Poling of ferroelectrics

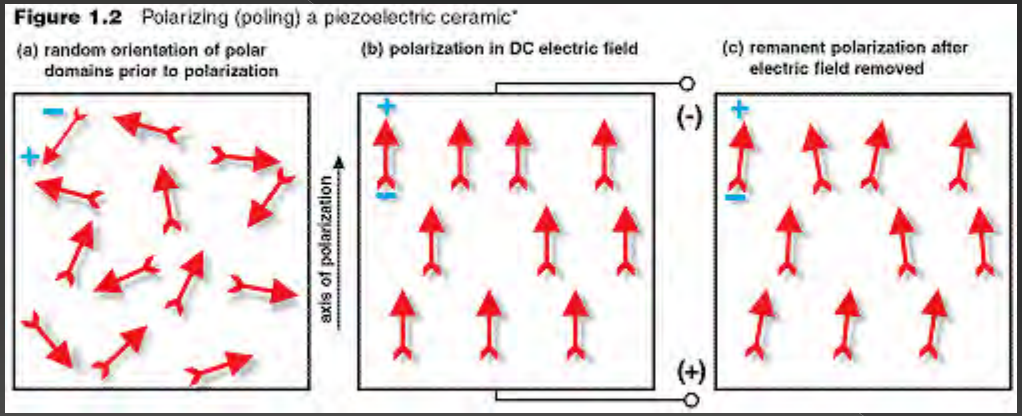

Ferroelectric domain in a ferroelectric materials

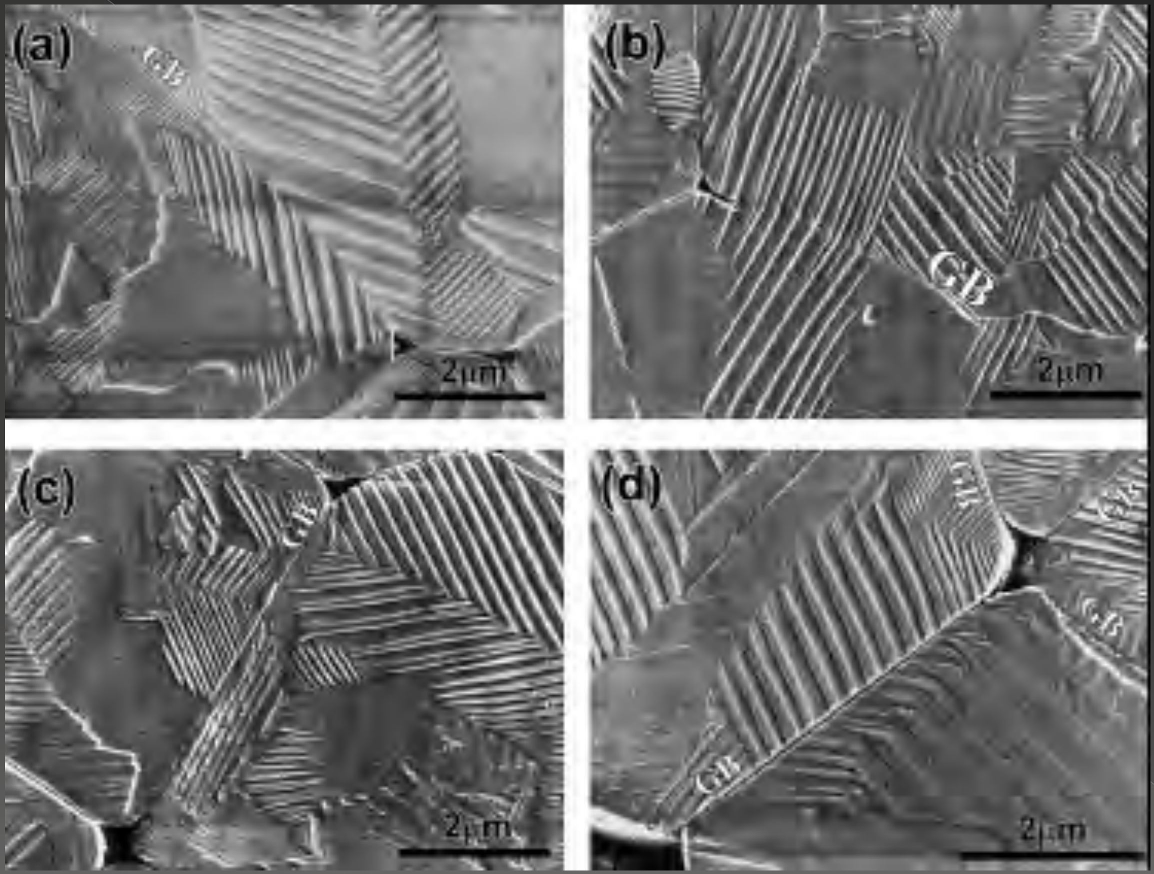

Piezoelectric Ceramics: mostly $PbZrO_3/PbTiO_3$

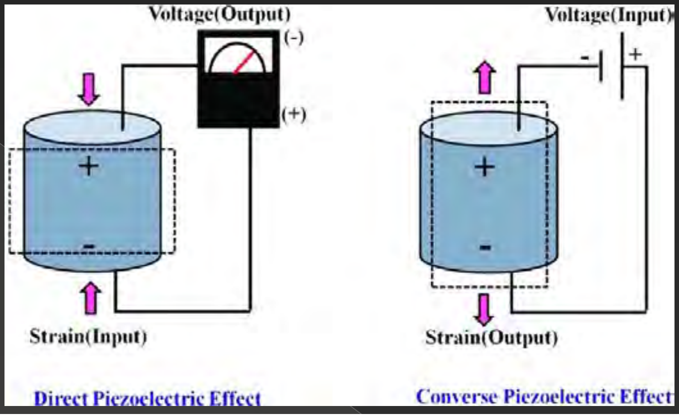

$P = d\,\sigma$, direct effect

$\varepsilon = d\,E$, converse effect

- P: polarization (pC/m^2)
- σ : stress (N/m^2)
- ε :strain
- d: piezoelectric coefficient (pC/N or m/V)

Examples

$$Q = d\,F = d\,\sigma\,A = d\,\varepsilon\,E\,A$$

d = charge sensitivity coefficient (matrix)

for example :

$$V_z = \frac{Q_z}{C} = \frac{d_{zx}F_x}{C} = \frac{d_{zx}F_x z}{\varepsilon_0 \varepsilon_r A_z}$$

Typically, in PZT, lead zirconate ceramics, the Voltage obtainable is of the order of some volts, for loads of some Newton over 1 cm^2 (d33 is around 200-300 pC/N)

Typical applications: Sensors, transducers, actuators

High precision mirror mount

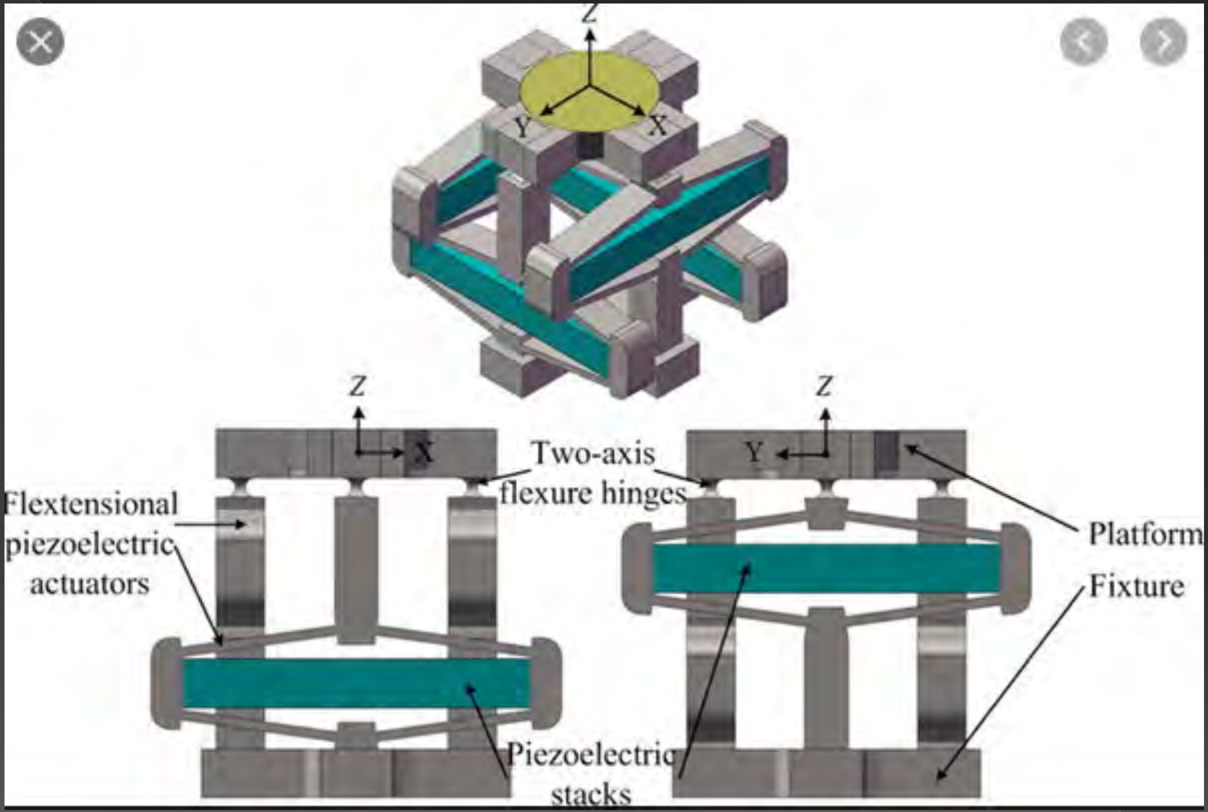

https://www.youtube.com/watch?v=VbTUsluY2xU

Positive Temperature coefficient, PTC of Barium Titanate

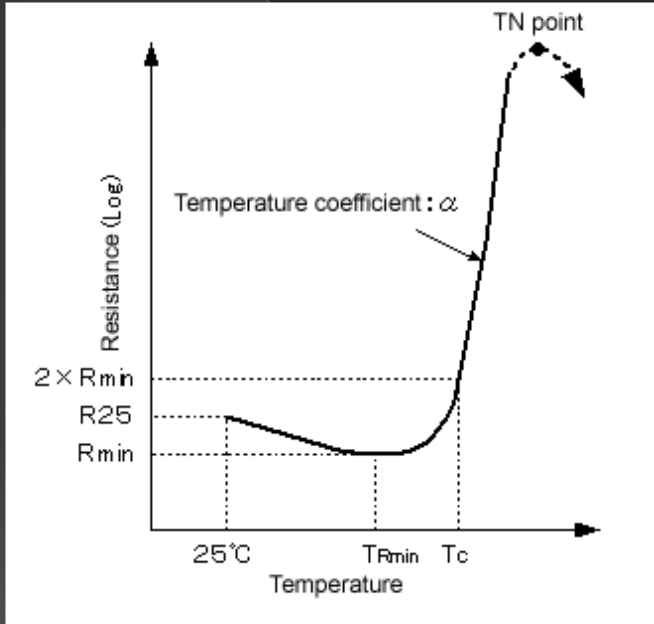

Fig. 2 Definition of resistance-temperature characteristics and Curie temperature

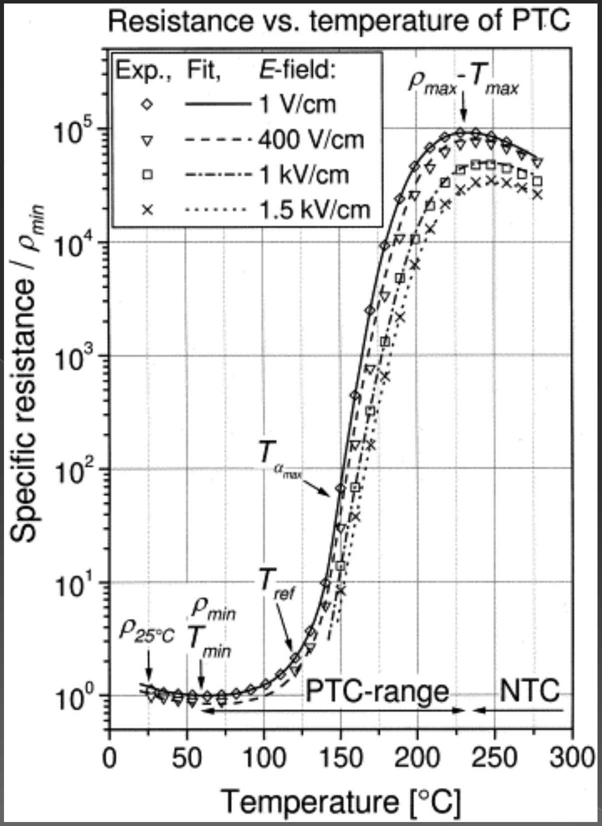

Explanation for PTC behavior of $BaTiO_3$

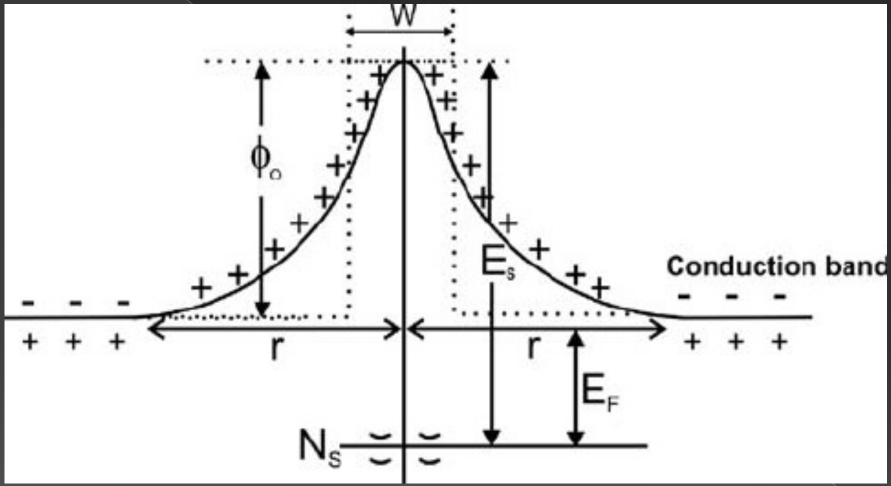

Use of PTC thermistor

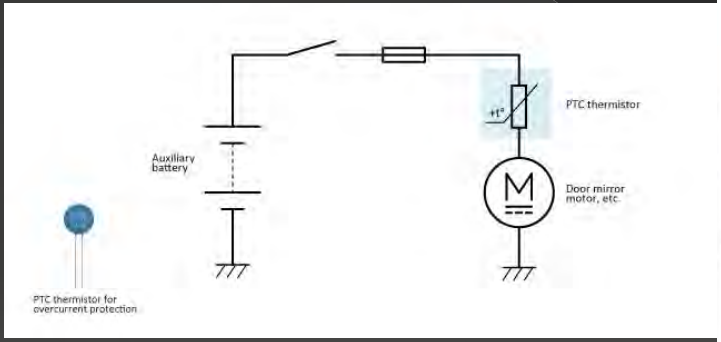

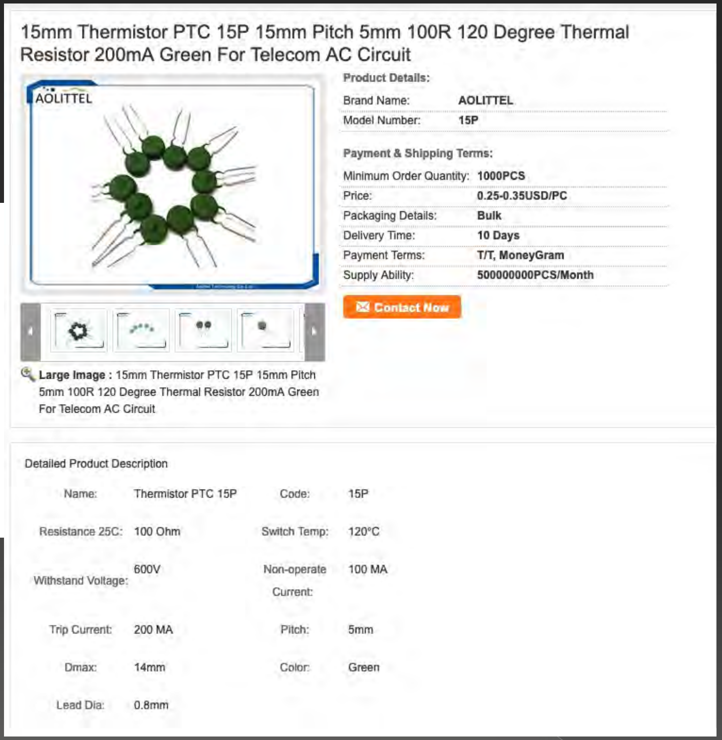

Transparent conducting oxide: Indium Tin Oxide (In_2O_3:Sn)

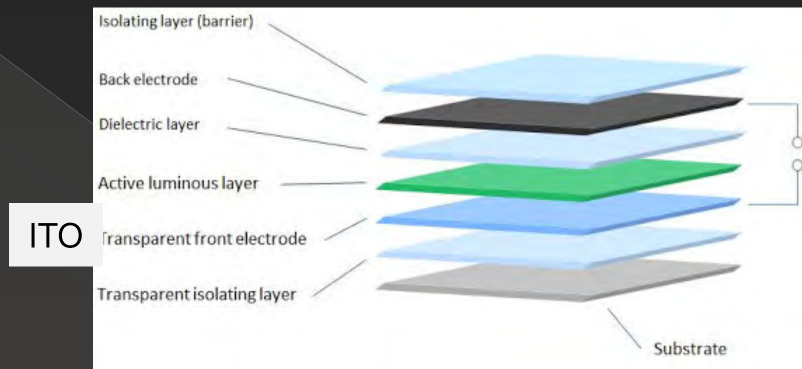

- https://www.boldmethod.com/blog/video/2016/04/watch-a-737-land-through-the-hud/

Optical properties of ceramics: Translucency (Na-vapour lamps)

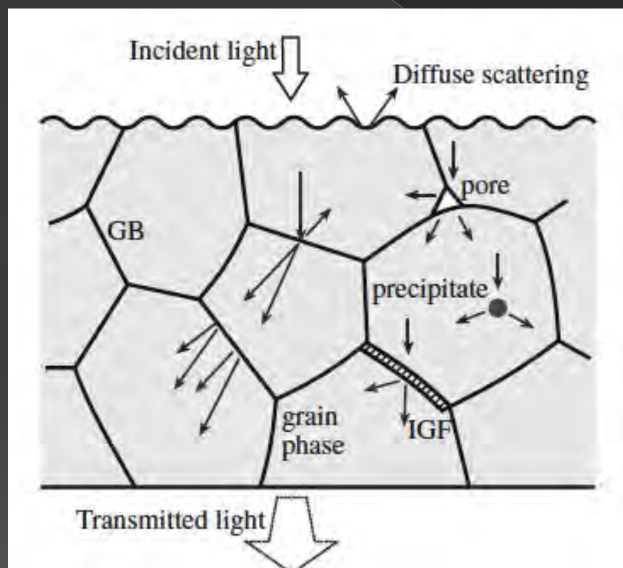

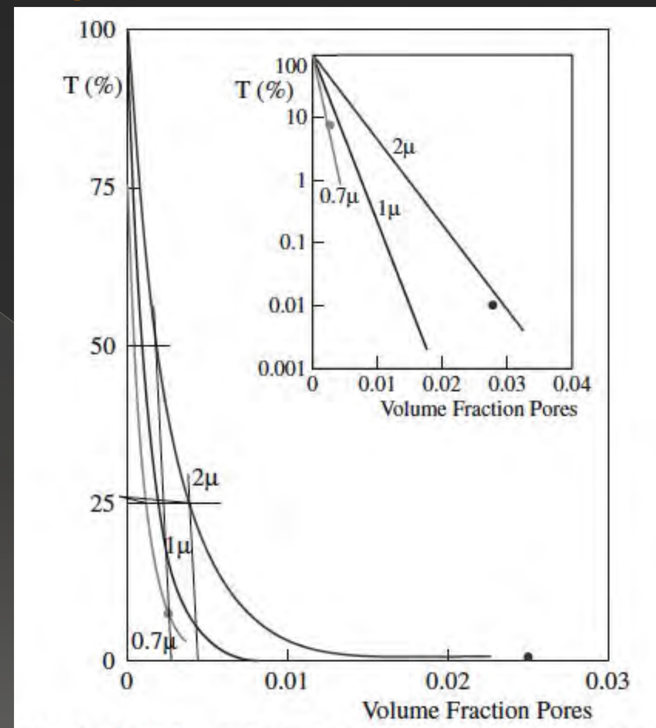

FIGURE 32.11 Effect of porosity on the transparency of polycrystalline alumina.

Optical fibers: based on Snell's law

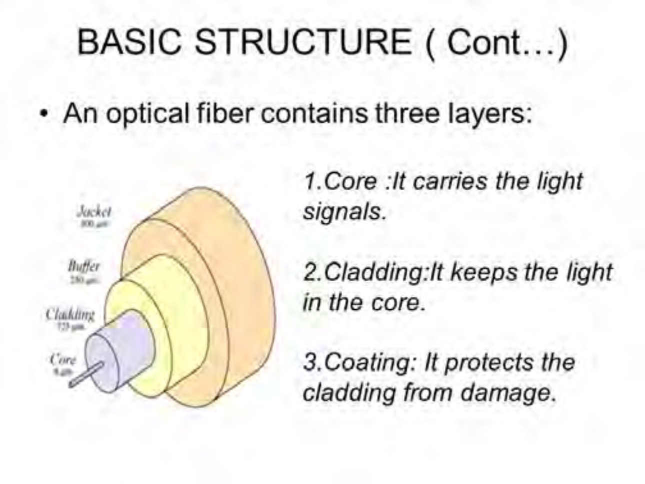
BASIC STRUCTURE (Cont…)

- An optical fiber contains three layers:

1.Core :It carries the light signals.

2.Cladding:It keeps the light in the core.

3.Coating: It protects the cladding from damage.

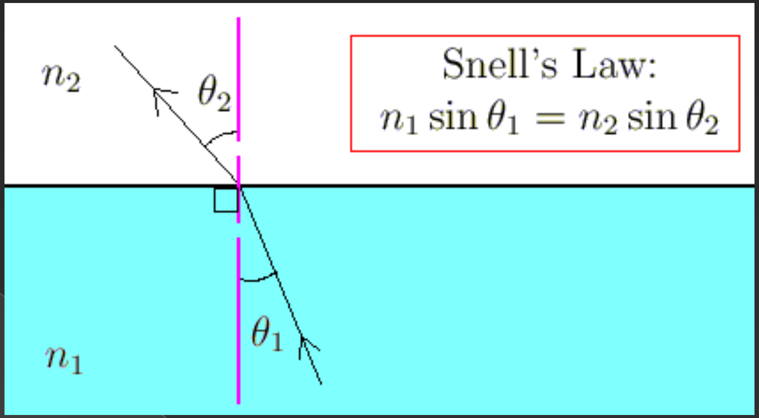

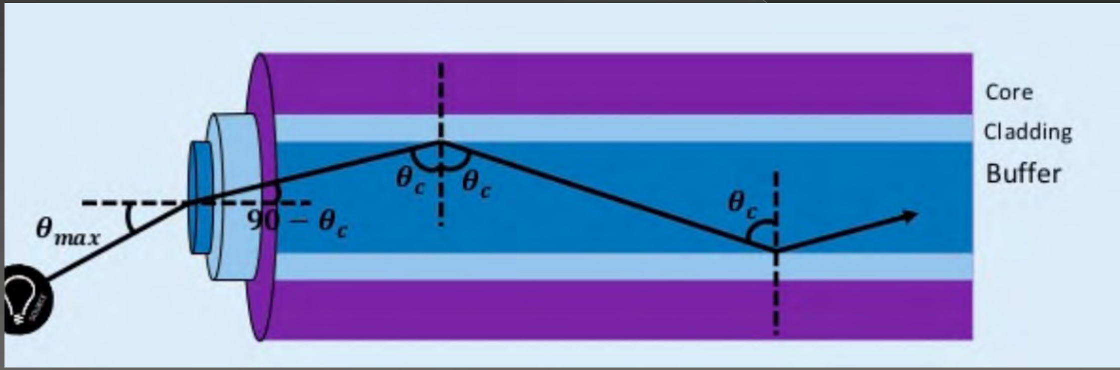

Type of optical fibers

- Pure or doped SiO_2: very small loss over distance
- Na_2O-CaO-SiO_2 (NCS) or NaO_2-B_2O_3-SiO_2 (NBS)
  Small distances, cheap
- Fluoride glasses (ZBLAN):
  ZrF_4-BaF_2-LaF_3-AlF_3-NaF; not yet industrial

Optical fibers: fabrication

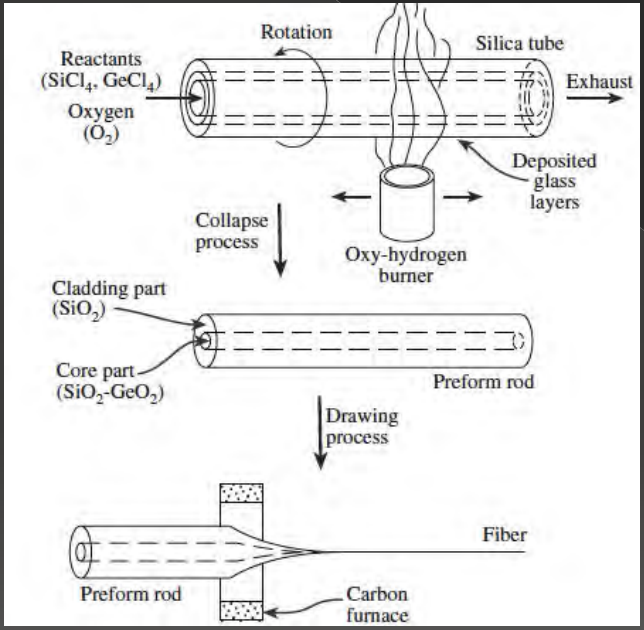

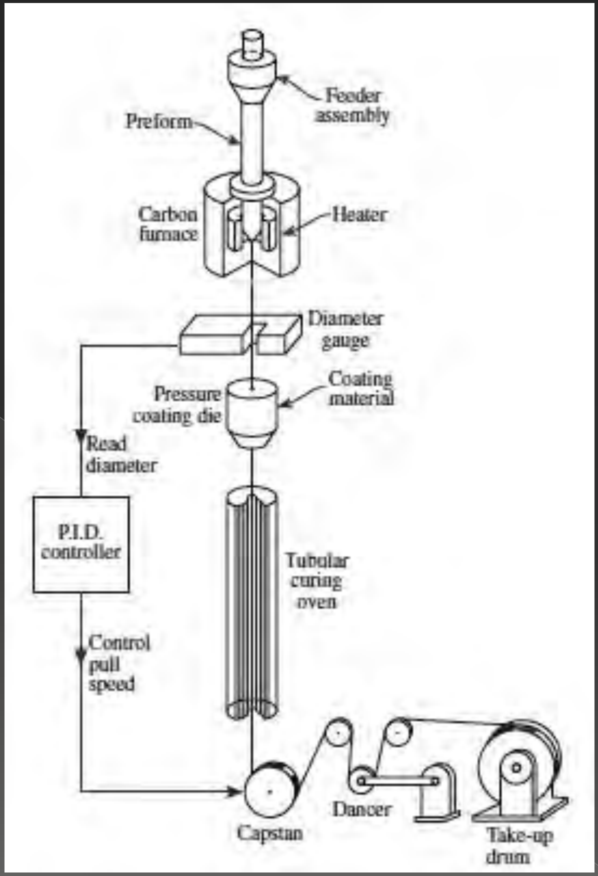

Fabrication: https://www.youtube.com/watch?v=uSnjo5tOGQA

Laser principle

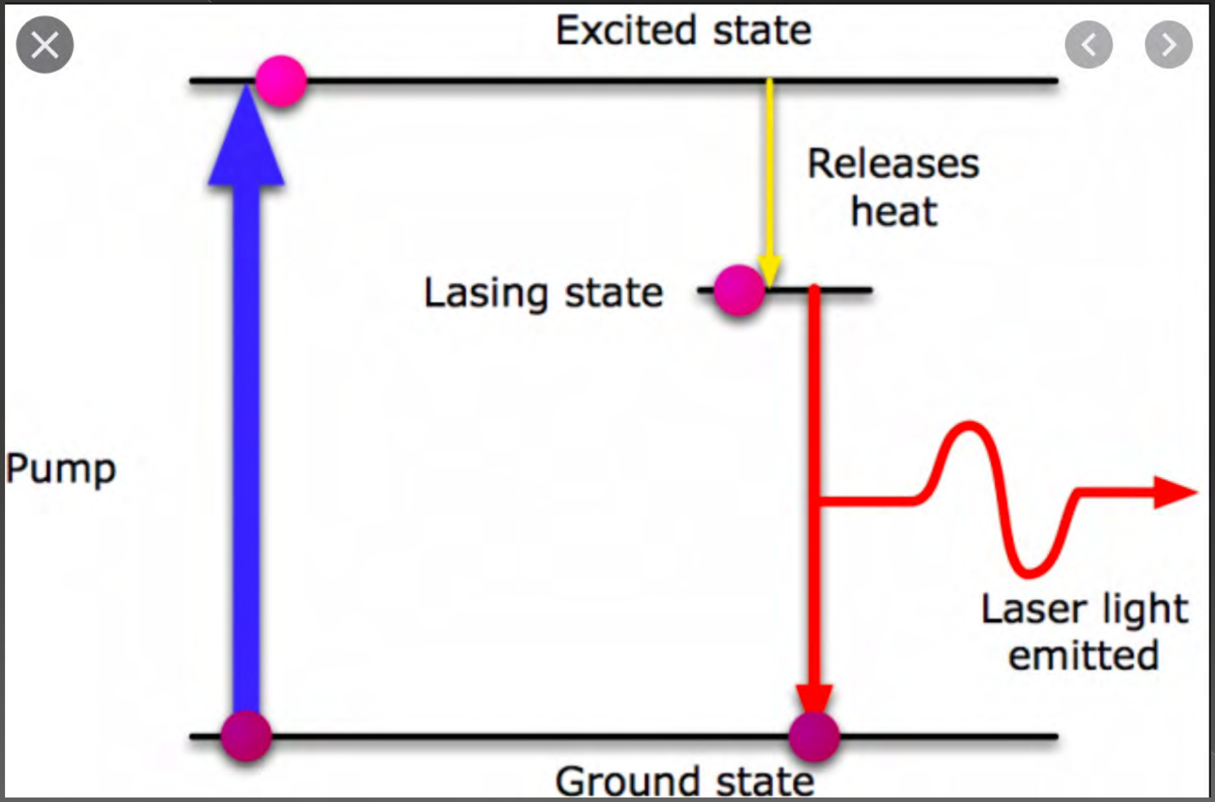

Ceramic lasers:

-) Ruby

-) Nd:YAG Yttrium Aluminium Garnet

$Y_3Al_5O_{12}$

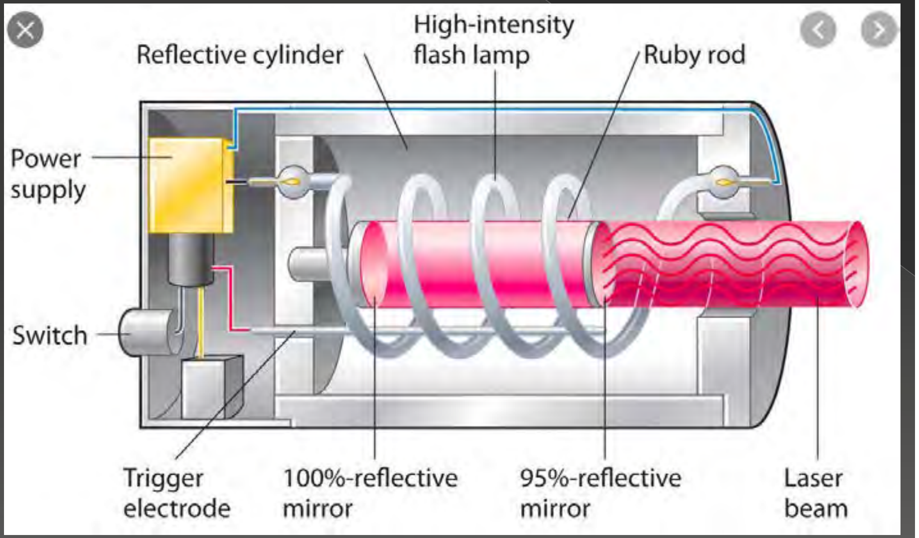

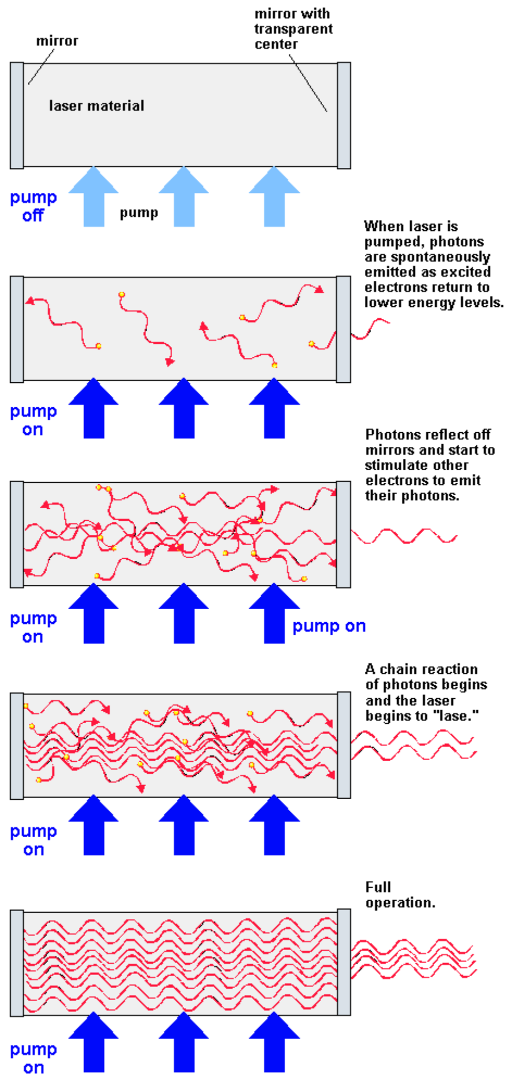

Electro-optic effects: $PbTiO_3$-$PbZrO_3$-La_2O_3 (PLZT)

$$\Delta n = n^3(r_c E + R E^2)$$

Linear POCKELS Effect

Quadratic KERR Effect

TABLE 32.12 Electrooptical Properties of Several Ceramics

Material	κ	*n at 633 nm*	r_c *m/V*	R *m²/V²*
Ceramic				
PLZT 8.5/65/35	5000	2.50	—	38.6×10^{-16}
PLZT 9/65/35	5700	2.50	—	3.8×10^{-16}
PLZT 9.5/65/35	5500	2.50	—	1.5×10^{-16}
PLZT 8/70/30	5400	2.48	—	11.7×10^{-16}
PLZT 8/40/60	980	2.57	1.02×10^{-10}	—
PLZT 12/40/60	1300	2.57	1.20×10^{-10}	—
PLZT 14/30/70	1025	2.59	1.12×10^{-10}	—
Single crystal				
$LiNbO_3$ (r_{33})	37	2.20	0.32×10^{-10}	—
$LiNbO_3$ (r_{13})	37	2.29	0.10×10^{-10}	—
$BaTiO_3$ (r_{33})	373	2.36	0.28×10^{-10}	—
$BaTiO_3$ (r_{51})	372	2.38	8.20×10^{-10}	—
$KNbO_3$ (r_{33})	30	2.17	0.64×10^{-10}	—
$KNbO_3$ (r_{42})	137	2.25	3.80×10^{-10}	—
Strontium barium niobate ($T = 560$ K)	119	2.22	0.56×10^{-10}	—
Strontium barium niobate ($T = 300$ K)	3400	2.30	13.40×10^{-10}	—
$Ba_2NaNb_5O_{15}$	86	2.22	0.56×10^{-10}	—

PLZT: optical switches

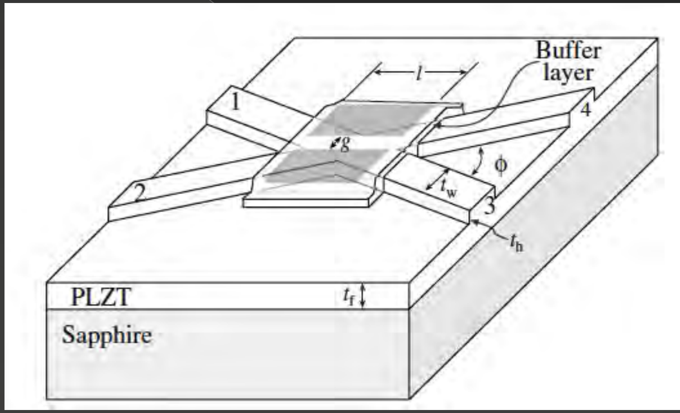

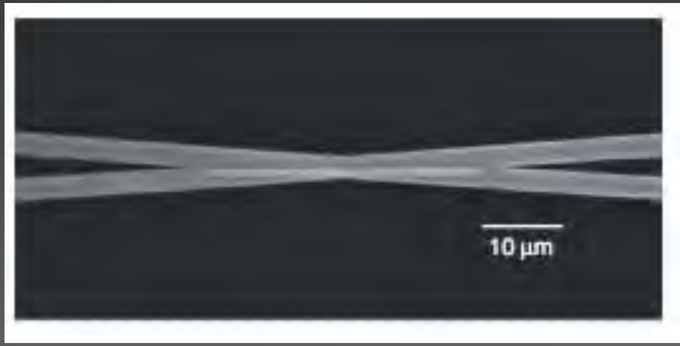

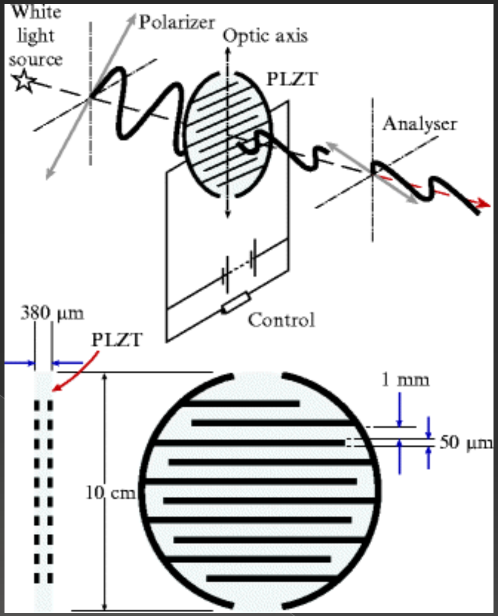

Magnetism

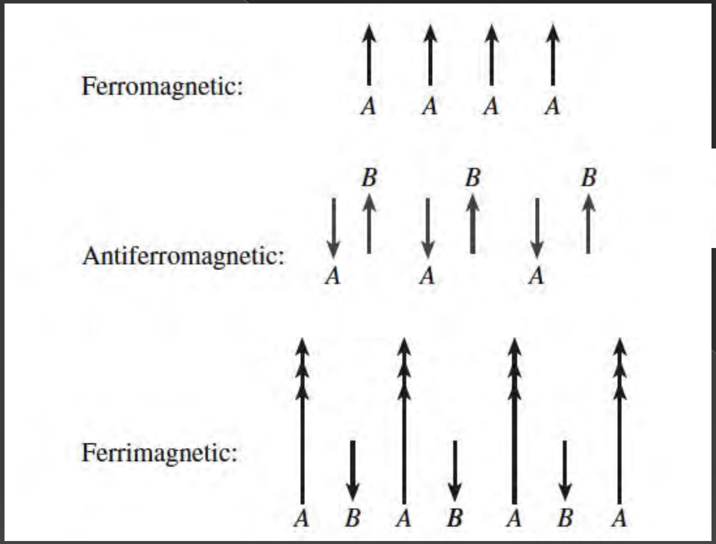

CrO_2

MnO (θ_N = 122 K) NiO (θ_N = 523 K)

CoO (θ_N = 293 K) FeO (θ_N = 198 K)

CMR Colossal Magneto Resistance
: $La_{1-x}(Ba, Sr, Ca)MnO_3$

Most relevant in ceramics

TABLE 33.6 Magnetic Properties of Several Ferrimagnetic Ceramics

Material	θ_c *(K)*	B_{sat} *(T) at RT*	*Calculated moments* *T site*	*O site*	*Net*	*Experimental*
		Spinel ferrites [AO·B_2O_3]				
$Fe^{3+}[Cu^{2+}Fe^{3+}]O_4$	728	0.20	−5	1.73 + 5	1	1.30
$Fe^{3+}[Ni^{2+}Fe^{3+}]O_4$	858	0.34	−5	2 + 5	2	2.40
$Fe^{3+}[Co^{2+}Fe^{3+}]O_4$	1020	0.50	−5	3 + 5	3	3.70–3.90
$Fe^{3+}[Fe^{2+}Fe^{3+}]O_4$	858	0.60	−5	4 + 5	4	4.10
$Fe^{3+}[Mn^{2+}Fe^{3+}]O_4$	573	0.51	−5	5 + 5	5	4.60–5.0
$Fe^{3+}[Li_{0.5}Fe_{1.5}]O_4$	943		−5	0 + 0.75		2.60
$Mg_{0.1}Fe_{0.9}[Mg_{0.9}Fe_{1.1}]O_4$	713	0.14	0–4.5	0 + 5.5	1	1.10
		Hexagonal ferrites				
$BaO:6Fe_2O_3$	723	0.48				1.10
$SrO:6Fe_2O_3$	723	0.48				1.10
$Y_2O_3:5Fe_2O_3$	560	0.16				5.00
$BaO:9Fe_2O_3$	718	0.65				
		Garnets				
$YIG\{Y_3\}[Fe_2]Fe_3O_{12}$	560	0.16			5	4.96
$(Gd_3)[Fe_2]Fe_3O_{12}$	560				16	15.20
		Binary oxides				
EuO	69					6.8
CrO_2	386	0.49				2.00

TABLE 33.8 Classes of Magnetic Ceramic

Structure	*Composition*	*Applications*
Spinel (cubic ferrites)	1 MeO : 1Fe_2O_3 MeO = transition metal oxide, e.g., Ni,Co, Mn, Zn	Soft magnets
Garnet (rare earth ferrites)	3 Me_2O_3 : 5Fe_2O_3 Me_2O_3 = rare earth metal oxide, e.g., Y_2O_3, Gd_2O_3	Microwave devices
Magnetoplumbite (hexagonal ferrites)	1 MeO : 6Fe_2O_3 MeO = divalent metal oxide from group IIA; e.g., BaO, CaO, SrO	Hard magnets

Hard and Soft ceramic magnets: mostly ferrites

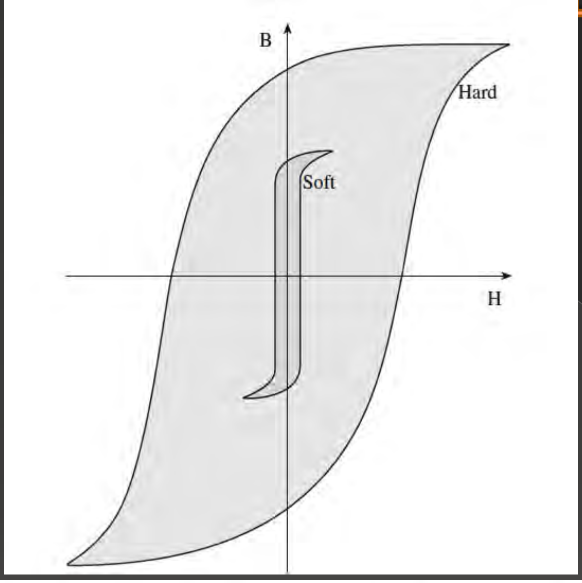

Hard Magnets:
Starter motors,
loudspeakers,
closing fixtures

Soft Magnets:
Memories,
Deflection coils

TABLE 33.11 Physical and Magnetic Properties of Magnetic Particles

Magnetic particle	*Particle length (μm)*	*Aspect ratio*	*Specific surface area (m^2/g)*	H_c *(kA/m)*	B_s *(T)*	θ_c *(°C)*
γ-Fe_2O_3	0.3–0.6	10	20–30	20–32	0.5	675
Co–γ-Fe_2O_3	0.3–0.4	10	20–30	30–70	0.5	400
CrO_2	0.2–0.7	10–20	24–40	30–50	0.5	113
Fe (metal)	0.2–0.4	~6	40–50	75–130	2.0	770

Magnetic memories

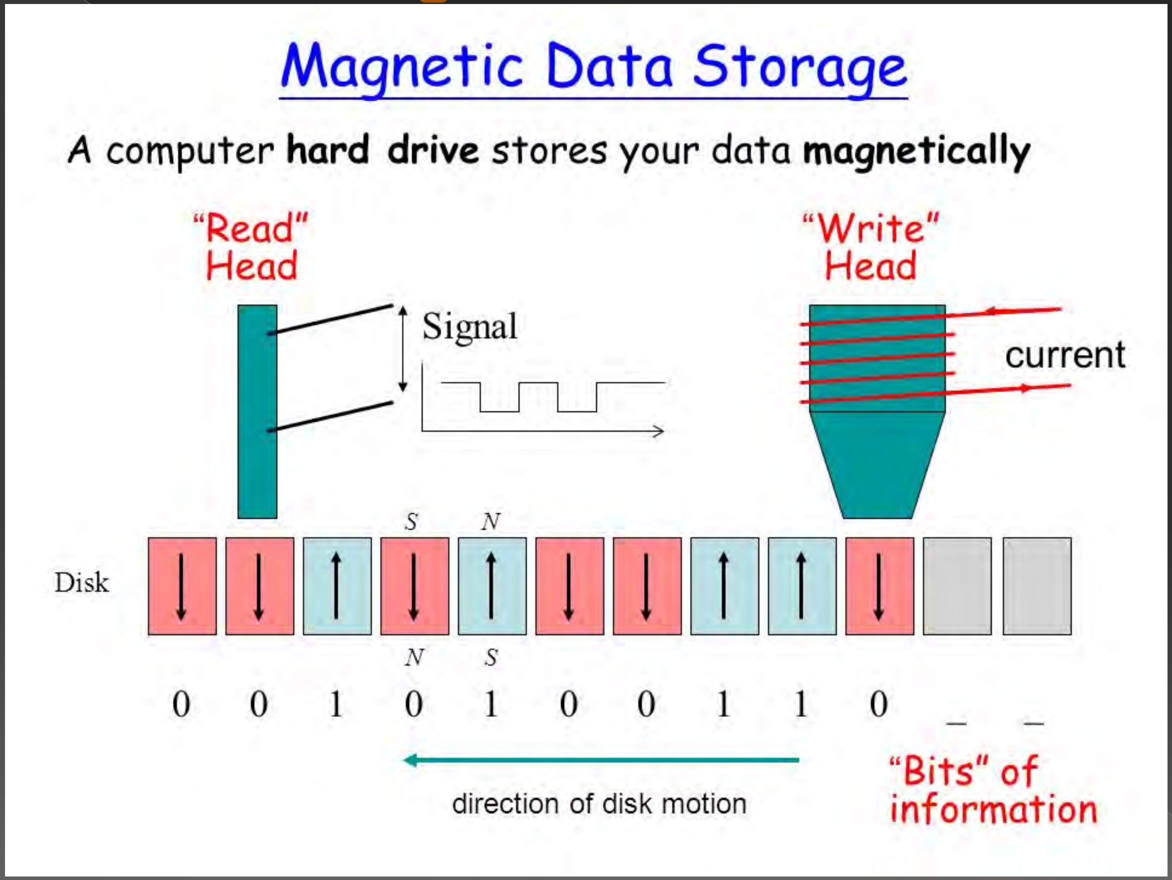

Table 14.2 Examples of Design Requirements of Various Applications and Ceramics with Properties Which Match the Requirements

Application	Requirements of the applications	Candidate ceramics	Key properties
Seal			
Turbine stator			
Heating element			
Rotary heat exchanger			
Heat sink for IC and transistor devices			
Furnace insulation			
Miniature capacitor			
High-speed, high-load bearing			
Segments of watch band			

CONSIDERAZIONI PROGETTUALI

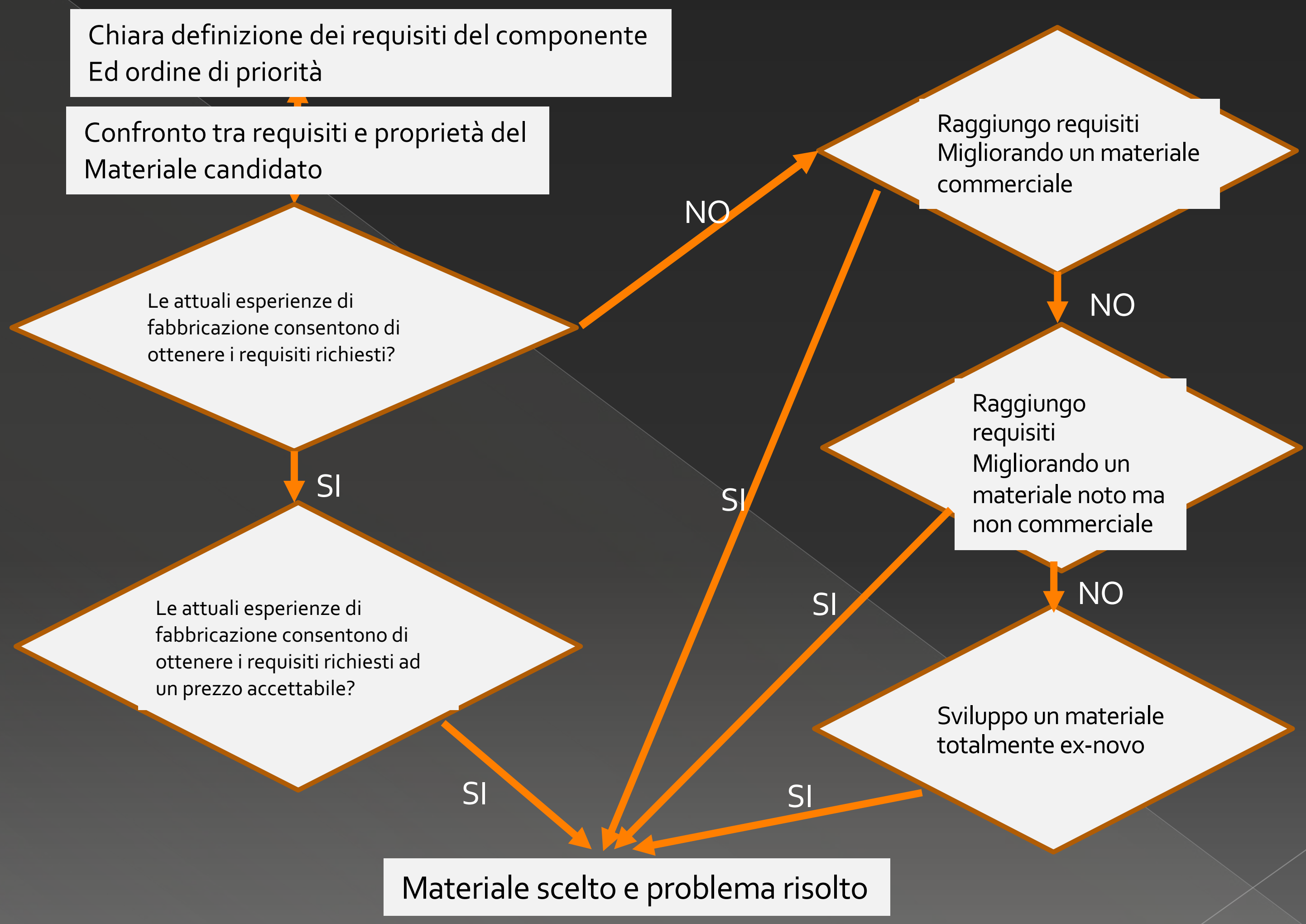

SiC Heat exchanger

Ceramic seal for taps

Sandblast nozzles

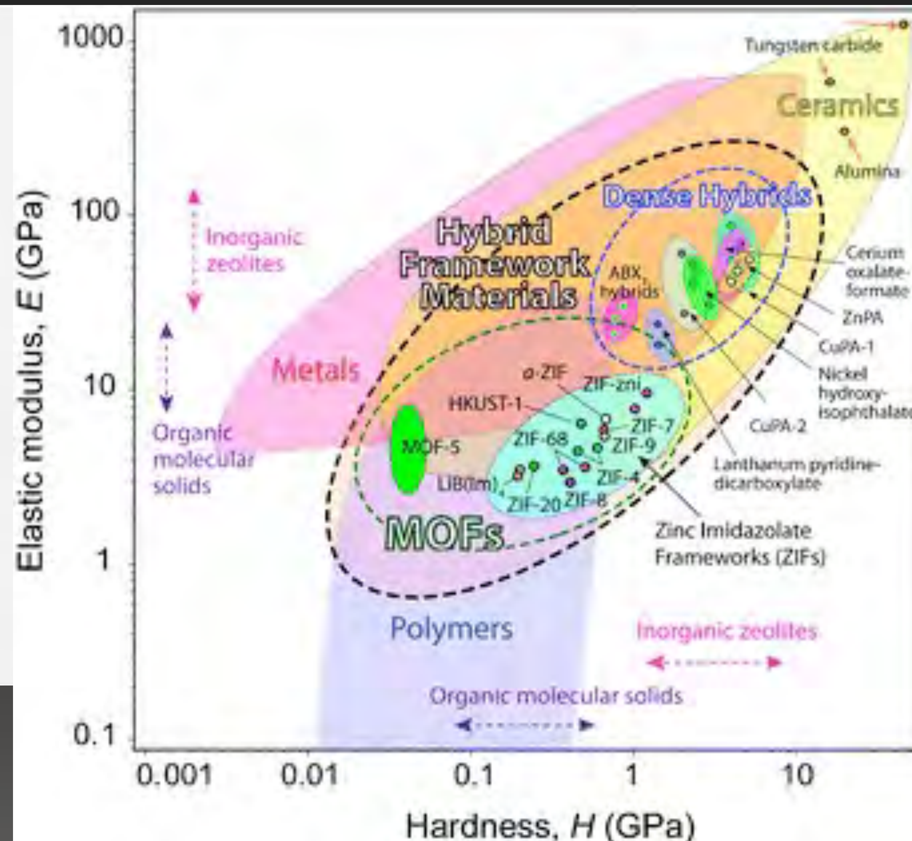

Rado watches

SEM fundamentals

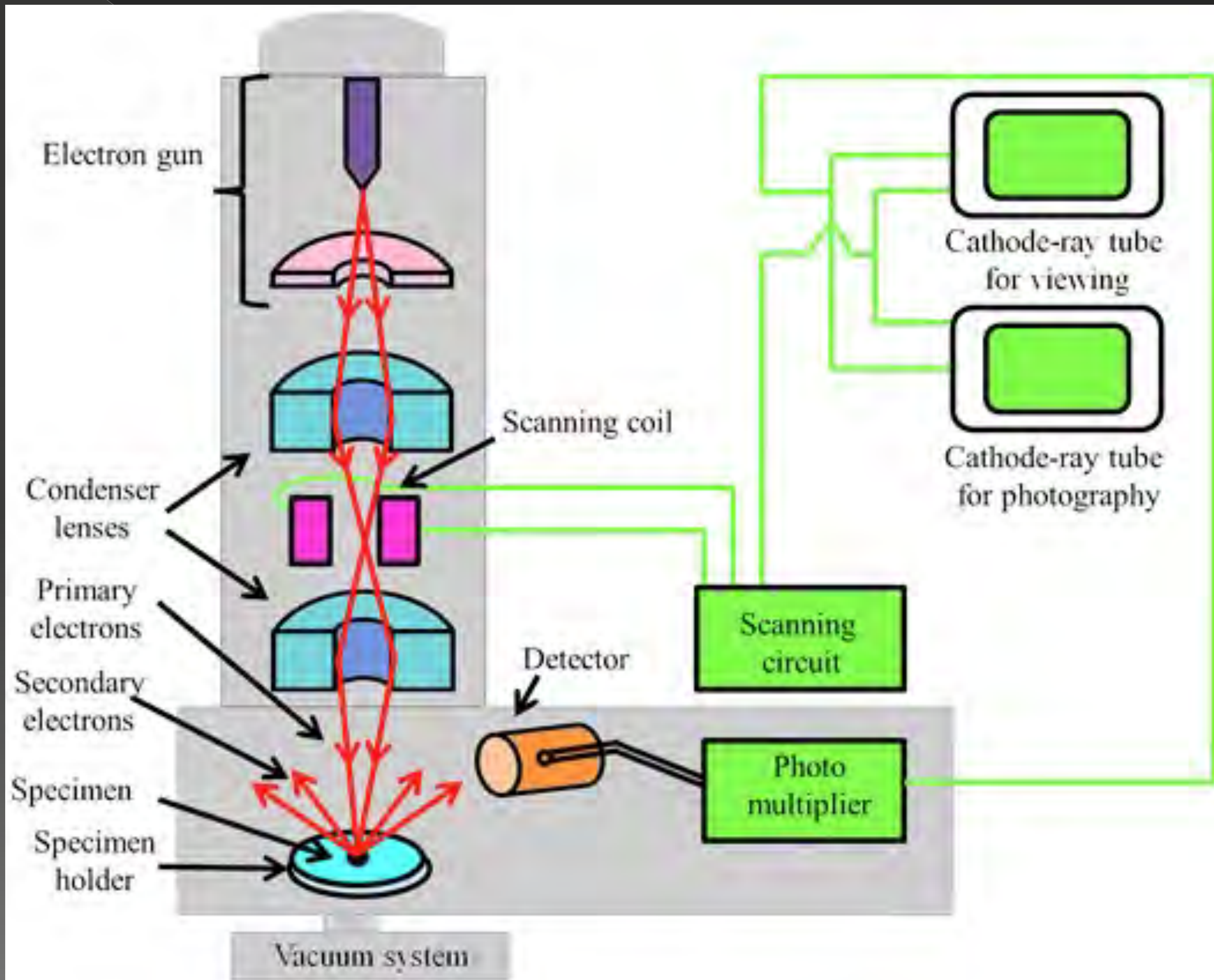

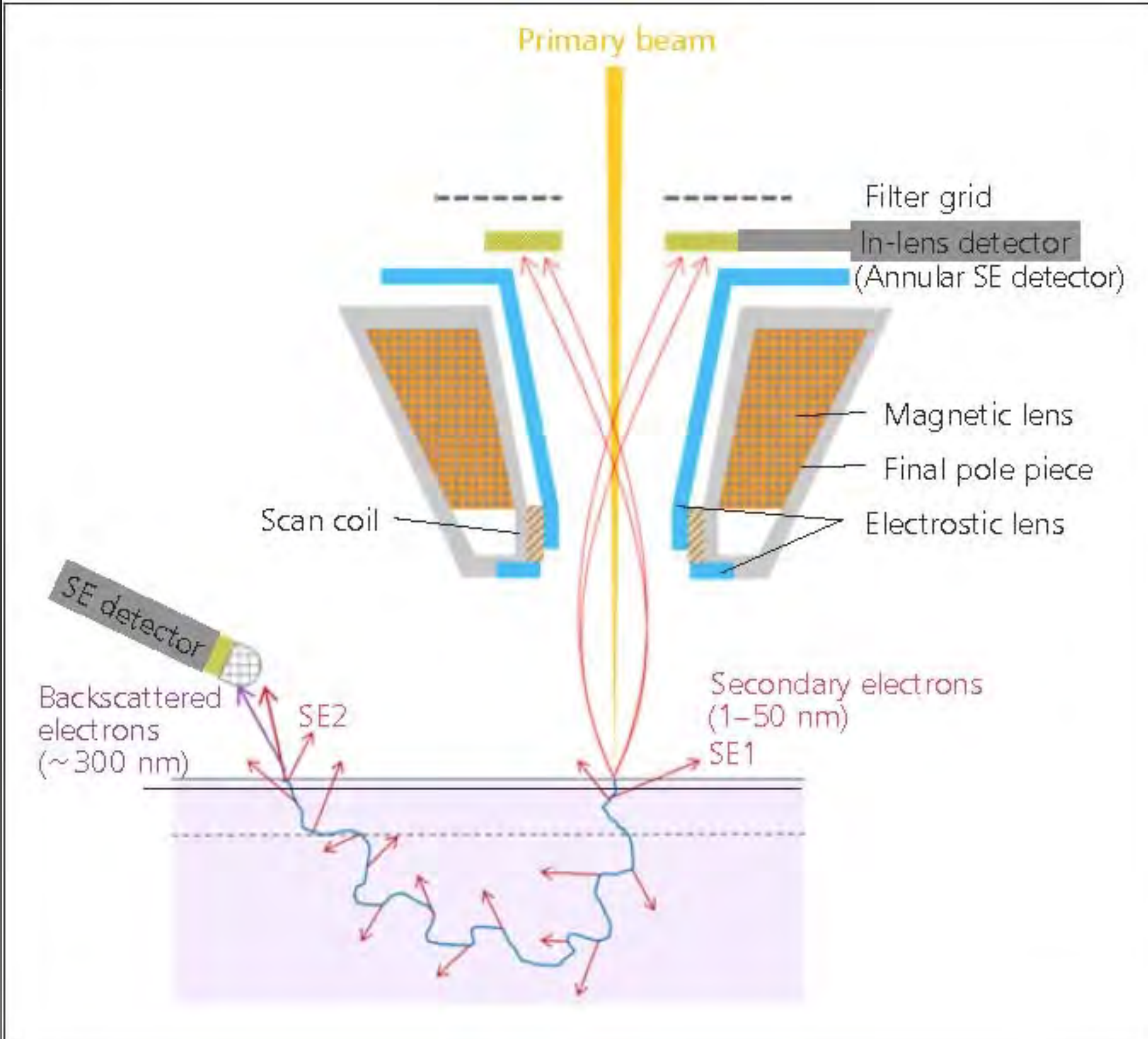

Primary beam
Filter grid
In-lens detector
(Annular SE detector)
Magnetic lens
Final pole piece
Scan coil
Electrostic lens
SE detector
Backscattered
electrons
(~300 nm)
SE2
Secondary electrons
(1–50 nm)
SE1

E-beam sample intercation

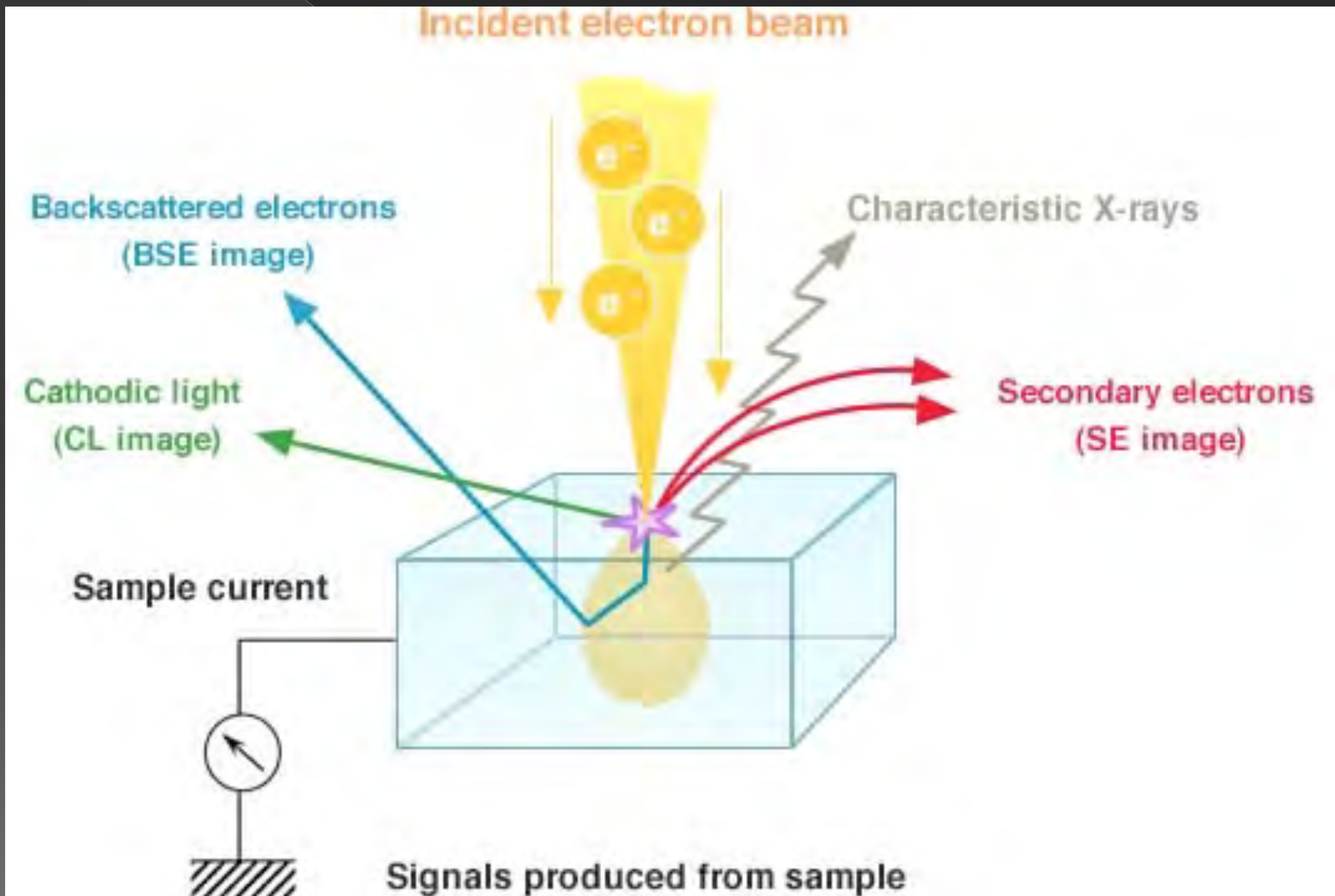

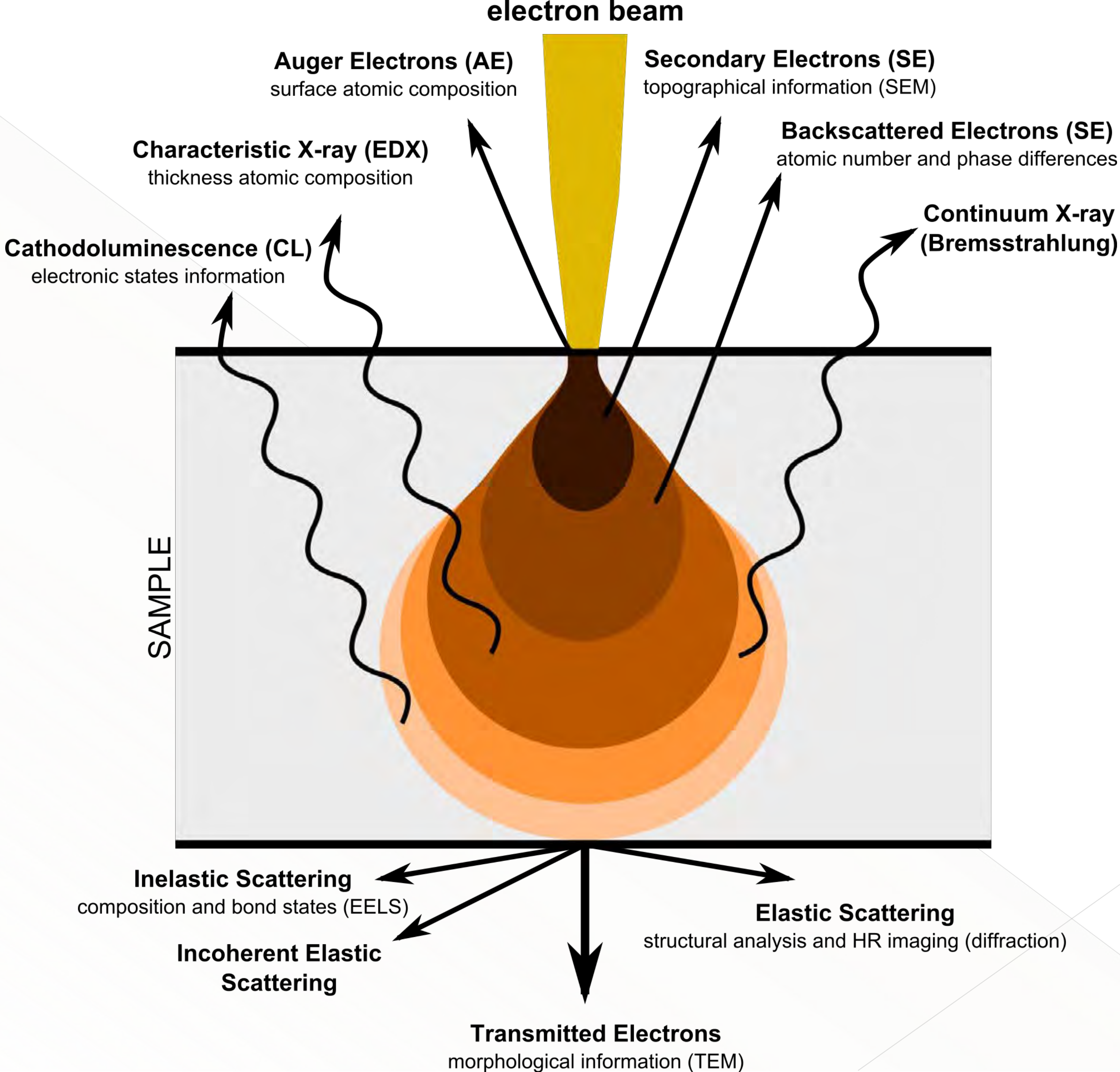
electron beam
Auger Electrons (AE)
surface atomic composition
Secondary Electrons (SE)
topographical information (SEM)
Characteristic X-ray (EDX)
thickness atomic composition
Backscattered Electrons (SE)
atomic number and phase differences
Cathodoluminescence (CL)
electronic states information
Continuum X-ray
(Bremsstrahlung)
SAMPLE
Inelastic Scattering
composition and bond states (EELS)
Elastic Scattering
structural analysis and HR imaging (diffraction)
Incoherent Elastic
Scattering
Transmitted Electrons
morphological information (TEM)

EDS spectrum of ZnO deposited on SiC

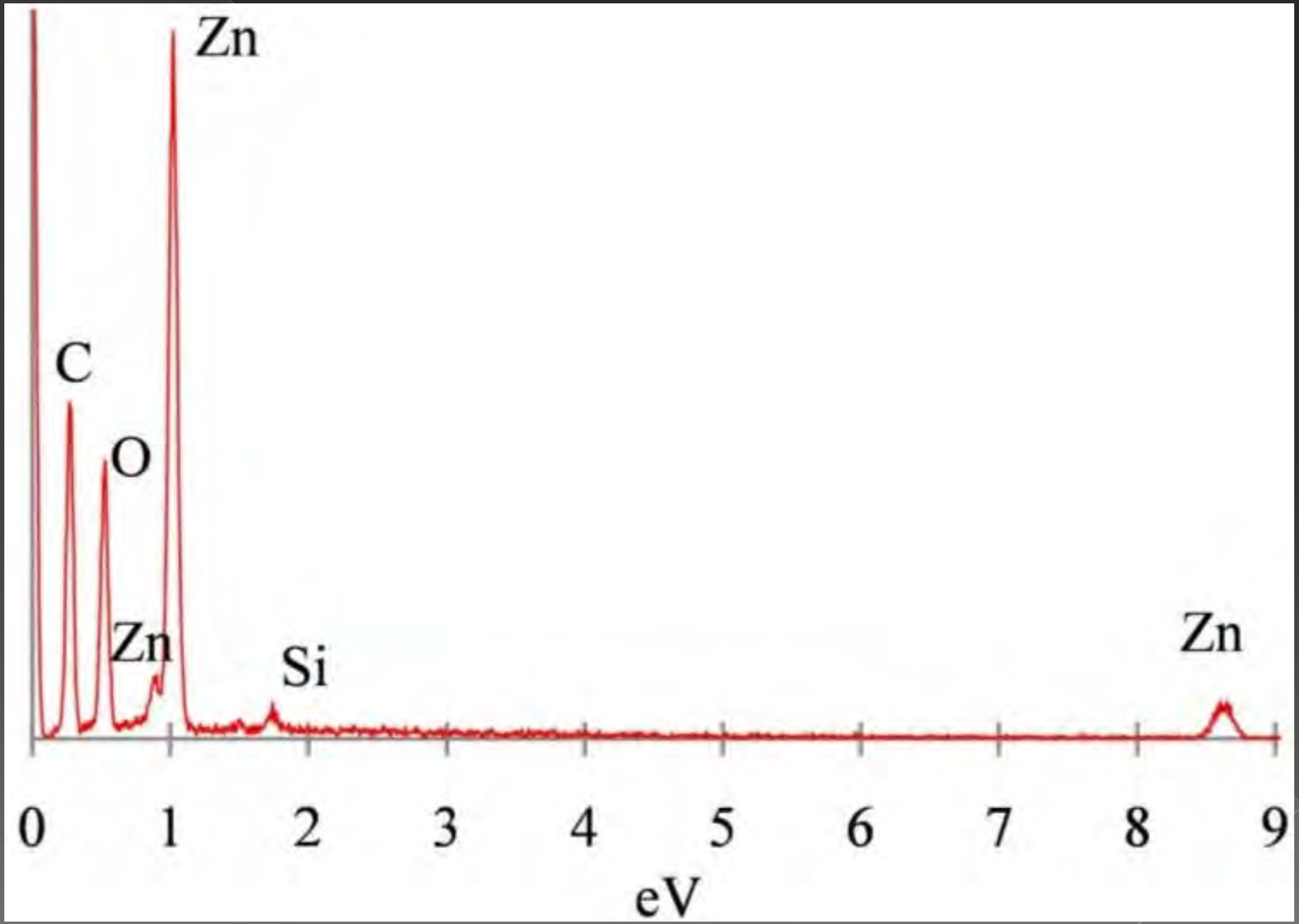

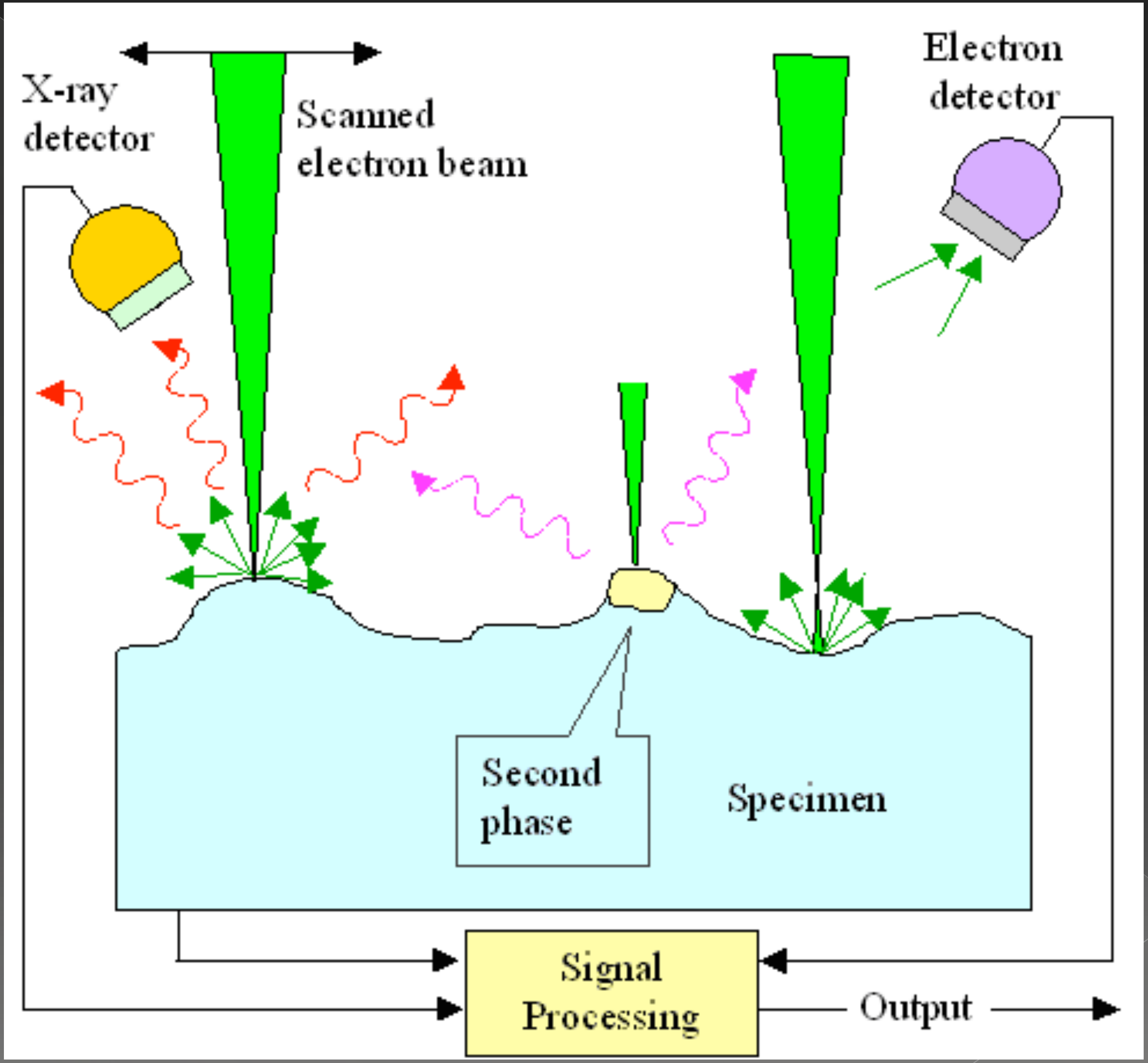
X-ray
detector
Scanned
electron beam
Electron
detector
Second
phase
Specimen
Signal
Processing
Output

Compositional contrast

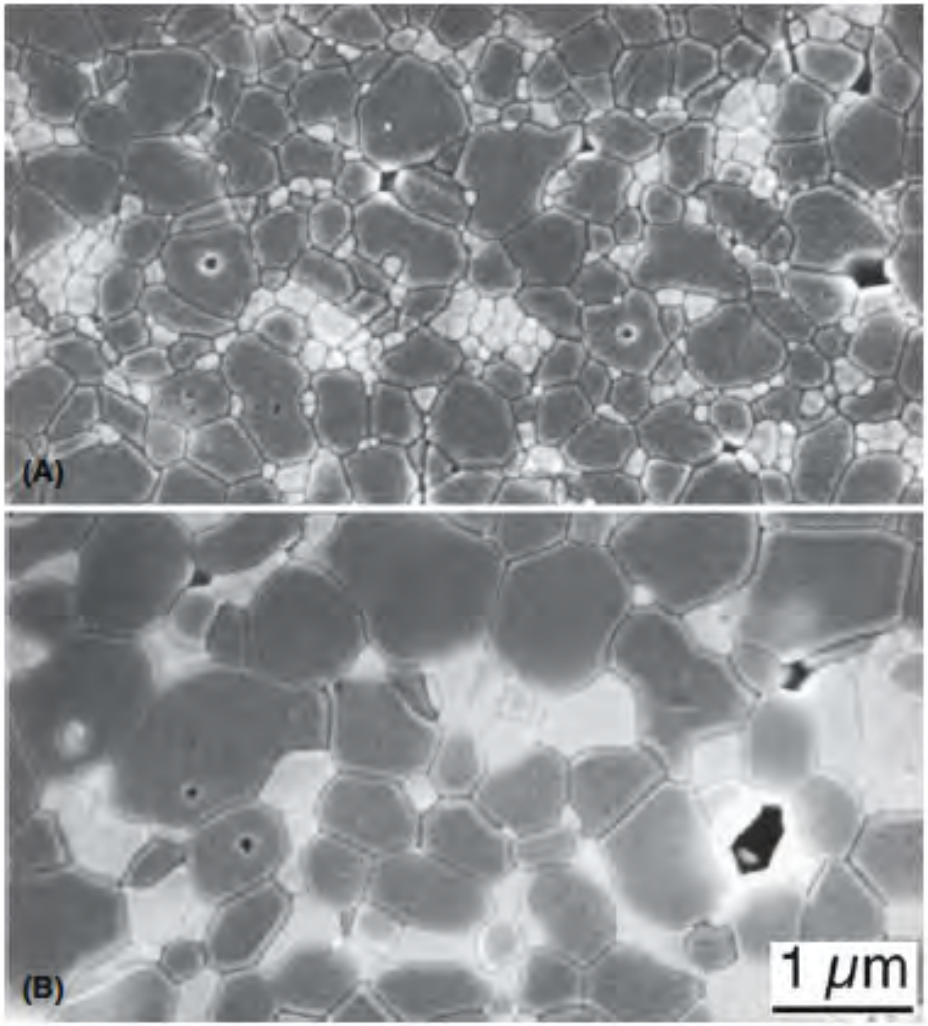

FIGURE 24.27 Two-phase ceramics. (a) As sintered and (b) heat treated at 1600°C for 30 hours. ZTA 30% (zirconia-toughened alumina with 30 vol% YSZ containing 10 molar% yttria).

Topographycal contrast

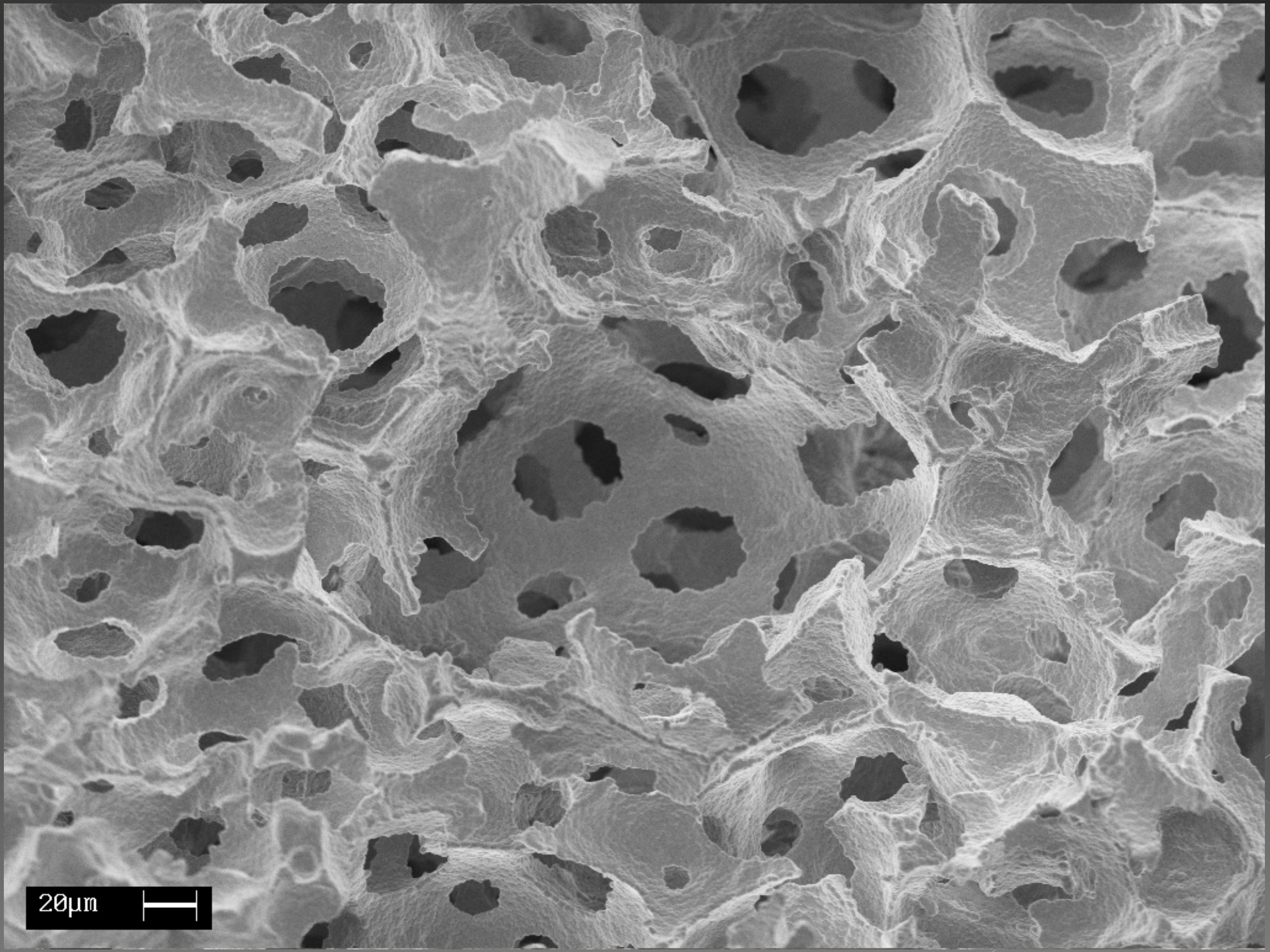

Magnification mechanism in SEM: reduce scanned region!

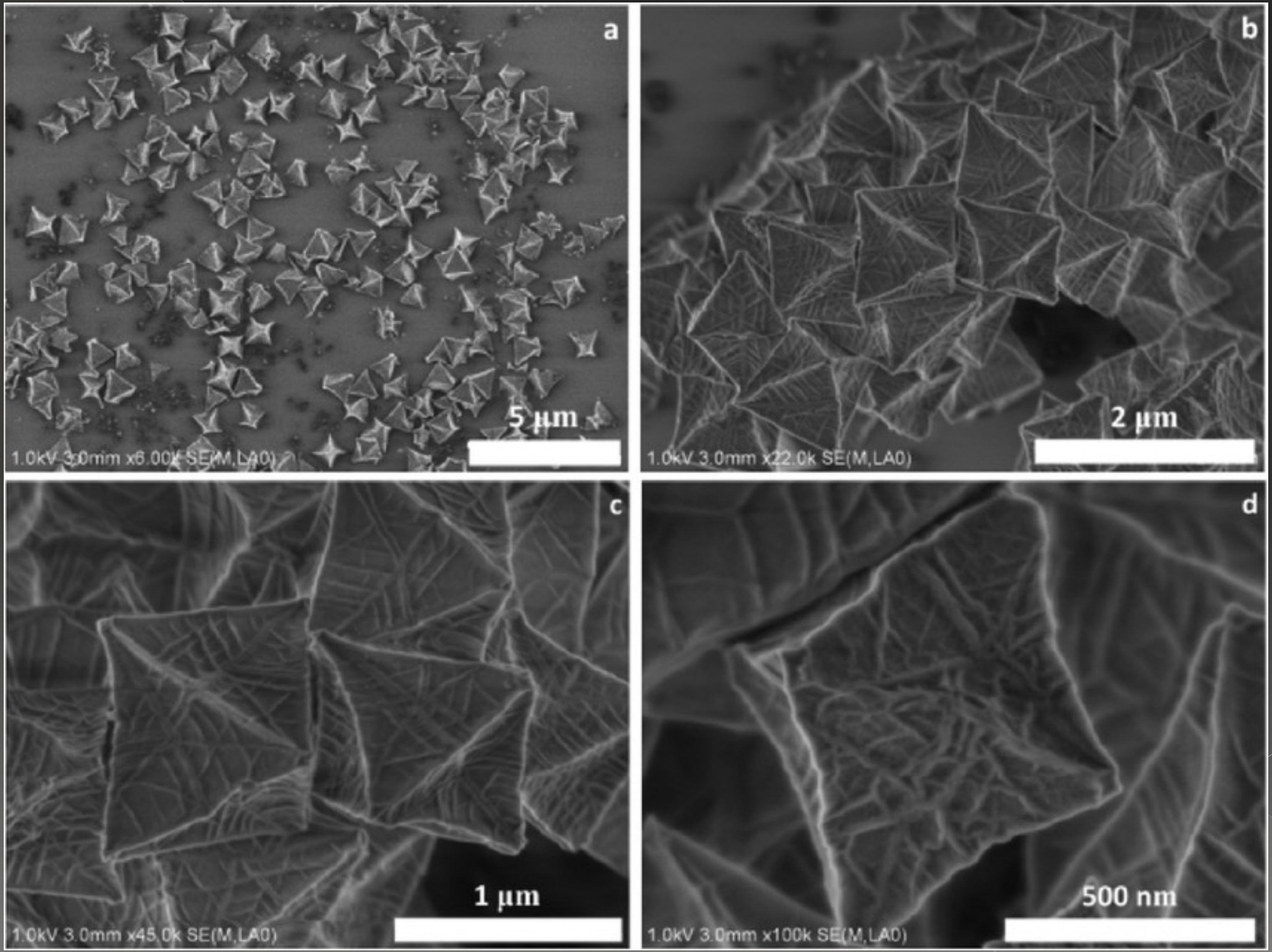

Data reported on original SEM Images

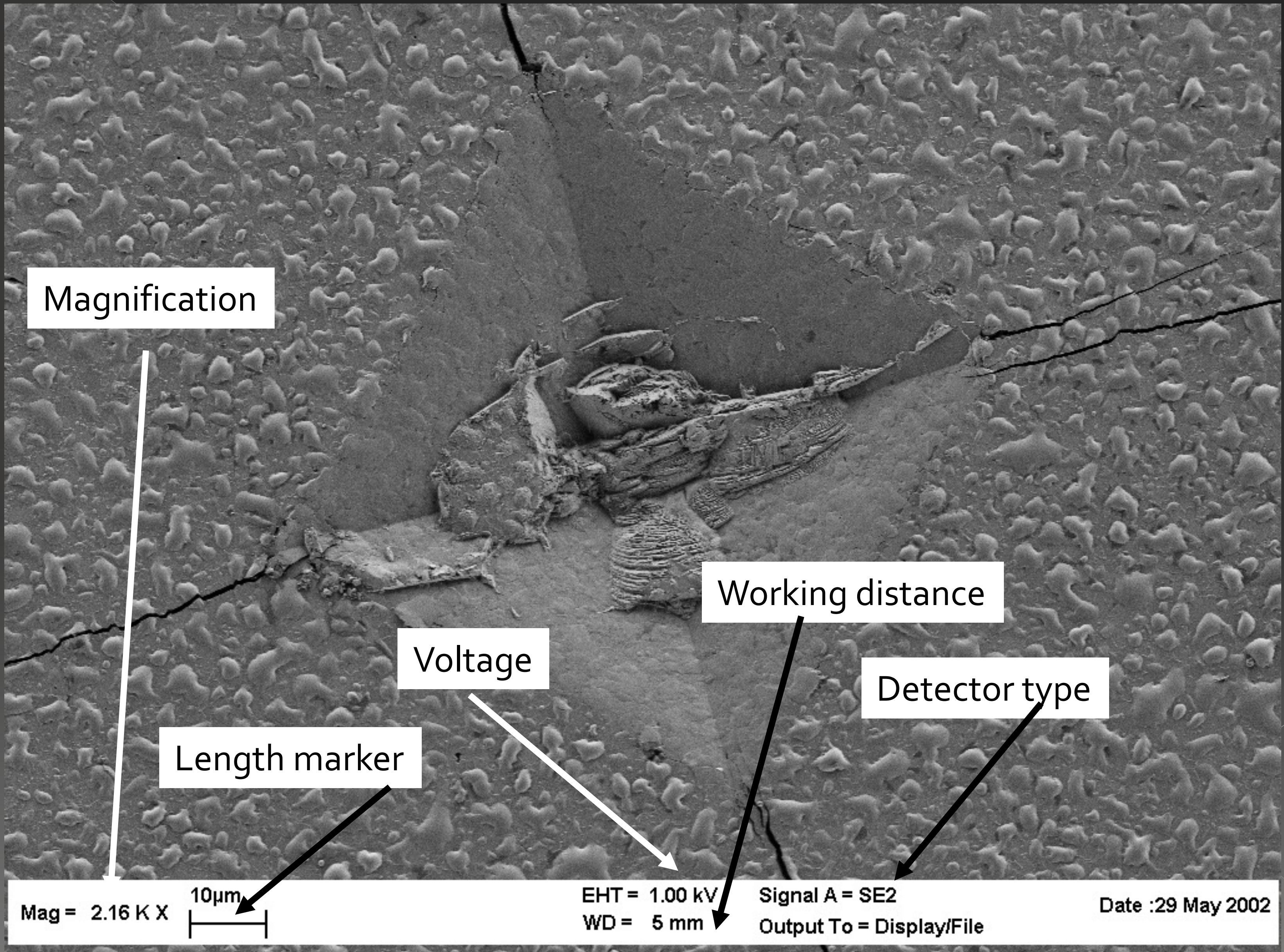

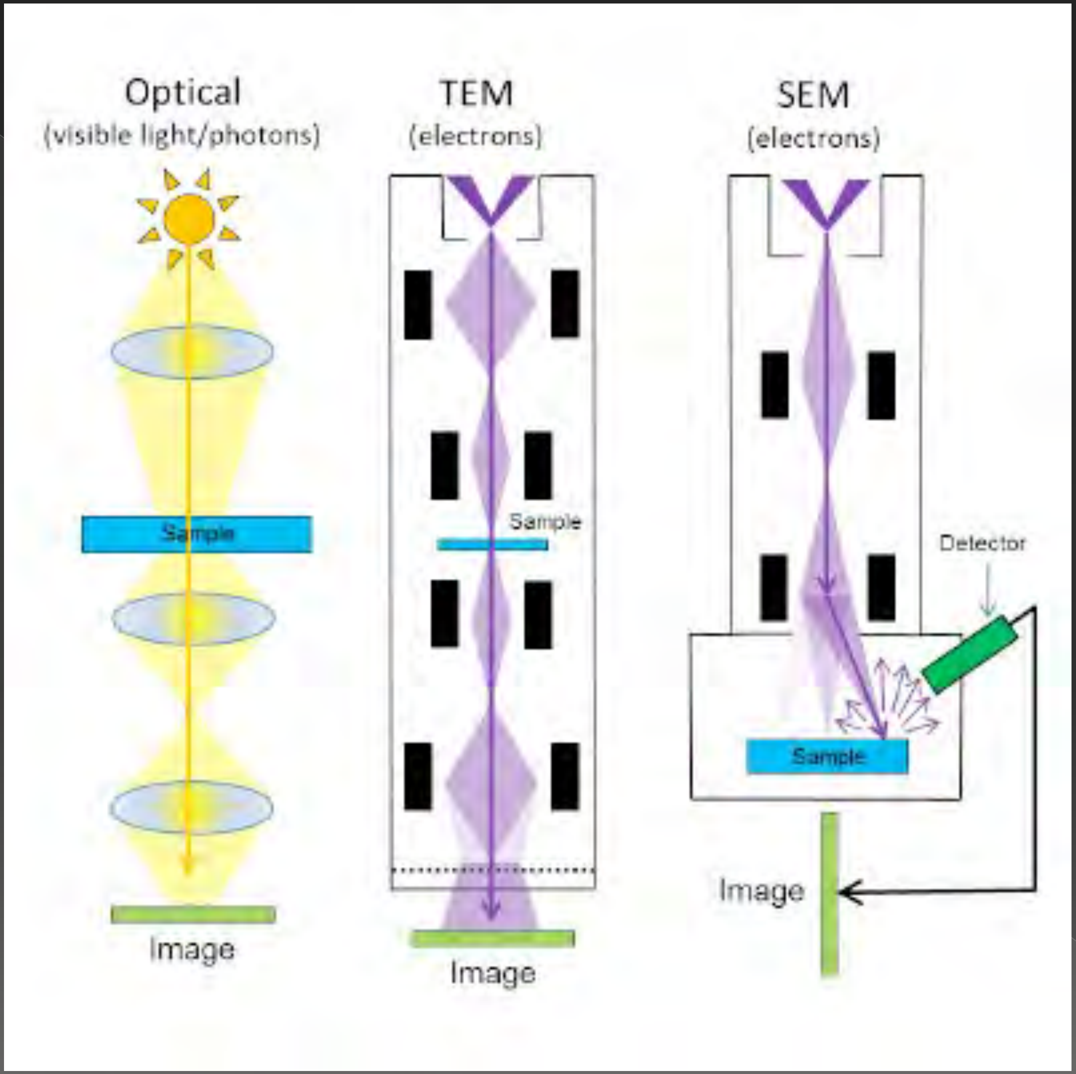
Optical
(visible light/photons)
TEM
(electrons)
SEM
(electrons)
Sample
Sample
Detector
Sample
Image
Image
Image

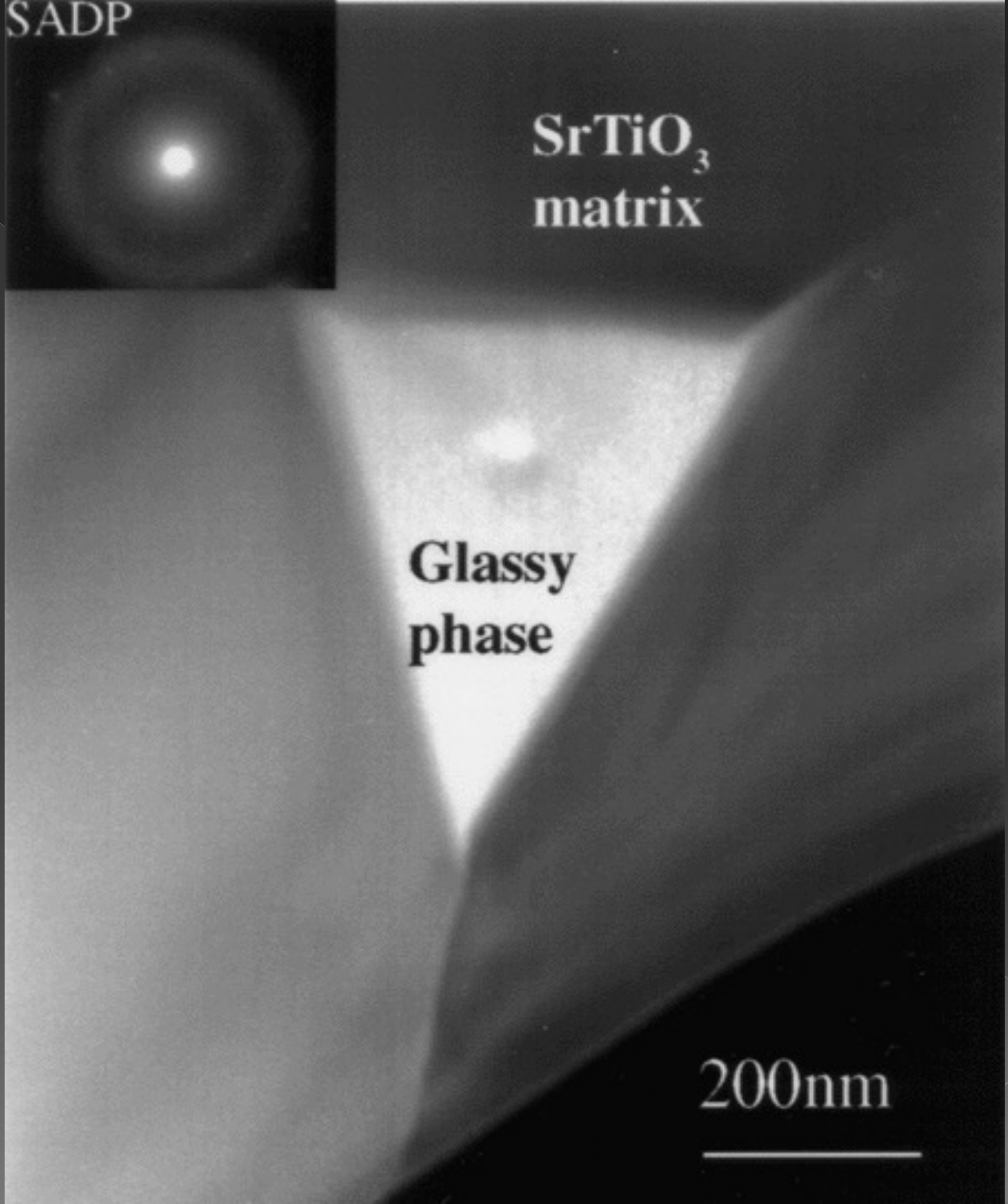
SADP
SrTiO3
matrix
Glassy
phase
200nm

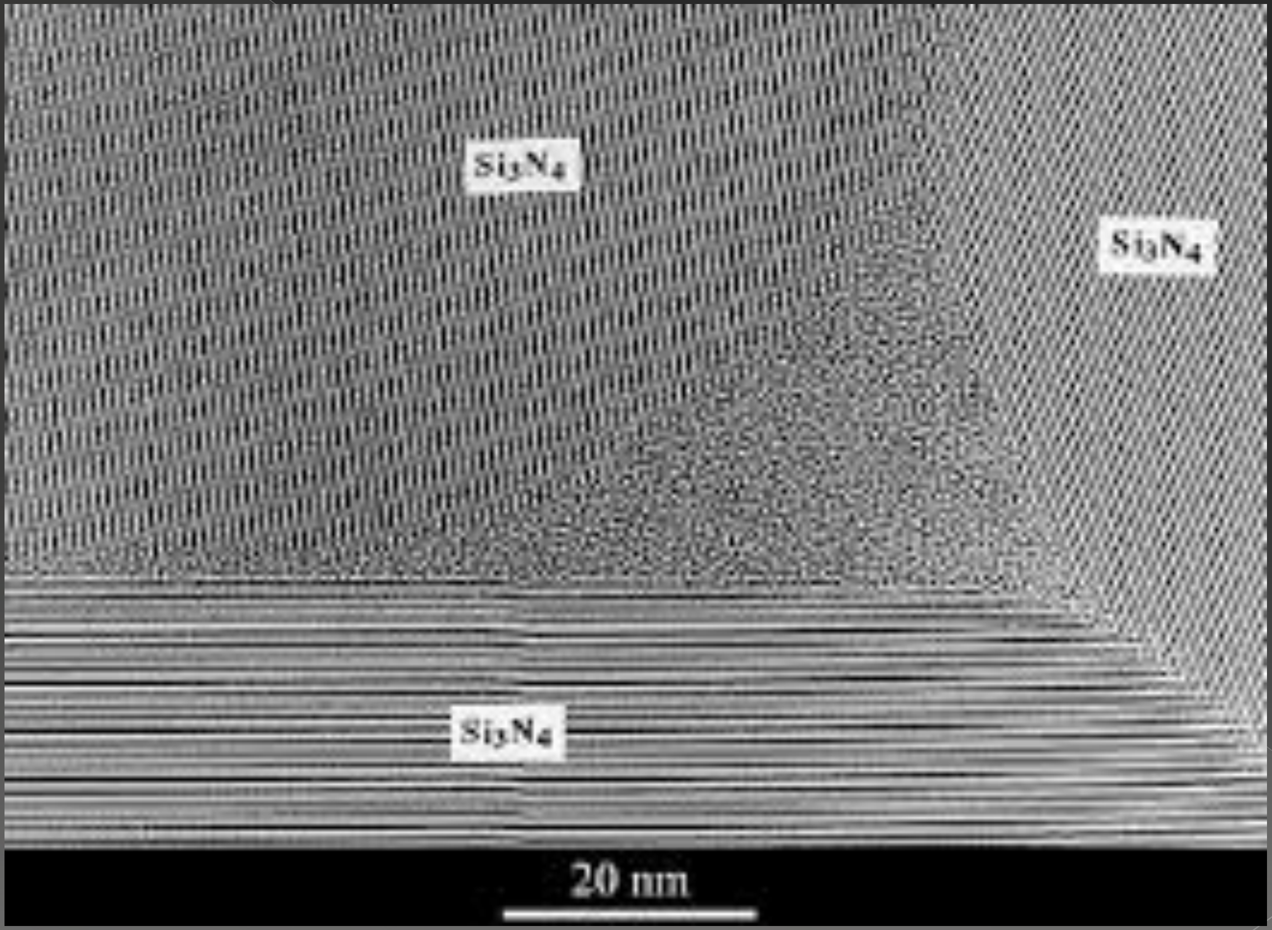

Si_3N_4
Si_3N_4
Si_3N_4
20 nm

Electron diffraction pattern

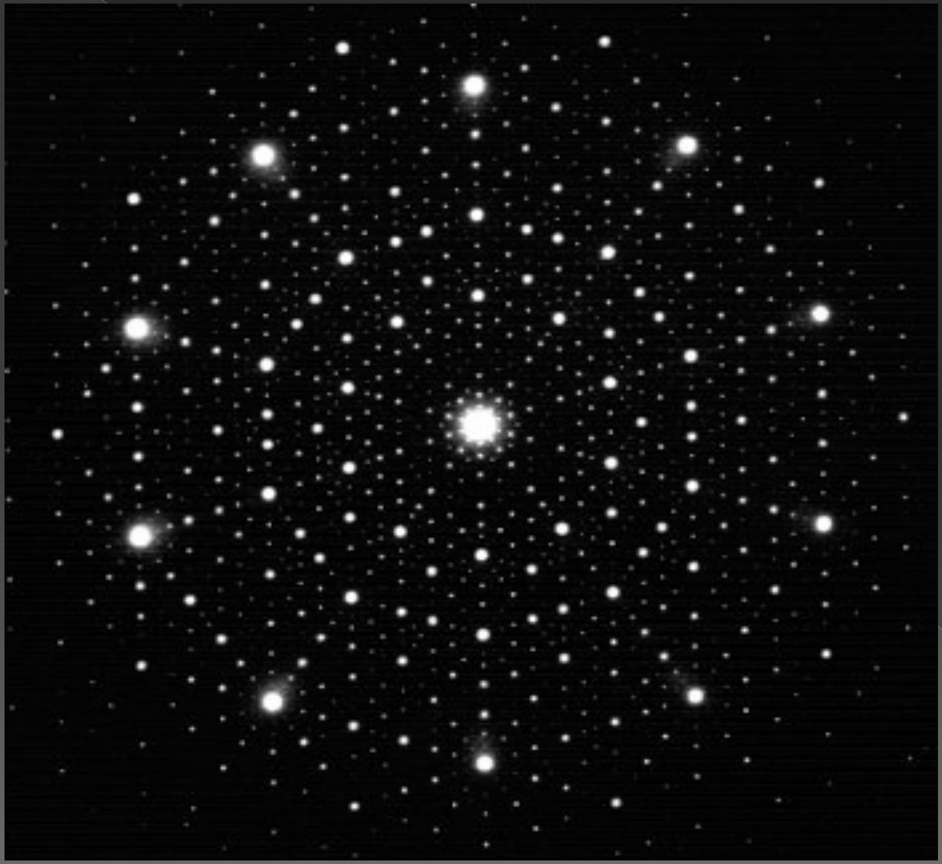

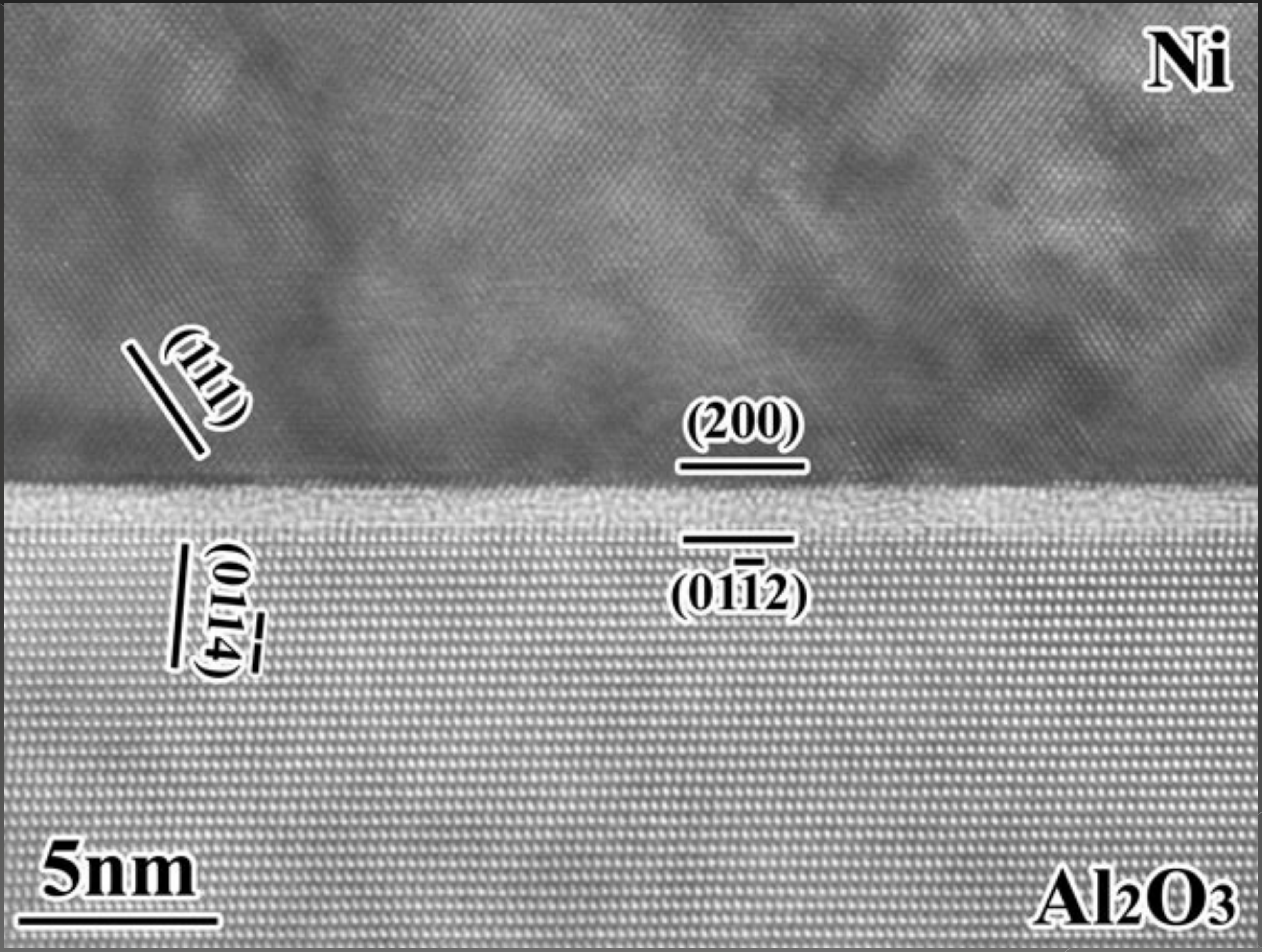

Ni
(200)
(01$\bar{1}$2)
5nm
Al_2O_3

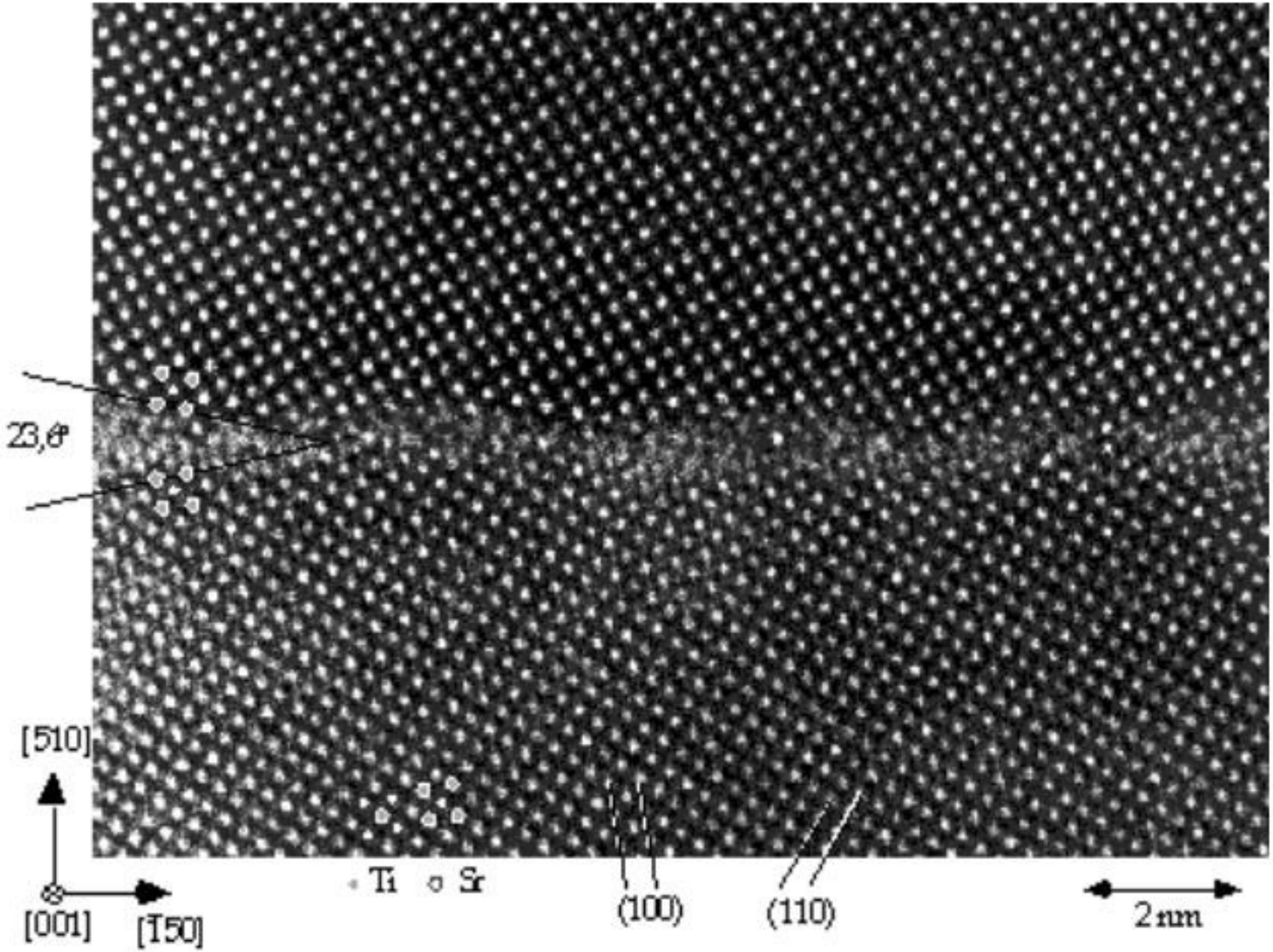
23,6°
[510]
[001]
[150]
Ti
Sr
(100)
(110)
2 nm

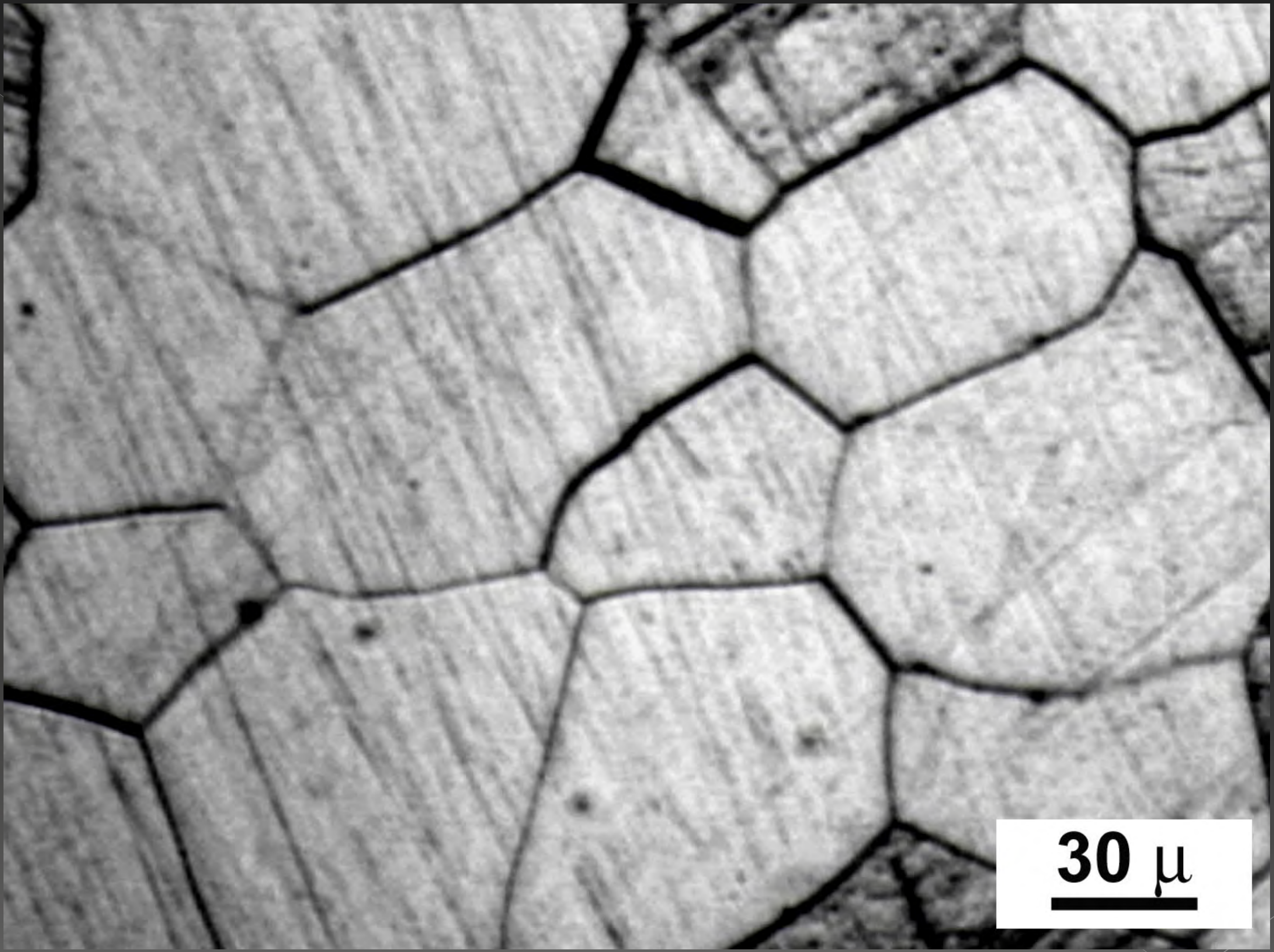
30 μ